



**Phase I Hydrologic Data for the
Groundwater Flow and
Contaminant Transport Model
of Corrective Action
Unit 99: Rainier Mesa/Shoshone
Mountain, Nevada Test Site,
Nye County, Nevada**



Revision No.: 1

May 2008

Prepared for U.S. Department of Energy under Contract No. DE-AC52-03NA99205.

Approved for public release; further dissemination unlimited.

Available for public sale, in paper, from:

U.S. Department of Commerce
National Technical Information Service
5285 Port Royal Road
Springfield, VA 22161
Phone: 800.553.6847
Fax: 703.605.6900
Email: orders@ntis.gov
Online ordering: <http://www.ntis.gov/ordering.htm>

Available electronically at <http://www.osti.gov/bridge>

Available for a processing fee to U.S. Department of Energy and its contractors,
in paper, from:

U.S. Department of Energy
Office of Scientific and Technical Information
P.O. Box 62
Oak Ridge, TN 37831-0062
Phone: 865.576.8401
Fax: 865.576.5728
Email: reports@adonis.osti.gov

Reference herein to any specific commercial product, process, or service by trade name, trademark, manufacturer, or otherwise, does not necessarily constitute or imply its endorsement, recommendation, or favoring by the United States Government or any agency thereof or its contractors or subcontractors.





**PHASE I HYDROLOGIC DATA FOR THE
GROUNDWATER FLOW AND
CONTAMINANT TRANSPORT MODEL
OF CORRECTIVE ACTION UNIT 99:
RAINIER MESA/SHOSHONE MOUNTAIN,
NEVADA TEST SITE, NYE COUNTY,
NEVADA**

Contributors:

Stoller-Navarro Joint Venture

John Londergan
William Fryer
Nathan Bryant

National Securities Technologies, LLC

Sigmund L. Drellack

Revision No.: 1

May 2008

Stoller-Navarro Joint Venture
7710 W. Cheyenne, Building 3
Las Vegas, NV 89129

Prepared for U.S. Department of Energy under Contract No. DE-AC52-03NA99205.

Approved for public release; further dissemination unlimited.

**PHASE I HYDROLOGIC DATA
FOR THE GROUNDWATER FLOW AND CONTAMINANT TRANSPORT MODEL
OF CORRECTIVE ACTION UNIT 99: RAINIER MESA/SHOSHONE MOUNTAIN,
NEVADA TEST SITE, NYE COUNTY, NEVADA**

Approved by: _____
Sam Marutzky, UGTA Project Manager
Stoller-Navarro Joint Venture

Date: _____

ACKNOWLEDGEMENT

We thank the many individuals who assisted in the creation of this report and especially appreciate the efforts of Chris Miller, Christy Morris, Ellen Cook, and the document production staff for their support in preparing this document for publication. We also thank Greg Ruskauff for his contributions and thorough review.

TABLE OF CONTENTS

| | |
|---|------|
| List of Figures..... | v |
| List of Plates..... | viii |
| List of Tables..... | ix |
| List of Acronyms and Abbreviations..... | x |
| List of Stratigraphic Unit Abbreviations and Symbols..... | xiii |
| 1.0 Introduction..... | 1-1 |
| 1.1 Role of the Hydrologic Data Document in the FFACO Process..... | 1-1 |
| 1.2 Role of the Document in CAU-Scale Modeling..... | 1-1 |
| 1.3 Underground Nuclear Testing in RMSM..... | 1-3 |
| 1.4 Supporting Documents..... | 1-3 |
| 1.5 References..... | 1-5 |
| 2.0 Geologic and Hydrologic Setting..... | 2-1 |
| 2.1 Geologic Overview of Rainier Mesa..... | 2-1 |
| 2.2 Geologic Overview of Shoshone Mountain..... | 2-2 |
| 2.3 Hydrologic Setting..... | 2-3 |
| 2.3.1 Surface Water..... | 2-3 |
| 2.3.2 Groundwater..... | 2-3 |
| 2.4 References..... | 2-4 |
| 3.0 Data Compilation and Analysis..... | 3-1 |
| 3.1 Data Types..... | 3-1 |
| 3.1.1 Saturated Media Hydraulic Properties..... | 3-1 |
| 3.1.2 Recharge from Precipitation..... | 3-1 |
| 3.1.3 Groundwater Surface Discharge..... | 3-1 |
| 3.1.4 Lateral Boundary Fluxes..... | 3-2 |
| 3.1.5 Hydraulic Head..... | 3-2 |
| 3.1.6 Temperature Data..... | 3-2 |
| 3.2 Data Quality..... | 3-3 |
| 3.3 Data Transferability..... | 3-3 |
| 3.4 References..... | 3-3 |
| 4.0 RMSM Hydrostratigraphic Framework and HSU Mineralogy..... | 4-1 |
| 4.1 RMSM HFM..... | 4-1 |
| 4.1.1 Hydrogeologic and Hydrostratigraphic Units of the RMSM HFM..... | 4-1 |
| 4.2 HFM Model Overview..... | 4-2 |
| 4.3 References..... | 4-3 |
| 5.0 Saturated Media Hydraulic Properties..... | 5-1 |
| 5.1 Data Compilation and Evaluation..... | 5-1 |
| 5.2 Data Sources..... | 5-3 |
| 5.3 Data Quality Evaluation..... | 5-3 |

TABLE OF CONTENTS (CONTINUED)

| | | |
|------|---|------|
| 5.4 | Hydraulic Property Characterization Groups | 5-4 |
| 5.5 | Assignment of Data to Characterization Groups | 5-5 |
| 5.6 | Data Transfer | 5-6 |
| 5.7 | Spatial Distribution of Data | 5-7 |
| 5.8 | Hydraulic Conductivity. | 5-7 |
| | 5.8.1 Scales of Test Data and Applicability | 5-8 |
| | 5.8.2 Test Analyses and Associated Uncertainties | 5-9 |
| 5.9 | Analysis of Hydraulic Conductivity Data. | 5-9 |
| | 5.9.1 Multiple Test Results for One Well | 5-9 |
| | 5.9.2 Methodology. | 5-10 |
| 5.10 | Analysis Results | 5-10 |
| 5.11 | Conversion of Hydraulic Conductivity to Permeability | 5-16 |
| 5.12 | Anisotropy of K | 5-19 |
| 5.13 | Depth Dependence of Hydraulic Conductivity. | 5-19 |
| | 5.13.1 Depth-Decay Formulation | 5-19 |
| | 5.13.2 Analysis of NTS Datasets for Depth Decay. | 5-20 |
| 5.14 | Specific Storage | 5-23 |
| 5.15 | LCA Hydraulic Conductivity, Dual-Porosity Analysis | 5-26 |
| | 5.15.1 Previous Dual-Porosity Analyses. | 5-26 |
| | 5.15.2 Reanalysis of LCA Test Data. | 5-27 |
| 5.16 | Comparison of the YFCM HDD and the RMSM HDD Hydraulic Conductivity Analyses. | 5-28 |
| 5.17 | Limitations | 5-28 |
| 5.18 | Summary. | 5-30 |
| 5.19 | References. | 5-31 |
| 6.0 | Precipitation Recharge | 6-1 |
| 6.1 | Objectives | 6-1 |
| 6.2 | Approach. | 6-1 |
| 6.3 | Data Types and Prioritization | 6-1 |
| 6.4 | South-Central Great Basin Recharge Processes | 6-1 |
| 6.5 | Recharge Model Descriptions. | 6-2 |
| | 6.5.1 Revised UGTA Recharge Model | 6-3 |
| | 6.5.1.1 Methodology | 6-3 |
| | 6.5.1.2 Construction of the Digital Precipitation Map and Grid File | 6-5 |
| | 6.5.1.3 Recharge Distribution and Reallocation | 6-5 |
| | 6.5.2 USGS Recharge Model | 6-5 |
| | 6.5.3 DRI Recharge Model | 6-7 |
| | 6.5.4 USGS DVRFS Model. | 6-7 |
| 6.6 | Limitations | 6-7 |
| 6.7 | References. | 6-11 |
| 7.0 | Groundwater Discharge | 7-1 |

TABLE OF CONTENTS (CONTINUED)

| | | |
|---------|---|------|
| 7.1 | Well Discharge | 7-1 |
| 7.2 | Spring Discharge | 7-4 |
| 7.3 | Tunnel Discharge | 7-4 |
| 7.4 | References | 7-5 |
| 8.0 | Lateral Boundary Flux Evaluations | 8-1 |
| 8.1 | Introduction | 8-1 |
| 8.2 | Models Used | 8-1 |
| 8.3 | Recharge Scenarios | 8-2 |
| 8.4 | DVRFS Model Flows Calculated for the Recharge Scenarios | 8-4 |
| 8.4.1 | NTS Flow Model Calibration | 8-9 |
| 8.4.1.1 | Calibration Procedure | 8-9 |
| 8.4.1.2 | Discussion of Results | 8-11 |
| 8.5 | RMSM Model Area Flows Calculated for the AFMs | 8-17 |
| 8.6 | Summary of Modeling Results | 8-31 |
| 8.7 | Limitations | 8-33 |
| 8.8 | References | 8-33 |
| 9.0 | Hydraulic Heads | 9-1 |
| 9.1 | Objectives | 9-1 |
| 9.2 | Data Types | 9-1 |
| 9.2.1 | Data Uncertainties | 9-1 |
| 9.2.2 | Data Sources | 9-2 |
| 9.2.3 | Data Compilation | 9-2 |
| 9.2.4 | Data Analysis Methods | 9-3 |
| 9.3 | RMSM Hydraulic Head Distribution | 9-3 |
| 9.4 | References | 9-6 |
| 10.0 | Subsurface Temperature Data | 10-1 |
| 10.1 | Groundwater Temperature Data for the RMSM Model Area | 10-1 |
| 10.2 | References | 10-6 |

Appendix A - RMSM HFM Data

| | | |
|-------|-----------------------|-----|
| A.1.0 | Introduction | A-1 |
| A.2.0 | Dataset Summary | A-1 |
| A.3.0 | References | A-1 |

Appendix B - Hydraulic Properties Additional Analysis

| | | |
|-------|--|-----|
| B.1.0 | Introduction | B-1 |
| B.2.0 | Characterization Group Datasets | B-1 |
| B.3.0 | Alternate Evaluation and Presentation of Depth Decay | B-8 |

TABLE OF CONTENTS (CONTINUED)

Appendix C - Areal Recharge Supplementary Information

| | |
|-----------------------------|-----|
| C.1.0 Introduction..... | C-1 |
| C.2.0 Dataset Summary | C-1 |

Appendix D - Groundwater Discharge Supplementary Information

| | |
|-----------------------------|-----|
| D.1.0 Introduction..... | D-1 |
| D.2.0 Dataset Summary | D-1 |

Appendix E - Hydraulic Head Supplementary Information

| | |
|-----------------------------|-----|
| E.1.0 Introduction..... | E-1 |
| E.2.0 Dataset Summary | E-1 |
| E.3.0 References..... | E-1 |

Appendix F - Comments from Nevada Division of Environmental Protection

LIST OF FIGURES

| NUMBER | TITLE | PAGE |
|---------------|---|-------------|
| 1-1 | Underground Test Area Corrective Action Units Process Flow Diagram | 1-2 |
| 5-1 | NTS Data Compilation Area Hydraulic Property Data Locations | 5-2 |
| 5-2 | Relationship of CG Hydraulic Conductivity Distributions | 5-15 |
| 5-3 | Overlay of NTS Data Compilation Area Hydraulic Conductivity Distributions | 5-16 |
| 5-4 | Comparison of Pumping-Scale and Lab-Scale K Distributions, 95% Bounds | 5-17 |
| 5-5 | Hydraulic Conductivity Versus Depth for the NTS Data Compilation Area Dataset . . | 5-24 |
| 5-6 | Specific Storage Data for the NTS Data Compilation Area Dataset | 5-25 |
| 5-7 | LCA Dual-Porosity Analyses | 5-26 |
| 5-8 | LCA Dual-Porosity Reanalyses | 5-29 |
| 6-1 | UGTA Revised Modified ME Recharge Model | 6-4 |
| 6-2 | USGS DPWM Recharge Model | 6-6 |
| 6-3 | RMSM DRI CMB Recharge Model Mean | 6-8 |
| 6-4 | RMSM DRI CMB Recharge Model Coefficient of Variation | 6-9 |
| 6-5 | USGS DVRFS Recharge Model | 6-10 |
| 7-1 | RMSM Area Discharge Features | 7-2 |
| 7-2 | RMSM Area Well Discharge Graphs | 7-3 |
| 8-1 | Geographic and Prominent Topographic Features of the DVRFS Region, Nevada and California | 8-3 |
| 8-2 | Unweighted Residual Hydraulic Heads for the DVRFS Regional Recharge Scenario . . | 8-6 |
| 8-3 | Unweighted Residual Hydraulic Heads for the DVRFS Revised UGTA Recharge Scenario | 8-7 |
| 8-4 | Unweighted Residual Hydraulic Heads for the DVRFS DRI Recharge Scenario | 8-8 |
| 8-5 | Map Showing Locations of All UGTA HFM Areas | 8-10 |

LIST OF FIGURES (CONTINUED)

| NUMBER | TITLE | PAGE |
|---------------|---|-------------|
| 8-6 | Unweighted Residual Hydraulic Heads for the NTS CAU Insert Model Regional Recharge Scenario | 8-18 |
| 8-7 | Unweighted Residual Hydraulic Heads for the NTS CAU Insert Model Revised UGTA Recharge Scenario | 8-19 |
| 8-8 | Unweighted Residual Hydraulic Heads for the NTS CAU Insert Model DRI Recharge Scenario. | 8-20 |
| 8-9 | West-East Profiles through the Base Model and the No Redrock Valley Caldera AFM. | 8-21 |
| 8-10 | Comparison of the Base Model with the More Extensive LCA3 AFM. | 8-22 |
| 8-11 | Comparison of the Base Model with the Shoshone Mountain Thrust Sheet AFM | 8-23 |
| 8-12 | West-East Profiles through the Base Model and the Shoshone Mountain Thrust Sheet AFM | 8-24 |
| 8-13 | Unweighted Residual Hydraulic Heads for the No Redrock Valley Caldera AFM Regional Recharge Scenario | 8-27 |
| 8-14 | Unweighted Residual Hydraulic Heads for the More Extensive LCA3 AFM Regional Recharge Scenario | 8-28 |
| 8-15 | Unweighted Residual Hydraulic Heads for the Shoshone Mountain Thrust AFM Regional Recharge Scenario | 8-29 |
| 8-16 | Unweighted Residual Hydraulic Heads for the Initial Run of the No Redrock Valley Caldera AFM Regional Recharge Scenario. . . . | 8-30 |
| 9-1 | RMSM Hydraulic Head Calibration Targets | 9-4 |
| 10-1 | RMSM Locations of Existing Groundwater Temperature Profiles | 10-5 |
| B.2-1 | AA Pumping-Scale CDF | B-2 |
| B.2-2 | AA Pumping-Scale Depth Decay. | B-2 |
| B.2-3 | LFA Pumping-Scale CDF | B-3 |
| B.2-4 | LFA Pumping-Scale Depth Decay | B-3 |

LIST OF FIGURES (CONTINUED)

| NUMBER | TITLE | PAGE |
|---------------|--|-------------|
| B.2-5 | WTA Pumping-Scale CDF | B-4 |
| B.2-6 | WTA Pumping-Scale Depth Decay | B-4 |
| B.2-7 | TCU Pumping-Scale CDF | B-5 |
| B.2-8 | TCU Pumping-Scale Depth Decay | B-5 |
| B.2-9 | LCA Pumping-Scale CDF | B-6 |
| B.2-10 | LCA Pumping-Scale Depth Decay | B-6 |
| B.2-11 | LCA3 Pumping-Scale CDF | B-7 |
| B.2-12 | LCA3 Pumping-Scale Depth Decay | B-7 |
| B.3-1 | Depth-Decay K HSU CDFs | B-9 |
| B.3-2 | Brittle Rock Depth Decay | B-11 |
| B.3-3 | Ductile Rock Depth Decay | B-12 |

LIST OF PLATES

NUMBER

TITLE

Plate 1 Rainier Mesa/Shoshone Mountain Hydrostratigraphic Area
and Corrective Action Sites Pocket

LIST OF TABLES

| NUMBER | TITLE | PAGE |
|---------------|--|-------------|
| 1-1 | Major Supporting Documents | 1-4 |
| 5-1 | Hydraulic Property Characterization Groups | 5-2 |
| 5-2 | Summary of RMSM HFM Area Hydraulic Conductivity Analysis | 5-11 |
| 5-3 | Summary of NTS Data Compilation Area Hydraulic Conductivity Analysis. | 5-12 |
| 5-4 | Statistical Comparison of RMSM Data to NTS Data | 5-14 |
| 5-5 | Comparison of Mean and Standard Deviation by Scale of Measurement. | 5-17 |
| 5-6 | Variation of Water Properties with Temperature | 5-18 |
| 5-7 | Summary of Depth-Decay Analysis | 5-21 |
| 5-8 | Summary of Specific Storage Data by Characterization Group | 5-25 |
| 5-9 | Comparison of K Statistics for All LCA Analyses and Dual-Porosity Analyses | 5-27 |
| 5-10 | Comparison of YFCM and RMSM Hydraulic Conductivity Analyses. | 5-30 |
| 6-1 | Recharge Models Considered | 6-2 |
| 8-1 | DVRFS Model Run Results. | 8-5 |
| 8-2 | Comparison of Model Calibration Parameters | 8-11 |
| 8-3 | NTS Flow Model Run Results. | 8-16 |
| 8-4 | Alternate Framework Model Run Results | 8-26 |
| 8-5 | Summary of Model Results | 8-32 |
| 10-1 | Key Reports Providing Temperature Data and Information for the NTS Area. | 10-2 |
| 10-2 | Wells with Temperature Logs in the RMSM Model Area | 10-3 |
| 10-3 | Wells with Temperature Logs in the RMSM Model Area | 10-4 |
| B.3-1 | Statistics for K_0 Datasets | B-9 |
| B.3-2 | Regression Statistics for $\log_{10} K$ Versus Depth | B-10 |

LIST OF ACRONYMS AND ABBREVIATIONS

| | |
|----------------------|---|
| 2-D | Two-dimensional |
| 3-D | Three-dimensional |
| AFM | Alternative framework model |
| amsl | Above mean sea level |
| bgs | Below ground surface |
| CADD | Corrective Action Decision Document |
| CAI | Corrective Action Investigation |
| CAIP | Corrective Action Investigation Plan |
| CAP | Corrective Action Plan |
| CAS | Corrective Action Site |
| CAU | Corrective Action Unit |
| CDF | Cumulative distribution function |
| CG | Characterization group |
| cm/yr | Centimeters per year |
| cm ² /sec | Square centimeters per second |
| CMB | Chloride mass balance |
| CR | Closure Report |
| DDE_F | Data documentation evaluation flag |
| DEM | Digital elevation model |
| DOE | U.S. Department of Energy |
| DPWS | Distributed parameter watershed |
| DQE_F | Data quality evaluation flag |
| DRI | Desert Research Institute |
| DVD | Digital video disc |
| ECDF | Empirical cumulative distribution function |
| ER | Environmental Restoration |
| ERP | Environmental Restoration Project |
| FAI | Formation access interval |
| FFACO | <i>Federal Facility Agreement and Consent Order</i> |
| ft | Foot |
| g/cm-sec | Grams per centimeter-second |
| g/cm ³ | Grams per cubic centimeter |
| GMG | Geometric Multigrid |

LIST OF ACRONYMS AND ABBREVIATIONS (CONTINUED)

| | |
|---------------------|--|
| GMS | Groundwater Modeling System |
| GRFM | Generalized radial flow model |
| HDD | Hydrologic data document |
| HFM | Hydrostratigraphic framework model |
| HGU | Hydrogeologic unit |
| HSU | Hydrostratigraphic unit |
| HUF | Hydrogeologic-unit flow |
| K-S | Kolmogorov-Smirnov |
| K | Hydraulic conductivity |
| k | Intrinsic permeability |
| km | Kilometer |
| kt | Kiloton |
| Lpm | Liters per minute |
| LLNL | Lawrence Livermore National Laboratory |
| LMG | Link-Algebraic Multigrid |
| m | Meter |
| m/day | Meters per day |
| M&O | Management and operating |
| m ³ | Cubic meter |
| m ³ /day | Cubic meters per day |
| m ³ /yr | Cubic meters per year |
| ME | Maxey-Eakin |
| mi | Mile |
| mm/yr | Millimeters per year |
| MODFLOW | Modular Three-Dimensional Finite Difference Ground-Water Flow |
| NA | Not applicable |
| NAD | North American Datum |
| NDEP | Nevada Division of Environmental Protection |
| NNSA/NSO | U.S. Department of Energy, National Nuclear Security Administration Nevada Site Office |
| NTS | Nevada Test Site |
| NWIS | National Water Information System |
| PDF | Probability density function |
| pdf | Portable Document Format |

LIST OF ACRONYMS AND ABBREVIATIONS (CONTINUED)

| | |
|------|--------------------------------|
| PMOV | Pahute Mesa/Oasis Valley |
| QA | Quality assurance |
| QAPP | Quality Assurance Project Plan |
| RMSM | Rainier Mesa/Shoshone Mountain |
| S | Storativity |
| SNJV | Stoller-Navarro Joint Venture |
| Ss | Specific storage |
| T | Transmissivity |
| UGTA | Underground Test Area |
| USGS | U.S. Geological Survey |
| UTM | Universal Transverse Mercator |
| WW | Water Well |
| YFCM | Yucca Flat/Climax Mine |
| YMP | Yucca Mountain Project |
| °C | Degrees Celsius |

LIST OF STRATIGRAPHIC UNIT ABBREVIATIONS AND SYMBOLS

| | |
|-------|---|
| AA | Alluvial aquifer |
| ATICU | Ammonia Tanks intrusive confining unit |
| ATCU | Argillic tuff confining unit |
| BRA | Belted Range aquifer |
| CA | Carbonate aquifer |
| CCU | Clastic confining unit |
| CHICU | Calico Hills intrusive confining unit |
| DVRFS | Death Valley Regional Flow System |
| FCCM | Fortymile Canyon composite unit |
| GCU | Granite confining unit |
| IICU | Intra-caldera intrusive confining unit |
| LCA | Lower carbonate aquifer |
| LCA3 | Lower carbonate aquifer-thrust plate |
| LCCU | Lower clastic confining unit |
| LCCU1 | Lower clastic confining unit-thrust plate |
| LFA | Lava-flow aquifer |
| LTCU | Lower tuff confining unit |
| LTCU1 | Lower tuff confining unit 1 |
| LVTA1 | Lower vitric-tuff aquifer 1 |
| LVTA2 | Lower vitric-tuff aquifer 2 |
| MGCU | Mesozoic granite confining unit |
| OAA | Older alluvium |
| OSBCU | Oak Spring Butte confining unit |
| PCU | Playa confining unit |
| RMBCU | Rainier Mesa breccia confining unit |
| RMICU | Rainier Mesa intrusive confining unit |
| RVA | Redrock Valley aquifer |
| RVBCU | Redrock Valley breccia confining unit |
| RVICU | Redrock Valley intrusive confining unit |
| SCICU | Silent Canyon intrusive confining unit |
| SWA | Stockade Wash aquifer |
| TCU | Tuff confining unit |
| TMCM | Timber Mountain composite unit |

LIST OF STRATIGRAPHIC UNIT ABBREVIATIONS AND SYMBOLS (CONTINUED)

| | |
|---------|---|
| TM-LVTA | Timber Mountain lower vitric-tuff aquifer |
| TM-UVTA | Timber Mountain upper vitric-tuff aquifer |
| TM-WTA | Timber Mountain welded-tuff aquifer |
| TPA | Twin Peaks aquifer |
| TSA | Topopah Spring aquifer |
| TUBA | Tub Spring aquifer |
| UCA | Upper carbonate aquifer |
| UCCU | Upper clastic confining unit |
| VA | Volcanic aquifer |
| VTA | Vitric-tuff aquifer |
| WTA | Welded-tuff aquifer |

1.0 INTRODUCTION

This document presents a summary and framework of the available hydrologic data and other information directly relevant to the development of the Rainier Mesa/Shoshone Mountain (RMSM) Corrective Action Unit (CAU) 99 groundwater flow models. Where appropriate, data and information documented elsewhere are briefly summarized with reference to the complete documentation.

1.1 Role of the Hydrologic Data Document in the FFACO Process

The U.S. Department of Energy (DOE), National Nuclear Security Administration Nevada Site Office (NNSA/NSO) initiated the Underground Test Area (UGTA) Project to assess and evaluate the effects of the underground nuclear weapons tests on groundwater beneath the Nevada Test Site (NTS) and vicinity. The framework for this evaluation is provided in Appendix VI, Revision No. 2 of the *Federal Facility Agreement and Consent Order* (FFACO) [1]. Section 3.0 of Appendix VI “Corrective Action Strategy” of the FFACO describes the process that will be used to complete corrective actions specifically for the UGTA Project. The objective of the UGTA corrective action strategy is to define contaminant boundaries for each UGTA CAU where groundwater may have become contaminated from the underground nuclear tests. The contaminant boundaries are determined based on modeling of groundwater flow and contaminant transport. [Figure 1-1](#) outlines the FFACO process. This document fits within the “Develop CAU Flow and Transport Model” block of the diagram.

1.2 Role of the Document in CAU-Scale Modeling

The hydrologic data document (HDD) is one of several documents produced as part of the modeling process. The HDD identifies sources of data and analyses of data that can be used for flow modeling. The RMSM HDD is being produced concurrently with the RMSM contaminant transport parameters document. The transport parameters document is similar to the HDD, but contains data and analysis related to transport modeling and not directly applicable to flow modeling. The RMSM modeling approach strategy document is also currently in development and will be released shortly after this document. The modeling approach/strategy document describes the modeling process that will be used for RMSM.

Modeling groundwater flow and transport in an area as complex as the RMSM CAU is a difficult process. In past UGTA CAUs, model sensitivity analysis has shown some parameters to be far more important than others, and the important parameters are not always consistent between models. An iterative approach to modeling works best, whereby datasets are refined to fill gaps and correct inconsistencies discovered during the modeling process. As such, the data and data characterizations used in this document are not final and are subject to revision during the modeling process. The

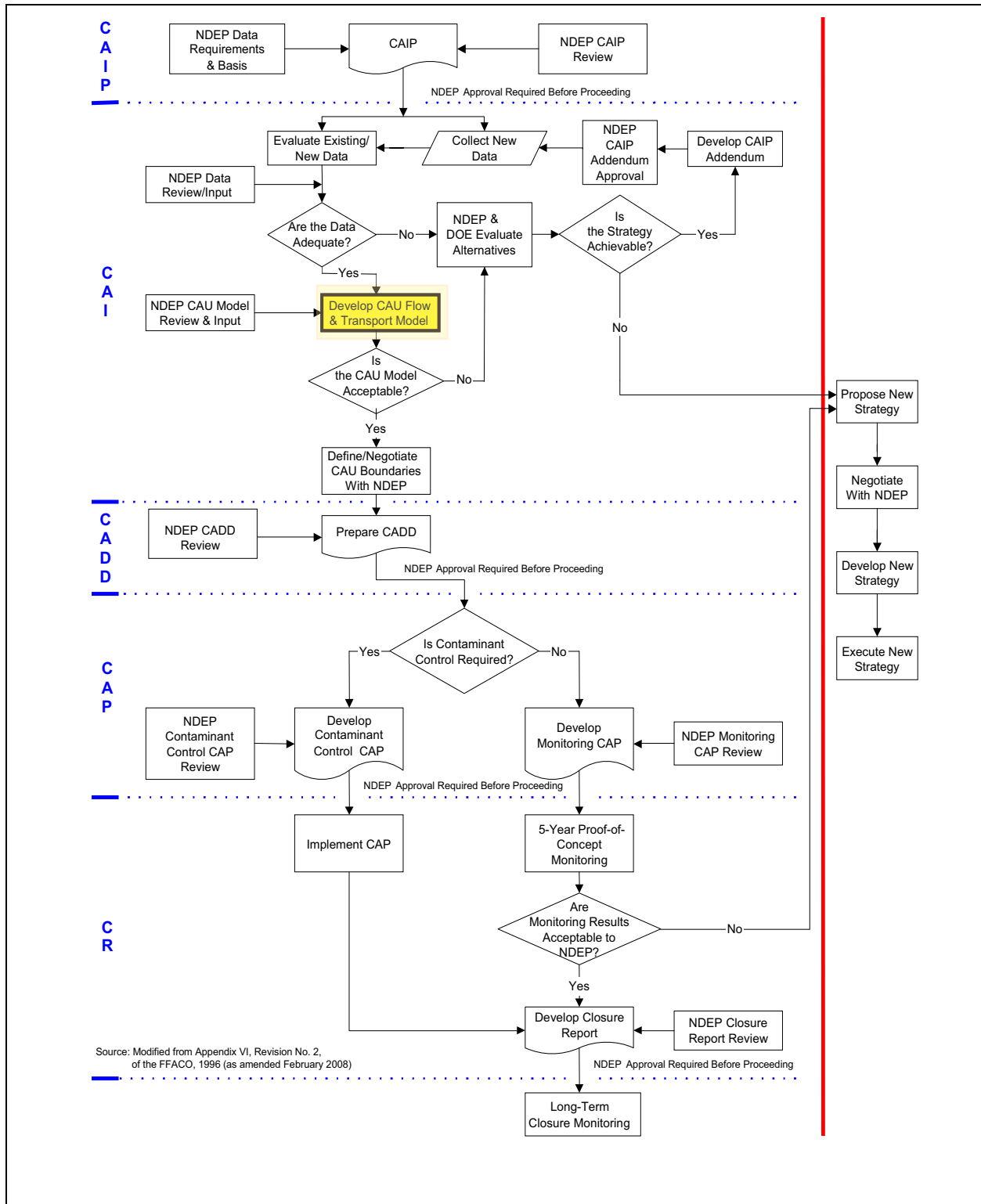


Figure 1-1
Underground Test Area Corrective Action Units Process Flow Diagram

emphasis for this document is to compile and evaluate datasets rather than to perform exhaustive analyses of all possible parameters, many of which will prove to be superfluous during modeling.

1.3 Underground Nuclear Testing in RMSM

Plate 1 is an overview of the RMSM model area with a digital elevation model (DEM) hillshade that shows physiography. Physiographic features are labeled in dark gray lettering. The RMSM CAU includes two distinct areas of nuclear testing, as outlined on Plate 1. The northern area in Area 12 where the majority of the RMSM tests are located includes all of Rainier Mesa and a small portion of Aqueduct Mesa to the northeast. The entire northern testing area is commonly referred to as Rainier Mesa, despite the inclusion of the portion of Aqueduct Mesa. The southern area in Area 16 is located beneath Tippihah Point, which is at the northeastern edge of the topographically high area generally referred to as Shoshone Mountain. Between 1957 and 1992, a total of 68 underground nuclear detonations were conducted in tunnels and shafts in this CAU. These tests included 62 detonations in the Rainier Mesa area and six detonations in Shoshone Mountain [2]. Cavities resulting from underground nuclear detonations are designated as corrective action sites (CASs) in the FFACO [1]. Multiple simultaneous detonations at one location are assigned to a single CAS. There are 60 CASs in Rainier Mesa and six in Shoshone Mountain for a total of 66 in the CAU. Section 5.0 of the contaminant transport parameters document for the RMSM CAU contains a complete list of the underground nuclear tests and related test information. The locations of the CASs, tunnel complexes, and UGTA wells in the RMSM CAU are shown in Plate 1.

Announced test yields for the RMSM CAU range from zero to 200 kilotons (kt), and the depths of burial range from 30 to 545 meters (m) below ground surface (bgs) [3]. Nuclear devices were emplaced in the Tertiary volcanics in RMSM. All of these detonations were conducted above the regional water table; however, perched groundwater has accumulated in some of the tunnel complexes [4]. Transport in the groundwater flow system is the primary avenue by which contaminants can move away from the test areas.

1.4 Supporting Documents

The NTS and surrounding areas have been the subject of intensive scientific study for more than half a century by a constellation of projects, programs, and organizations. A large body of literature and data supports a variety of activities at the NTS, much of which is useful to illuminate conditions and processes that affect radionuclide transport at the site. Table 1-1 lists documents that either provide a regional framework of the area around the NTS or document a variety of different types of information specific to the RMSM CAU. Each section of this report contains a number of references that are generally more specific to individual phenomena as well.

**Table 1-1
Major Supporting Documents**

| Title | Description |
|--|--|
| <i>Corrective Action Investigation Plan for Corrective Action Unit 99: Rainier Mesa/Shoshone Mountain, Nevada Test Site, Nevada [3]</i> | An FFACO [1] requirement that summarizes the historical data for the RMSM CAU. Describes the characterization activities that will be implemented to evaluate the extent of contamination in groundwater due to underground nuclear testing and support the development of groundwater flow and transport models to predict the contaminant boundary. |
| <i>Hydrogeologic and Hydrochemical Framework, South-Central Great Basin, Nevada-California, with Special Reference to the Nevada Test Site [5]</i> | The first report published on the regional groundwater flow system in southern Nevada, specifically focused on the NTS area. It provides comprehensive background information describing data and information on the regional flow system as well as detailed information on the NTS. |
| <i>Summary of Hydrogeologic Controls on Ground-Water Flow at the Nevada Test Site, Nye County, Nevada [6]</i> | Summarizes what is known and inferred about groundwater flow throughout the UGTA region. Major controls on groundwater flow are identified, some uncertainties about groundwater flow are highlighted, and technical needs are prioritized and identified relative to the Environmental Restoration Project (ERP). |
| <i>Value of Information Analysis for Corrective Action Unit 99: Rainier Mesa/Shoshone Mountain, Nevada Test Site, Nevada [7]</i> | Describes the evaluation of the sufficiency of existing information to support the corrective action investigation (CAI) and identifies the major problems anticipated in developing the geologic, flow, and transport models. Potential data collection activities to improve characterization data are evaluated for potential benefit and prioritization. |
| <i>Death Valley Regional Ground-Water Flow System, Nevada and California - Hydrogeologic Framework and Transient Ground-Water Flow Model [8]</i> | Presents an updated regional flow model that was developed by the U.S. Geological Survey (USGS) in collaboration with the Yucca Mountain Project (YMP) and the UGTA Project. |
| <i>A Hydrostratigraphic Model and Alternatives for the Groundwater Flow and Contaminant Transport Model of Corrective Action Unit 99: Rainier Mesa-Shoshone Mountain, Nye County, Nevada [9]</i> | Presents the hydrostratigraphic framework model (HFM) for the RMSM CAU that will be used for Phase I groundwater flow and contaminant transport modeling. |
| <i>Groundwater Flow Model Documentation Package (Phase I Data Analysis Documentation, Volume VI) [10]</i> | Presents the original UGTA regional groundwater flow model. |

1.5 References

FFACO, 1996; as amended, February 2008, see [1].

1. *Federal Facility Agreement and Consent Order*. 1996 (as amended February 2008). Agreed to by the State of Nevada; U.S. Department of Energy, Environmental Management; U.S. Department of Defense; and U.S. Department of Energy, Legacy Management.
2. U.S. Department of Energy, Nevada Operations Office. 2000. *United States Nuclear Tests, July 1945 through September 1992*, DOE/NV--209, Rev. 15. Las Vegas, NV.
3. U.S. Department of Energy, National Nuclear Security Administration Nevada Site Office. 2004. *Corrective Action Investigation Plan for Corrective Action Unit 99: Rainier Mesa/Shoshone Mountain, Nevada Test Site*, DOE-NV--1031. Las Vegas, NV.
4. Fenelon, J.M. 2006. *Database of Ground-Water Levels in the Vicinity of Rainier Mesa, Nevada Test Site, Nye County, Nevada, 1957-2005*. Carson City, NV: U.S. Geological Survey.
5. Winograd, I.J., and W. Thordarson. 1975. *Hydrogeologic and Hydrochemical Framework, South-Central Great Basin, Nevada-California, with Special Reference to the Nevada Test Site*, Professional Paper 712-C. Washington, DC: U.S. Geological Survey.
6. Laczniak, R.L., J.C. Cole, D.A. Sawyer, and D.A. Trudeau. 1996. *Summary of Hydrogeologic Controls on the Ground-Water Flow at the Nevada Test Site, Nye County, Nevada*, WRIR-96-4109. Carson City, NV: U.S. Geological Survey.
7. Stoller-Navarro Joint Venture. 2004. *Value of Information Analysis for Corrective Action Unit 99: Rainier Mesa/Shoshone Mountain, Nevada Test Site, Nevada*, S-N/99205-031. Las Vegas, NV.
8. Belcher, W.R., J.B. Blainey, F.A. D'Agnesse, C.C. Faunt, M.C. Hill, R.J. Laczniak, G.M. O'Brien, C.J. Potter, H.M. Putnam, C.A. San Juan, and D.S. Sweetkind. 2004. *Death Valley Regional Ground-Water Flow System, Nevada and California - Hydrogeologic Framework and Transient Ground-Water Flow Model*, Scientific Investigations Report 2004-5205. U.S. Geological Survey.
9. National Security Technologies, LLC. 2007. *A Hydrostratigraphic Model and Alternatives for the Groundwater Flow and Contaminant Transport Model of Corrective Action Unit 99: Rainier Mesa-Shoshone Mountain, Nye County, Nevada*, DOE/NV/29546--146. Las Vegas, NV.
10. IT Corporation. 1997. *Groundwater Flow Model Documentation Package (Phase I Data Analysis Documentation, Volume VI)*. Prepared for the U.S. Department of Energy, Nevada Operations Office. Las Vegas, NV.

2.0 GEOLOGIC AND HYDROLOGIC SETTING

Geologic and hydrologic descriptions in this section are largely derived from discussions in Sections 1.4.3, 1.4.4, and 1.4.5 of the RMSM HFM report [1]. The report is distributed on the digital video disc (DVD) accompanying this document and should be consulted for more detail.

Rainier Mesa is a high volcanic plateau dissected by drainages. The mesa is preserved by the presence of a thick caprock of welded tuff, which overlies much less-resistant bedded tuff layers. The top of the mesa is relatively flat, though incised in some areas by deep canyons. Ground-level elevations on Rainier Mesa are generally over 2,225 m (7,300 feet [ft]) above mean sea level (amsl), and average about 2,286 m (7,500 ft). The highest point on the NTS, 2,341 m (7,679 ft), is on Rainier Mesa. Aqueduct Mesa has slightly rougher and lower terrain, generally above 1,920 m (6,300 ft) in elevation. The edges of the mesas drop off abruptly on the west, south, and east sides.

Shoshone Mountain is a topographically high area located west of Yucca Flat, approximately 17 kilometers (km) (10.5 miles [mi]) due south of Rainier Mesa. Ground-level elevations at Shoshone Mountain range from 1,707 to 2,073 m (5,600 to 6,800 ft), but are generally above 1,830 m (6,000 ft). Tippipah Point, located at the northeast end of Shoshone Mountain and above the U16a Tunnel, has an elevation of 2,015 m (6,612 ft). The lowest region within the RMSM area is Mid Valley in the southeast portion of the model area at approximately 1,400 m (4,600 ft).

2.1 Geologic Overview of Rainier Mesa

Rainier Mesa consists of a layered volcanic rock sequence, with each layer exhibiting different physical and mechanical properties. The geology of the mesa can be briefly summarized as a thick sequence of relatively young Tertiary-age volcanic tuffs draped over an irregular substrate of much older Paleozoic sedimentary and Mesozoic intrusive rocks. The lower bedded tuffs have undergone significant *in situ* zeolitic alteration as a result of water percolating through them. In most places, the lower zeolitized section is overlain by a section of vitric bedded tuff, which lies just below the welded tuff caprock [2].

The geologic structure of the volcanic rocks of Rainier Mesa is well documented. Several high-angle normal faults have been mapped in the volcanic rocks; however, faults with greater than about 30 m (100 ft) of displacement are notably absent. The structure of the pre-Tertiary section is poorly known, though some geologists speculate that the trace of the Belted Range thrust fault is present in the pre-Tertiary rocks beneath Rainier Mesa. A broad synclinal feature mapped at the surface [3, 4] and in the tuffs of Rainier and Aqueduct Mesas may reflect a paleo-topographic low beneath the tuffs, but the exact character of this feature is unknown. It may be a “strike valley” related to the Belted Range thrust fault.

The structure of the pre-Tertiary rocks is complex and poorly known, but it is important because the pre-Tertiary section is very thick and extensive, and includes units that form regional aquifers. The main pre-Tertiary structures in the RMSM model area are related to the east-vergent Belted Range thrust fault, which placed Late Proterozoic to Cambrian-age rocks over rocks as young as Late Mississippian [5, 6]. In several places along the western margin of Yucca Flat, east-vergent structures related to the Belted Range thrust were deformed by younger west-vergent structural activity [6]. This west-vergent deformation is related to the CP thrust fault, which also placed older Paleozoic-age carbonate rocks over younger Paleozoic-age rocks (commonly the Eleana formation or Chainman shale) [7].

More recent large-scale extensional faulting in the NTS area is significant because the resulting faults have profoundly affected the hydrogeology of the Tertiary volcanic units by controlling to a large extent their alteration potential and final geometry. In addition, the faults themselves may facilitate flow of potentially contaminated groundwater from sources in the younger rocks into the underlying regional aquifers. The major Tertiary-age faults trend largely north-northeast consistent with the modern maximum compressive stress direction. Rainier Mesa is not as heavily faulted as central Pahute Mesa to the west.

2.2 Geologic Overview of Shoshone Mountain

The U16a Tunnel complex, the only tunnel complex at Shoshone Mountain used for nuclear testing, is located in zeolitized ash-fall and ash-flow tuffs [8], similar in age and physical properties to the rocks that are found at the southern end of Rainier Mesa (e.g., U12g and U12e Tunnels). A simplified description of the geologic section at U16a includes from the top of the mesa:

- A welded tuff “caprock” of Tiva Canyon tuff approximately 15 m (50 ft) thick; moderately to densely welded and related bedded tuff of the Topopah Spring tuff about 150 m (450 ft) thick;
- A sequence of bedded, vitric ash-fall tuffs related to the Calico Hills formation, approximately 38 m (125 ft) thick; and another 335-m (1,100-ft)-thick sequence of zeolitized ash-fall and interbedded welded ash-flow tuffs related to the Tunnel formation and older tuffs [9, 10].

The pre-Tertiary section in the vicinity of Shoshone Mountain consists of up to 300 m (1,000 ft) of Tippipah limestone overlying several hundred to perhaps 1,000 m of Eleana formation/Chainman shale. The Eleana formation/Chainman shale conformably overlies the thick section of Paleozoic carbonate rocks that form the lower carbonate aquifer (LCA).

The structural geology of the U16a area is quite complex, with many faults and fractures found throughout the tunnel system. Fault displacements range from a few centimeters (inches) to more than 30 m (100 ft). The strata strike generally north-south, and dip to the west. The dip of bedding measured along the tunnels ranges from about 8 to 18 degrees, with an average dip of approximately 15 degrees. This general attitude is mirrored in the gravity-postulated pre-Tertiary surface, which also dips gently toward the west.

Several faults have been mapped at Shoshone Mountain but, in general, the structure is less well known there than at Rainier Mesa. Shoshone Mountain is located at the northern limit of more extended terrain to the south and adjacent to the Mine Mountain basin. This area is more disrupted by basin-range faulting than the Rainier Mesa area, and there is evidence that Shoshone Mountain is more heavily faulted as well. The tunnel complex is cut by several faults with more than 30 m (100 ft) of displacement, and the strikes of the larger-displacement faults are more variable in orientation.

A conservative interpretation of the large-displacement faults found at tunnel level would indicate at least the potential for additional surface faulting, and a large displacement fault was logged near the 152 m (500 ft) depth in core from UE16a#1, which can be easily projected to the surface. Also, post-test surface mapping following the last underground test in the U16a Tunnel complex revealed a rather lengthy north-south-striking fault with up to 1.0 m (3.3 ft) of displacement.

2.3 Hydrologic Setting

The hydrologic character of the NTS and vicinity reflects the region's arid climatic conditions and complex geology [11]. The hydrology of the NTS has been extensively studied for more than 50 years [12], and numerous scientific reports and large databases are available. The following subsections present an overview of the hydrologic setting of the NTS and vicinity, including summary descriptions of surface water and groundwater, hydrogeologic framework, and finally a summary of the hydrogeology for the RMSM area.

2.3.1 Surface Water

The NTS is located within the Great Basin, a closed hydrographic province that includes numerous closed hydrographic basins. In general, rivers and streams on the NTS are ephemeral and flow only in response to precipitation events or snowmelt. The runoff is conveyed through normally dry washes toward playa lakes in flats such as Yucca Flat and Frenchman Flat, where the majority evaporates. There is minor infiltration. With the exception of a few infrequent, short-duration flash floods in Fortymile Canyon, Fortymile Wash, and Topopah Wash, long-distance surface water flow has not been observed on the NTS [13].

A few minor springs emanate from local perched groundwater systems in the foothills surrounding Rainier and Aqueduct Mesa. Most water discharged from springs travels only a short distance from the source before evaporating or infiltrating into the ground.

2.3.2 Groundwater

The NTS is located within the Death Valley regional groundwater flow system, one of the major hydrologic subdivisions of the southern Great Basin [14, 15]. Groundwater in southern Nevada is conveyed within several flow-system sub-basins in the Death Valley regional flow system. A groundwater sub-basin is defined as the area that contributes water to a major surface discharge area [15]. Three principal groundwater sub-basins, named for their downgradient discharge areas, have

been identified within the NTS region: the Ash Meadows, Oasis Valley, and Alkali Flat-Furnace Creek Ranch sub-basins [14]. Rainier Mesa lies along the boundary between the Ash Meadows and Alkali Flat-Furnace Creek Ranch groundwater sub-basins. Shoshone Mountain is thought to lie within the western portion of the Ash Meadows groundwater sub-basin; however, it is close to the boundary, which is somewhat uncertain.

The groundwater-bearing rocks at the NTS have been classified into several aquifers and confining units, the largest of which is the LCA, a thick sequence of Paleozoic carbonate rock. This unit extends throughout the subsurface of central and southeastern Nevada, and is considered to be a regional aquifer [15-17]. Various volcanic aquifers (VAs) and alluvial aquifers (AAs) are also locally important as water sources. Groundwater chemistry ranges from a sodium-potassium-bicarbonate type to a calcium-magnesium-carbonate type, depending on the mineralogical composition of the aquifer source [18].

The depth to groundwater in wells at the NTS varies from about 210 m (690 ft) below the land surface under the Frenchman Flat playa in the southeastern NTS, to more than 760 m (2,500 ft) below the land surface beneath Shoshone Mountain at ER-16-1 [19]. Perched groundwater (isolated lenses of water lying above the regional groundwater level) occurs locally throughout the NTS, mainly within the volcanic rocks.

Recharge areas for the Death Valley groundwater system are the higher mountain ranges of central and southern Nevada, where there can be significant precipitation and snowmelt. Groundwater flow is generally from these upland areas to natural discharge areas in the south and southwest. Groundwater at the NTS is also derived from underflow from basins upgradient of the area [20]. The direction of groundwater flow may locally be influenced by structure, rock type, or other geologic conditions. Existing water-level data [21-23] and results of modeling groundwater flow [11, 17] indicate that the general groundwater flow direction within major water-bearing units beneath the NTS is to the south and southwest.

Most of the natural discharge from the Death Valley flow system is via transpiration by plants or evaporation from soil and playas in the Amargosa Desert and Death Valley rather than overland flow. Groundwater discharge at the NTS is minor, consisting of small springs that drain perched water lenses and artificial discharge at a limited number of water supply wells [16, 24].

2.4 References

1. National Security Technologies, LLC. 2007. *A Hydrostratigraphic Model and Alternatives for the Groundwater Flow and Contaminant Transport Model of Corrective Action Unit 99: Rainier Mesa-Shoshone Mountain, Nye County, Nevada*, DOE/NV/29546--146. Las Vegas, NV.
2. Sargent, K.A., and P.P. Orkild. 1973. *Geologic Map of the Wheelbarrow Peak-Rainier Mesa Area, Nye County, Nevada*. U.S. Geological Survey Miscellaneous Geologic Investigations Map 1-754, scale 1:48,000. Washington, DC.

3. U.S. Department of Energy, National Nuclear Security Administration Nevada Site Office. 2006. *Completion Report for Well ER-12-3*, DOE/NV/11718--1182. Prepared by Bechtel Nevada, Las Vegas, NV.
4. U.S. Department of Energy, National Nuclear Security Administration Nevada Site Office. 2006. *Completion Report for Well ER-12-4*, DOE/NV--1208. Prepared by Bechtel Nevada, Las Vegas, NV.
5. Cole, J.C. 1997. *Major Structural Controls on the Distribution of Pre-Tertiary Rocks, Nevada Test Site Vicinity, Southern Nevada*. U.S. Geological Survey Open-File Report 97-533, scale 1:100,000, 19 pp. Denver, CO.
6. Cole, J.C., and P.H. Cashman. 1999. *Structural Relationships of Pre-Tertiary Rocks in the Nevada Test Site Region, Southern Nevada*. U.S. Geological Survey Professional Paper 1607.
7. Caskey, S.J., and R.A. Schweickert. 1992. "Mesozoic Deformation in the Nevada Test Site and Vicinity: Implications for the Structural Framework of the Cordilleran Fold and Thrust Belt and Tertiary Extension North of Las Vegas." In *Tectonics*, v. 11, no. 6, pp. 1314-1331.
8. Davis, R.E. 1962. *Preliminary Report on the Geology of the U16a Tunnel, Nevada Test Site*. U.S. Geological Survey Technical Letter: Marshmallow-4.
9. Orkild, P.P. 1963. *Geologic Map of the Tippipah Spring Quadrangle, Nye County, Nevada*. U.S. Geological Survey, Quadrangle Map GQ-213, scale 1:24,000. Washington, DC.
10. Slate, J.L., M.E. Berry, P.D. Rowley, C.J. Fridrich, K.S. Morgan, J.B. Workman, O D. Young, G.L. Dixon, V.S. Williams, E.H. McKee, D.A. Ponce, T.G. Hildenbrand, W.C. Swadley, S.C. Lundstrom, E.B. Ekren, R.G. Warren, J.C. Cole, R.J. Fleck, M.A. Lanphere, D.A. Sawyer, S.A. Minor, D.J. Grunwald, R.J. Laczniaak, C.M. Menges, J.C. Yount, and A.S. Jayko. 1999. *Digital Geologic Map of the Map of the Nevada Test Site and Vicinity, Nye, Lincoln, and Clark Counties, Nevada and Inyo County, California*. U.S. Geological Survey Open-File Report 99B554BA, scale 1:120,000.
11. D'Agnese, F.A., C.C. Faunt, A.K. Turner, and M.C. Hill. 1997. *Hydrogeologic Evaluation and Numerical Simulations of the Death Valley Regional Groundwater Flow System, Nevada and California*. U.S. Geological Survey Water-Resources Investigations Report 96-4300, 133 pp. Denver, CO: U.S. Geological Survey.
12. U.S. Department of Energy, Nevada Operations Office. 1996. *Final Environmental Impact Statement for the Nevada Test Site and Off-site Locations in the State of Nevada*, DOE/EIS-0243. Las Vegas, NV.
13. U.S. Geological Survey. 2001. *Flooding in the Amargosa River Drainage Basin, February 23-24, 1998, Southern Nevada and Eastern California, Including the Nevada Test Site*. U.S. Geological Survey Fact Sheet 036-01.
14. Waddell, R.K., J.H. Robison, and R.K. Blankennagel. 1984. *Hydrology of Yucca Mountain and Vicinity, Nevada-California Investigative Results through Mid-1983*. U.S. Geological Survey Water-Resources Investigation Report 84-4267, 72 pp. Denver, CO.

15. Laczniaak, R.J., J.C. Cole, D.A. Sawyer, and D.A. Trudeau. 1996. *Summary of Hydrogeologic Controls on the Ground-water Flow at the Nevada Test Site, Nye County, Nevada*. U.S. Geological Survey Water-Resources Investigation Report 96-4109. Carson City, NV.
16. Winograd, I.J., and W. Thordarson. 1975. *Hydrogeologic and Hydrochemical Framework, South-Central Great Basin, Nevada-California, with Special Reference to the Nevada Test Site*. U.S. Geological Survey Professional Paper 712-C, 126 pp. Washington, DC.
17. IT Corporation. 1996. *Regional Geologic Model Data Documentation Package (Phase I, Data Analysis Documentation, Volume I, Parts 1 and 2)*, ITLV/10972--181. Las Vegas, NV.
18. Chapman, J.B. 1994. *Classification of Groundwater at the Nevada Test Site*. Desert Research Institute Report 45069, DOE/NV/10384-28.
19. U.S. Department of Energy, National Nuclear Security Administration Nevada Site Office. 2006. *Completion Report for Well ER-16-1 Corrective Action Unit 99: Rainier Mesa - Shoshone Mountain*, DOE/NV--1180.
20. IT Corporation. 1996. *Potentiometric Data Task Documentation Package (Phase I, Data Analysis Documentation, Volume II)*, ITLV/10972--181. Las Vegas, NV.
21. Reiner, S.R., G.L. Locke, and L.S. Robie. 1995. *Ground-Water Data for the Nevada Test Site and Selected Other Areas in South-Central Nevada 1992-1993*. U.S. Geological Survey Open-File Report 95-160.
22. Harrill, J.R., J.S. Gates, and J.M. Thomas. 1988. *Major Groundwater Flow Systems in the Great Basin Region of Nevada, Utah and Adjacent States*. Hydrological Investigation Atlas HA-694-C, scale 1:1,000,000. Denver, CO: U.S. Geological Survey.
23. U.S. Department of Energy, National Nuclear Security Administration Nevada Site Office. 2003. *Routine Radiological Environmental Monitoring Plan*, DOE/NV/11718--804. Prepared by Bechtel Nevada, Las Vegas, NV.
24. Hansen, D.J., P.D. Greger, C.A. Wills, and W.K. Ostler. 1997. *Nevada Test Site Wetlands Assessment*. Las Vegas, NV: Bechtel Nevada.

3.0 DATA COMPILATION AND ANALYSIS

As stated in [Section 1.0](#), this document strives to provide data to support the development of CAU-scale flow and transport modeling in the RMSM CAU. This section provides a general overview of each property presented in this document and a general overview of the methods used to determine the applicability of the data.

3.1 Data Types

3.1.1 Saturated Media Hydraulic Properties

Hydraulic properties are basic properties of a geologic medium that govern the flow of a fluid through it. Hydraulic conductivity describes the ease with which a saturated medium transmits water and is the primary hydraulic property for a steady-state groundwater flow model. Geologic media are heterogeneous with hydraulic properties that vary with scale. The objective of data analysis is to collate and evaluate representative hydraulic property parameter values within the context of the HFM discussed in [Section 4.0](#). This evaluation is preparatory to and supports analysis required for the CAU flow model, recognizing that the parameter data may be further modified as required for development of calibrated flow models. [Section 5.0](#) presents a detailed discussion of the analysis of hydraulic properties applicable to the RMSM HFM area.

3.1.2 Recharge from Precipitation

Precipitation recharge is the input of water to a flow system from areal precipitation. In the RMSM area, precipitation occurs primarily as rain and snow in high topographic areas. Uncertainty in recharge is addressed through the use of multiple methods to estimate precipitation recharge and inclusion of variance within some individual methods. Generally, the methods used to estimate precipitation recharge include some consideration of the loss of water that occurs due to evapotranspiration at the surface and shallow subsurface before the water is transported. [Section 6.0](#) presents a detailed discussion of the analysis of precipitation recharge for the RMSM area. The number of models presented here has been reduced from previous CAU modeling efforts to simplify modeling.

3.1.3 Groundwater Surface Discharge

Groundwater surface discharge accounts for processes that remove water from a flow system at the surface. In the RMSM area, the primary surface discharge processes are spring discharge, well discharge, and tunnel discharge. The spring discharge occurring in the area comes from several small springs close to the mesas producing very recently precipitated water. For the past 50 to 60 years,

water supply wells and test wells have withdrawn water from the aquifers around the NTS. In the Rainier Mesa area, tunnels mined into the mesa intercept perched water and drain it to the surface. In general, these tunnels behave like artificial springs; however, their production rate has fallen with time, and several have been plugged and no longer discharge to the surface. [Section 7.0](#) presents a detailed discussion of the analysis of groundwater discharge for the RMSM area.

3.1.4 Lateral Boundary Fluxes

Lateral boundary flux accounts for water that flows through the model area. For the RMSM model area, the surface and four vertical sides of the model formed the boundaries across which water flux was calculated. The bottom of the model was a no-flow barrier. There is no practical method to directly measure groundwater fluxes at the scale and spatial frequency needed to represent the conditions at the CAU flow-model boundary so lateral boundary fluxes are calculated by evaluating flow across the boundaries of the RMSM model in the larger regional Death Valley Regional Flow System (DVRFS) model [1]. Uncertainty is characterized through the use of calibrated alternative models. [Section 8.0](#) presents a detailed discussion of the lateral boundary flux analyses for the RMSM CAU model area.

3.1.5 Hydraulic Head

Hydraulic head provides the state of hydraulic potential throughout a saturated media flow system. Hydraulic head is a spatial potential field and varies both laterally and vertically. In the RMSM area, hydraulic heads are provided by measurements of water levels in wells. Uncertainty in the representativeness of individual well completions is addressed through examination of the temporal trends in measurements as well as other factors that may have influence on the water levels. In general, there are more wells and hydraulic head measurements in the vicinity of underground testing. [Section 9.0](#) presents a detailed discussion of the hydraulic head analyses for the RMSM CAU model area.

3.1.6 Temperature Data

Water temperature provides the state of thermal potential throughout a saturated media flow system. In the RMSM area, temperature data are provided by vertical temperature logs in groundwater wells and temperature measurements of spring discharge. Where temperature gradients exist, temperature data have several uses in evaluating flow in saturated media. Hydraulic conductivity and hydraulic head are both dependent on fluid density, which varies with water temperature. Heat can also be used as a tracer in groundwater flow systems to characterize flow direction and magnitude, because advection generally transports heat more readily than conduction in such systems. In general, temperature measurements tend to be highly accurate; however, the natural temperature distribution in a groundwater well can be disturbed by intra-well flow and other processes. [Section 10.0](#) presents a detailed discussion of the temperature data for the RMSM CAU model area.

3.2 Data Quality

Data provided in this report have been collected over the past 50 to 60 years for a variety of purposes. The measurement methods and quality of documentation for different datasets included in this report vary. Where data of varying quality are used together, the data are evaluated in the framework outlined in the UGTA Quality Assurance Project Plan (QAPP) [2] and further refined in the UGTA data transferability document [3]. When datasets are not combined or directly comparable, the nature of the dataset is discussed in the text.

3.3 Data Transferability

The RMSM area covers a large geographic area. Data points are not available uniformly across the model area for all the data types examined in this report. To develop property distributions, it is necessary to transfer data from other areas where it is reasonable to assume that properties are similar.

Geologic similarity is the primary basis for transferring properties from one area to another for the data types examined in this document. The HFM [4] generally provides the framework used to determine geologic similarity, although it is used in different ways for different data types. The UGTA data transferability document [3] discusses a number of the factors that affect data transferability, such as rock type, structural history, and alteration. The importance of a given factor to the transfer of a data type varies, so the methods used to transfer data types are discussed in the section with each data type.

3.4 References

1. Belcher, W.R., J.B. Blainey, F.A. D'Agnesse, C.C. Faunt, M.C. Hill, R.J. Laczniak, G.M. O'Brien, C.J. Potter, H.M. Putnam, C.A. San Juan, and D.S. Sweetkind. 2004. *Death Valley Regional Ground-Water Flow System, Nevada and California - Hydrogeologic Framework and Transient Ground-Water Flow Model*, Scientific Investigations Report 2004-5205. U.S. Geological Survey.
2. U.S. Department of Energy, National Nuclear Security Administration Nevada Site Office. 2003. *Underground Test Area Quality Assurance Project Plan, Nevada Test Site, Nevada*, DOE/NV--341-REV. 4. Las Vegas, NV.
3. Stoller-Navarro Joint Venture. 2004. *Transferability of Data Related to the Underground Test Area Project, Nevada Test Site, Nye County, Nevada*, Rev. 0, S-N/99205--020. Las Vegas, NV.
4. National Security Technologies, LLC. 2007. *A Hydrostratigraphic Model and Alternatives for the Groundwater Flow and Contaminant Transport Model of Corrective Action Unit 99: Rainier Mesa-Shoshone Mountain, Nye County, Nevada*, DOE/NV/29546--146. Las Vegas, NV.

4.0 RMSM HYDROSTRATIGRAPHIC FRAMEWORK AND HSU MINERALOGY

A three-dimensional (3-D) HFM and alternatives for the RMSM CAU were constructed in 2007 and are documented in the report *A Hydrostratigraphic Model and Alternatives for the Groundwater Flow and Contaminant Transport Model of Corrective Action Unit 99: Rainier Mesa-Shoshone Mountain, Nye County, Nevada* [1]. This section gives a brief overview of the model and describes how it relates to data compiled in this report. Detailed information about the HFM can be found in the original report. Most of the data types in this document are analyzed in the context of the HFM and it is recommended that users familiarize themselves with the original HFM report.

4.1 RMSM HFM

The HFM provides the 3-D framework for flow and transport models. The base RMSM HFM incorporates numerous structural elements, including volcanic calderas, thrust faults, and 56 basin-and-range normal faults. The foundation of the model is the hydrostratigraphic system. The RMSM hydrostratigraphic classification system was developed through the rigorous evaluation and analysis of stratigraphic, lithologic, and alteration data from surface exposures and drill holes in and around the RMSM model area. The RMSM hydrostratigraphic system includes 44 hydrostratigraphic units (HSUs) that form individual 3-D volumes in the model. The boundaries of the HFM in relation to the CASs are shown in [Plate 1](#).

The RMSM HFM consists of five models: a base HFM and four alternative HFMs. These alternative models are generally alternative structural interpretations of the geology and can contain HSUs not present in the base model. A detailed explanation of the differences between the base model and the alternatives is provided in Section 5.0 of the RMSM HFM report [1]. The four alternative models are:

- No Redrock Valley Caldera
- More Extensive LCA3
- Shoshone Mountain Thrust Sheet
- LCA3 at Bottom of ER-12-1

4.1.1 Hydrogeologic and Hydrostratigraphic Units of the RMSM HFM

The RMSM HFM classifies rocks hydrologically using a two-level classification scheme: hydrogeologic units (HGUs) and HSUs [1-5]. Descriptions of the HGUs and HSUs in the RMSM HFM are given in Tables 4-3 and 4-4 of the HFM report [1].

The HGUs categorize rocks according to their ability to transmit groundwater (i.e., aquifers or confining units), which is a function of a primary lithologic properties such as rock type, degree of fracturing, and mineral alteration. The rocks of the RMSM model area are classified as one of the following nine HGUs: alluvial aquifer (AA), welded-tuff aquifer (WTA), vitric-tuff aquifer (VTA), lava-flow aquifer (LFA), tuff confining unit (TCU), intra-caldera intrusive confining unit (IICU), granitic confining unit (GCU), clastic confining unit (CCU), and carbonate aquifer (CA). A spreadsheet table of HGUs with descriptions is included in the RMSM_HFM.xls workbook in the Appendix\A folder on the DVD accompanying this report.

Adjacent stratigraphic units with the same HGU type are grouped into larger HSUs to facilitate mapping and 3-D model construction. For the RMSM model, most HSUs consist of a single HGU (e.g., the Timber Mountain lower vitric-tuff aquifer [TM-LVTA] essentially is 100% VTA). There are eight exceptions that may consist of several HGUs but are defined so a single general type of HGU dominates (e.g., mostly WTA). These exceptions are the Fortymile Canyon composite unit (FCCM), Timber Mountain upper vitric-tuff aquifer (TM-UVTA), Timber Mountain welded-tuff aquifer (TM-WTA), Timber Mountain composite unit (TMC), Rainier Mesa breccia confining unit (RMBCU), Redrock Valley breccia confining unit (RVBCU), Stockade Wash aquifer (SWA), and Topopah Spring aquifer (TSA). A full list of the HSUs in the base RMSM HFM with brief descriptions is included in the RMSM_HFM.xls workbook in the Appendix\A folder on the accompanying DVD.

4.2 HFM Model Overview

The geology of the RMSM HFM, like most of the Basin and Range province, is complex. However, there are a few generalities that can be applied to the model. The LCA is the principal aquifer in the model and modeled at a thickness of up to 4,000 m. The LCA is present throughout the entire model area with the exception of those areas containing intrusive HSUs. These exceptions are the Mesozoic granite confining unit (MGCU), Silent Canyon intrusive confining unit (SCICU), Redrock Valley intrusive confining unit (RVICU), Calico Hills intrusive confining unit (CHICU), Rainier Mesa intrusive confining unit (RMICU), and Ammonia Tanks intrusive confining unit (ATICU). The lower clastic confining unit (LCCU) is a siliciclastic confining unit below the LCA.

The LCA is covered by another clastic confining unit, the upper clastic confining unit (UCCU), in all but the southeast corner of the model area. The thickness of the unit varies but is generally 500 to 1,000 m thick in most of the model area. The lower carbonate aquifer-thrust plate (LCA3) is a thrust sheet of LCA stratigraphic units that is on top of the UCCU in the northeastern and eastern part of the model, and directly on top of the LCA in the southeast part of the model.

The Paleozoic units (LCA, LCA3, UCCU, LCCU, lower clastic confining unit-thrust plate [LCCU1], and upper carbonate aquifer [UCA]) are capped by a section of Tertiary volcanic HSUs. With some exceptions, the bottom units are TCU HGU dominated. These exceptions are the Twin Peaks aquifer (TPA), Redrock Valley aquifer (RVA), Tub Spring aquifer (TUBA), lower vitric-tuff aquifer 1 (LVTA1), Belted Range aquifer (BRA), lower vitric-tuff aquifer 2 (LVTA2), and SWA. The Tertiary volcanic units are generally thinner and less continuous than the Paleozoic units.

Section 4.0 of the RMSM HFM report contains detailed descriptions and block diagrams that better illustrate the location, extent, and relationships of the HSUs in the model [1]. Several large cross sections are included in Appendix C of the HFM report. The files included in the Appendix\A folder on the accompanying DVD also include these block diagrams, cross sections, and spreadsheets with HGU and HSU descriptions in reorganized, more user-friendly formats.

4.3 References

1. National Security Technologies, LLC. 2007. *A Hydrostratigraphic Model and Alternatives for the Groundwater Flow and Contaminant Transport Model of Corrective Action Unit 99: Rainier Mesa-Shoshone Mountain, Nye County, Nevada*, DOE/NV/29546--146. Las Vegas, NV.
2. IT Corporation. 1996. *Regional Geologic Model Data Documentation Package (Phase I, Data Analysis Documentation, Volume I, Parts 1 and 2)*, ITLV/10972--181. Las Vegas, NV.
3. Bechtel Nevada. 2002. *A Hydrostratigraphic Model and Alternatives for the Groundwater Flow and Contaminant Transport Model of Corrective Action Units 101 and 102: Central and Western Pahute Mesa, Nye County, Nevada*, DOE/NV/11718--706. Las Vegas, NV.
4. Bechtel Nevada. 2005. *A Hydrostratigraphic Model and Alternatives for the Groundwater Flow and Contaminant Transport Model of Corrective Action Unit 98: Frenchman Flat, Clark, Lincoln, and Nye County, Nevada*, DOE/NV/11718--1064. Las Vegas, NV.
5. Bechtel Nevada. 2006. *A Hydrostratigraphic Model and Alternatives for the Groundwater Flow and Contaminant Transport Model of Corrective Action Unit 97: Yucca Flat-Climax Mine, Lincoln and Nye Counties, Nevada*, DOE/NV/11718--1119. Las Vegas, NV.

5.0 SATURATED MEDIA HYDRAULIC PROPERTIES

Representative hydraulic property values at the scale of model discretization for the formations modeled are required to produce defensible groundwater flow model predictions. This criterium guided the analysis and is the basis for evaluating the results. Statistical analysis of available hydraulic parameter data produced estimates for the range and distributions of hydraulic parameter values for the formations in the RMSM CAU. This section primarily addresses hydraulic conductivity, the depth dependence of hydraulic conductivity, and specific storage.

The RMSM HFM is complex with many HSUs of similar HGU character. The data were aggregated by HGU-based characterization groups (CGs) for data transfer and statistical analysis. There are very few RMSM CAU-specific data. Those that are available do not provide specific data for all CGs or sufficient data to determine statistics for those CGs for which data exist. Data specific to the RMSM CAU (RMSM HFM area) were analyzed to the extent possible. To obtain datasets of statistically relevant size, analysis was conducted for all data in the NTS Data Compilation Area (Section 5.1) using additional transferred data. The analysis considers three scales of measurement: pumping test, slug test, and laboratory scale. Discussion includes uncertainties in the data; uncertainty in the analysis regarding scale; and other characteristics of hydraulic properties for which data are very limited, such as the spatial variation of properties, anisotropy, and uncertainty due to temperature variation.

5.1 Data Compilation and Evaluation

The UGTA Project maintains a database of hydraulic property analyses for various hydraulic tests and testing activities for the NTS and nearby surrounding area, referred to as the “NTS Data Compilation Area.” The boundary of the data compilation (Figure 5-1) is defined as (Universal Transverse Mercator [UTM] Zone 11 North American Datum [NAD] 27 [m]):

- N 4,150,000 (just north of the NTS into adjacent valleys)
- S 4,035,000 (south of U.S. 95, including the Nye County Early Warning Drilling Program wells and Amargosa Desert wells)
- E 630,000 - 650,000 (east to include the Watertown wells and Indian Springs Valley wells)
- W 520,000 (just west of U.S. 95 and Beatty, including Oasis Valley wells)

The database contains hydraulic parameter values compiled for interpretations of aquifer, packer and slug tests, laboratory permeability tests, and grain-size analyses. Included are supporting information for each test on the well, test parameters, stratigraphy and lithology for the borehole, the type of analysis, and the data source. The data compilation was updated from Section 6.0 of the previous Yucca Flat/Climax Mine (YFCM) Phase I HDD analysis, with additional data from recent UGTA testing activities as well as several corrections to existing entries [1].

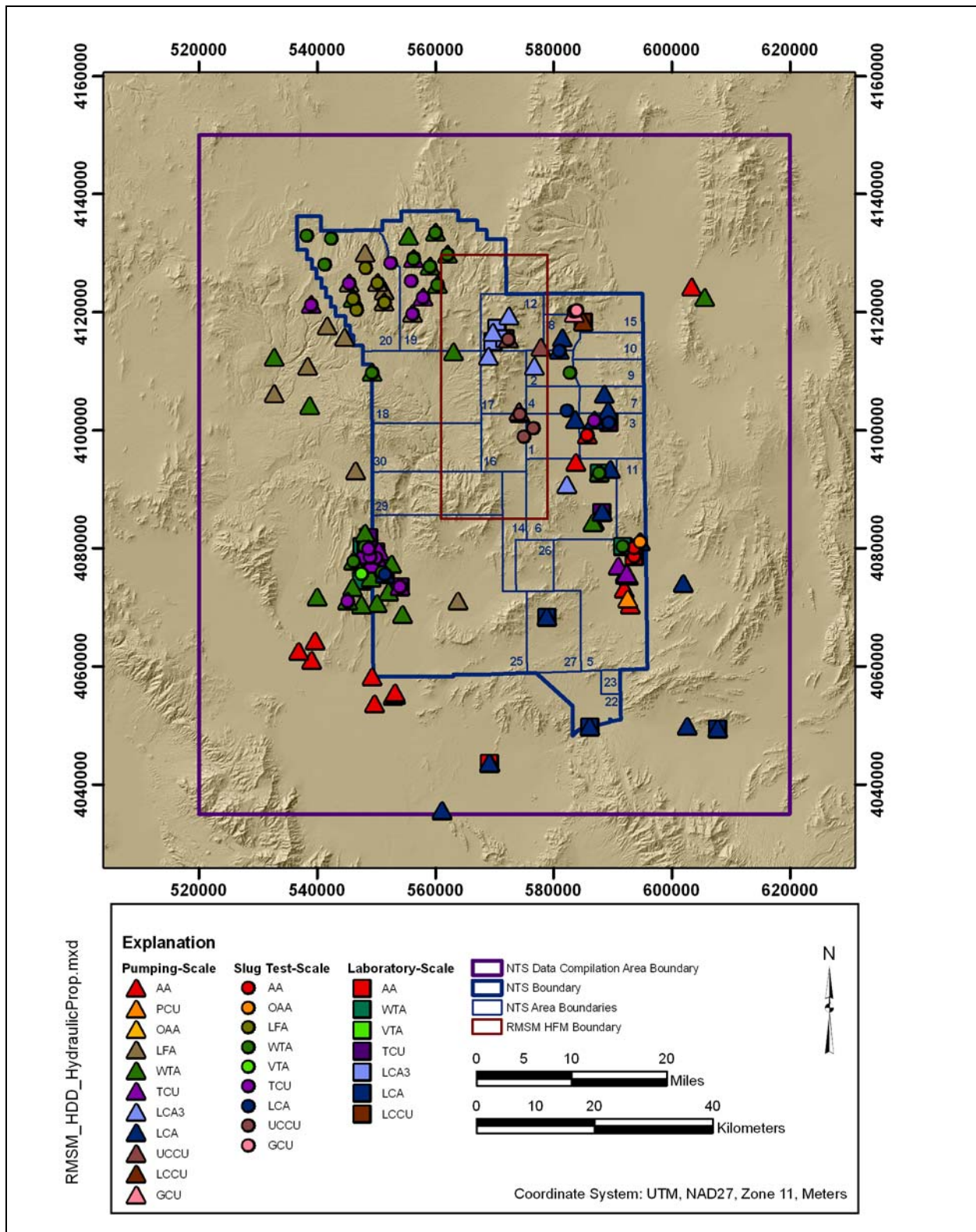


Figure 5-1
NTS Data Compilation Area Hydraulic Property Data Locations

5.2 Data Sources

Hydraulic property data were obtained from published and unpublished sources. Published data were obtained from reports of a large number of organizations that have worked on the NTS and in the surrounding area. Publications providing hydraulic parameter values may or may not include the raw and/or reduced drawdown and/or recovery data and specifics for the interpretation. An effort was made to acquire full documentation for each test; the extent of documentation acquired is reflected in the data documentation evaluation flag (DDE_F) qualifiers, discussed in [Section 5.3](#). Specific references for data sources are recorded in the database. Unpublished data and interpretations from the Desert Research Institute (DRI), the USGS, and the Environmental Restoration (ER) Contractor files are also included in the database. Unpublished data are evaluated and incorporated into the analyses according to the same quality assurance (QA)/quality control procedures as published data. Copies of all original data sources used for analysis are housed in the ER Contractor Central Files, Library, and/or electronic library.

5.3 Data Quality Evaluation

Data quality for the hydraulic parameter data was judged by the contribution of the data to the representativeness of the derived parameter characterization within the context of the flow model. Two very different aspects of this criterion that are specifically addressed in this analysis are scale of measurement and analysis uncertainty. These are difficult to assess and quantify.

The scale of measurement is addressed at a basic level in the statistical analysis of the data by grouping and analyzing the data for three different general scales of measurement that are distinguished primarily by test types: pumping tests, slug tests, and laboratory tests. While this does not closely relate the scale of each measurement to the discretization scale or zonation scale of the flow model, it provides a breakdown that approximates the different scales of parameters as they may be applied in modeling. The information on hydraulic properties at the various scales of measurement can be used to infer or construct appropriate equivalent hydraulic property values for the model scale. The approach to scaling this characterization to the flow model will depend upon the nature of the flow model and is not addressed.

The appropriateness of the analytical model and assumptions used for analysis of hydraulic tests is a significant uncertainty in the determination of property values. Selection of these by the analyst is dependent upon available site-specific information, background knowledge, test data collected, and the analytic intent. Coordinated evaluation of the dataset of tests may produce different conclusions than independent evaluations of individual tests. Analytic model(s) used for analysis should also coordinate with the flow model conceptualization. Analysis of a test is greatly influenced by the conceptual model for the test, which in turn is influenced by the form of the test response. Interpretation of the response form depends upon the length of the test (revealing different characteristics at varying time scales), the detail of the observed response, and knowledge of physical and structural characteristics of the tested formations.

A particular analysis uncertainty examined in this section is between single- and dual-porosity analyses of LCA pumping tests. The full dataset compiled includes analyses based on both single- and dual-porosity analytic models, depending upon the interpretation of the analyst. The use of all types of analyses captures the full extent of analysis uncertainty but results in apparent variability that is not necessarily appropriate relative to the flow model conceptualization. However, reinterpretation of all tests within the conceptual framework of CAU-specific flow models has not been pursued. An example of the effect of such reinterpretation is presented in [Section 5.15.2](#). The appropriateness of the assumptions used in the interpretation is a matter of specific test knowledge (and supporting information collected during testing), broad knowledge of the hydrogeology, and coordination with the flow model. The quality of the analysis regarding methodology and model fitting is most amenable to direct evaluation, but is generally a relatively minor factor. These considerations are further discussed in [Section 5.8](#).

It has been judged that the most inclusive statistics incorporating analysis uncertainty best meet analysis objectives to quantify variability with uncertainty, rather than only using the highest quality, but very limited data. The evaluation of the quality of tests and analyses has many aspects, some of which are substantially subjective. All data in the database were considered suitable for this approach. In cases where there were many data values for a CG, the statistical analysis is expected to provide a good estimate of the mean and preclude the undue influence of any particular data value. In cases where there were few data for a CG, there is an insufficient basis to identify questionable data. Consequently, data quality evaluation flag (DQE_F) levels were not assigned to the hydraulic property data, and all data were used with equal weight. This approach, while not the norm, is consistent with the UGTA QAPP [2] as an alternate regarding the type and intended use of the data.

5.4 Hydraulic Property Characterization Groups

The hydraulic properties of the formations in the RMSM HFM area have been characterized within general categories of distinct hydrogeologic character, CGs, that can be directly related to the geologic model structure upon which the flow model structure will be based. The geologic model (HFM) is discussed in detail in Section 4.0 of the RMSM HFM document [3]. The RMSM HFM is composed of HSUs, which are units of generally consistent hydrogeologic character that are defined by stratigraphic position. The HSUs are stratigraphic units comprising rocks of primarily one dominant HGU. The HGU properties can be characterized based on the summary characteristics of all HSUs with a common dominant HGU. In some cases, HGU distinctions also are made for intervals within HSUs with distinctly different hydrogeologic character [3]. For example, the TM-WTA HSU describes a stratigraphically defined rock unit that is predominantly welded tuff at the scale of the stratigraphic unit. In some locations, this HSU may adjoin other welded tuff HSUs that all belong to the WTA HGU. However, within the TM-WTA, there are intervals of vitric tuff that correlate to the VTA HGU. In this case, the overall character of the TM-WTA HSU is determined by the dominant welded tuff component, which is most prevalent and most hydraulically conductive. The HGU distinctions within HSUs were accounted for in assigning data to CGs.

The hydraulic property CGs shown in [Table 5-1](#) were used for the hydraulic property analyses. These categories are primarily HGUs, with three of the HGUs subdivided by HSU distinctions. Where

Table 5-1
Hydraulic Property Characterization Groups

| CG | Title | HGU |
|------|------------------------------|------|
| AA | Alluvial Aquifer | AA |
| OAA | Older Alluvium | AA |
| PCU | Playa Confining Unit | AA |
| LFA | Lava-Flow Aquifer | LFA |
| WTA | Welded-Tuff Aquifer | WTA |
| VTA | Vitric-Tuff Aquifer | VTA |
| TCU | Tuff Confining Unit | TCU |
| LCA3 | Overthrust Carbonate Aquifer | CA |
| LCA | Lower Carbonate Aquifer | CA |
| UCCU | Upper Clastic Confining Unit | CCU |
| LCCU | Lower Clastic Confining Unit | CCU |
| GCU | Granite Confining Unit | IICU |

possible, HSU distinctions were maintained for application to flow modeling where these HSUs are discretely modeled. The AA HGU is subdivided by the HSU distinctions of AA, older alluvium (OAA), and playa confining unit (PCU). The CA HGU is subdivided into the LCA (the regional carbonate aquifer, which includes the LCA3 of the CP thrust in Yucca Flat) and the LCA3 (the overthrust carbonate aquifer in RMSM, including the UCA). The CCU HGU is subdivided into the UCCU and the LCCU. These HSU distinctions generally reflect differences in the distributions of property values. The differences are due to the variation in physical properties attributed to the distinct HSUs, such as the degree of fracturing and the condition of the fractures.

5.5 Assignment of Data to Characterization Groups

The hydraulic property values most appropriate for use in flow models are primarily determined from large-scale *in situ* hydraulic tests that commonly test long vertical intervals. Such long test intervals may span more than one HSU and often include intervals of more than one HGU. Generally, there is no specific test information available to separately determine properties for different HGU intervals occurring within the test interval when there are more than one. Specifically, the hydraulic response in a well is an average weighted by the differing transmissivities of each HGU in the test interval, and further modified by well hydraulics. The simplest approach to assign the hydraulic conductivity from a test analysis to a CG is to attribute the test to the CG with the greatest transmissivity. This would typically be the CG that has the greatest mean hydraulic conductivity (K). For test intervals with combinations of VA HGUs, they were ordered as WTA>LFA>VTA. However, the relative lengths of different HGU intervals in the test interval were taken into account when the most conductive HGU interval (dominant HGU) does not constitute a high proportion of the interval length.

Test intervals were assigned a top and bottom depth, which are within the completed interval, and a length. The top and bottom depths correspond to the uppermost and lowermost extent of the dominant HGU intervals within the assigned HGU. The assigned test interval defines the portion of the formation considered to be represented by the test results. The top/bottom depths are used to assign the hydraulic conductivity value to the midpoint depth of the interval for determination of the depth-decay function. The test interval length, the total length of the dominant HGU intervals within the top and bottom depth, is used in conjunction with the transmissivity determined from the test analysis to calculate the hydraulic conductivity for that test analysis. When multiple HSU intervals within the open formation interval contain different proportions of high-conductivity HGUs (WTA/VTA/LFA), the proportions of each HGU were determined by summing lengths for each HGU using the typical percentage for each HGU within the HSU. This situation occurs mainly in the volcanic formations of the Pahute Mesa/Oasis Valley (PMOV) area. Non-dominant high-conductivity HGU interval lengths were also included in the total test interval length.

In a substantial number of cases, test intervals contained almost equal parts WTA and LFA, and the test was attributed to the WTA per the specified ranking. However, the distinction between the WTA and the LFA is poor due to this situation. It was also found that there were no pumping-scale data for test intervals in which the VTA was dominant. Short intervals of VTA are found in some test intervals where the WTA or the LFA are dominant, and the length of those intervals was included in the total length.

The CG assignments for the UCCU data were re-evaluated, and most data were reassigned to LCA3 based on the actual formation type tested. The LCA3 is not mapped in the HFM in the completion interval for those wells due to the small scale of the formation type.

5.6 Data Transfer

Data transfer concerns the use of hydraulic property data for the NTS Data Compilation Area outside of the RMSM HFM area to characterize the HSUs within the RMSM HFM area. Considerations and requirements for data transfer are presented in the UGTA data transferability document [4]. The basis for transfer of hydraulic testing data has been addressed by characterizing at the HGU level with the HSU distinctions that are important. While only some HSUs are continuous from the RMSM HFM area into adjacent CAUs, at the HGU level, formation classifications are common throughout the NTS as defined for all CAU HFMs. The HSU(s) within the tested formation interval for each analysis were determined using the drill-hole database for each CAU HFM, and the HSU(s) were then cross-referenced to HGUs (Section 5.5). Consideration of hydrogeologic character is embodied in HSUs and HGUs, as described in the RMSM HFM document [3]. While data transfer necessarily generalizes the characterization, the lack of data for specific RMSM HFM area characterization required the generalization to capture the potential variability. Because of the limited amount of RMSM-specific information, transfer of information from other areas is required, resulting in greater uncertainty in parameter values.

The analysis was conducted for datasets for both the NTS Data Compilation Area and RMSM-specific HFM area. Note that the RMSM and NTS Data Compilation datasets for LCA3 and

UCCU are the same and, consequently, the NTS Data Compilation dataset analysis results are appropriate for use in the RMSM CAU. The only other RMSM-specific dataset was for the WTA CG. The RMSM-specific dataset was tested with respect to the NTS Data Compilation Area dataset for inconsistency, which is discussed in [Section 5.10](#).

5.7 Spatial Distribution of Data

[Figure 5-1](#) shows the locations of the wells and boreholes for which there are hydraulic parameter data within the RMSM area. The locations are identified with three different symbols corresponding to the three test scales. The categorization category nomenclature is presented in [Table 5-1](#). In some cases, data at more than one test scale are available for a single location. The data are not uniformly distributed throughout the NTS Data Compilation Area. Rather, the data are clustered in areas on the NTS where underground nuclear testing was performed, major construction facilities were located, or where ER drilling and testing activities have taken place. Off the NTS, data are generally located in areas of human settlement and activity, or in areas that are of interest due to the presence of natural resources. Note the cluster of data on the southwestern border of the NTS associated with the YMP. As shown on the map, a relatively small number of locations with hydraulic property data are available for the RMSM CAU.

5.8 Hydraulic Conductivity

Transmissivity (T) is the bulk hydraulic property determined from a field-scale test characterizing groundwater flow in a formation. Hydraulic conductivity (K), or intrinsic permeability ([k], hereafter referred to as permeability) in the case of flow models that include temperature, is the hydraulic parameter used to simulate steady-state groundwater flow. Transmissivity is conceptually defined as the product of hydraulic conductivity and transmissive thickness, and is related to numeric flow models as the product of nodal K values and node spacing. Hydraulic conductivity is calculated from the transmissivity determined for a test using an assumed transmissive thickness for that part of the formation that determined the response to a test. The appropriate thickness depends upon a number of factors which may not be well determined for a field test. Matching the calculation of hydraulic conductivity to the application of the value in the flow model requires consideration of interpretation and scaling issues. At the laboratory scale, the dimensions of the test volume are controlled, and hydraulic conductivity can be specifically determined for the sample tested.

Hydraulic conductivity varies with location within a rock unit and is necessarily averaged over the volume of rock tested. The value determined for K depends on the particular volume of rock tested (i.e., location, completion depth interval, and radius of influence). Hydraulic conductivity variability can be the result of spatial variation. Different test types or test specifications can also produce different results at any particular location as a function of the scale of the test (i.e., the specific volume of rock tested). When the subject rock type (HGU across the area of interest) is very extensive, only a small percentage of the total volume of the subject unit is typically characterized. Conducting many tests at different locations or of different volumes within a particular rock type (defined by CGs for this analysis) produces a range of K values that characterize the variability of the property inclusive of both location and scale variability.

A parametric probability model for the test parameter values can be used to define a probability density function (PDF) for the data. The distribution fitted to the data can be used to constrain the fitting of generalized values for hydraulic conductivity. Comparison of the parameter values used for HGUs in the calibrated flow model to the PDFs of test values for the CGs can provide confidence in the appropriateness of the calibrated values.

5.8.1 Scales of Test Data and Applicability

The scale of a test is an important factor for the representativeness of the test result for use in modeling. Hydraulic properties representative of the scale of discretization of the flow model are most appropriate. Values representative of smaller scales of measurement do not capture the hydrologic features present at the discretization scale of the flow model such as the average effect of fracturing variability on the overall properties. In fractured rocks, the smaller scale test data may reflect the extremes of fracturing variability or may only represent unfractured matrix properties. The data were analyzed in separate groups for the three distinct scales of tests as follows:

- Pumping-scale tests assess hydraulic properties representative of the greatest aquifer volume and are more likely to reflect high hydraulic conductivity structures in tested formations.
- Slug-test-scale tests (including packer tests) provide information for much smaller volumes of formations (both vertical interval and radius) and are more affected by local variability.
- Laboratory-scale tests provide data only somewhat applicable to unfractured and/or granular media formations, and for matrix properties of fractured formations.

Pumping-scale tests in the database were conducted with a wide range of specifications for test interval lengths, pumping rates, and durations. These factors as well as the formation hydraulic properties affect the volume of formation tested. An estimate of the radius tested for each test can be made based on assumptions about the formation tested and the test analysis results. However, the uncertainty is difficult to quantify, and the number of tests with test volumes closely matching the model discretization would be small. Consequently, all pumping-scale tests were grouped as the “large-scale” dataset. Pumping-scale tests have an associated scale as a function of the test duration and the hydraulic properties of the formation tested. Generally, the largest scale that the available test data represent is on the order of the flow model discretization. There are limited larger-scale data available, but they generally include effects of structures (faults) that are included in flow models discretely and, consequently, may not provide appropriate hydraulic properties for equivalent porous media representation of entire formations.

Slug- and packer-test scale tests were also conducted with a wide range of operational specifications. These methods test a relatively small volume of rock in the immediate area of the borehole, and the results may be substantially influenced by near-borehole conditions both reflecting local variability in the formations and effects from well drilling and completion. The results are also very dependent upon appropriate test specifications relative to formation hydraulic properties.

Laboratory-scale data comprise measurements made on small samples in a test apparatus in the laboratory. Samples may be chosen as representative for a particular purpose, but the rock/core samples tested are representative of very small formation volumes that necessarily exclude natural variability and important hydrologic features such as fractures. Measurements generally represent the hydraulic conductivity of the intact matrix, which may be appropriate for certain uses such as for modeling of matrix flow processes (i.e., matrix diffusion).

5.8.2 Test Analyses and Associated Uncertainties

Uncertainties related to the analysis of tests include the limitations of the test method, the test measurement accuracy, appropriateness of the analysis model, and assumptions made about the test and interval tested. The analysis of a field test is highly interpretive because these factors are difficult to determine and assess the associated uncertainty. In particular, the selection of the analysis model and the assumptions made about the tested formation interval can result in variation of hydraulic property values of an order of magnitude or more, in some cases, for the same test. Analysis uncertainty is difficult to quantify and is not readily separable from the variability described by the parametric probability model. The total uncertainty resulting from these factors may be substantial and increases the apparent variability. This is evidenced in cases where several different analyses of the same test, or analyses of different tests on the same well, produced very different results. [Section 5.15](#) provides a view of the difference between the analysis uncertainty of the complete dataset for the LCA and the imposition of a consistent analysis model and assumptions. [Section 5.16](#) discusses the change in the 95% confidence intervals between the NTS Investigation Area YFCM hydraulic property analysis and the NTS Data Compilation Area RMSM analysis due to the revision of the method for assignment of CGs, as discussed in [Section 5.5 \[1\]](#).

5.9 Analysis of Hydraulic Conductivity Data

The K data were separately analyzed at the pumping-scale, slug-test-scale, and laboratory-scale data. A more detailed review of the pumping-scale data is presented because these data are most relevant for use in large-scale modeling.

5.9.1 Multiple Test Results for One Well

Several situations can result in multiple test analysis results for a single well. First, there may be multiple analyses of a single test including analyses by different analysts, different analysis models applied to a test, or variations of assumptions made for a particular test analysis. Second, there may be multiple independent tests conducted in a well, usually with different test parameters. Third, there may be multiple test intervals for a well resulting from changes in the well completion or test interval for multiple tests, or different interpretations of the test interval. To characterize the variability of hydraulic conductivity within the context of the relationship of the HFM to the flow model, location and tested formation interval (as defined by the formation access interval [FAI] and HFM HSUs) were used to determine “independent” measurements. That is, where there were multiple results for the same well and the same transmissive interval, multiple K values were averaged (arithmetic average of K, assuming a normal distribution of errors is most likely) for the multiple tests and

analysis models used. This assumes that the variability represents testing and analysis uncertainty. However, different tested intervals were treated as independent results because the particular volume of formation tested, as embodied in the analysis (tested interval thickness, conceptual/analytic model), was interpreted to be different.

5.9.2 Methodology

The hydraulic test analysis database contains information on hydraulic tests and test analyses as reported in the data sources. The data are typically reported in a variety of units, and for several forms and variations of properties such as transmissivity or hydraulic conductivity, fracture and matrix hydraulic conductivity, and storativity or specific storage. For this analysis, these data were converted to a common basis. As discussed earlier, the primary analysis result is transmissivity, and hydraulic conductivity is calculated based on the assumed transmissive thickness. Where hydraulic conductivity was reported, the reported test interval length was used to back-calculate transmissivity, and hydraulic conductivity was then recalculated from the recalculated transmissivity using the revised test interval length. This was also done for specific storage (Section 5.14). The data were sorted by test scale and CG. Multiple values for a location and interval were averaged (arithmetic average, assuming a normal distribution for error), $\log_{10} K$ was calculated, and statistics for each dataset computed. The individual CG datasets were tested for conformity of the $\log_{10} K$ data to a normal distribution (lognormal distribution of K) using the Kolmogorov-Smirnov (K-S) test.

5.10 Analysis Results

The results for all of the CGs are presented in this section in tables and summary figures. The CG-specific figures for K distributions and depth decay can be found in Appendix B for CGs for which there were sufficient data to determine distributions. These figures show the data used to determine the distribution, the fitted distribution, and the 95% confidence bounds of the distribution. Table 5-2 presents a summary of the analyses of RMSM-specific K data, and Table 5-3 presents a summary of the analyses of all K data within the NTS Data Compilation Area. The column labeled “Count” indicates the number of data values (unique as to location and vertical interval) used to determine the statistics for each CG. In the last two columns, “Number of Entries” indicates the total number of test analyses for each CG (includes multiple analyses of a test and multiple tests at a well), and the “Number of Wells” indicates the number of different wells for which there were test analyses. The standard deviation of the mean of the population was estimated at the 95% confidence level. To indicate that the result of the K-S test did not reject the lognormality hypotheses, “Yes” is listed in the column “Accept Lognormality Hypothesis.”

Table 5-2
Summary of RMSM HFM Area Hydraulic Conductivity Analysis

| CG | Mean | Standard Deviation | | Count ^b | Minimum Value | Maximum Value | K-S Critical Statistic D* | K-S Statistic D at 95% | Accept Lognormality Hypothesis | 95% Confidence Interval Bounds | | Number of Entries ^c / Number of Wells ^d | |
|------------------------------|-----------------------------|--------------------|-----------------------------|--------------------|-----------------------------|---------------|---------------------------|------------------------|--------------------------------|--------------------------------|-------|--|---|
| | | Data | Population ^a | | | | | | | Lower | Upper | | |
| | log ₁₀ K (m/day) | | log ₁₀ K (m/day) | | log ₁₀ K (m/day) | | | | | | | | |
| Pumping-Scale Data | | | | | | | | | | | | | |
| WTA | 0.50 | 0.61 | 0.25 | 6 | -0.45 | 1.07 | 0.17 | 0.56 | Yes | -0.70 | 1.70 | 28 | 1 |
| LCA3 | -0.70 | 0.95 | 0.32 | 9 | -2.94 | 0.10 | 0.20 | 0.45 | Yes | -2.56 | 1.15 | 48 | 6 |
| UCCU | -3.30 | -3.30 | -- | 2 | -3.49 | -3.11 | -- | -- | -- | -- | -- | 2 | 2 |
| Slug Test-Scale Data | | | | | | | | | | | | | |
| LCA | -1.39 | -- | -- | 2 | -1.77 | -1.02 | -- | -- | -- | -- | -- | 2 | 2 |
| LCA3 | -0.20 | -- | -- | 2 | -0.32 | -0.08 | -- | -- | -- | -- | -- | 2 | 1 |
| UCCU | -2.12 | -- | -- | 3 | -2.65 | -1.16 | -- | -- | -- | -- | -- | 4 | 4 |
| Laboratory-Scale Data | | | | | | | | | | | | | |
| LCA3 | -5.11 | -- | -- | 2 | -5.52 | -4.70 | -- | -- | -- | -- | -- | 2 | 2 |

^a Estimate of the standard deviation of the mean of the population = standard deviation of the data/square root of count

^b Number of independent data used to determine statistics and test for a normal distribution

^c Total number of test analyses

^d Total number of wells for which there are test analyses

Table 5-3
Summary of NTS Data Compilation Area Hydraulic Conductivity Analysis
 (Page 1 of 2)

| CG | Mean | Standard Deviation | | Count ^b | Minimum | Maximum | K-S Critical Statistic D* | K-S Statistic D at 95% | Accept Lognormality Hypothesis | 95% Confidence Interval Bounds | | Number of Entries ^c / Number of Wells ^d | |
|-----------------------------|-----------------------------|--------------------|-----------------------------|--------------------|-----------------------------|---------|------------------------------|---------------------------|--------------------------------------|-----------------------------------|-------|--|----|
| | | Data | Population ^a | | | | | | | Lower | Upper | | |
| | log ₁₀ K (m/day) | | log ₁₀ K (m/day) | | log ₁₀ K (m/day) | | | | | | | | |
| Pumping-Scale Data | | | | | | | | | | | | | |
| AA | 0.08 | 0.86 | 0.17 | 27 | -1.26 | 1.66 | 0.12 | 0.26 | Yes | -1.61 | 1.78 | 70 | 19 |
| PCU | -0.64 | -- | -- | 3 | -0.76 | -0.55 | -- | -- | -- | -- | -- | 30 | 1 |
| OAA | -1.01 | -- | -- | 1 | -- | -- | -- | -- | -- | -- | -- | 1 | 1 |
| LFA | -0.14 | 0.91 | 0.19 | 24 | -1.94 | 0.93 | 0.12 | 0.28 | -- | -1.92 | 1.64 | 71 | 16 |
| WTA | 0.21 | 0.94 | 0.11 | 79 | -1.92 | 1.74 | 0.10 | 0.15 | Yes | -1.63 | 2.06 | 212 | 36 |
| TCU | -0.94 | 1.21 | 0.14 | 71 | -5.02 | 1.35 | 0.08 | 0.16 | Yes | -3.31 | 1.44 | 132 | 14 |
| UCCU | -3.30 | -- | -- | 2 | -3.49 | -3.11 | -- | -- | -- | -- | -- | 2 | 2 |
| LCA | 0.14 | 1.31 | 0.17 | 60 | -2.12 | 2.65 | 0.13 | 0.18 | Yes | -2.43 | 2.71 | 260 | 29 |
| LCA3 | -0.70 | 0.95 | 0.32 | 9 | -2.94 | 0.20 | 0.20 | 0.45 | Yes | -2.56 | 1.15 | 48 | 6 |
| LCCU | -2.21 | -- | -- | 1 | -- | -- | -- | -- | -- | -- | -- | 1 | 1 |
| GCU | -2.49 | -- | -- | 1 | -- | -- | -- | -- | -- | -- | -- | 1 | 1 |
| Slug Test-Scale Data | | | | | | | | | | | | | |
| AA | -0.60 | -- | -- | 4 | -1.00 | 0.04 | -- | -- | -- | -- | -- | 15 | 3 |
| OAA | -0.37 | -- | -- | 1 | -- | -- | -- | -- | -- | -- | -- | 1 | 1 |
| LFA | -1.86 | 0.84 | 0.10 | 74 | -4.10 | -0.59 | 0.11 | 0.16 | Yes | -3.50 | -0.22 | 343 | 9 |
| WTA | -2.34 | 1.08 | 0.08 | 170 | -5.51 | 0.08 | 0.04 | 0.10 | Yes | -4.45 | -0.23 | 666 | 22 |
| VTA | -2.71 | -- | -- | 11 | -3.92 | -0.83 | -- | -- | -- | -- | -- | 18 | 4 |
| TCU | -2.45 | 1.20 | 0.13 | 86 | -6.00 | -0.01 | 0.06 | 0.15 | Yes | -4.80 | -0.11 | 199 | 14 |
| UCCU | -1.99 | -- | -- | 4 | -2.65 | -1.16 | -- | -- | -- | -- | -- | 4 | 4 |
| LCA | -1.44 | -- | -- | 15 | -2.63 | -0.67 | -- | -- | -- | -- | -- | 67 | 6 |
| LCA3 | -0.20 | -- | -- | 2 | -0.32 | -0.08 | -- | -- | -- | -- | -- | 2 | 1 |
| GCU | -1.16 | -- | -- | 3 | -3.19 | 0.15 | -- | -- | -- | -- | -- | 3 | 3 |

Table 5-3
Summary of NTS Data Compilation Area Hydraulic Conductivity Analysis
 (Page 2 of 2)

| CG | Mean | Standard Deviation | | Count ^b | Minimum | Maximum | K-S Critical Statistic D* | K-S Statistic D at 95% | Accept Lognormality Hypothesis | 95% Confidence Interval Bounds | | Number of Entries ^c / Number of Wells ^d | |
|-----------------------|-----------------------------|--------------------|-----------------------------|--------------------|-----------------------------|---------|------------------------------|---------------------------|--------------------------------------|-----------------------------------|-------|--|----|
| | | Data | Population ^a | | | | | | | Lower | Upper | | |
| | log ₁₀ K (m/day) | | log ₁₀ K (m/day) | | log ₁₀ K (m/day) | | | | | | | | |
| Laboratory-Scale Data | | | | | | | | | | | | | |
| AA | -0.37 | 0.79 | 0.10 | 63 | -3.09 | 0.84 | 0.09 | 0.17 | Yes | -1.92 | 1.18 | 63 | 4 |
| WTA | -4.37 | 1.82 | 0.08 | 531 | -8.13 | 2.51 | 0.09 | 0.06 | No | -7.93 | -0.80 | 531 | 22 |
| VTA | -3.45 | 2.20 | 0.15 | 210 | -7.75 | 4.60 | 0.15 | 0.09 | No | -7.75 | 0.86 | 210 | 17 |
| TCU | -4.66 | 1.34 | 0.09 | 201 | -7.47 | -1.70 | 0.09 | 0.10 | Yes | -7.28 | -2.04 | 201 | 11 |
| LCA | -4.16 | 1.48 | 0.33 | 20 | -6.33 | -1.67 | 0.16 | 0.30 | Yes | -7.06 | -1.26 | 20 | 4 |
| LCA3 | -5.21 | -- | -- | 4 | -5.52 | -4.70 | -- | -- | -- | -- | -- | 4 | 3 |
| LCCU | -6.56 | 0.66 | 0.18 | 30 | -7.54 | -4.69 | 0.16 | 0.25 | Yes | -7.86 | -5.26 | 30 | 1 |

^a Estimate of the standard deviation of the mean of the population = standard deviation of the data/square root of count

^b Number of independent data used to determine statistics and test for a normal distribution

^c Total number of test analyses

^d Total number of wells for which there are test analyses

As can be seen by comparing Tables 5-2 and 5-3, there are not many RMSM-specific data, but extensive datasets for the NTS Data Compilation Area are available for many of the CGs at all three test scales. The RMSM datasets for the UCCU and LCA3 are the same as the NTS Data Compilation Area, as are the analysis results. Note that the LCA3 category, as previously defined, is specific to the RMSM HFM model area, and the results are also the same in both tables. The RMSM WTA dataset was statistically tested with respect to the NTS Data Compilation Area dataset for inconsistency of the variances and means, and found not to be inconsistent. Table 5-4 shows the comparison. The lognormal hypothesis was not rejected for any datasets at the “Pumping Scale” and “Slug-Test Scale.” The lognormal hypothesis was rejected for two datasets at the “Laboratory Scale.” However, these data were probably not random data points but, rather, data collected to characterize specific intervals in wells that could not be generally characterized by other methods. The 95% confidence interval bounds for lognormal distributions determined from the data analyses were calculated and are presented in the table.

Table 5-4
Statistical Comparison of RMSM Data to NTS Data

| | NTS Data Compilation Area | RMSM CAU |
|--|------------------------------|----------|
| F-Test Two-Sample for Variances | | |
| Mean | 0.21 | 0.50 |
| Variance | 0.88 | 0.38 |
| Observations | 79 | 6 |
| df | 78 | 5 |
| F | 2.35 | |
| P(F<=f) one-tail | 0.17 | |
| F Critical one-tail | 4.42 | |
| t-Test: Two-Sample Assuming Equal Variances | | |
| Mean | 0.21 | 0.50 |
| Variance | 0.88 | 0.38 |
| Observations | 79 | 6 |
| Pooled Variance | 0.85 | |
| Hypothesized Mean Difference | 0.00 | |
| df | 83 | |
| t-Stat | -0.73 | |
| P(T<=t) one-tail | 0.23 | |
| t Critical one-tail | 1.66 | |
| P(T<=t) two-tail | 0.47 | |
| t Critical two-tail | 1.99 | |

Figure 5-2 illustrates the relationships of the pumping-scale K data distributions for the different CG categories for the NTS Data Compilation Area. The central diamond for each HGU indicates the mean value, and the bar indicates the 95% confidence bounds. This diagram shows the relationship between the K distributions for aquifer unit and confining unit CG. In general, the mean \log_{10} K meters per day (m/day) of aquifer units is > -0.5 , and < -0.5 for confining units (vertical divider on Figure 5-2). Note that the inclusion of VTA intervals within the overall length of the assigned test interval for the WTA and LFA may reduce the calculated K values for those tests because the VTA, in general, is believed to have lower but undetermined hydraulic conductivity. An alternate analysis with VTA intervals removed from the calculation would bound the analysis on the high side. A better determination of values for the WTA and LFA would require knowledge of the VTA K distribution, which is lacking. The mean \log_{10} K for the LCA3 is in the confining unit range. The LCA3 was separated from the LCA for the reason that the K values are much different. For this CG, the hydraulic conductivity would primarily be a function of fracturing. Fractures in the LCA3 are typically less open and more healed or filled.

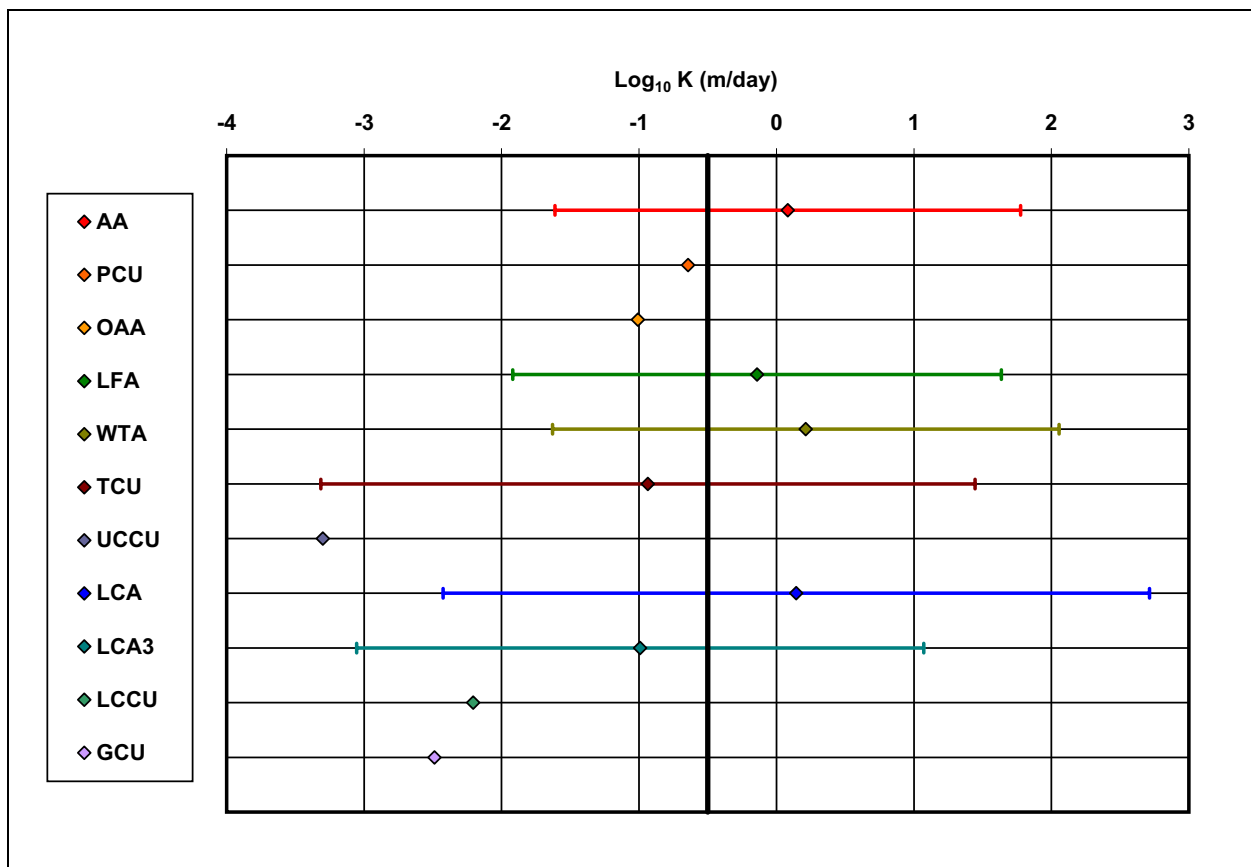


Figure 5-2
Relationship of CG Hydraulic Conductivity Distributions

Note: The central diamond for each CG indicates the mean value; the bar indicates the 95% confidence bounds.

Figure 5-3 shows an overlay of the lognormal distributions determined for CGs from the NTS Data Compilation Area dataset. Shown are 95% confidence intervals for the different CG distributions as well as the general differences in K between CGs. Figure 5-4 shows both the pumping-scale distributions, reflecting large-scale properties, and the lab-scale distributions, reflecting matrix properties. The lab-scale distributions have the same color-codes as the pumping-scale distributions, but the lines are crosshatched. This illustrates that the large-scale K is typically about four orders of magnitude greater than the matrix K for fractured formations. Again, the VTA data are somewhat anomalous. For the AA, the difference is only about one order of magnitude.

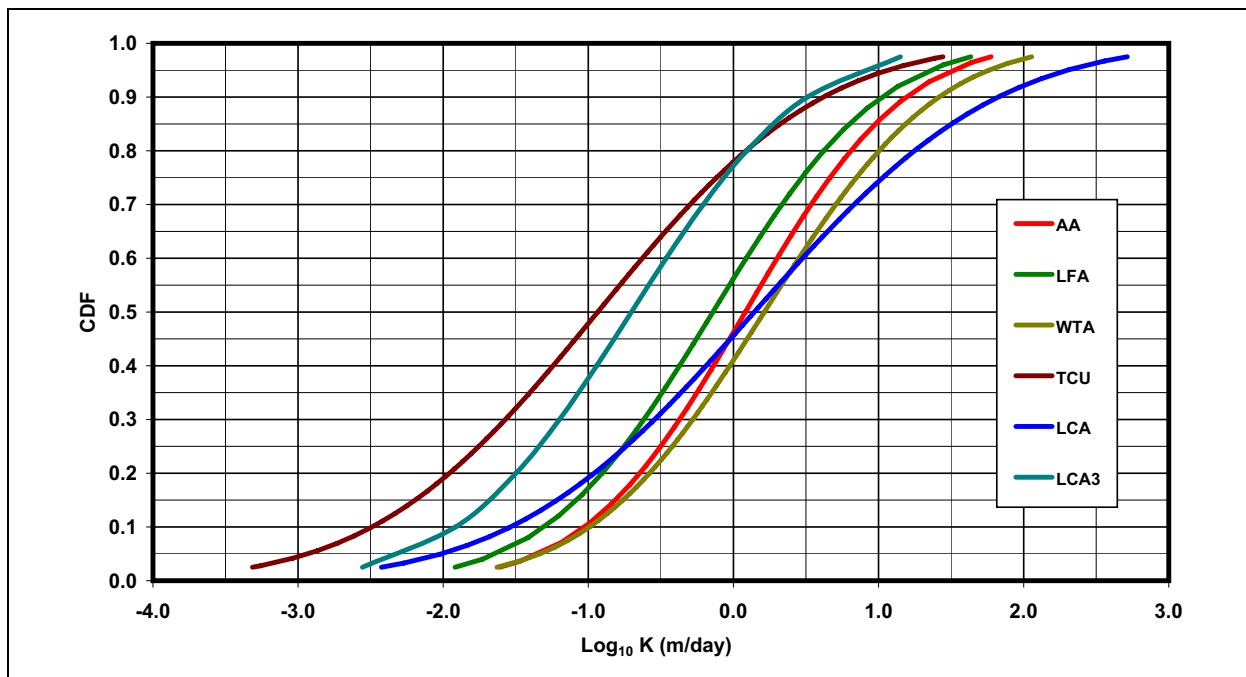


Figure 5-3
Overlay of NTS Data Compilation Area Hydraulic Conductivity Distributions

Table 5-5 compares the mean and standard deviation of the NTS data compilation datasets for the three different measurement scales (see Table 5-3). In general, the mean K decreases with decreasing measurement scale. As previously mentioned, this is consistent with the concept that the larger-scale measurements encompass and preferentially reflect high-conductivity hydrologic features such as fracturing and faults much more than smaller-scale measurements. Within the formations at the NTS, fracturing is common and is the most significant factor for groundwater flow. The laboratory-scale values reflect unfractured matrix properties. For fractured formations, the large-scale mean values are several orders of magnitude larger than the matrix hydraulic conductivity. The higher hydraulic conductivity values are more appropriate to the discretization scale for the flow model.

5.11 Conversion of Hydraulic Conductivity to Permeability

Hydraulic conductivity values reflect the properties of the fluid used for testing. The flow model will use intrinsic permeability rather than hydraulic conductivity. Conversion from hydraulic conductivity

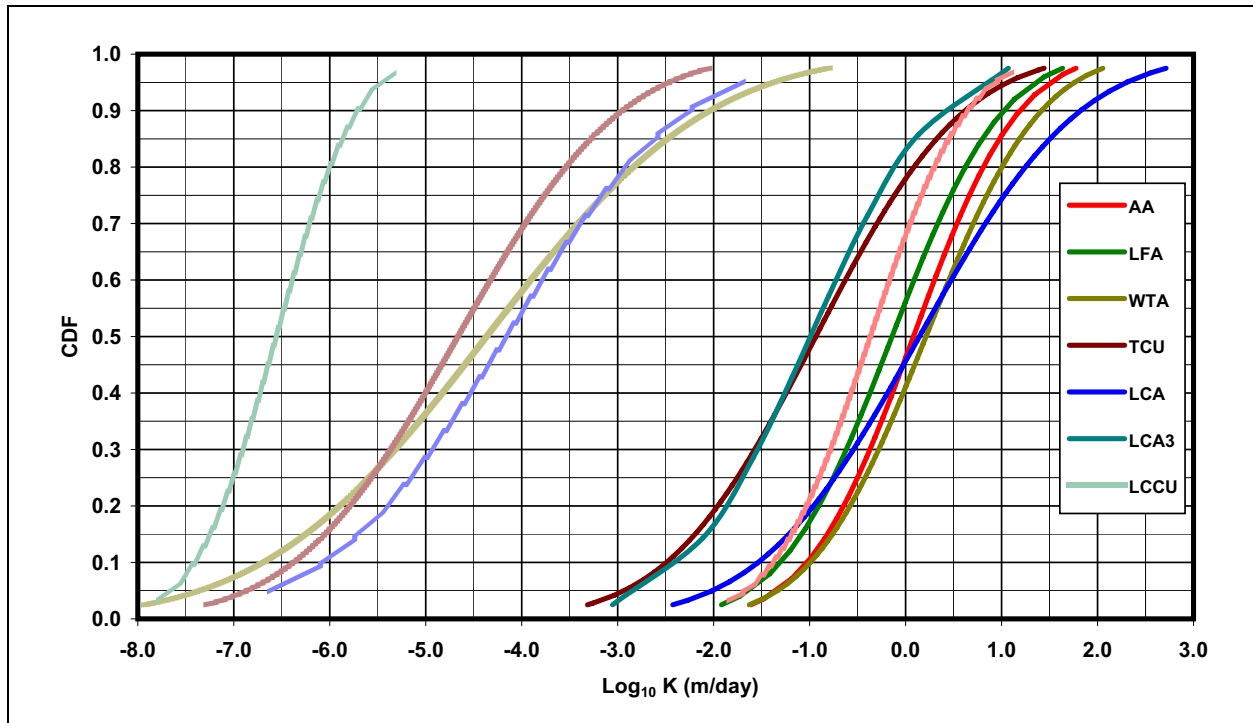


Figure 5-4
Comparison of Pumping-Scale and Lab-Scale K Distributions, 95% Bounds

Table 5-5
Comparison of Mean and Standard Deviation by Scale of Measurement

| CG | Pumping-Scale Data | | | Slug Test-Scale Data | | | Laboratory-Scale Data | | |
|------|-----------------------------|--------------------|-------------------------|----------------------|--------------------|-------------------------|-----------------------|--------------------|-------------------------|
| | Mean | Standard Deviation | | Mean | Standard Deviation | | Mean | Standard Deviation | |
| | | Data | Population ^a | | Data | Population ^a | | Data | Population ^a |
| | log ₁₀ K (m/day) | | | | | | | | |
| AA | 0.08 | 0.86 | 0.17 | -0.60 | -- | -- | -0.37 | 0.79 | 0.10 |
| PCU | -0.64 | -- | -- | -- | -- | -- | -- | -- | -- |
| OAA | -1.01 | -- | -- | -0.37 | -- | -- | -- | -- | -- |
| LFA | -0.14 | 0.91 | 0.19 | -1.86 | 0.84 | 0.10 | -- | -- | -- |
| WTA | 0.21 | 0.94 | 0.11 | -2.34 | 1.08 | 0.08 | -4.37 | 1.82 | 0.08 |
| TCU | -0.94 | 1.21 | 0.11 | -2.45 | 1.20 | 0.13 | -4.66 | 1.34 | 0.09 |
| UCCU | -3.30 | -- | -- | -1.99 | -- | -- | -- | -- | -- |
| LCA | 0.14 | 1.31 | 0.17 | -1.44 | -- | -- | -4.16 | 1.48 | 0.33 |
| LCA3 | -0.70 | 0.95 | 0.32 | -0.20 | -- | -- | -5.21 | -- | -- |
| LCCU | -2.21 | -- | -- | -- | -- | -- | -6.56 | 0.66 | 0.12 |
| GCU | -2.49 | -- | -- | -1.16 | -- | -- | -- | -- | -- |

^a Standard error of the estimate of the mean = standard deviation X (1/n)^{0.5}; Source: [5]

to intrinsic permeability normalizes the formation hydraulic properties with respect to fluid property variation. Intrinsic permeability (k) is calculated from hydraulic conductivity (K) as $k = K\mu/\rho g$, where μ is the dynamic viscosity of the fluid, ρ is the density of the fluid, and g is the force of gravity [6]. Both μ and ρ vary with the temperature of the fluid. The fluid used in testing was water, with known properties, and the conversion can be calculated if the temperature of the water produced from the formation is known. However, these data are not always recorded. The temperature of the water in formations at the NTS varies widely, both spatially, in relation to geologic features, and with depth in relation to the geothermal gradient.

Table 5-6 shows the variation of μ and ρ with temperature for pure water. Water in the formations beneath the NTS is generally considered fresh, and the variation of water properties shown here is representative. Specific data for NTS waters are not available. The fourth column in Table 5-6 shows the ratio of μ/ρ , which is the factor of the conversion from hydraulic conductivity to intrinsic permeability that would vary with temperature. The ratio of the values of this factor for the uncertainty in temperature reflects the uncertainty in the conversion due to temperature. The downhole temperatures in the NTS Data Compilation area range from a minimum of 14.7 degrees Celsius ($^{\circ}\text{C}$) to a maximum of 83.8 $^{\circ}\text{C}$. The uncertainty due to the unknown temperature of the groundwater during testing for this temperature range is a factor of up to 3.4 (ratio of the conversion factors for the temperature endpoints).

Table 5-6
Variation of Water Properties with Temperature

| Temperature ($^{\circ}\text{C}$) | ρ - Density (g/cm^3) | μ - Dynamic Viscosity ($\text{g}/\text{cm}\text{-sec} \times 10^2$) | μ/ρ ($\text{cm}^2/\text{sec} \times 10^2$) |
|---------------------------------------|--|--|--|
| 0 | 0.99984 | 1.793 | 1.793 |
| 10 | 0.99970 | 1.307 | 1.307 |
| 20 | 0.99821 | 1.002 | 1.004 |
| 30 | 0.99565 | 0.798 | 0.801 |
| 40 | 0.99222 | 0.653 | 0.658 |
| 50 | 0.98803 | 0.547 | 0.554 |
| 60 | 0.98320 | 0.467 | 0.475 |
| 70 | 0.97778 | 0.404 | 0.413 |
| 80 | 0.97182 | 0.354 | 0.364 |
| 90 | 0.96535 | 0.315 | 0.326 |
| 100 | 0.95840 | 0.282 | 0.294 |

Source: [7]

g/cm^3 = Grams per cubic centimeter
 $\text{g}/\text{cm}\text{-sec}$ = Grams per centimeter-second
 cm^2/sec = Square centimeters per second

5.12 Anisotropy of K

Generally, hydraulic conductivity is not a scalar value but a second rank tensor where hydraulic conductivity at a point in space is a function of direction. Commonly, anisotropy within a formation is described as two distinct factors, horizontal anisotropy and vertical anisotropy, which are determined and applied separately. Determination of anisotropy requires testing that can distinguish vector properties. This typically requires tests with responses recorded in multiple wells, which are not common at the NTS, and there are none in the RMSM HFM area. Anisotropy in fractured formations is primarily a function of the fracturing orientations [8, 9]. Fracture data for the RMSM CAU could be used to assess theoretical anisotropy as a function of fracturing. However, data transfer from other CAUs is not appropriate because fracturing is the product of the stress history of the rock, which is specific to the RMSM CAU.

5.13 Depth Dependence of Hydraulic Conductivity

Depth dependence for hydraulic conductivity has been used in previous UGTA flow models. The relationship of hydraulic conductivity to depth is controversial because the data contain great scatter and the regression of the log of hydraulic conductivity against depth exhibits poor correlation. However, there is considerable support in the literature for the relationship. A literature review of the relationship of hydraulic conductivity or permeability to depth was presented in the YFCM HDD [1]. This review identifies and discusses studies of the depth dependence of hydraulic conductivity for unconsolidated sediments, sedimentary, carbonate, metamorphic, and crystalline rocks but did not locate any studies for volcanic tuffs.

The hydraulic conductivity data have been analyzed for the depth-dependence relationship, and the results are presented in this section. The analysis has been conducted in terms of hydraulic conductivity due to the lack of specific temperature information for all tests to support conversion of hydraulic conductivity to permeability. It is recognized that the general temperature increase with depth has an effect on this analysis which may be separated when hydraulic conductivity is converted to permeability. The potential for uncertainty related to the variation in temperature is generally addressed in Section 5.11, but not specifically as it relates to this depth-dependence analysis. There is also potential for bias in this analysis due to generally increasing test interval lengths with depth for NTS wells. Removal of such a bias has not been attempted.

5.13.1 Depth-Decay Formulation

The relationship of hydraulic conductivity to depth, commonly termed depth decay, is of interest for flow modeling to properly represent large-scale systematic hydraulic property variation in the vertical dimension. A decreasing linear trend is commonly observed in the logarithm of hydraulic conductivity with increasing depth, although the data show great scatter. Despite the data scatter, which indicates that there is great variability of hydraulic conductivity at different depths for many formulations, the general conclusion in the literature addressing the question of the relationship of hydraulic conductivity to depth is that hydraulic conductivity decreases with depth. The relationship of hydraulic conductivity to depth used for analysis is given below. Another relationship may provide

slightly better correlation in some cases, but the simple relationship prescribed is consistent with the degree of scatter in the data.

$$K_{Depth} = K_0 (10^{-\lambda d}) \quad (5-1)$$

where:

K_{Depth} = Horizontal hydraulic conductivity at specified depth (m/day)

K_0 = Horizontal hydraulic conductivity at land surface (m/day)

λ = Decay coefficient (calculated from linear regression) (1/m)

d = Depth from land surface (m)

The rate of decrease of hydraulic conductivity with depth is determined by the value of λ , (the decay coefficient), and K_0 provides the reference hydraulic conductivity at the ground surface, from which depth is measured.

5.13.2 Analysis of NTS Datasets for Depth Decay

The depth dependence of hydraulic conductivity was analyzed for the pumping-scale datasets for both RMSM-specific and the NTS Data Compilation Area CG datasets. The “All-Data” analysis provides a generalized view of depth dependence of hydraulic conductivity. Depth versus hydraulic conductivity trends may be specific to individual CGs according to variations in physical properties affecting the hydraulic conductivity and the response to increasing effective stress with depth.

Table 5-7 presents the results of correlation and regression analysis (using Excel 2002 Analysis Toolpak statistical calculation tools) of the depth dependence of hydraulic conductivity for each dataset. The columns on the left in Table 5-7 provide the regression parameter values and statistics for the best-fit linear regression line for K_{Depth} versus depth. The “p-Value(s),” indicating the probability for no relationship, are low for many of the regressions for the NTS Data Compilation Area dataset. From this, it can be inferred there is a relationship. The R values (correlation coefficient) in the column labeled “Data” in Table 5-7 indicate the correlation between the hydraulic conductivity data and the assigned depth. The correlation coefficient values indicate that there is significant correlation (0.27 - 0.65) for many CGs of the NTS Data Compilation Area dataset, and the negative sign indicates that hydraulic conductivity values decrease with increasing depth. By significant, it is meant that K appears correlated with depth to a degree that has proven significant for flow modeling. The relationship is understood to be superimposed upon natural variability. The two columns under the heading “Regression” present statistics for the regression of hydraulic conductivity against depth. The R^2 value for the regression gives the proportion of the total variability in the hydraulic conductivity that can be accounted for by increasing depth. The NTS Data Compilation Area dataset, which is much larger than the RMSM-specific dataset, shows greater correlation. These values reflect the data scatter and are consistent with the understanding that other factors, such as heterogeneity and spatial variability, are also factors in the variability of hydraulic conductivity. The R value under the “Par” heading indicates the correlation between the two regression parameters.

Table 5-7
Summary of Depth-Decay Analysis
 (Page 1 of 2)

| CG | Par ^a | Value | SE ^b | t-Stat ^c | p-Value ^d | Confidence Bounds | | | | Data | Regression | | Par's |
|----------------------------------|-----------------------------|-----------|-----------------|---------------------|----------------------|-------------------|-----------|--------------|--------------|----------------|----------------|-----------------|----------------|
| | | | | | | Lower 95% | Upper 95% | Lower 68.27% | Upper 68.27% | R ^e | R ² | SE ^b | R ^e |
| RMSM-Specific Data | | | | | | | | | | | | | |
| WTA | K ₀ ^f | 5.95E-01 | 6.84E-01 | 8.71E-01 | 4.33E-01 | -1.30E+00 | 2.49E+00 | -1.85E-01 | 1.38E+00 | -0.08 | 0.01 | 0.68 | -0.91 |
| | λ | -1.30E-04 | 8.31E-04 | -1.56E-01 | 8.83E-01 | -2.44E-03 | 2.18E-03 | -1.08E-03 | 8.19E-04 | | | | |
| LCA3 | K ₀ ^f | 1.20E-01 | 6.75E-01 | 0.18 | 8.64E-01 | -1.48E+00 | 1.72E+00 | -6.07E-01 | 8.46E-01 | -0.47 | 0.21 | 0.90 | -0.87 |
| | λ | -1.18E-03 | 8.69E-04 | -1.36 | 2.16E-01 | -3.24E-03 | 8.73E-04 | -2.12E-03 | -2.46E-04 | | | | |
| NTS Data Compilation Area | | | | | | | | | | | | | |
| All Data | K ₀ ^f | 6.59E-01 | 1.44E-01 | 4.57 | 7.39E-06 | 3.75E-01 | 9.43E-01 | 5.17E-01 | 8.00E-01 | -0.42 | 0.15 | 1.13 | -0.83 |
| | λ | -1.23E-03 | 1.77E-04 | -6.94 | 2.72E-11 | -1.58E-03 | -8.80E-04 | -1.40E-03 | -1.05E-03 | | | | |
| AA | K ₀ ^f | 7.96E-01 | 2.52E-01 | 3.16 | 4.11E-03 | 2.77E-01 | 1.32E+00 | 5.39E-01 | 1.05E+00 | -0.56 | 0.32 | 0.73 | -0.83 |
| | λ | -2.02E-03 | 5.93E-04 | -3.41 | 2.22E-03 | -3.24E-03 | -8.00E-04 | -2.63E-03 | -1.42E-03 | | | | |
| LFA | K ₀ ^f | 1.05E+00 | 4.26E-01 | 2.46 | 2.21E-02 | 1.65E-01 | 1.93E+00 | 6.13E-01 | 1.48E+00 | -0.54 | 0.29 | 0.78 | -0.93 |
| | λ | -1.44E-03 | 4.76E-04 | -3.01 | 6.41E-03 | -2.42E-03 | -4.47E-04 | -1.92E-03 | -9.48E-04 | | | | |
| WTA | K ₀ ^f | 9.68E-01 | 2.23E-01 | 4.34 | 4.28E-05 | 5.24E-01 | 1.41E+00 | 7.43E-01 | 1.19E+00 | -0.39 | 0.16 | 0.87 | -0.90 |
| | λ | -1.08E-03 | 2.85E-04 | -3.77 | 3.21E-04 | -1.64E-03 | -5.07E-04 | -1.36E-03 | -7.88E-04 | | | | |

Table 5-7
Summary of Depth-Decay Analysis
 (Page 2 of 2)

| CG | Par ^a | Value | SE ^b | t-Stat ^c | p-Value ^d | Confidence Bounds | | | | Data | Regression | | Par's |
|------|-----------------------------|-----------|-----------------|---------------------|----------------------|-------------------|-----------|--------------|--------------|----------------|----------------|-----------------|----------------|
| | | | | | | Lower 95% | Upper 95% | Lower 68.27% | Upper 68.27% | R ^e | R ² | SE ^b | R ^e |
| TCU | K ₀ ^f | 7.68E-02 | 4.59E-01 | 0.17 | 8.68E-01 | -8.38E-01 | 9.91E-01 | -3.85E-01 | 5.39E-01 | -0.27 | 0.07 | 1.18 | -0.95 |
| | λ | -1.35E-03 | 5.83E-04 | -2.32 | 2.35E-02 | -2.51E-03 | -1.88E-04 | -1.94E-03 | -7.63E-04 | | | | |
| LCA | K ₀ ^f | 1.57E+00 | 2.57E-01 | 6.11 | 9.00E-08 | 1.06E+00 | 2.09E+00 | 1.31E+00 | 1.83E+00 | -0.65 | 0.42 | 1.01 | -0.86 |
| | λ | -1.66E-03 | 2.58E-04 | -6.44 | 2.57E-08 | -2.18E-03 | -1.14E-03 | -1.92E-03 | -1.40E-03 | | | | |
| LCA3 | K ₀ ^f | 1.21E-01 | 6.75E-01 | 0.18 | 8.62E-01 | -1.48E+00 | 1.72E+00 | -6.06E-01 | 8.48E-01 | -0.47 | 0.21 | 0.90 | -0.87 |
| | λ | -1.18E-03 | 8.70E-04 | -1.36 | 2.15E-01 | -3.24E-03 | 8.72E-04 | -2.12E-03 | -2.48E-04 | | | | |

^a Par = Parameter, referring to the two parameters in the depth-decay formulation

^b Standard error

^c t-Statistic

^d Level of significance

^e Correlation coefficient

^f As log₁₀ K (m/day)

Figure 5-5 is a graph of the NTS Data Compilation Area dataset showing the regression trendline and two standard deviations for both K_0 and λ . The degree of data scatter shown for plots of hydraulic conductivity versus depth for the NTS Data Compilation Area data is consistent with the degree of scatter in other published studies in the literature. To the extent that depth decay is related to increasing overburden stress on fractures with depth, the depth-decay relationship may be subject to a lower limit for K related to the matrix K of the formation. Such a limit has not been evaluated due to lack of appropriate data.

5.14 Specific Storage

Storage properties for formations is not of primary importance because the flow model will be based on steady-state groundwater flow conditions, which does not require storage. However, storage property values are needed for transient simulations of groundwater flow, which may be used for model verification. Storage is parameterized in test analyses as storativity (S), bulk storage for the formation tested (conceptually similar to transmissivity), and defined as the product of specific storage and formation thickness. Storage is analyzed in terms of specific storage (Ss), normalizing storage with respect to formation thickness, for use in numeric groundwater flow models.

Table 5-8 presents a summary of the data for “Specific Storage” for both the RMSM and NTS Data Compilation Area datasets. These datasets contain all storage parameter values reported in analyses of pumping-scale tests, including results from both single- and multi-well tests. It is recognized that results for storage from single-well tests are much less reliable than results from multi-well tests. However, few multi-well tests have been conducted, and there are consequently few storage values determined from such testing.

Figure 5-6 shows the distributions of the specific storage data for the NTS Data Compilation Area dataset, identified by CG. The specific storage probability distribution for the data spans nine orders of magnitude. The values at the upper end (above ~ 0.0001) are suspect because such high values are not consistent with physical properties of the formations affecting storage properties. As noted, analysis of single-well tests does not provide storage values with high confidence because determination of storage is greatly affected by near-well and in-well head losses associated with water production. These high values may also be the result of inappropriate conceptual models used for analysis, indicating that analysis may be faulty. Values determined for storage are also sensitive to the analysis model used. In particular, a single porosity model will require an unrealistic storage value to model a dual-porosity response, which is relevant to fractured formations.

Sanchez-Vila et al. show that in the presence of heterogeneity, which always occurs in reality, storativity estimates will often vary strongly as a function of the relative transmissivity of the flow path between the pumping and observation well [10]. Thus, storativity estimates depend on the degree of heterogeneity in the transmissivity. Sanchez-Vila et al. also suggest that a good estimate of true storativity is rarely obtained in practice from pumping tests [10]. It is possible that much of the apparent scatter in specific storage values is unrelated to the actual variability of storage properties. General survey information on storage properties of formations in southern Nevada can be found in Kilroy [11]. The large variation in values may also be due to variation in the analysis models used for

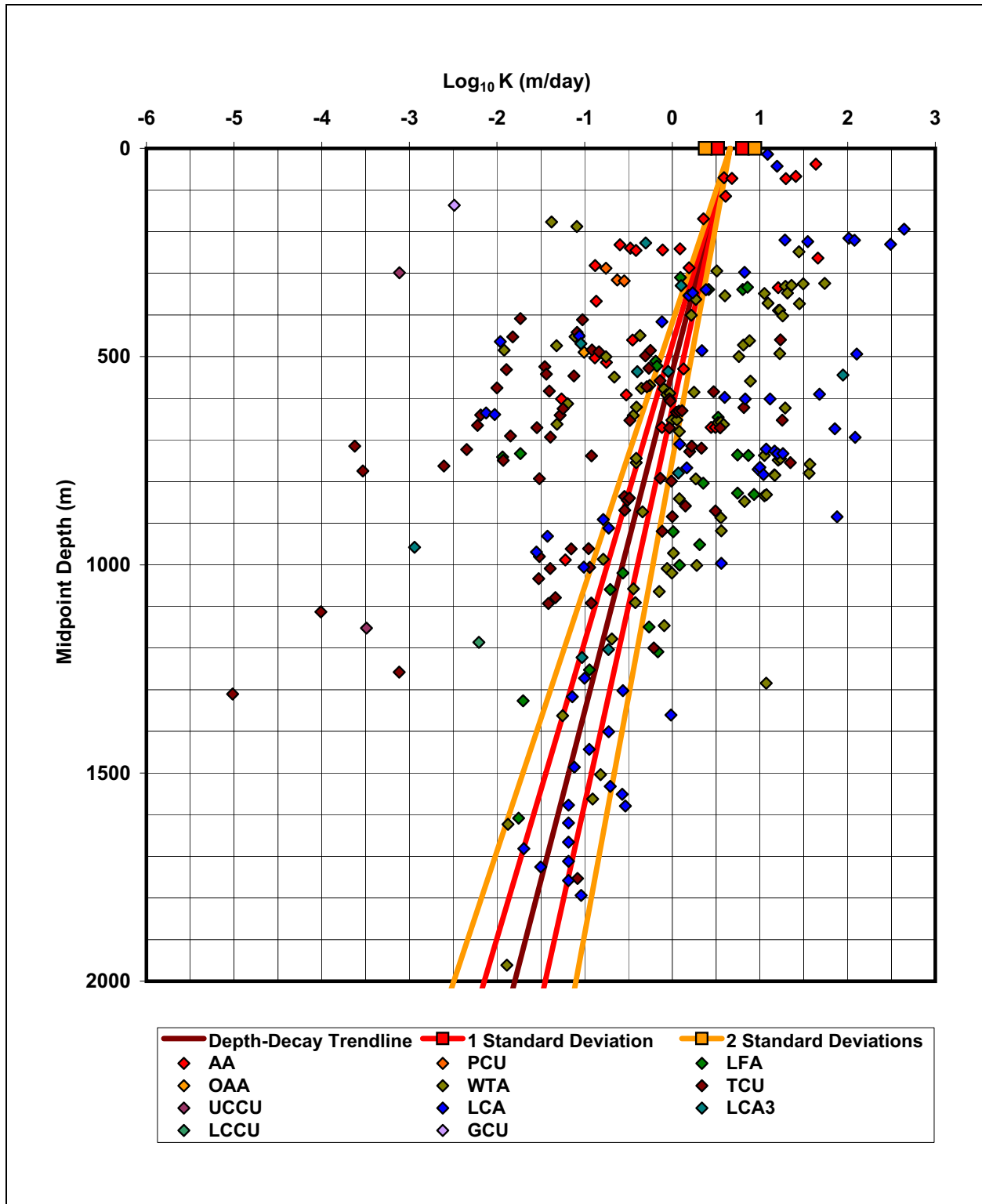


Figure 5-5
Hydraulic Conductivity Versus Depth for the NTS Data Compilation Area Dataset

Table 5-8
Summary of Specific Storage Data by Characterization Group

| CG | Mean | Std Dev | Min | Max | Count |
|----------------------------------|----------|----------|----------|----------|-------|
| | (1/m) | | | | |
| RMSM HFM Area | | | | | |
| WTA | 5.65E-02 | 1.24E-01 | 8.98E-08 | 2.78E-01 | 5 |
| LCA3 | 3.77E-01 | 7.22E-01 | 1.02E-09 | 1.83 | 6 |
| NTS Data Compilation Area | | | | | |
| AA | 1.34E-04 | 2.57E-04 | 1.71E-07 | 7.90E-04 | 9 |
| OAA | 4.78E-06 | -- | -- | -- | 1 |
| LFA | 1.05E-03 | 3.41E-03 | 2.30E-07 | 1.13E-02 | 11 |
| WTA | 1.03E-02 | 4.80E-02 | 1.13E-07 | 2.78E-01 | 42 |
| TCU | 4.55E-02 | 1.00E-01 | 2.85E-08 | 3.37E-01 | 15 |
| LCA | 1.79E-02 | 3.81E-02 | 5.58E-09 | 1.69E-01 | 28 |
| LCA3 | 1.25E-03 | 1.78E-03 | 1.02E-09 | 4.25E-03 | 6 |

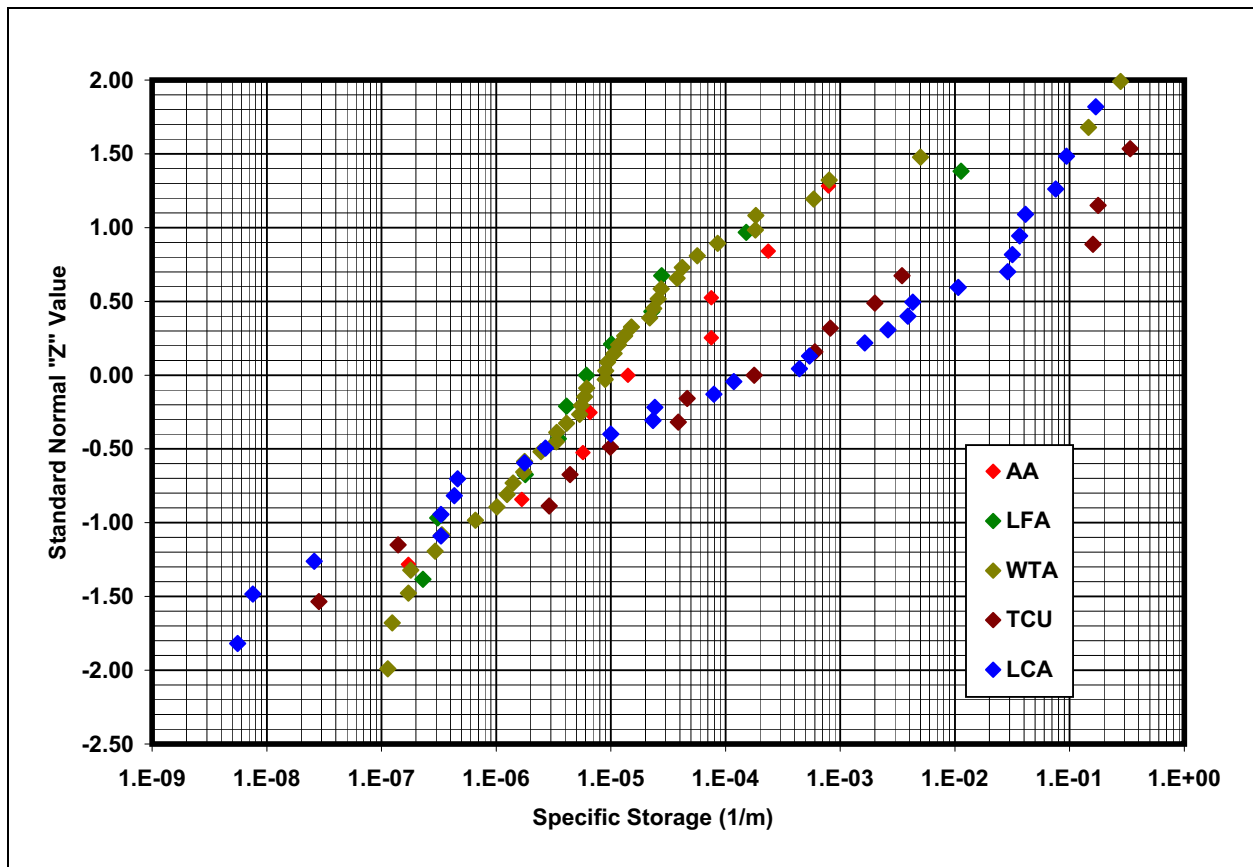


Figure 5-6
Specific Storage Data for the NTS Data Compilation Area Dataset

various tests, which can produce greatly differing values for storage properties, and the fact that most NTS tests are single-well tests that do not yield data that constrain storage values very well.

5.15 LCA Hydraulic Conductivity, Dual-Porosity Analysis

5.15.1 Previous Dual-Porosity Analyses

Some of the analyses of LCA tests contained in the database have used dual-porosity analytic models (terminology consistent with the analysis models references), which produces both an estimate of fracture hydraulic conductivity and matrix hydraulic conductivity. These models are more properly classified as dual-permeability or dual-continuum models. A dual-porosity model is consistent with the physical nature of the LCA as a highly fractured formation of low permeability matrix rock. The hydraulic properties database contains 49 dual-porosity analyses of LCA tests. Figure 5-7 shows the fracture and matrix hydraulic conductivity distributions for those dual-porosity analyses. Also plotted is the laboratory-scale K value distribution, which addresses matrix K and can be seen to be similar to the matrix K distribution from pumping-scale dual-porosity test analyses. This graph shows the great difference in the hydraulic conductivity between the matrix rock and the fracture system. The dual-porosity LCA fracture K values have a much narrower range than the complete LCA K-value dataset as shown in Figure 5-3. This difference suggests that some of the great variability in the complete dataset is due to uncertainty related to the analysis model used.

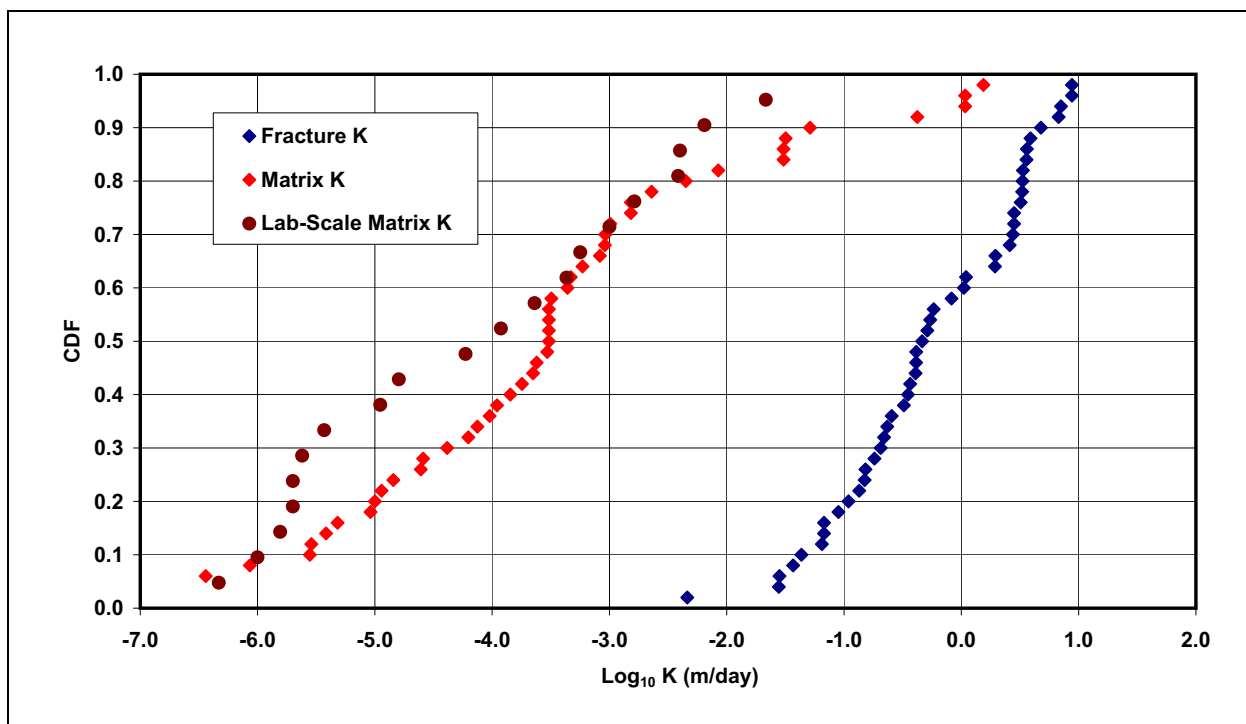


Figure 5-7
LCA Dual-Porosity Analyses

Table 5-9 presents the statistics for the LCA K data. The table is divided into two sections. The data listed under the “NTS Data Compilation Area” heading show the results of analyses extracted from existing reports. The data listed under “Dual-Porosity Reanalyses” are presented here for the sake of comparison and described in more detail in Section 5.15.2. The Pumping-Scale K and the Lab-Scale K information is from Table 5-2. The Pumping-Scale Fracture K- and Matrix K- information is for the dual-porosity analyses in the NTS Data Compilation Area dataset. Reference to the NTS Data Compilation Area data shows that the mean dual-porosity fracture $\log_{10} K$ for this dataset is -0.26 m/day, the mean matrix $\log_{10} K$ is -3.58 m/day, and the mean laboratory-scale $\log_{10} K$ is -4.16 m/day. Of note is the fact that the fracture K values are approximately three orders of magnitude larger than the matrix K values.

Table 5-9
Comparison of K Statistics for All LCA Analyses and Dual-Porosity Analyses

| Dataset | Count | Mean | Standard Deviation | Minimum | Maximum | 95% Confidence Interval | |
|----------------------------------|-------|--|--------------------|---------|---------|-------------------------|-------------|
| | | | | | | Lower Bound | Upper Bound |
| NTS Data Compilation Area | | $\log_{10}K$ (m/day) | | | | | |
| Pumping-Scale K values | 59 | 0.11 | 1.30 | -2.12 | 2.65 | -2.44 | 2.66 |
| Pumping-Scale Fracture K values | 49 | -0.26 | 0.78 | -2.34 | 0.94 | -1.80 | 1.27 |
| Pumping-Scale Matrix K values | 49 | -3.58 | 1.74 | -7.41 | 0.19 | -6.99 | -0.18 |
| Lab-Scale Data | 20 | -4.16 | 1.48 | -6.33 | -1.67 | -7.06 | -1.26 |
| Dual-Porosity Reanalyses | | $\log_{10}K$ (m/day) | | | | | |
| Pumping-Scale Fracture K values | 16 | -0.18 | 0.94 | -2.14 | 1.66 | -2.02 | 1.66 |
| Pumping-Scale Matrix K values | 16 | -5.88 | 0.76 | -7.56 | -5.06 | -7.38 | -4.39 |

The last two columns in the table list the 95% confidence interval upper and lower bounds. Reviewing the ranges defined by the upper and lower bounds shows that the dual-porosity fracture K values vary more than three orders of magnitude while the overall range for matrix analyses is about five orders of magnitude. The lab-scale analyses agree well with the pumping scale matrix values in both the mean and bounds as core sample tests do not capture the fracture properties present at the field scale.

5.15.2 Reanalysis of LCA Test Data

Test analyses in the hydraulic properties database are not consistent regarding the analysis model or assumptions used for each analysis, either for tests within a particular formation or even the same test, which introduces considerable analysis variability. To evaluate the importance of standardizing the method of analysis, a group of tests in the LCA within the NTS Data Compilation Area were

reanalyzed using the same analysis model, methodology, and assumptions for all analyses. The generalized radial flow model (GRFM) with a dual-porosity formulation was used in recognition that the formation is fractured and that known hydrologic features such as fracturing and faults affect the radial nature of the response [12, 13]. Storage parameter values were constrained to a range consistent with porosity and rock compressibility data (Fracture Ss, 3.3E-7 to 3.3E-8 [1/m]; and Matrix Ss, 3.3E-5 to 3.3E-6 [1/m]).

The results of the reanalyses are summarized in Table 5-9 under the “Dual-Porosity Reanalyses” heading. Figure 5-8 shows the results of the reanalyses as an empirical cumulative distribution function (ECDF), including the flow dimension (n) that corresponds to each reanalysis. Flow dimension is a parameter describing the geometry of the flow field, ranging from 1 (linear) to 2 (radial) to 3 (spherical). Non-integer flow dimension indicates an intermediate flow geometry such as bi-linear flow, n=1.5, which is simultaneous linear flow from the matrix to a fracture, and linear flow along the fracture. Reference to the table shows that the results have a mean \log_{10} K fracture K of -0.18 m/day, with a standard deviation of 0.94. The dual-porosity analyses in the hydraulic parameters database for the LCA (Figure 5-7 and Table 5-9) have a mean \log_{10} K of -0.26 m/day and a standard deviation of 0.78, with a similar range. The reanalyses produced a mean matrix \log_{10} K value of -5.88 and standard deviation of 0.76, with both values significantly smaller than those previously developed for the NTS Data Compilation Area. Reviewing the ranges found by reanalysis as compared to those reported for the NTS Data Compilation Area, the range for the fracture K values is somewhat larger. However, standardizing the analysis decreased the range for the matrix K values from five to three orders of magnitude. Grouping all the LCA test analyses (Table 5-3) produces a mean \log_{10} value for K of 0.14 m/day with a standard deviation of 1.31. The higher \log_{10} mean K for all analyses may be due to the inclusion of multiple analyses of some tests included in the database (typically, the higher conductivity tests) or bias due to analysis with single-porosity models.

5.16 Comparison of the YFCM HDD and the RMSM HDD Hydraulic Conductivity Analyses

The major change for the RMSM hydraulic property analysis from the previous YFCM analysis is the change in the approach to assigning the tested intervals to the hydraulic property CGs, and revision of the tested interval lengths based on a hierarchy of the HGU dominance in each test (see Section 5.5). Table 5-10 compares the results of this change. The variability of K values for individual CGs were generally reduced, as was the range of the 95% confidence interval for each category. This was expected because the approach removed extreme low values that were associated with very long test intervals containing intervals of low permeability rocks. This approach adapted the standard test analysis results (focused on T for the specific test interval) for the purpose of characterizing the hydraulic conductivity of HGU-based CGs, removing inconsistency.

5.17 Limitations

The amount of RMSM HFM area data available to characterize hydraulic conductivity for RMSM CGs is very limited; there are no data for many CGs. Pumping-scale measurements have been made within the RMSM HFM area for only three CGs and for only two CGs at multiple locations.

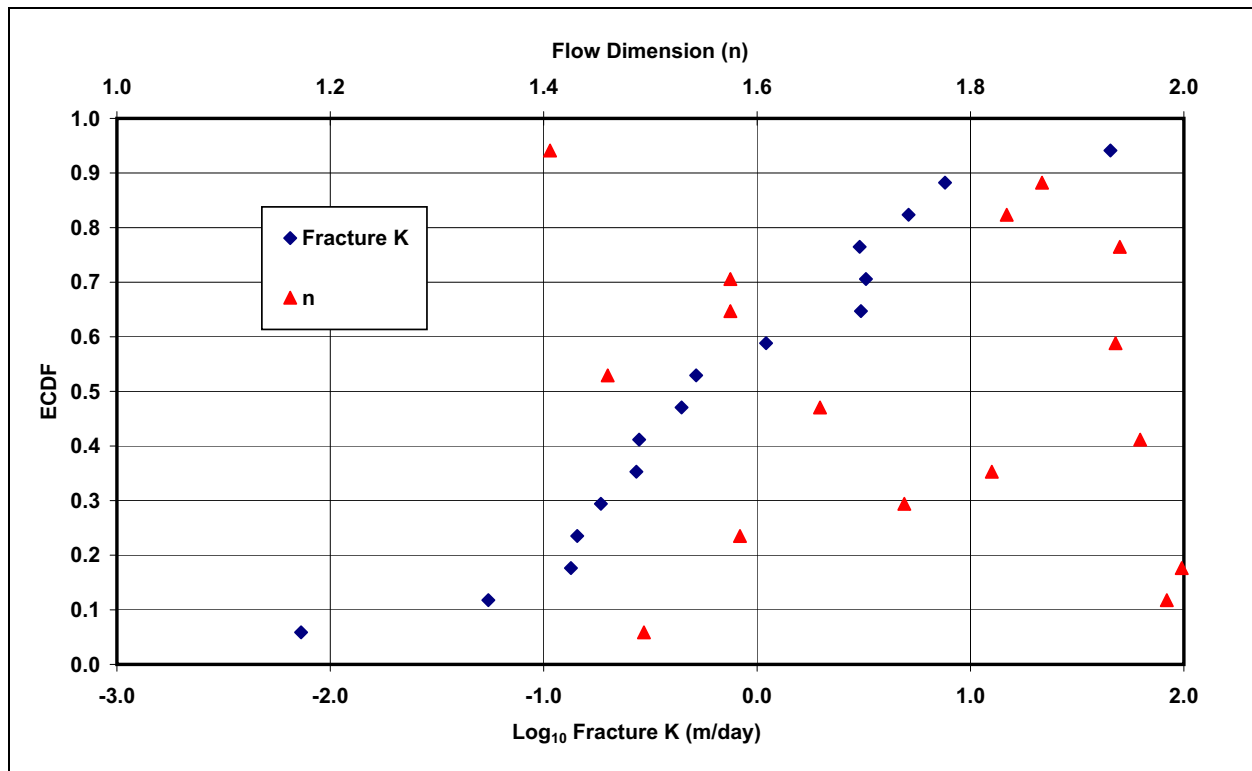


Figure 5-8
LCA Dual-Porosity Reanalyses

Characterization of hydraulic properties using data for the NTS Data Compilation Area at the HGU/CG level of characterization provides consistency through the HFM models. The use of HGU-based CGs as characterization groups allows the aggregation of large datasets for statistical analysis, generally defining the range of properties for different formation types (CGs). However, many HSUs appear to have their own distinct character, and their specific properties may differ from the average properties determined for the CG. Individual HSUs could have properties within the 95% confidence range of the overall CG but with a substantially different distribution within the wide ranges determined for CGs.

The data available for the RMSM HFM area alone are not well distributed through the area and do not provide complete, comprehensive characterization across the extent of the HFM area. The aggregate area tested for any HSU constitutes only a small percentage of the total area of the HSU. There are insufficient data to assess spatial trends given the apparent great variability of property values. For this reason, the area from which data for analyses were gathered was expanded to encompass all of the NTS.

The data for hydraulic properties are of variable quality resulting from a variety of factors, but it is believed that much of the variability observed in the property data is real. However, different analysis models and assumptions have been used to interpret the testing data. Some of the variability could be reduced by imposing consistency in analysis based on the flow model conceptualization, as was illustrated in [Section 5.15](#) with the LCA dual-porosity analyses.

Table 5-10
Comparison of YFCM and RMSM Hydraulic Conductivity Analyses

| CG | Mean | Standard Deviation | Minimum | Maximum | 95% Confidence Interval Bounds | | |
|----------------------|-----------------------------|--------------------|-----------------------------|---------|--------------------------------|-------|-------|
| | | | | | Lower | Upper | Range |
| | log ₁₀ K (m/day) | | log ₁₀ K (m/day) | | log ₁₀ K (m/day) | | |
| YFCM Analysis | | | | | | | |
| AA | 0.45 | 0.93 | -1.47 | 2.54 | -1.37 | 2.27 | 3.64 |
| LFA | -0.26 | 0.95 | -2.53 | 1.54 | -2.12 | 1.61 | 3.73 |
| VA | -0.12 | 1.29 | -4.80 | 3.41 | -2.66 | 2.42 | 5.08 |
| TCU | -0.91 | 1.43 | -4.82 | 1.90 | -3.72 | 1.90 | 5.62 |
| UCCU | -2.64 | 1.15 | -3.48 | -1.33 | -- | -- | -- |
| LCA | 0.16 | 1.34 | -2.85 | 3.12 | -2.46 | 2.78 | 5.24 |
| LCCU | -0.78 | 2.02 | -2.21 | 0.65 | -- | -- | -- |
| GCU | -2.49 | -- | -- | -- | -- | -- | -- |
| RMSM Analysis | | | | | | | |
| AA | 0.08 | 0.86 | -1.26 | 1.66 | -1.61 | 1.78 | 3.39 |
| PCU | -0.64 | -- | -0.76 | -0.55 | -- | -- | -- |
| OAA | -1.01 | -- | -- | -- | -- | -- | -- |
| LFA | -0.14 | 0.91 | -1.94 | 0.93 | -1.92 | 1.64 | 3.56 |
| WTA | 0.21 | 0.94 | -1.92 | 1.74 | -1.63 | 2.06 | 3.69 |
| TCU | -0.94 | 1.21 | -5.02 | 1.35 | -3.31 | 1.44 | 4.75 |
| LCA3 | -0.70 | 0.95 | -2.94 | 0.10 | -2.56 | 1.15 | 3.71 |
| UCCU | -3.30 | -- | -3.49 | -3.11 | -- | -- | -- |
| LCA | 0.14 | 1.31 | -2.12 | 2.65 | -2.43 | 2.71 | 5.14 |
| LCCU | -2.21 | -- | -- | -- | -- | -- | -- |
| GCU | -2.49 | -- | -- | -- | -- | -- | -- |

The data sampling (tested part of the formation) may be biased because many of the wells tested were specifically targeted for the most productive intervals of the formations penetrated. Tests in wells generally do not characterize the entire HSU (or a specific formation) in aggregate but only shorter intervals selected during drilling or testing, usually because of the particular productivity of the interval. In general, UGTA characterization drilling and well completion decisions have focused on the more productive intervals under the assumption that the transport of contaminants will preferentially occur in those intervals. This bias is evident in cases of high hydraulic conductivity values for ostensible confining units. This generally results from testing a fractured interval within an otherwise low-conductivity formation.

5.18 Summary

The data presented in this summary come from a variety of sources and represent hydraulic property values measured at different scales. There were few pumping-scale tests within the RMSM HFM

area. The NTS Data Compilation Area database provides considerably more basis for determining representative distributions of hydraulic conductivity for generalized CGs. This analysis defines the range of property values and statistics for lognormal distribution of property values for CGs with sufficient data. The data available for hydraulic properties of HSUs are not definitive for the RMSM HFM area and do not provide specific characterization for the large-scale aggregate hydraulic properties of HSUs.

5.19 References

1. Stoller-Navarro Joint Venture. 2006. *Phase I Hydrologic Data for the Groundwater Flow and Contaminant Transport Model of Corrective Action Unit 97: Yucca Flat/Climax Mine, Nevada Test Site, Nye County, Nevada*, S-N/299205--077. Las Vegas, NV.
2. U.S. Department of Energy, National Nuclear Security Administration Nevada Site Office. 2003. *Underground Test Area Quality Assurance Project Plan, Nevada Test Site, Nevada*, DOE/NV--341-REV. 4. Las Vegas, NV.
3. National Security Technologies, LLC. 2007. *A Hydrostratigraphic Model and Alternatives for the Groundwater Flow and Contaminant Transport Model of Corrective Action Unit 99: Rainier Mesa-Shoshone Mountain, Nye County, Nevada*, DOE/NV/29546--146. Las Vegas, NV.
4. Stoller-Navarro Joint Venture. 2004. *Transferability of Data Related to the Underground Test Area Project, Nevada Test Site, Nye County, Nevada*, Rev. 0, S-N/99205--020. Las Vegas, NV.
5. Davis, J.C. 1986. *Statistics and Data Analysis in Geology*, Second Edition. John Wiley and Sons, Inc.
6. Freeze, R.A., and J.A. Cherry. 1979. *Groundwater*. Englewood Cliffs, NJ: Prentice Hall.
7. CRC Press. 2000. *CRC Handbook of Chemistry and Physics*, 81st edition.
8. National Research Council. 1996. *Rock Fractures and Fluid Flow. Contemporary Understanding and Applications*. Washington DC: National Academy Press.
9. Snow, D.T. 1969. "Anisotropic Permeability of Fractured Media." In *Water Resources Research*, Vol. 5, No. 6. Colorado School of Mines, Golden, CO.
10. Sanchez-Vila, X., P.M. Meier, and J. Carrera. 1999. "Pumping Tests in Heterogeneous Aquifers: An Analytical Study of What Can Be Obtained from their Interpretation Using Jacob's Method." In *Water Resources Research*, v. 35 (4): 943-952. Washington, DC: American Geophysical Union.
11. Kilroy, K.C. 1992. *Aquifer Storage Characteristics of Paleozoic Carbonate Rocks in Southeastern Nevada Estimated from Harmonic Analysis of Water-Level Fluctuations*. University of Nevada at Reno, Ph. D. Dissertation.
12. Barker, J.A., 1988. "A Generalized Radial Flow Model for Hydraulic Tests in Fractured Rock." In *Water Resources Research*, vol. 24, no. 10, pp. 1796-1804.
13. Duffield, G. 1996-2007. AQTESOLV for Windows Version 4.50 Professional, HydroSOLVE.

6.0 PRECIPITATION RECHARGE

Precipitation recharge is the input of water to a flow system due to subsurface infiltration of precipitation. In the RMSM area, there is no sustained surface flow, and precipitation recharge is an important part of the water budget [1].

6.1 Objectives

This section provides an overview of the processes that affect precipitation recharge in the RMSM area and provides spatial characterizations of precipitation recharge to the regional flow system.

6.2 Approach

There are many physical processes that affect the transport of water from the atmosphere to an aquifer that are difficult to accurately characterize. The quantity of precipitation that falls is the most important, but variability in topography causes uneven spatial distribution of precipitation. After a precipitation event occurs, the water must make its way from the surface to the water table to be considered recharge. Processes such as runoff and evapotranspiration affect the distribution and quantity of precipitation that becomes recharge. To characterize recharge, it is necessary to use a model that accounts for the processes that affect recharge by making assumptions about these processes; however, these assumptions can create systematic error. To characterize uncertainty inherent to a given modeling methodology, results from three recharge models employing different methodologies and assumptions are presented here.

6.3 Data Types and Prioritization

The recharge models presented here are predominantly developed and documented separate from the CAU-scale modeling effort. The data output from these models are datasets that contain recharge volumes for a uniform grid that covers the area of interest. The input data required for these models vary based on the methodology used, but all require precipitation and land surface elevation data. Various other data required for the models are spring, recharge, and soil chloride concentrations; land surface vegetation cover; and land surface lithology.

6.4 South-Central Great Basin Recharge Processes

The area surrounding the NTS lies principally within the most arid part of Nevada, the most arid state in the country [1]. As discussed in [Section 2.0](#), the NTS and surrounding areas are composed of north-south-trending mountain blocks separated by valleys. Orographic effects in the area cause a strong correlation between elevation and precipitation. Most of the precipitation in the area occurs as

rain and snowfall on the mountains. This correlation between recharge and elevation is the primary basis used to develop precipitation distributions.

To become recharge, precipitation must make its way into the ground and past the shallow subsurface root zone. The percentage of precipitation that becomes recharge is lower with lower amounts of precipitation. This idea was first quantified by Maxey and Eakin in 1949 in a study of recharge in southern Nevada [2]. To estimate recharge, they assume that areas receiving less than 20.3 centimeters per year (cm/yr) of precipitation have zero recharge. Areas with more precipitation are assigned increasingly larger percentages of precipitation as recharge.

Russell and Minor looked at soil chloride concentration profiles in 40 borehole sites in the alluvial vadose zone around the NTS area [3]. The average estimated recharge as a percentage of precipitation is 0.1% for all 40 borehole sites, with a maximum of 1.3% and average of 0.4% in wash environment sites, and a maximum of 0.06% and average of 0.02% in nonwash environment sites [3]. Although runoff from mountainous areas to low elevation and alluvial areas does occur through ephemeral streams and washes, the effect on overall recharge appears to be negligible. There are a few larger canyons, such as Fortymile Canyon, where significant flow has been observed after intense rainfall [4]. However, the effect of these features on overall recharge is debated.

6.5 Recharge Model Descriptions

Table 6-1 lists the four recharge models examined in this report:

Table 6-1
Recharge Models Considered

| Model | Total RMSM Recharge Rate (m ³ /day) |
|--|--|
| Revised UGTA Recharge Model [5] | 13,931 |
| USGS Distributed-Parameter Watershed Model [6] | 11,835 |
| DRI Chloride Mass Balance Model [3] | 19,296 |
| USGS DVRFS Model [7] | 14,192 |

m³/day = Cubic meters per day

The number of recharge models (as compared to previous CAUs) has been reduced to reduce overall complexity. For modeling methods where alternative models rely on slightly different assumptions, the primary recharge model using the most realistic set of assumptions is used. This simplification was done because results from previous CAU-scale modeling showed little difference in results between similar models.

6.5.1 Revised UGTA Recharge Model

The original UGTA recharge model was first developed during the regional model evaluation [8, 9]. This recharge model was derived using a modification to the Maxey-Eakin (ME) method [2] that involves reallocating recharge into canyons and washes. A revised version of the modified ME method was developed for the Frenchman Flat HDD [5] to incorporate new precipitation data and to correct errors and inconsistencies found in the original UGTA recharge model. The distribution of surface recharge across the site derived from this model is presented in Figure 6-1.

6.5.1.1 Methodology

The Revised UGTA Recharge Model uses a modification of the ME method. The ME method assigns areas to five different zones based on the amount of annual precipitation they receive. Recharge at a single location is calculated by the formula:

$$R_i = r_i P_i \quad (6-1)$$

where:

R_i = Recharge [L/T]

r_i = ME recharge coefficient for each delineated precipitation zone

P_i = Precipitation [L/T]

Recharge volume can be calculated over an area by multiplying R by the area for which R is representative. The zones defined in the original source [2] are: 0% recharge for precipitation of less than 20.3 cm/yr; 3% for 20.3 to 30.5 cm/yr; 7% for 30.5 to 38 cm/yr; 15% for 38 to 50.8 cm/yr; and 25% for greater than 50.8 cm/yr. This basic method has been used in a number of studies since its original publication with the coefficients changing slightly, but the same pattern is preserved with low coefficients for low precipitation zones.

The steps used in the modified ME method for the Revised UGTA Recharge Model are:

- Construct and update a precipitation map using new and existing data.
- Calculate recharge using ME coefficients.
- Calculate total recharge volumes for individual hydrographic areas.
- Redistribute a percentage of the total recharge within selected sub-areas to low-lying areas in wash or canyon reaches.
- Multiply the resulting recharge estimates for the entire model area by a coefficient calculated to make the estimated recharge value match the estimated discharge for the hydrographic area.

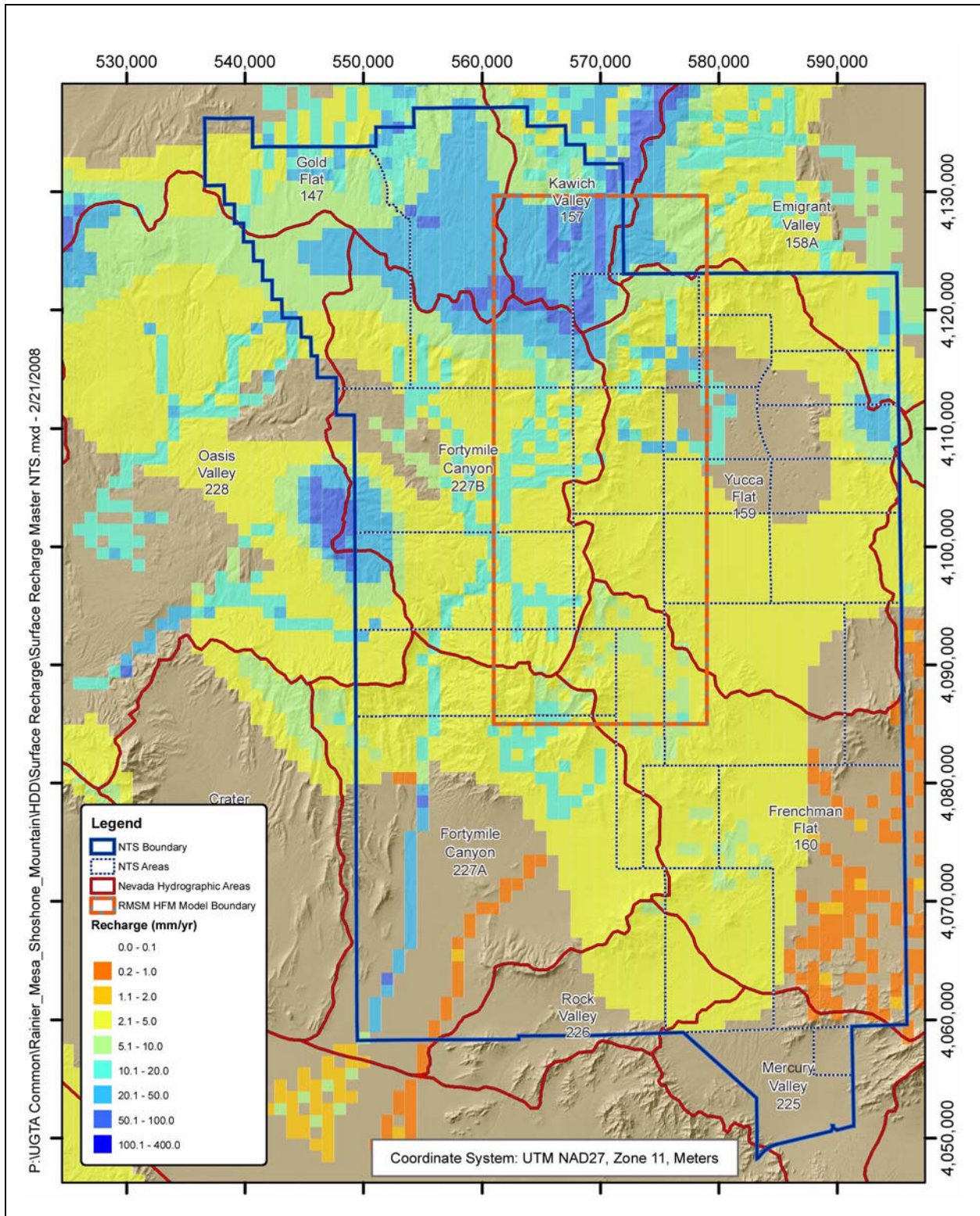


Figure 6-1
UGTA Revised Modified ME Recharge Model

6.5.1.2 Construction of the Digital Precipitation Map and Grid File

The precipitation map used for the Revised UGTA Recharge Model is a combination of two existing maps, Hardman [10] and James et al. [11]. The Hardman map covers Nevada but not the Death Valley portion of the UGTA regional groundwater flow system [10]. The James et al. map is used to fill in the Death Valley portion of the flow system [11]. Precipitation station data are also added to the map and used to make minimal changes to the map contours. The resulting contours are gridded on a 1-by-1-km cell grid. The Frenchman Flat HDD [5] presents the total recharge values for individual hydrographic areas.

6.5.1.3 Recharge Distribution and Reallocation

Preliminary recharge amounts are calculated from the precipitation map grid and the ME coefficients above. The redistribution of recharge by runoff in large canyons is taken into account by the Revised UGTA Recharge Model via a process outlined in detail in the Frenchman Flat HDD [5]. The redistribution routine moves a portion of the recharge from higher-elevation canyons to lower-elevation washes.

6.5.2 USGS Recharge Model

The distributed parameter watershed (DPWS) model uses net-infiltration estimates to quantify the downward percolation of water across the lower boundary of the root zone. The water that makes it past the root zone is interpreted as recharge [6]. The model is based on a water-balance conceptual model of net infiltration for arid to semiarid environments. The major components of this conceptual model include:

- Precipitation
- Infiltration of rain, snowmelt, and surface water into soil or bedrock
- Surface-water runoff
- Surface-water run-on (overland flow and stream flow)
- Bare soil evaporation
- Transpiration from the root zone
- Redistribution of water content in the root zone
- Net infiltration across the lower boundary of the root zone

The DPWS model report examines the effect of several different parameters on recharge by creating four different models [6]. Model 1 in the report has been called the “USGS Redistribution Model” in previous CAU reports and is the model data used for this report. The DPWS model report contains the documentation of the distributed parameter model, and a summary of the model is presented in the DVRFS report [7]. The spatial distribution of recharge is presented in [Figure 6-2](#).

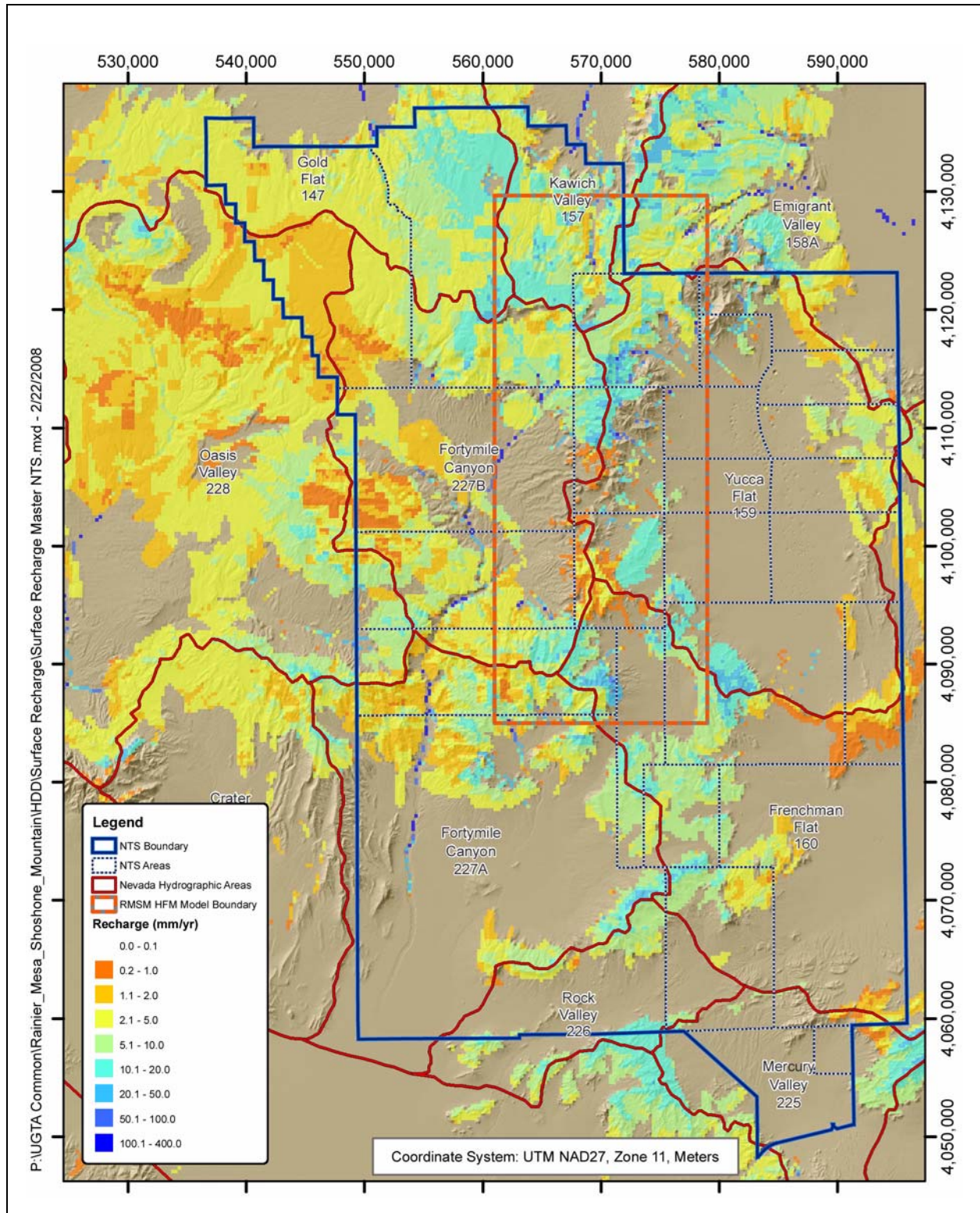


Figure 6-2
USGS DPWM Recharge Model

6.5.3 DRI Recharge Model

The DRI model uses the flux of chloride through the hydrologic system to determine basin inputs and outputs. This model is often referred to as the DRI Chloride Mass Balance (CMB) Model. Chloride is a conservative ion involved in few reactive processes in groundwater flow systems. In the area of the NTS, the primary source of chloride is precipitation, and the primary sink is dissolved chloride in water that leaves the system.

The CMB model was originally developed in Russell and Minor [3]. The original report examines discharge rates and chloride and bromide concentrations at 17 springs located in the Sheep Range, the Spring Mountains, and within the NTS, and provides estimates for 15 hydrographic basins. Since the original report, the DRI has performed work to expand the results to the entire DVRFS model area. These expanded results are used in this report. The results are gridded on the same grid as the DVRFS. Two models are presented in Russell and Minor [3]. The results of the alluvial and elevation mask model are presented here.

Statistical procedures are used to evaluate uncertainty in measurements of the chloride concentration from individual springs, disagreement among isohyetal maps of the area, the spatial and temporal variability in the chloride flux, and the elevation of the watershed for any given spring. The uncertainty associated with each of the variables is incorporated into 1,000 Monte Carlo simulations to estimate the uncertainty in the prediction of recharge rates. The mean recharge value and coefficient of variation for each grid cell are shown in [Figures 6-3 and 6-4](#).

6.5.4 USGS DVRFS Model

The DVRFS recharge model is based mainly on the USGS 2003 DPWS model with redistribution. The DVRFS recharge model is regridded at the DVRFS grid spacing of 1.5 km, and the results are adjusted in zones to better match input recharge with output discharge modeled in the DVRFS. Creation of the DVRFS model is documented in Belcher et al. [7] and Blainey et al. [12]. The spatial distribution of recharge from the model is shown in [Figure 6-5](#).

6.6 Limitations

Numerous limitations are documented in the development of each of the reported recharge models. The reader is directed to those reports to obtain a complete description of each limitation, including how and at what point in the application of the methodology it affects the resultant recharge estimate. However, there are several limitations that all authors of the reports found in common.

First, all authors agree that the sparsity of precipitation data, especially at higher elevations and in remote areas, greatly increases the uncertainty in the resultant recharge. In addition, the length of record and conversion of snowpack to liquid precipitation have a significant impact on the outcome of the estimates.

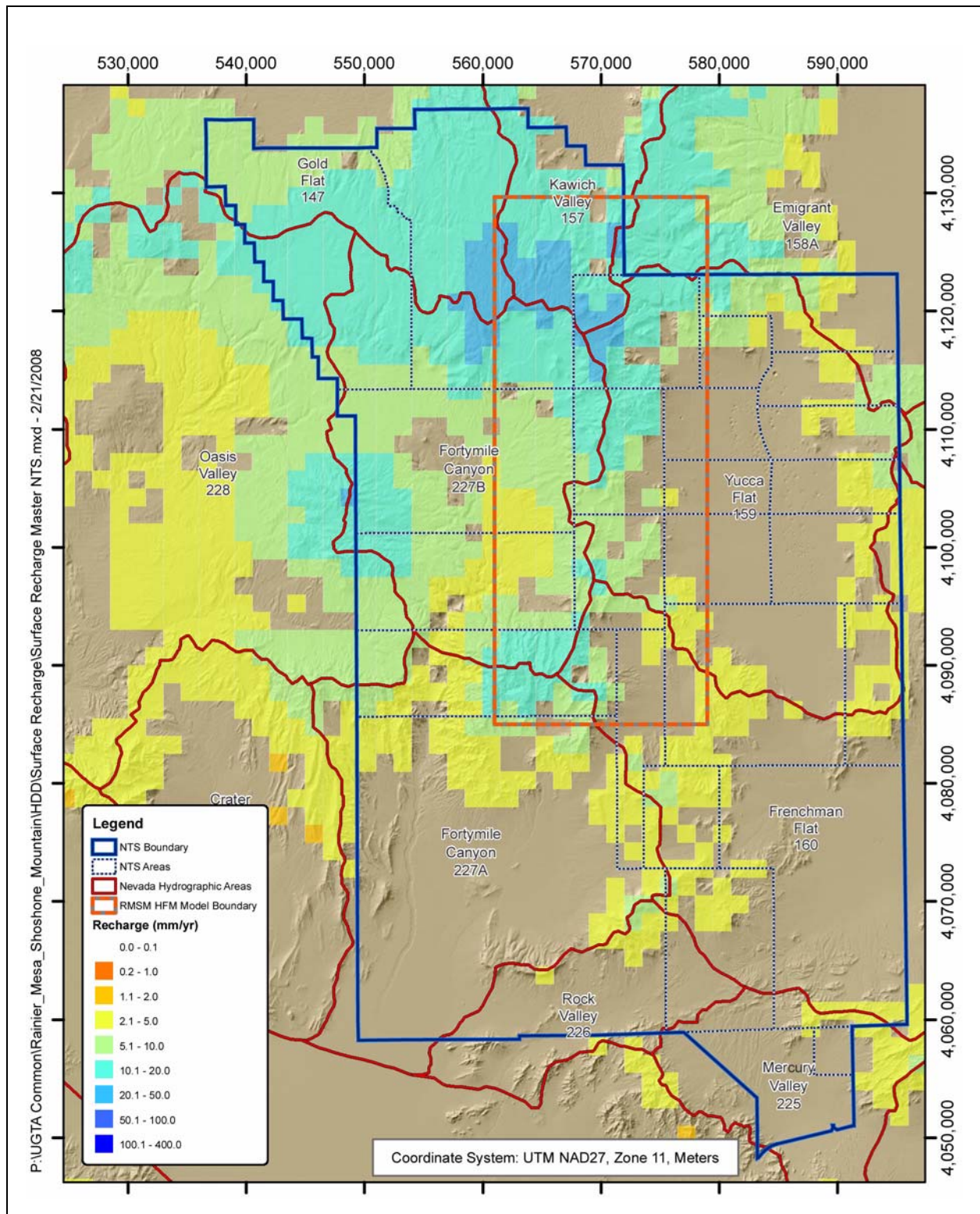


Figure 6-3
RSM DRI CMB Recharge Model Mean

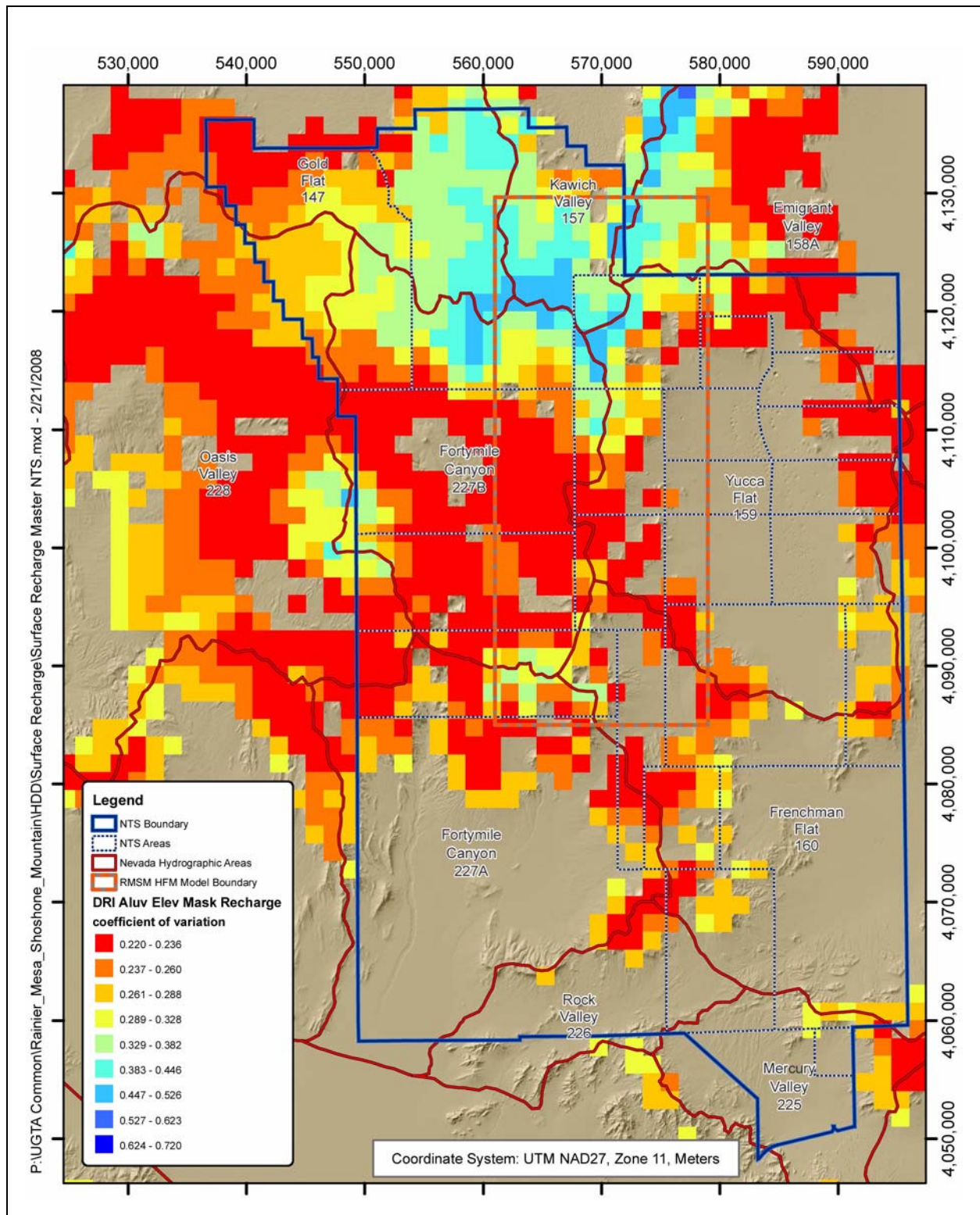


Figure 6-4
RMSM DRI CMB Recharge Model Coefficient of Variation

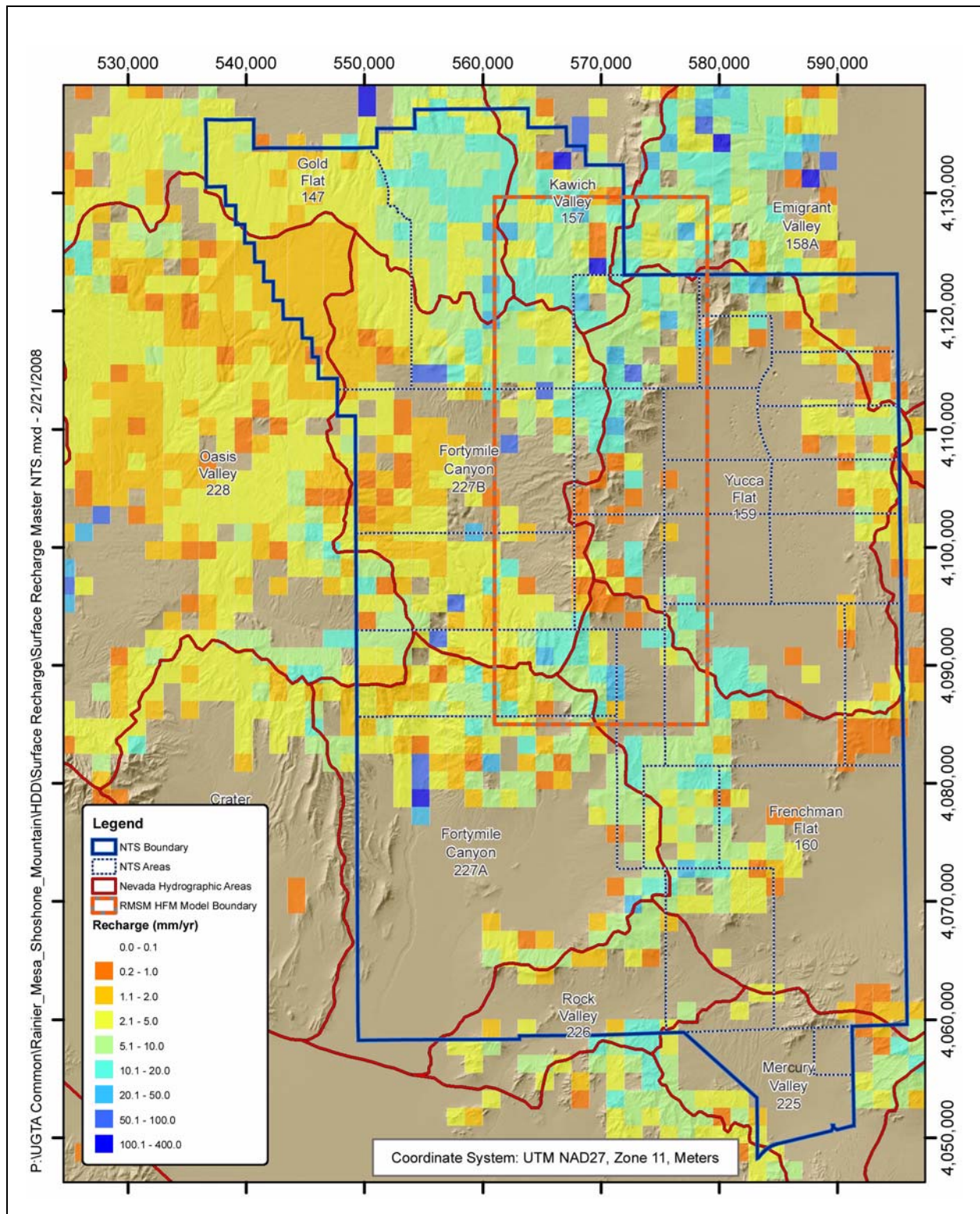


Figure 6-5
USGS DVRFS Recharge Model

Second, the other data types necessary to support each of the methods discussed in this section are limited (e.g., chloride and bromide concentrations in the DRI method [3]). The regional aspect of the model makes it very difficult and costly to collect sufficient detailed data to develop more than coarse estimates of recharge. Recharge models with many uncertain parameters may introduce more uncertainty, as variability in each parameter would potentially compound the overall uncertainty in the recharge distribution.

Third, the ME method and, to a smaller extent, the other methods depend on a mass balance approach that involves the quantification of discharge, which is uncertain because it cannot be measured directly. Finally, the unsaturated zone is thick and could redistribute water before it reaches the water table.

6.7 References

1. Winograd, I.J., and W. Thordarson. 1975. *Hydrogeologic and Hydrochemical Framework, South-Central Great Basin, Nevada-California, with Special Reference to the Nevada Test Site*, USGS-PP-712-C. Denver, CO: U.S. Geological Survey.
2. Maxey, G.B., and T.E. Eakin. 1949. "Groundwater in White River Valley, White Pine, Nye and Lincoln Counties, Nevada." In *Water Resources Bulletin* No. 8. Carson City, NV: State of Nevada, Office of the State Engineer.
3. Russell, C.E., and T. Minor. 2002. *Reconnaissance Estimates of Recharge Based on an Elevation-dependent Chloride Mass-balance Approach*, DOE/NV/11508-37, Publication No. 45164. Prepared for the U.S. Department of Energy, National Nuclear Security Administration Nevada Operations Office. Las Vegas, NV: Desert Research Institute.
4. Savard, C.S. 1994. "Groundwater Recharge in Fortymile Wash Near Yucca Mountain, Nevada, 1992-1993." In *Radioactive Waste Management*, Vol. 4: 1,805-1,813. Washington, DC: American Nuclear Society.
5. Stoller-Navarro Joint Venture. 2004. *Phase II Hydrologic Data for the Groundwater Flow and Contaminant Transport Model of Corrective Action Unit 98: Frenchman Flat, Nevada*, S-N/99205-032. Las Vegas, NV.
6. Hevesi, J.A., A.L. Flint, and L.E. Flint. 2003. *Simulation of Net Infiltration Using a Distributed Parameter Watershed Model for the Death Valley Regional Flow System, Nevada and California*, Water-Resources Investigations Report 03-4090. Sacramento, CA: U.S. Geological Survey.
7. Belcher, W.R., J.B. Blainey, F.A. D'Agnesse, C.C. Faunt, M.C. Hill, R.J. Lacznia, G.M. O'Brien, C.J. Potter, H.M. Putnam, C.A. San Juan, and D.S. Sweetkind. 2004. *Death Valley Regional Ground-Water Flow System, Nevada and California - Hydrogeologic Framework and Transient Ground-Water Flow Model*, Scientific Investigations Report 2004-5205. U.S. Geological Survey.
8. U.S. Department of Energy, Nevada Operations Office. 1997. *Regional Groundwater Flow and Tritium Transport Modeling and Risk Assessment of the Underground Test Area, Nevada Test Site, Nevada*, DOE/NV--477. Las Vegas, NV.

9. IT Corporation. 1996. *Groundwater Recharge and Discharge Data Documentation Package (Phase I Data Analysis Documentation, Volume III)*. Prepared for the U.S. Department of Energy, Nevada Operations Office. Las Vegas, NV.
10. Hardman, G. 1965. *Nevada Precipitation and Acreages of Land by Rainfall Zones*. Reno, NV: U.S. Department of Agriculture, University of Nevada Experimental Station.
11. James, J.W., T. Hendricks, and K. Sorenson. 1993. *Climate of the Death Valley Region, Nevada/California*. Prepared for the National Park Service. Reno, NV: State of Nevada, Office of the State Climatologist.
12. Blainey, J.B., C.C. Faunt, and M.C. Hill. 2006. *A Guide for Using the Transient Ground-Water Flow Model of the Death Valley Regional; Ground-Water Flow System, Nevada and California*. Open-File Report 2006-1104. U.S. Geological Survey.

7.0 GROUNDWATER DISCHARGE

Groundwater discharge in a flow system is water that leaves the system at the surface. In the RMSM area, there are three processes that represent surface discharge:

- Production of water from wells for water supply and investigative purposes
- Natural discharge of groundwater from springs
- Artificial discharge of water created by the drilling of tunnels in Rainier Mesa

Figure 7-1 shows the locations of these discharge features in the RMSM area.

7.1 Well Discharge

Well discharge is water that is pumped from an aquifer by means of a well. Wells that produce water in the RMSM area are used for industrial water supply purposes and for scientific investigative purposes. The USGS/USDOE Cooperative Studies website catalogs most major long-term production of water from wells on the NTS [1]. Short-term withdrawals from wells as part of the ER UGTA testing program can be large and are examined here; however, in the RMSM area, they do not appear to be significant.

Well WW-8 was completed in January 1963. The well is located at the western edge of the RMSM HFM area at the northern edge of Area 18. It is completed to a depth of 1,673.4 m with an open interval from 1,145.9 to 1,726.6 amsl producing from the BRA. From the commencement of water production in 1963 through 2006, the last year of record, this well had produced some 5.5 million cubic meters of water. Figure 7-2 shows total water production from the well by year.

Water production at UE-16d WW started in 1981 for water supply purposes, and the well is still active. The well is located in the northeast corner of Area 16. The UE-16d WW was originally drilled to a total depth of 914.4 m (513.3 m amsl); however, the bottom of the hole is sealed off with a bridge plug near the bottom of the main casing, and the well is open from 835.2 to 1,198.2 m amsl. This producing interval is within the UCA, a carbonate section hydraulically isolated from the LCA in this area. The well produced about 2.8 million cubic meters (m³) of water from 1981 to 2005 [1]. Figure 7-2 shows total water production from the well by year.

Well UE-2ce is located in the western part of Area 2 in Yucca Flat and is 183 m from the site of the NASH test. The well was used from May 1977 to August 1984, and the average annual production was 5,200 m³ [1]. The well was drilled after the NASH test, and water production from the well was used to monitor tritium in the groundwater. Production measurements for this well are from a status report for the Radionuclide Migration Project [2]. Well UE-2ce is open from 949.3 to 1,011.1 m amsl within the LCA3, which is hydraulically separated from the LCA by a thick section of UCCU at this

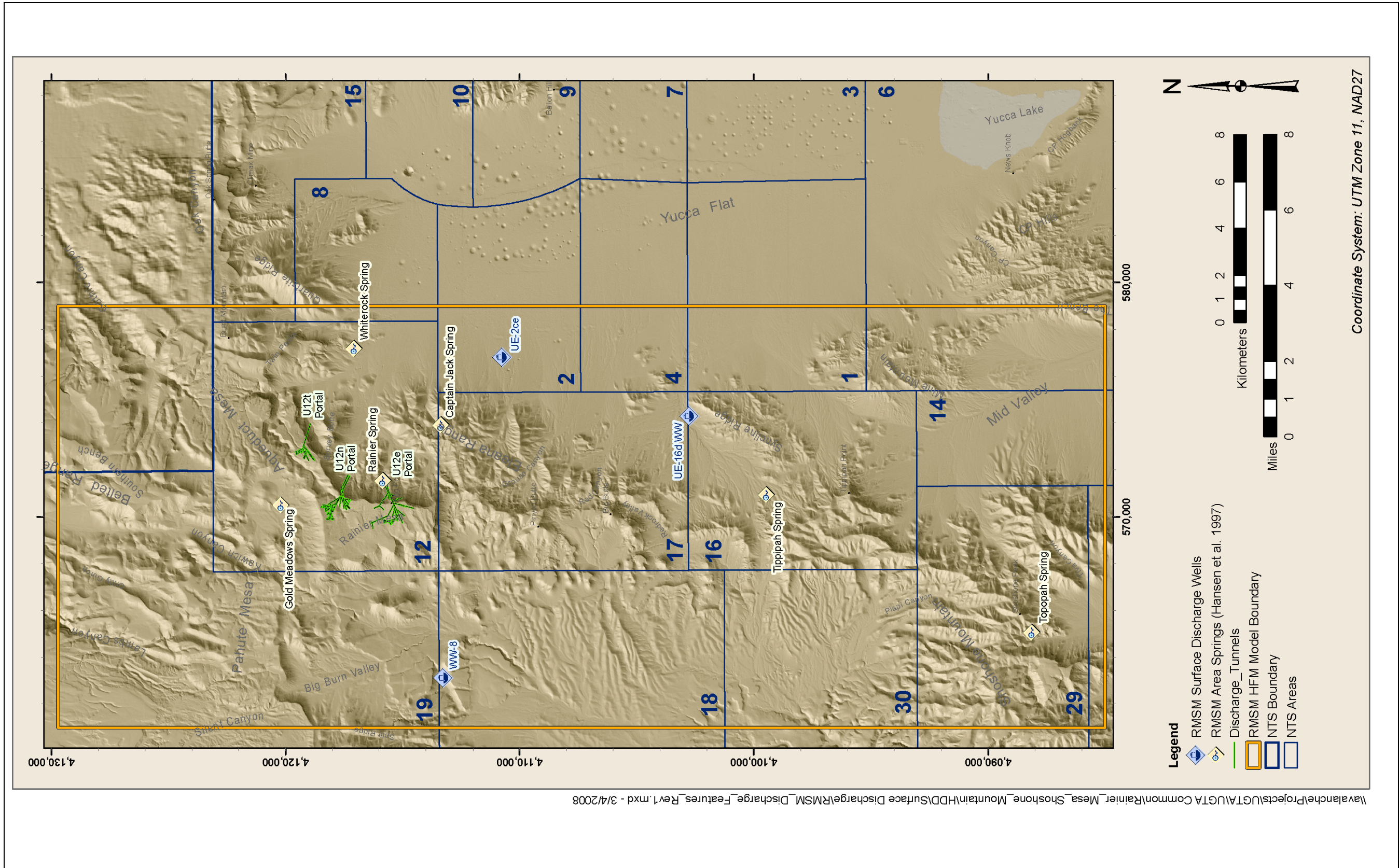


Figure 7-1
RMSM Area Discharge Features

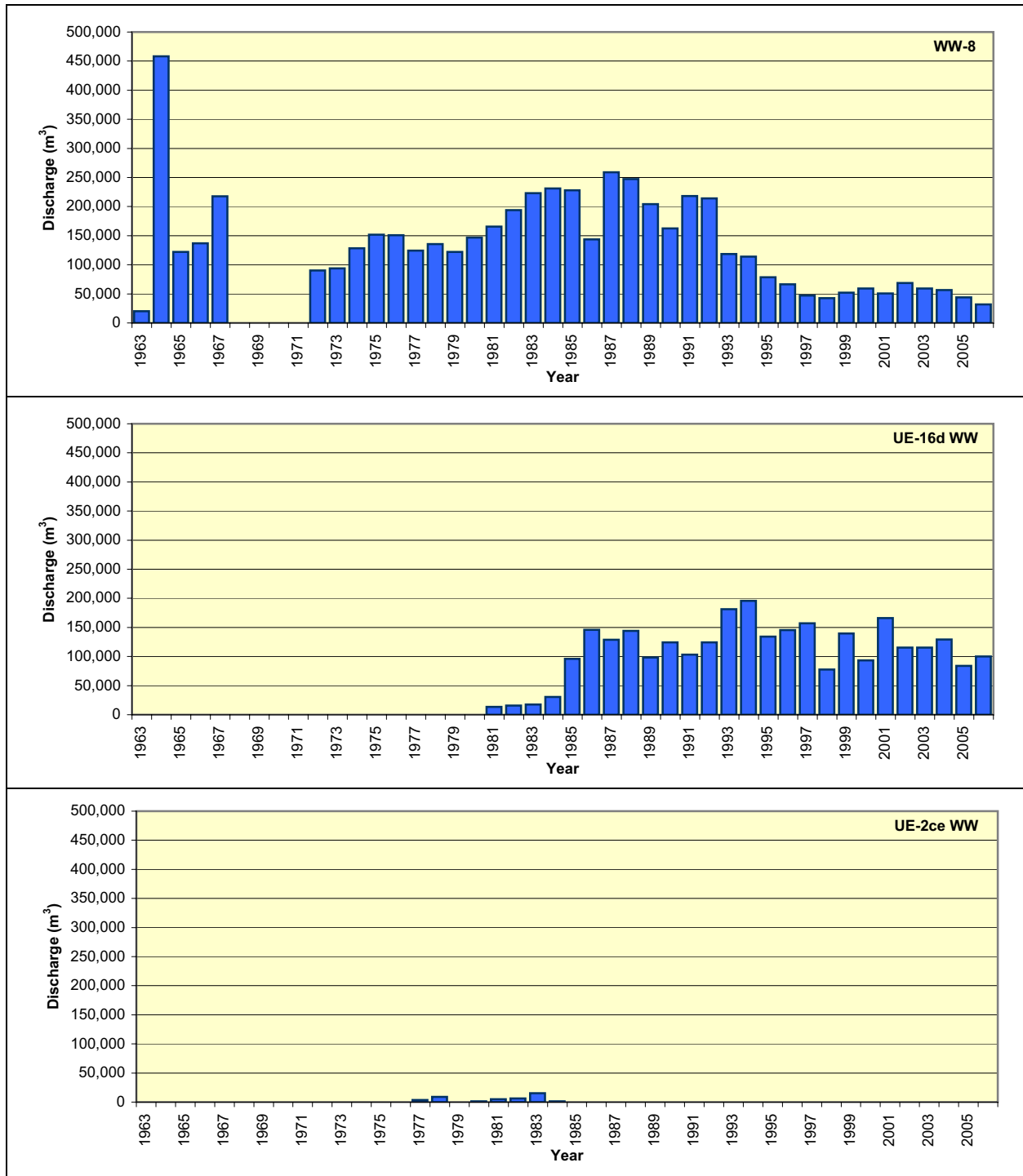


Figure 7-2
RMSM Area Well Discharge Graphs

location. Production from this well ceased when the pump failed. The well produced a total of 0.042 million m³ of water from 1977 to 1984. [Figure 7-2](#) shows total water production from the well by year.

In some areas of the NTS, large multiple-well aquifer tests have produced significant quantities of water for aquifer characterization as part of the UGTA ER program. These types of tests have not been performed in the RMSM area, and the tests are generally short term. There are six wells in the RMSM area that have produced water for the ER testing program. The wells are U-12s, ER-12-1, ER-12-2, ER-12-3, ER-12-4, and ER-16-1. The total volume of water produced from these wells is small (< 2,500 m³ per well). Water introduced into the well during drilling is generally close to the amount produced from them during testing. More information on the production of water from these wells is included in the RMSM_Well_Discharge.xls workbook in the Appendix\D folder on the accompanying DVD.

7.2 Spring Discharge

Springs are groundwater discharges to the ground surface at locations where the ground surface locally intersects the level of saturation in the formation. The springs in the RMSM area have very low discharges at elevations well above the regional water-table level [\[3\]](#). The discharge rates of some of the springs are shown to be closely correlated with short-term precipitation events [\[4\]](#). The water discharged from these springs flows only a short distance to small wetlands where some proportion of the water is lost to evapotranspiration and the remainder reinfilters [\[4\]](#). The net effect of these springs on the groundwater flow system is to decrease and redistribute the net infiltration to the regional water table.

The spring discharges in the RMSM area are variable, and there have been several studies that characterize them. Sustained flow for the larger springs is as much as 2.7 liters per minute (Lpm) (about 1,400 cubic meters per year [m³/yr]), and the smallest springs discharge only intermittently after rainfall [\[3\]](#). Springflow measurement data with sources are provided in the RMSM_Spring_Discharge.xls workbook in the Appendix\D folder on the accompanying DVD. Spring discharge is not believed to have a significant effect on the regional groundwater flow.

7.3 Tunnel Discharge

A number of tunnels were mined into Rainier and Aqueduct Mesas and Shoshone Mountain for the purpose of conducting underground nuclear tests. At Shoshone Mountain, the groundwater level is deep, and very little groundwater was encountered during tunneling. Rainier and Aqueduct Mesas (located in close proximity to each other) receive relatively large amounts of precipitation relative to the flats on the NTS. Water that infiltrates is temporarily retained in the mesas by a layer of low permeability zeolitic tuffs. Tunnels mined into the lower portion of these tuffs encounter fractures containing water and drain it to the surface [\[5\]](#).

There are three tunnel complexes in Rainier Mesa that have had significant groundwater discharge: U12t, U12n, and U12e. Discharge from these complexes has been variable. Tunnel discharge is

greatest immediately after mining and tapers off with time to a base discharge rate that varies with seasonal precipitation. The tunnels were expanded over time with new drifts in each of the tunnel complexes. The initial discharge of these tunnels was as high as 1,900 Lpm (about 1 million m³/yr), but the discharge quickly tapers off [5]. The largest sustained historic discharge for a single tunnel (U12t) is about 350 Lpm (180,000 m³/yr) [6]. The discharged water is redirected to unlined ponds where some portion evaporates and the rest reinfilters. Discharge data for the tunnels are contained in the RMSM_Tunnel_Discharge.xls workbook in the Appendix\D folder on the accompanying DVD.

The U12t Tunnel complex was sealed in 1993 [7], and the U12n Tunnel complex was sealed in 1994 [8]. These tunnels no longer discharge to the surface. An attempt to seal the U12e Tunnel complex in 1994 was unsuccessful, and the tunnel currently discharges water at 28 to 35 Lpm (about 14,000 to 18,000 m³/yr) [9].

Significant long-term discharge has not been observed at other tunnels in Rainier Mesa. A few small seeps were encountered during the mining of U12a, U12b, and U12g [5], but there is no evidence that these tunnels have had sustained discharge. No water was encountered during the mining of U12i, U12j, and U12k [5]. The U12c, U12d, and U12f Tunnels are short tunnels in close proximity to and at a slightly higher altitude than U12b, and no discharge has been observed at these locations. No information about U12p discharge is mentioned in the reports documenting perched water and tunnel discharge examined for this report. Finally, no water was found in the vicinity of the U16a chamber by exploratory drill holes created for the express purpose of exploring for perched water [10].

7.4 References

Hansen et al., 1997, see [3].

1. U.S. Geological Survey. 2007. "USGS/USDOE Cooperative Studies in Nevada; Water-Use Wells, Nevada Test Site and Vicinity." As accessed at: http://nevada.usgs.gov/doe_nv/wateruse/wu_map.htm on 26 October.
2. Buddemeier and Isherwood. 1985. *Radionuclide Migration Project 1984 Progress Report*, UCRL-53628. Livermore, CA: Lawrence Livermore National Laboratory.
3. Hansen, D.J., P.D. Greger, C.A. Wills, and W.K. Ostler. 1997. *Nevada Test Site Wetlands Assessment*, Las Vegas, NV: Bechtel Nevada.
4. Lyles, B.F., J. Edkins, R.L. Jacobson, and J.W. Hess. 1990. *Time-Series Analysis of Ion and Isotope Geochemistry of Selected Springs of the Nevada Test Site, Nye County, Nevada*, Water Resources Center, DOE/NV/10384-27; Publication, No. 45068. Las Vegas, NV: Desert Research Institute.
5. Thordarson, W. 1965. *Perched Groundwater in Zeolitized-Bedded Tuff, Rainier Mesa and Vicinity, Nevada Test Site*, Trace Elements Investigations-862. U.S. Geological Survey.

6. Russell, C.E., L. Gillespie, and D. Gillespie. 1993. *Geochemical and Hydrologic Characterization of the Effluent Draining from U12E, U12N, and U12T Tunnels, Area 12 Nevada Test Site*. DOE/NV/10845-21, Pub. #45105. Las Vegas, NV.
7. Defense Threat Reduction Agency. 2007. *Corrective Action Decision Document/Closure Report for Corrective Action Unit 478: Area 12 T-Tunnel Ponds, Nevada Test Site, Nevada*. Las Vegas, NV.
8. Defense Threat Reduction Agency. 2007. *Corrective Action Decision Document/Closure Report for Corrective Action Unit 480: Area 12 N-Tunnel Ponds, Nevada Test Site, Nevada*. Las Vegas, NV.
9. Defense Nuclear Agency, Nevada Operations Office. 1996. *E-Tunnel Discharge Elimination Review Committee Final Report*. Mercury, Nevada.
10. Davies, R.E. 1962. *Technical Letter: Marshmallow-3, Results of Exploration for Water Superjacent to the U16a Chamber, Nevada Test Site*. U.S. Geologic Survey.

8.0 LATERAL BOUNDARY FLUX EVALUATIONS

8.1 Introduction

The objective of the regional-scale modeling presented here is to provide a range of lateral boundary fluxes that can be used as calibration guidelines for the RMSM CAU-scale flow model. The fluxes reported here are for the current CAU boundaries. Should the boundaries of subsequent modeling efforts differ, reanalysis will be required. However, any reanalysis can use the models and parameters resulting from this work, greatly reducing the effort required.

Inflow and outflow through the lateral boundaries of the RMSM CAU-scale groundwater flow model constitute an important portion of the water budget components of the system to be modeled. The other water budget components include precipitation recharge and internal groundwater system discharge (springs and well discharge). Precipitation recharge is addressed in [Section 6.0](#), and discharge is addressed in [Section 7.0](#). Estimating the flux of groundwater through the model area, as described in this section, was undertaken as it is an important physical aspect of the groundwater flow system and will be used as a calibration target in future contaminant transport modeling.

There are no practical means of directly measuring groundwater fluxes at the scale and spatial frequency needed to represent the conditions at the CAU flow-model boundary. Estimates can be made using hydraulic gradients and conductivities to derive the groundwater fluxes as was done for the eastern part of Pahute Mesa [1]. However, the lateral boundary fluxes for the CAU flow model are best estimated indirectly using a regional-scale flow model, which conserves the mass of water over the entire regional flow system and is controlled by a more detailed conceptualization of flow within the system. The DVRFS model developed by the USGS and variations thereof were calibrated to capture the variability in the boundary fluxes resulting from differences in the conceptualizations of the RMSM CAU HFM (see [Section 8.5](#)) and regional recharge distribution (see [Section 6.0](#)).

8.2 Models Used

This section discusses five different models:

- USGS DVRFS Model
- NTS Flow Model
- No Redrock Valley Caldera Alternative
- More Extensive LCA3 Alternative
- Shoshone Mountain Thrust Sheet Alternative

The DVRFS was the base model used [2]. Figure 8-1 shows the area encompassed by the model as well as prominent topographic features. The DVRFS model is a Modular Three-Dimensional Finite Difference Ground-Water Flow (MODFLOW) model developed by the USGS [3]. MODFLOW is a computer code that solves the groundwater flow equation in three dimensions using finite differences. The program is used to simulate the flow of groundwater through saturated media.

The NTS Flow Model is the DVRFS model with the four NTS CAU-scale HFM models inserted into it. The four CAU-scale HFM models were developed for Pahute Mesa, RMSM, Yucca Flat, and Frenchman Flat. The three alternative models are the NTS Flow Model with different configurations of the geological units incorporated into the RMSM CAU model. These models represent possible geological configurations for the RMSM CAU that the current data do not rule out.

The DVRFS model was run first. Following this evaluation of the groundwater fluxes through the RMSM HFM area, the NTS Flow Model was calibrated and groundwater fluxes through the RMSM HFM determined. This work was followed by calibration of the three alternate framework models (AFMs) and the determination of groundwater fluxes. The individual NTS CAU models and their alternatives are described in the hydrostratigraphic model and alternatives documents for Pahute Mesa, RMSM, Yucca Flat, and Frenchman Flat [4-7].

The version of MODFLOW 2000 installed to run the models is included in the Groundwater Modeling System (GMS) Version 6.0 software bundle [8]. The GMS software was used to post-process and visualize the results of each run. The post-processing included extracting the boundary flows presented here for the RMSM HFM area. With the exception of the QA run done to verify the proper installation and running of the DVRFS model, all runs were completed using the single precision code mf2k.exe and the Geometric Multigrid (GMG) solver. The DVRFS QA run was done using the double precision code mf2k_13_00-dp.exe and Link-Algebraic Multigrid (LMG) solver to match the work done by the USGS. All runs were steady state.

8.3 Recharge Scenarios

Three different recharge scenarios were used in the lateral boundary flux modeling. The scenarios, described in Section 6.0, are the USGS DVRFS Model (regional), Revised UGTA Recharge Model (revised UGTA), and DRI Chloride Mass Balance Model (DRI). The DVRFS and NTS Flow Model analyses were completed for all three scenarios. Detailed descriptions of the models can be found in Section 5.0 of the RMSM HFM report [5]. The AFM runs were analyzed for the regional recharge scenario only. The recharge scenarios were selected to provide a full range of values for analysis. The USGS Distributed-Parameter Watershed Model, discussed in Section 6.0, was not selected for use as the values for that scenario are not significantly different from those of the USGS DVRFS Model.



Figure 8-1
Geographic and Prominent Topographic Features of the DVRFS Region, Nevada and California

8.4 DVRFS Model Flows Calculated for the Recharge Scenarios

The DVRFS model was run under the three recharge scenarios using the parameter values as defined in [2]. The only exceptions to this statement being that the recharge multiplier variables RCH_2, RCH_35, RCH_467, and RCH_9 were modified for the revised UGTA recharge run to further lower the overall difference between observed and estimated values of hydraulic head.

The sums of weighted residual errors calculated for the three recharge scenarios range from a low of 12,611 to a high of 22,115. Table 8-1 presents a summary of the results.

In addition to the residual errors, Table 8-1 also presents a summary of the flows calculated passing through the top of the RMSM HFM area (recharge) as well as through the northern, southern, eastern, and western sides. The bottom of the model was simulated as a no-flow zone. (The lateral boundaries of the RMSM HFM area are shown in Figure 8-2.) Reference to the table shows the revised UGTA recharge scenario yielded the greatest overall flow through the RMSM HFM area at 28,058 m³/day and the DRI recharge scenario the lowest at 18,646 m³/day. For all three scenarios, there was net flow into the model area through the northern face of the model area and the surface (recharge). There was net flow out the eastern, western, and southern boundaries with the greatest net flow out through the eastern model face toward Yucca Flat. In all cases, the net flow calculated through the model area was balanced with 0% difference, to two significant digits, between the flows in and out.

When considering flow through the entire model area, the DRI recharge scenario at 659,528 m³/day exhibits the greatest flow volume and the revised UGTA recharge scenario at 584,056 the lowest. However, the values are not greatly different. The constant-head boundary fluxes for the DVRFS Model Area Flows presented here and throughout this section are based on the original USGS weighting factors. The values are summarized in Table 8-1.

Figures 8-2 through 8-4 show two-dimensional (2-D) plots of the residual heads determined for each of the recharge scenarios. Each data point is a location with an observed hydraulic head. The values shown are in meters and represent the absolute values of unweighted calculated minus observed heads. Reference to the figures shows that a similar overall pattern is present in each. The majority of the residuals are in the range of no more than 50 m. Comparing the various results, the most remarkable difference is the lack of excessive groundwater mounding over the Spring Mountains in the southeastern quadrant for the regional recharge scenario (Figure 8-2). The groundwater mounding is most pronounced here for the DRI recharge scenario (Figure 8-4) and represents an excess in the amount of recharge applied to this area. One large residual that is present in all of the simulations is found at the southern extreme of the DVRFS model area. This point is represented by a large orange point in Figures 8-2 through 8-4, indicating a residual in the range of 401 to 450 m. This hydraulic head measurement is for a relatively shallow well at a significant elevation above the valley floor in this area. The sediments in which this well is installed are hydraulically separate from those monitored in the valley by the points to the east of this large residual. The residuals at those points vary between 0 and 150 m.

**Table 8-1
DVRFS Model Run Results**

| | Recharge Scenario | | |
|--|--------------------------|--------------------------|--------------------------|
| | Regional | Revised UGTA | DRI |
| Sum of Squared Weighted Residuals | | | |
| Heads Only | 11,531.0 | 19,130.0 | 16,800.0 |
| Drain Flows Only | 536.93 | 1,870.9 | 1,300.3 |
| Constant Head Boundary Flows | 543.34 | 1,114.4 | 284.0 |
| Sum | 12,611.27 | 22,115.0 | 18,385.0 |
| RMSM HFM Area Boundary Flows | m³/day | m³/day | m³/day |
| North | 9,814.3 | 5,306.5 | 9,997.9 |
| South | -6,513.2 | -8,395.7 | -6,559.2 |
| East | -9,450.8 | -12,844.2 | -7,956.9 |
| West | -7,589.7 | -6,817.6 | -4,130.3 |
| Recharge | 13,739.3 | 22,751.0 | 8,648.4 |
| Total In | 23,553.7 | 28,057.5 | 18,646.3 |
| Total Out | -23,553.7 | -28,057.5 | -18,646.3 |
| Cumulative | 0.0 | 0.0 | 0.0 |
| Percent Difference ^a | 0.00% | 0.00% | 0.00% |
| DVRFS Model Area Flows | m³/day | m³/day | m³/day |
| IN | | | |
| CONSTANT HEAD | 349,591.3 | 388,437.3 | 346,831.2 |
| DRAINS | 0.0 | 0.0 | 0.0 |
| RECHARGE | 303,415.3 | 195,618.5 | 312,696.9 |
| TOTAL IN | 653,006.6 | 584,055.8 | 659,528.1 |
| OUT | | | |
| CONSTANT HEAD | 283,122.9 | 265,104.7 | 311,345.2 |
| DRAINS | 369,884.4 | 318,951.2 | 348,182.9 |
| RECHARGE | 0.0 | 0.0 | 0.0 |
| TOTAL OUT | 653,007.3 | 584,055.9 | 659,528.1 |
| IN - OUT | -0.6 | -0.1 | 0.0 |
| % DISCREPANCY | 0.0 | 0.0 | 0.0 |

^a Calculated as ((inflow + recharge) – (outflow)) / (outflow)

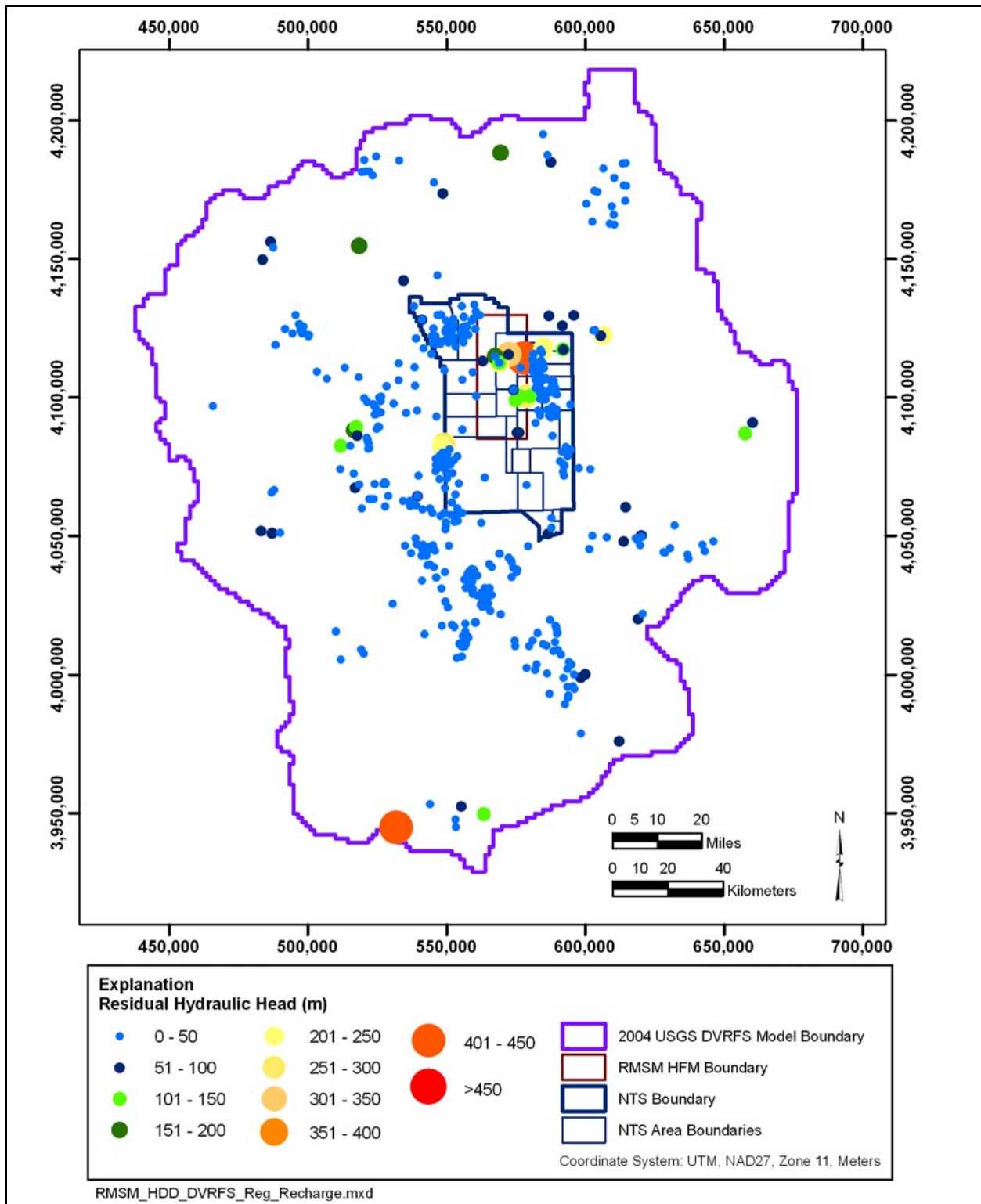


Figure 8-2
Unweighted Residual Hydraulic Heads for the DVRFS Regional Recharge Scenario

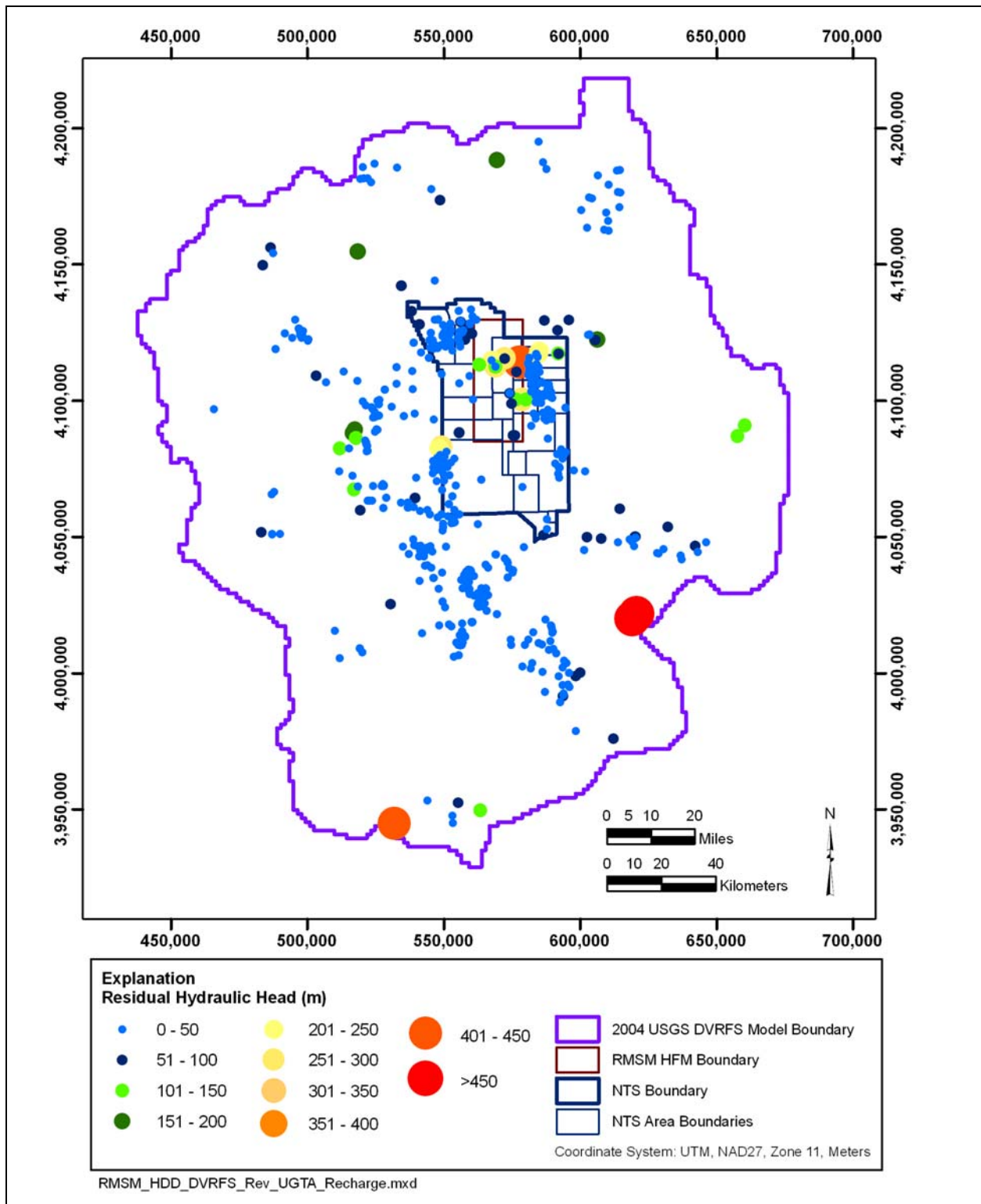


Figure 8-3
Unweighted Residual Hydraulic Heads for the DVRFS
Revised UGTA Recharge Scenario

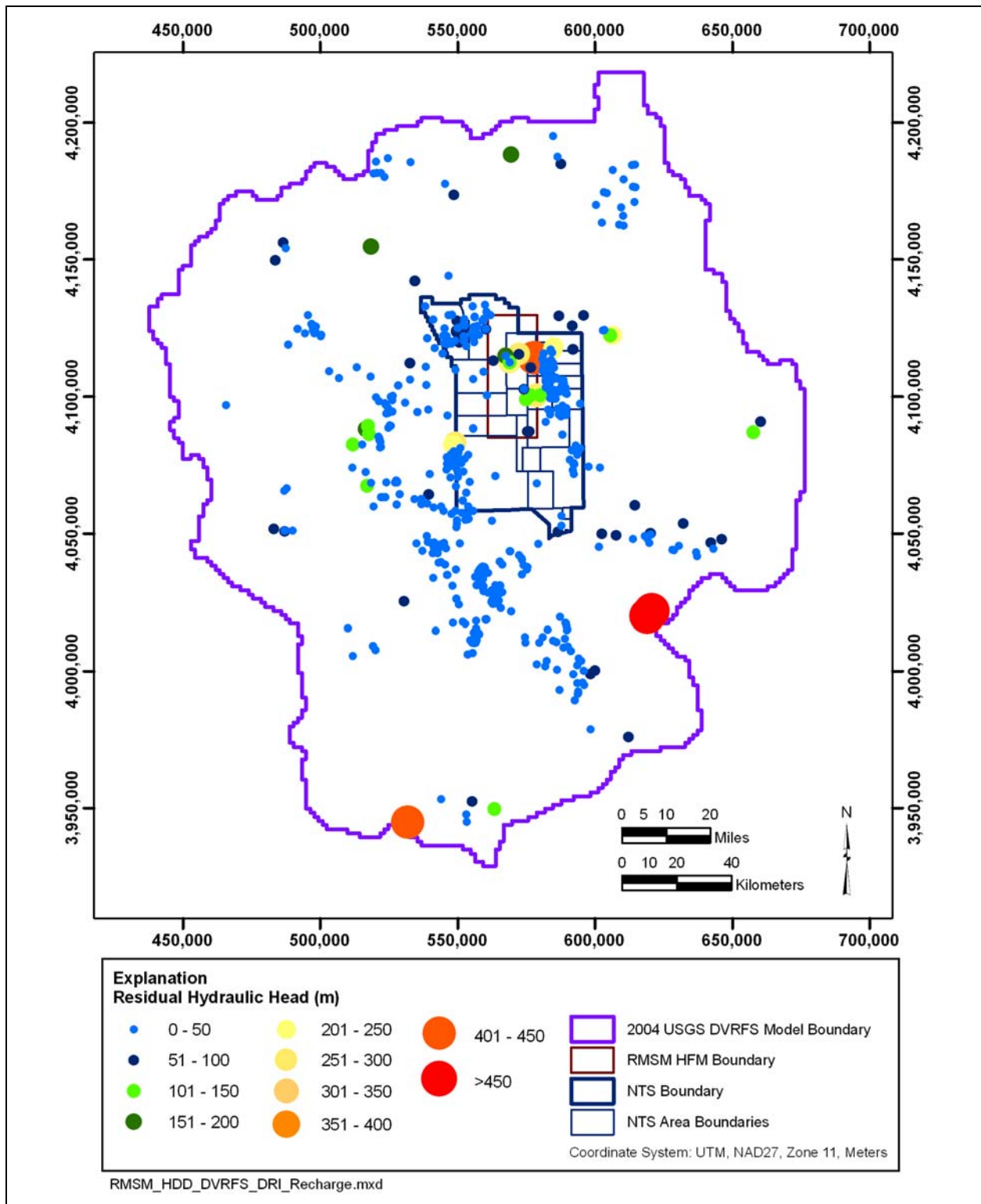


Figure 8-4
Unweighted Residual Hydraulic Heads for the DVRFS
DRI Recharge Scenario

Figures 8-2 through 8-4 show some relatively large residual heads in the RMSM HFM area. Large residuals highlight the difficulty in matching all observed heads due to the steep terrain, faulting, localized higher recharge, and large hydraulic gradients found in some areas. In addition, some of the observation water levels used represent perched versus regional water levels. Runs using the calibrated NTS Flow Model and alternative models showed similar residuals. During the calibration process, modifications to the model parameters to reduce the residuals at one well often led to increases in the residuals calculated for other wells. The presence of these residuals in the calibrated models increases the uncertainty in the groundwater fluxes calculated and must be considered when the data are used as calibration targets for the flow and transport modeling.

8.4.1 NTS Flow Model Calibration

Corrective Action Unit-specific HFM models have been developed for the Pahute Mesa, RMSM, Yucca Flat, and Frenchman Flat areas for the NTS project. These models are documented in [4-7]. The HFM models were inserted in the USGS DVRFS Model producing the NTS Flow Model. Figure 8-5 shows the model areas imposed over a map with the NTS boundaries. The DVRFS model grid served as the base grid for the NTS CAU inserts [2].

The NTS CAU models include a much finer division of the units used to represent the groundwater flow environment within the individual model areas. By way of example, a total of 72 hydrogeologic-unit flow (HUF) packages are used versus just 27 in the base USGS DVRFS Model. Calibrating the NTS Flow Model to flow for all three recharge scenarios was the first objective of work undertaken. Completing the calibration required changing HUF unit flow properties (e.g., horizontal conductivity, vertical anisotropy, and depth of hydraulic conductivity decay) in addition to adjusting the multipliers associated with the recharge zones for each scenario. Work proceeded, and a set of flow parameters was developed for the regional recharge scenario as defined in the sensitivity and KDEP files used. Once this set of parameters was established, only the recharge zone multipliers (e.g., RCH_1, RCH_2 found in the sensitivity file) were adjusted to calibrate flow as the recharge scenarios were changed. Adjusting the recharge zone multipliers changed the amount of recharge applied for each model/recharge scenario.

8.4.1.1 Calibration Procedure

The focus of the model calibration process was to minimize the difference between the hydraulic heads calculated versus those observed. This effort began with the regional recharge scenario and the parameter sets (e.g., sensitivity file) used for the initial DVRFS model runs. However, given the greater number of HUF units used in the CAU inserts, the original DVRFS parameters were assigned to more units.

Successive runs were completed with areas of high residuals examined to determine which parameters were influencing the results. Parameter estimation runs were used to aid this process. The parameters identified were then modified and the model rerun to view the impact of the changes on the residuals. In some cases, the broad assignments of parameters to existing variables did not allow sufficient latitude to effectively reduce the error. Several new variables were defined to allow

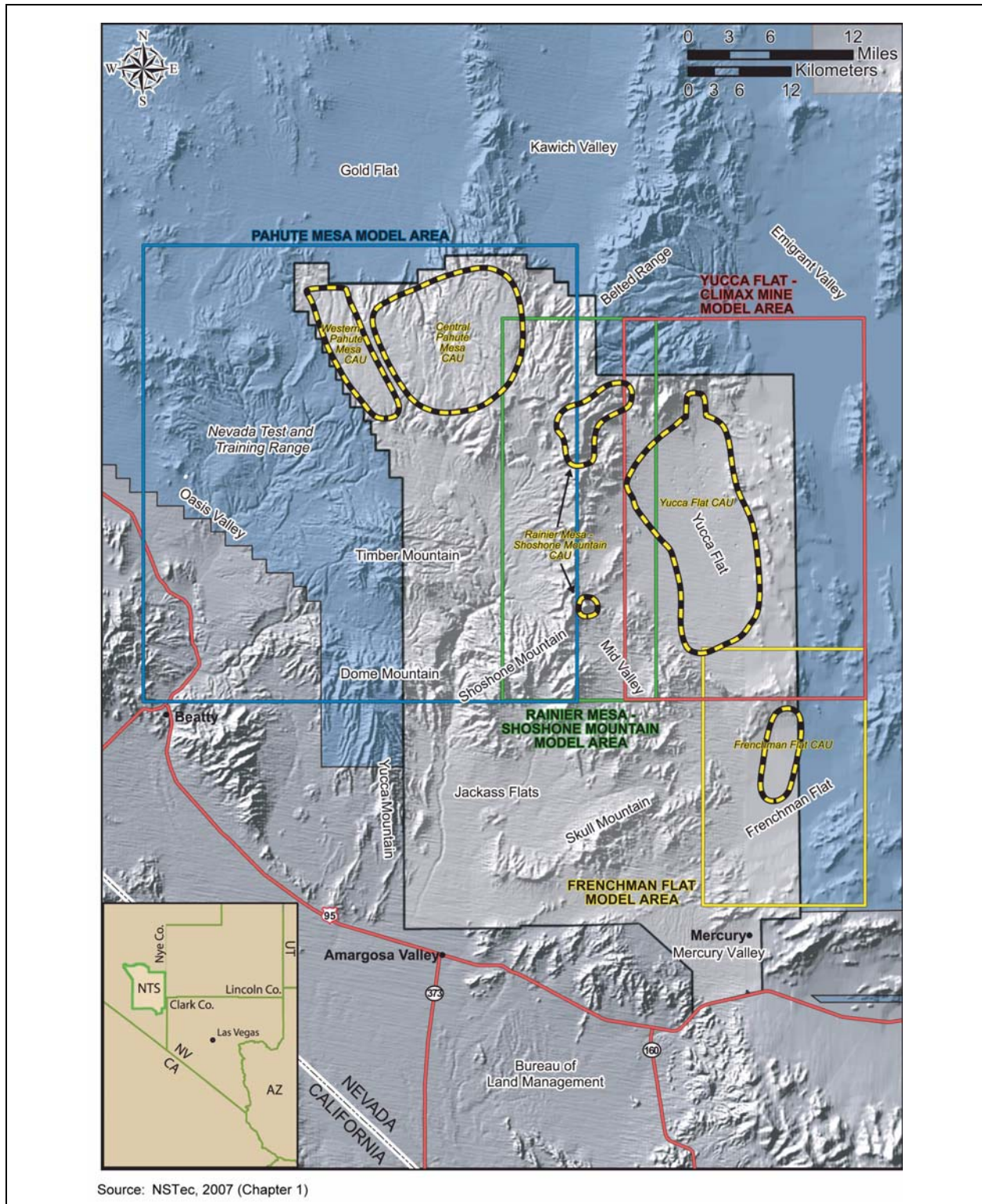


Figure 8-5
Map Showing Locations of All UGTA HFM Areas

greater parameter range. By way of example, the FCCM and TMCM were 2 of 20 HSUs using the single variable K3L11_utcu to assign a value for their horizontal hydraulic conductivity. To allow the use of a different value of hydraulic conductivity for these units, a new parameter was created for the NTS Flow Model and alternate HFM models called K3_TMCM. The FCCM and TMCM were then assigned to the new variable. In addition, some modifications were made to the recharge files where more recharge was being assigned than could infiltrate, leading to excessive residuals.

The result of the calibration process was a single set of hydraulic parameters, referred to here as the RMSM Base dataset, for use in all subsequent lateral boundary flux calculations. With one exception, the subsequent analyses adjusted only the recharge multiplier parameters to minimize the difference in calculated versus observed hydraulic heads. The exception is described in the description of the work done for the No Redrock Valley Caldera AFM (Section 8.5).

8.4.1.2 Discussion of Results

The USGS Base parameter values, as shown in Table 8-2, were used for the initial run calibrating the NTS Flow Model. Those parameters for which an “NA” is listed in the USGS Base column are new parameters that were created during the calibration process because the NTS Flow Model incorporates additional detail. The table also lists the parameter values or range of values as given in Appendix F of the USGS DVRFS [2]. Comparing the RMSM Base dataset to the USGS Base dataset, it can be noted that the majority have been changed. The last column to the right of the table shows whether the new value as calibrated for the NTS Flow Model is either less than or greater than the reference minimum and maximum as determined by the USGS. In many cases, the reference minimum and maximum values for a parameter are the same, reflecting only a single value cited rather than a range. For those parameters where a range is specified, the RMSM Base values generally fall within it.

Table 8-2
Comparison of Model Calibration Parameters
(Page 1 of 5)

| Parameter | Reference Minimum | Reference Maximum | USGS Base | RMSM Base | Compared to Reference |
|--|-------------------|-------------------|-----------|-----------|-----------------------|
| Hydraulic Flow Barriers (m/day/m) | | | | | |
| B_DV_N | 2.40E-07 | 2.40E-07 | 2.40E-07 | 2.40E-08 | LT MIN |
| B_DVFC_FCR | 1.00E-07 | 1.00E-07 | 1.00E-07 | 1.00E-08 | LT MIN |
| B_HWY95 | 2.95E-04 | 2.95E-04 | 2.95E-04 | 1.81E-05 | LT MIN |
| B_LVVSZ_1 | 9.00E-04 | 9.00E-04 | 9.00E-04 | 9.00E-04 | -- |
| B_LVVSZ_I2 | 4.19E-08 | 4.19E-08 | 4.19E-08 | 6.00E-07 | GT MAX |
| B_LVVSZ_IS | 1.10E-08 | 1.10E-08 | 1.10E-08 | 1.05E-06 | GT MAX |
| B_PAHRUMP | 5.52E-07 | 5.52E-07 | 5.52E-07 | 2.75E-07 | LT MIN |
| B_SOLTARIO | 4.45E-05 | 4.45E-05 | 4.45E-05 | 2.23E-05 | LT MIN |
| B_TC_LINE | 1.00E-07 | 1.00E-07 | 1.00E-07 | 1.00E-07 | -- |

Table 8-2
Comparison of Model Calibration Parameters
 (Page 2 of 5)

| Parameter | Reference Minimum | Reference Maximum | USGS Base | RMSM Base | Compared to Reference |
|---|-------------------|-------------------|-----------|-----------|-----------------------|
| Drain Conductance (m/day/m) | | | | | |
| DEEP_DRN | 4.56E+01 | 4.56E+01 | 4.56E+01 | 6.02E+01 | GT MAX |
| FRNCR_DRN | 1.00E+04 | 1.00E+04 | 1.00E+04 | 1.00E+04 | -- |
| UP_DV_DRN | 1.00E+04 | 1.00E+04 | 1.00E+04 | 1.00E+04 | -- |
| UP_DVN_DRN | 5.28E+01 | 5.28E+01 | 5.28E+01 | 5.28E+01 | -- |
| UP_PAH_DRN | 1.95E+02 | 1.95E+02 | 1.95E+02 | 1.95E+02 | -- |
| UP_PLY_DRN | 8.39E+01 | 8.39E+01 | 8.39E+01 | 1.22E+02 | GT MAX |
| UPPER_DRN | 1.08E+02 | 1.08E+02 | 1.08E+02 | 1.08E+02 | -- |
| Depth Decay Coefficient (%) | | | | | |
| KDEP_LCA | 1.00E-04 | 1.00E-04 | 1.00E-04 | 2.67E-04 | GT MAX |
| KDEP_NO | 1.00E-07 | 1.00E-07 | 1.00E-07 | 2.20E-05 | GT MAX |
| KDEP_UCCU | 1.50E-03 | 1.50E-03 | 1.50E-03 | 2.05E-03 | GT MAX |
| KDEP_VFVL | 1.23E-02 | 1.23E-02 | 1.23E-02 | 2.00E-02 | GT MAX |
| KDEP_VSUL | 1.20E-04 | 1.20E-04 | 1.20E-04 | 1.20E-04 | -- |
| KDEP_VSUU | 4.35E-03 | 4.35E-03 | 4.35E-03 | 4.35E-03 | -- |
| KDEP_XL | 6.20E-04 | 6.20E-04 | 6.20E-04 | 6.20E-04 | -- |
| KDP_LCANO | 2.89E-05 | 2.89E-05 | 2.89E-05 | 2.89E-05 | -- |
| KDP_LCAT1 | 1.50E-03 | 1.50E-03 | 1.50E-03 | 1.50E-03 | -- |
| KDP_VOL | 2.48E-03 | 2.48E-03 | 2.48E-03 | 8.00E-04 | LT MIN |
| Hydraulic Conductivity - Confining Units (m/day) | | | | | |
| K11_ICU | 6.00E-04 | 1.40E+00 | 2.46E-03 | 9.00E-03 | -- |
| K11_ICUCM | NA | NA | NA | 2.50E+00 | -- |
| K11C_XILCU | 3.00E-08 | 5.00E+00 | 1.94E-03 | 2.15E-05 | -- |
| K11DV_XCU | 1.09E-01 | 1.09E-01 | 1.09E-01 | 3.40E-03 | LT MIN |
| K1221UCCU | 2.00E-04 | 4.00E-01 | 3.88E-02 | 7.50E-03 | -- |
| K12223LCCU | 3.00E-08 | 5.00E+00 | 1.57E-03 | 8.00E-04 | -- |
| K122esLCCU | 3.00E-08 | 5.00E+00 | 1.85E-01 | 2.40E-03 | -- |
| K122fgLCCU | 3.00E-08 | 5.00E+00 | 6.00E-05 | 5.00E-05 | -- |
| K1LCCU_XCU | 3.00E-08 | 5.00E+00 | 4.08E-03 | 1.00E-03 | -- |
| Hydraulic Conductivity - Carbonate Aquifer (m/day) | | | | | |
| K2_DV_LCA | 1.00E-04 | 8.20E+02 | 3.00E+00 | 3.00E+00 | -- |
| K221_LCA | 1.00E-04 | 8.20E+02 | 6.09E+00 | 6.09E+01 | -- |

Table 8-2
Comparison of Model Calibration Parameters
 (Page 3 of 5)

| Parameter | Reference Minimum | Reference Maximum | USGS Base | RMSM Base | Compared to Reference |
|--|-------------------|-------------------|-----------|-----------|-----------------------|
| K232_LCA | 1.00E-04 | 8.20E+02 | 1.00E-03 | 2.00E-04 | -- |
| K2412_LCA | 1.00E-04 | 8.20E+02 | 8.06E-02 | 2.00E-01 | -- |
| K2412fLCA | 1.00E-04 | 8.20E+02 | 1.21E+01 | 1.21E+00 | -- |
| K241LCA_T1 | 1.00E-04 | 8.20E+02 | 9.87E-01 | 1.25E-01 | -- |
| K241LCA3 | NA | NA | NA | 8.00E-02 | -- |
| K241SM_LCA | 1.00E-04 | 8.20E+02 | 1.51E-03 | 2.15E-03 | -- |
| K241SMWLCA | 1.00E-04 | 8.20E+02 | 3.77E-01 | 3.75E-02 | -- |
| K2421_LCA | 1.00E-04 | 8.20E+02 | 1.57E-02 | 4.25E-02 | -- |
| K2422b_LCA | 1.00E-04 | 8.20E+02 | 6.45E-02 | 2.20E-03 | -- |
| K242A_LCA | 1.00E-04 | 8.20E+02 | 3.39E+00 | 7.52E+00 | -- |
| K242G_LCA | 1.00E-04 | 8.20E+02 | 6.46E-02 | 8.00E-02 | -- |
| K242YN_LCA | 1.00E-04 | 8.20E+02 | 1.17E-04 | 5.85E-05 | LT MIN |
| K243_LCA | 1.00E-04 | 8.20E+02 | 2.19E+00 | 1.10E+01 | -- |
| K243_UCA | 1.00E-04 | 8.20E+02 | 1.00E-04 | 1.50E-02 | -- |
| K243GV_LCA | 1.00E-04 | 8.20E+02 | 2.40E-03 | 2.40E-03 | -- |
| K243PP_LCA | 1.00E-04 | 8.20E+02 | 1.00E+00 | 1.00E+01 | -- |
| K244_LCA | 1.00E-04 | 8.20E+02 | 2.00E+02 | 2.50E+02 | -- |
| K2SHPLCA | 1.00E-04 | 8.20E+02 | 6.51E-02 | 1.50E-02 | -- |
| K2YMLCA | 1.00E-04 | 8.20E+02 | 4.23E-01 | 4.26E+00 | -- |
| Hydraulic Conductivity - Volcanic Units (m/day) | | | | | |
| K3_CHDV | NA | NA | NA | 2.00E-03 | -- |
| K3_TMCM | NA | NA | NA | 5.76E-02 | -- |
| K3211TMVA | 2.00E-04 | 2.00E+01 | 5.66E-01 | 1.16E-01 | -- |
| K321521_PP | 1.00E-03 | 1.80E+02 | 1.66E+02 | 4.00E-03 | -- |
| K3215BCU1 | 1.00E-03 | 1.80E+02 | 1.00E-02 | 1.00E-02 | -- |
| K3215BCU34 | 3.00E-04 | 5.50E+01 | 1.24E+00 | 1.24E+00 | -- |
| K3215TR | 3.00E-03 | 2.00E+00 | 5.60E-02 | 2.80E+00 | GT MAX |
| K32BR4CH13 | 8.00E-03 | 4.00E+00 | 1.60E-01 | 2.00E-01 | -- |
| K32CH24LF | 2.00E-03 | 4.00E+00 | 1.33E-01 | 1.20E+01 | GT MAX |
| K33_OVU | 1.00E-06 | 1.00E+00 | 9.90E-03 | 1.80E-02 | -- |
| K33_OVUSW | 1.00E-06 | 1.00E+00 | 4.86E-02 | 1.00E-01 | -- |
| K3BRU123 | 1.00E-02 | 4.00E+00 | 1.89E+00 | 8.00E-02 | -- |

Table 8-2
Comparison of Model Calibration Parameters
 (Page 4 of 5)

| Parameter | Reference Minimum | Reference Maximum | USGS Base | RMSM Base | Compared to Reference |
|---|-------------------|-------------------|-----------|-----------|-----------------------|
| K3C_PVA | 7.00E-07 | 1.70E+01 | 3.16E-01 | 8.31E-03 | -- |
| K3C_TM | 2.00E-04 | 2.00E+01 | 8.44E+00 | 5.00E-02 | -- |
| K3L09_LVTA | NA | NA | NA | 3.80E+00 | -- |
| K3L11_UTCU | NA | NA | NA | 1.00E-03 | -- |
| K3L12_TMLV | NA | NA | NA | 3.00E-04 | -- |
| K3L18_BLFA | NA | NA | NA | 4.00E+00 | -- |
| K3LFU_am | 2.00E-03 | 4.00E+00 | 5.09E-02 | 5.64E-02 | -- |
| K3PVA | 7.00E-07 | 1.70E+01 | 2.89E+02 | 3.89E-01 | -- |
| Hydraulic Conductivity - Valley Fill Units (m/day) | | | | | |
| K3L15_OAA1 | NA | NA | NA | 1.58E+00 | -- |
| K3L16_AA1 | NA | NA | NA | 5.97E-01 | -- |
| K4_VF_AQ | 6.00E-05 | 1.30E+02 | 5.97E-01 | 2.60E+01 | -- |
| K4_VF_CU | 3.00E-03 | 3.40E+01 | 1.58E+00 | 1.05E+00 | -- |
| K4_VF_OAA | 6.00E-05 | 1.30E+02 | 5.92E-02 | 5.92E-02 | -- |
| K42222_VSU | 4.00E-05 | 6.00E+00 | 5.00E-03 | 7.50E-03 | -- |
| K4222P_VSU | 4.00E-05 | 6.00E+00 | 5.81E-01 | 1.00E-01 | -- |
| K4222S_VSU | 4.00E-05 | 6.00E+00 | 1.26E-01 | 2.52E-03 | -- |
| K422DV_VSU | 4.00E-05 | 6.00E+00 | 8.80E-03 | 8.80E-03 | -- |
| K422GV_VSU | 4.00E-05 | 6.00E+00 | 4.63E-02 | 4.63E-02 | -- |
| K422GW_VSU | 4.00E-05 | 6.00E+00 | 1.52E-02 | 1.35E-02 | -- |
| K422LNEVSU | 4.00E-05 | 6.00E+00 | 1.85E-01 | 1.85E-01 | -- |
| K422LNWVSU | 4.00E-05 | 6.00E+00 | 1.92E-01 | 1.45E-03 | -- |
| K42UP_VSU | 4.00E-05 | 6.00E+00 | 7.06E+00 | 5.52E-02 | -- |
| K4UP_VSUC | 4.00E-05 | 6.00E+00 | 9.40E-01 | 9.40E-01 | -- |
| K4UP_VSUP | 4.00E-05 | 6.00E+00 | 2.08E+01 | 5.63E+00 | -- |
| Anisotropy (multiplier) | | | | | |
| K1_VANI | 1.27E+00 | 1.27E+00 | 1.27E+00 | 1.27E+00 | -- |
| K2CARBVANI | 1.00E+00 | 1.00E+00 | 1.00E+00 | 1.00E+00 | -- |
| K3_VOLVANI | 1.00E+00 | 1.00E+00 | 1.00E+00 | 1.00E+00 | -- |
| K4_VFVANIA | 5.00E+03 | 5.00E+03 | 5.00E+03 | 5.00E+02 | LT MIN |
| K4_VFVANIC | 5.00E+03 | 5.00E+03 | 5.00E+03 | 5.00E+02 | LT MIN |
| K4_VFVANVL | 2.18E+00 | 2.18E+00 | 2.18E+00 | 2.18E+00 | -- |

Table 8-2
Comparison of Model Calibration Parameters
 (Page 5 of 5)

| Parameter | Reference Minimum | Reference Maximum | USGS Base | RMSM Base | Compared to Reference |
|------------------------------|-------------------|-------------------|-----------|-----------|-----------------------|
| Recharge (multiplier) | | | | | |
| RCH_1 | NA | NA | NA | 8.00E-01 | -- |
| RCH_2 | 7.60E-01 | 7.60E-01 | 7.60E-01 | 8.00E-01 | GT MAX |
| RCH_3 | NA | NA | NA | 1.00E+00 | -- |
| RCH_35 | 1.12E+00 | 1.12E+00 | 1.12E+00 | NA | -- |
| RCH_4 | NA | NA | NA | 1.00E+00 | -- |
| RCH_467 | 1.00E+00 | 1.00E+00 | 1.00E+00 | NA | -- |
| RCH_5 | NA | NA | NA | 1.00E+00 | -- |
| RCH_6 | NA | NA | NA | 1.00E+00 | -- |
| RCH_7 | NA | NA | NA | 1.00E+00 | -- |
| RCH_8 | 1.00E+00 | 1.00E+00 | 1.00E+00 | 1.00E-02 | LT MIN |
| RCH_9 | 1.00E-06 | 1.00E-06 | 1.00E-06 | 1.00E-02 | GT MAX |

Source: Reference and USGS Base values taken from Appendix F of [2].

NA = Not applicable. Not every USGS and RMSM parameter is used in both datasets.

LT MIN = Value is less than the USGS suggested parameter value or range of values.

GT MIN = Value is greater than the USGS suggested parameter value or range of values.

The sums of weighted residual errors calculated for the three recharge scenarios range from a low of 19,253 for the regional recharge scenario to a high of 31,183 for the revised UGTA recharge scenario. [Table 8-3](#) presents a summary of the results.

[Table 8-3](#) also presents a summary of the flows calculated passing through the top of the RMSM HFM area (recharge) as well as through the northern, southern, eastern, and western sides. The bottom of the model was simulated as no flow. Reference to the table shows a somewhat smaller variation in the total flows calculated for each of the recharge scenarios than was seen in the difference in weighted residual errors. The DRI recharge scenario yielded the greatest overall flow through the RMSM HFM area at 20,374 m³/day and the revised UGTA recharge scenario the lowest at 17,619 m³/day. For all three scenarios, there was net flow into the model area through the northern and eastern faces of the model area as well as at the surface (recharge). There was net flow out the southern and western boundaries, with the greatest net flow out through the southern model face. Compared to the base USGS DVRFS Model, inclusion of the NTS CAU models changes direction of flow along the eastern RMSM HFM boundary. For the DVRFS model, the principal flow along the eastern boundary was out into Yucca Flat. For the NTS Flow Model, the principal direction of flow along the eastern boundary is inward, with the model area receiving flow from Yucca Flat. This difference highlights the impact of the finer definition of stratigraphy incorporated in the NTS HFMs as well as the changes in parameter values brought about by the calibration to flow. It also

**Table 8-3
NTS Flow Model Run Results**

| | Recharge Scenarios | | |
|--|--------------------------|--------------------------|--------------------------|
| | Regional | Revised UGTA | DRI |
| Sum of Squared Weighted Residuals | | | |
| Heads Only | 18,049.00 | 30,049.00 | 19,372.00 |
| Drain Flows Only | 1,156.60 | 911.72 | 982.72 |
| Constant Head Boundary Flows | 48.15 | 222.80 | 127.72 |
| Sum | 19,253.00 | 31,183.00 | 20,482.00 |
| RMSM HFM Area Boundary Flows | m³/day | m³/day | m³/day |
| North | 1,414.3 | 102.6 | 361.6 |
| South | -12,051.0 | -11,589.1 | -12,351.1 |
| East | 8,088.5 | 7,097.1 | 7,045.3 |
| West | -6,700.4 | -6,030.0 | -8,022.9 |
| Recharge | 9,248.7 | 10,419.3 | 12,967.1 |
| Total In | 18,751.4 | 17,619.0 | 20,373.9 |
| Total Out | -18,751.4 | -17,619.0 | -20,373.9 |
| Cumulative | 0.0 | 0.0 | 0.0 |
| Percent Difference ^a | 0.00% | 0.00% | 0.00% |
| DVRFS Model Area Flows | m³/day | m³/day | m³/day |
| IN | | | |
| CONSTANT HEAD | 201,144.28 | 238,172.11 | 204,860.63 |
| DRAINS | 0.00 | 0.00 | 0.00 |
| RECHARGE | 281,928.75 | 164,733.42 | 242,910.09 |
| TOTAL IN | 483,073.03 | 402,905.53 | 447,770.72 |
| OUT | | | |
| CONSTANT HEAD | 116,253.52 | 95,140.06 | 120,259.91 |
| DRAINS | 366,819.34 | 307,765.41 | 327,510.81 |
| RECHARGE | 0.00 | 0.00 | 0.00 |
| TOTAL OUT | 483,072.88 | 402,905.47 | 447,770.72 |
| IN - OUT | 0.16 | 0.06 | 0.00 |
| % DISCREPANCY | 0.0 | 0.0 | 0.0 |

^a Calculated as [(inflow + recharge) – (outflow)] / (outflow)

emphasizes the current uncertainty in flow direction through the Mid Valley area. In all cases, the net flow calculated through the model area was balanced with 0% difference, to two significant digits, between the flows in and out.

In terms of total flow through the entire DVRFS model area, the DRI and regional recharge scenarios change their ranking as compared to flow through the RMSM HFM area alone. The regional recharge scenario at 483,073 m³/day exhibits the greatest flow volume here with the revised UGTA recharge scenario still exhibiting the lowest flow volume at 402,905 m³/day. The results are summarized in [Table 8-3](#).

[Figures 8-6](#) through [8-8](#) show 2-D plots of the residual heads determined for each of the recharge scenarios. The values shown are in meters and represent unweighted calculated minus observed heads for each of the data points. Reference to the figures shows a broadly similar overall pattern in each. However, the differences in recharge applied between the various scenarios causes discernible differences with the revised UGTA scenario exhibiting larger residuals in the northeast quadrant ([Figure 8-7](#)) than seen for the other scenarios. The majority of the residuals are in the range of no more than 50 m.

8.5 RMSM Model Area Flows Calculated for the AFMs

Alternative geologic conceptual models of the RMSM HFM area have been developed. They present configurations of the geologic units that are different from that incorporated in the base RMSM CAU model insert used for the work described in the preceding sections. Specifically, the three alternative models considered here are:

1. No Redrock Valley Caldera: For this scenario, the Redrock Valley caldera is removed from the model. One major difference in this alternative is the replacement of the RVICU with an extension of the LCA as depicted in [Figure 8-9](#).
2. More Extensive LCA3: The LCA3 imbricate thrust sheet is not terminated by the Redrock Valley and Rainier Mesa calderas southwest of Rainier Mesa but rather extends further to the southwest. The scenario is shown in [Figure 8-10](#).
3. Shoshone Mountain Thrust Sheet: The carbonate rocks exposed along the west side of Mid Valley are not LCA but rather a thrust sheet of the LCA3 that overlies UCCU. The scenario is depicted in [Figures 8-11](#) and [8-12](#).

The AFMs are modifications of the NTS Flow Model. The modifications consist of changing the configurations of the geologic units in the RMSM HFM. The runs were done for the regional recharge scenario only and were calibrated by adjusting the recharge multiplier parameters to minimize the difference between the observed hydraulic heads and those calculated. Adjusting the recharge zone multipliers changed the amount of recharge applied for each model.

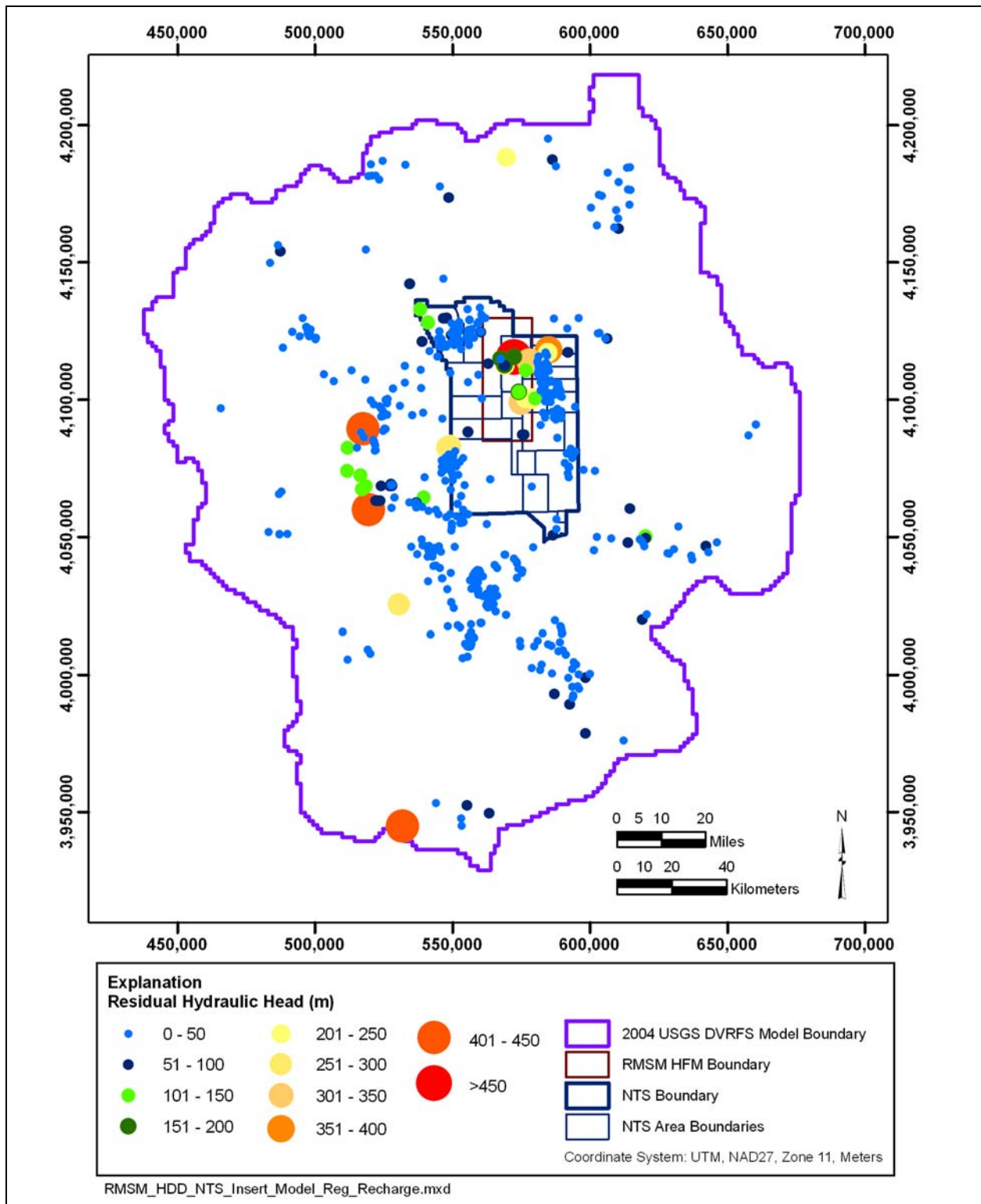


Figure 8-6
Unweighted Residual Hydraulic Heads for the NTS CAU
Insert Model Regional Recharge Scenario

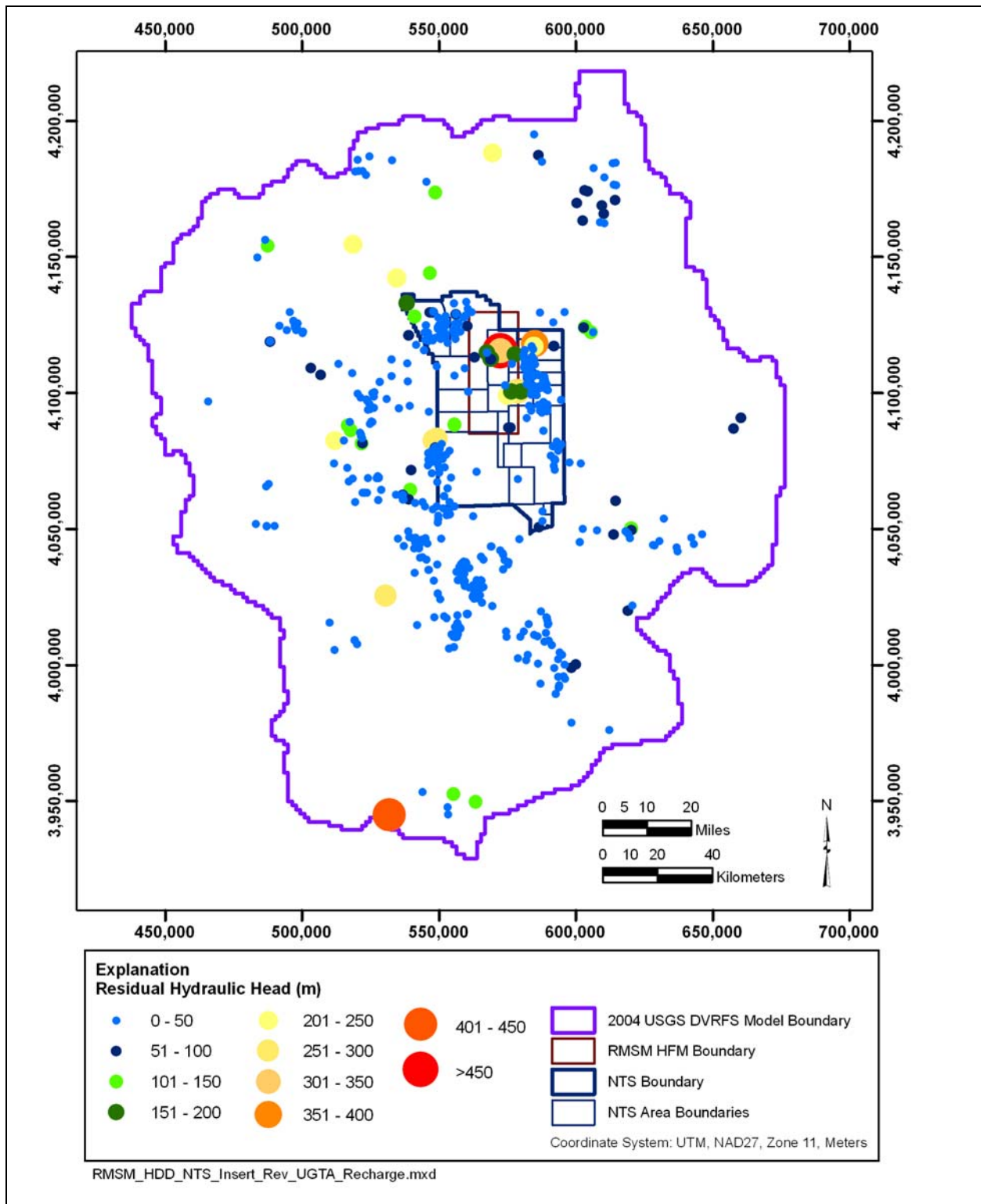


Figure 8-7
Unweighted Residual Hydraulic Heads for the NTS CAU
Insert Model Revised UGTA Recharge Scenario

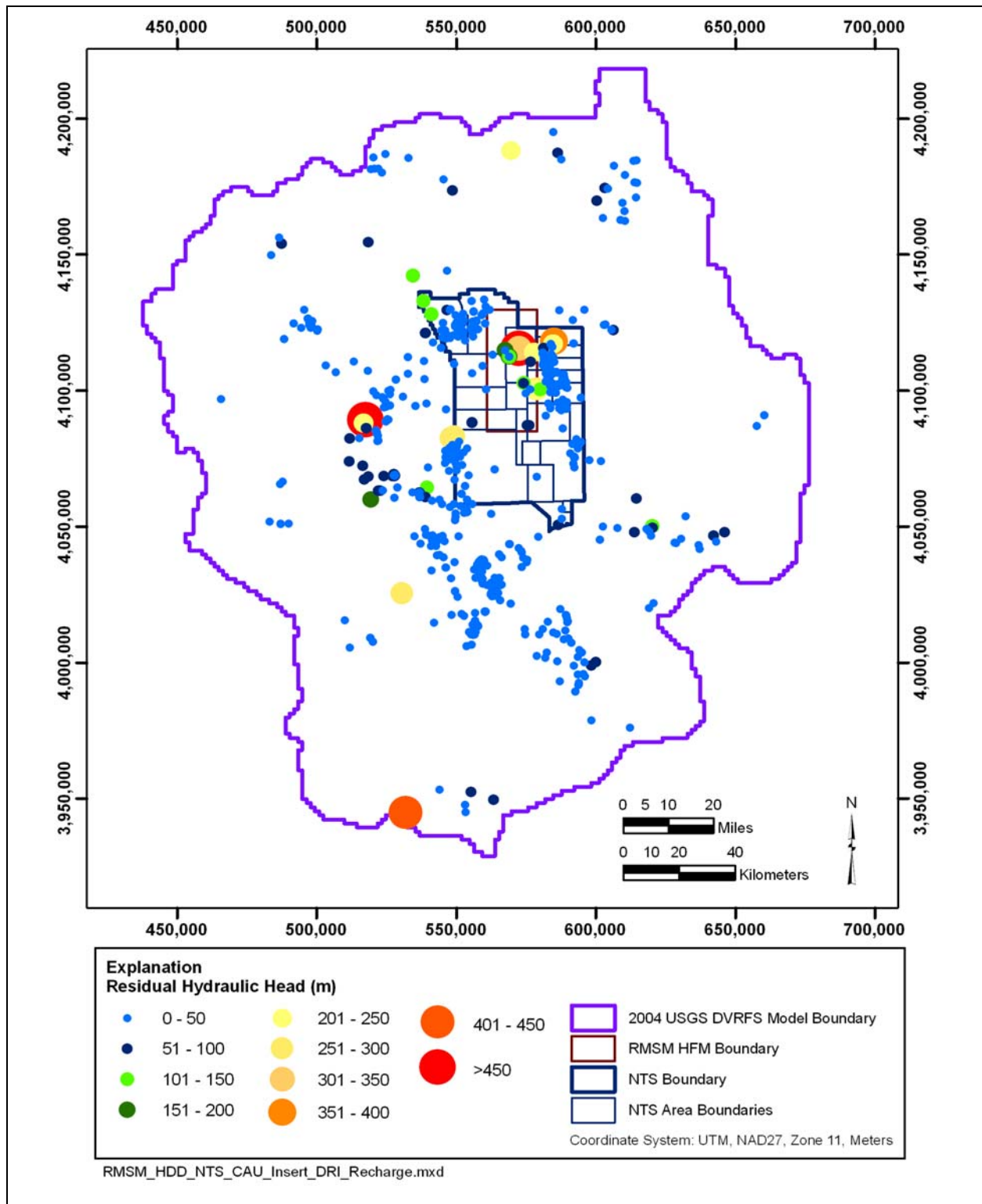


Figure 8-8
Unweighted Residual Hydraulic Heads for the NTS
CAU Insert Model DRI Recharge Scenario

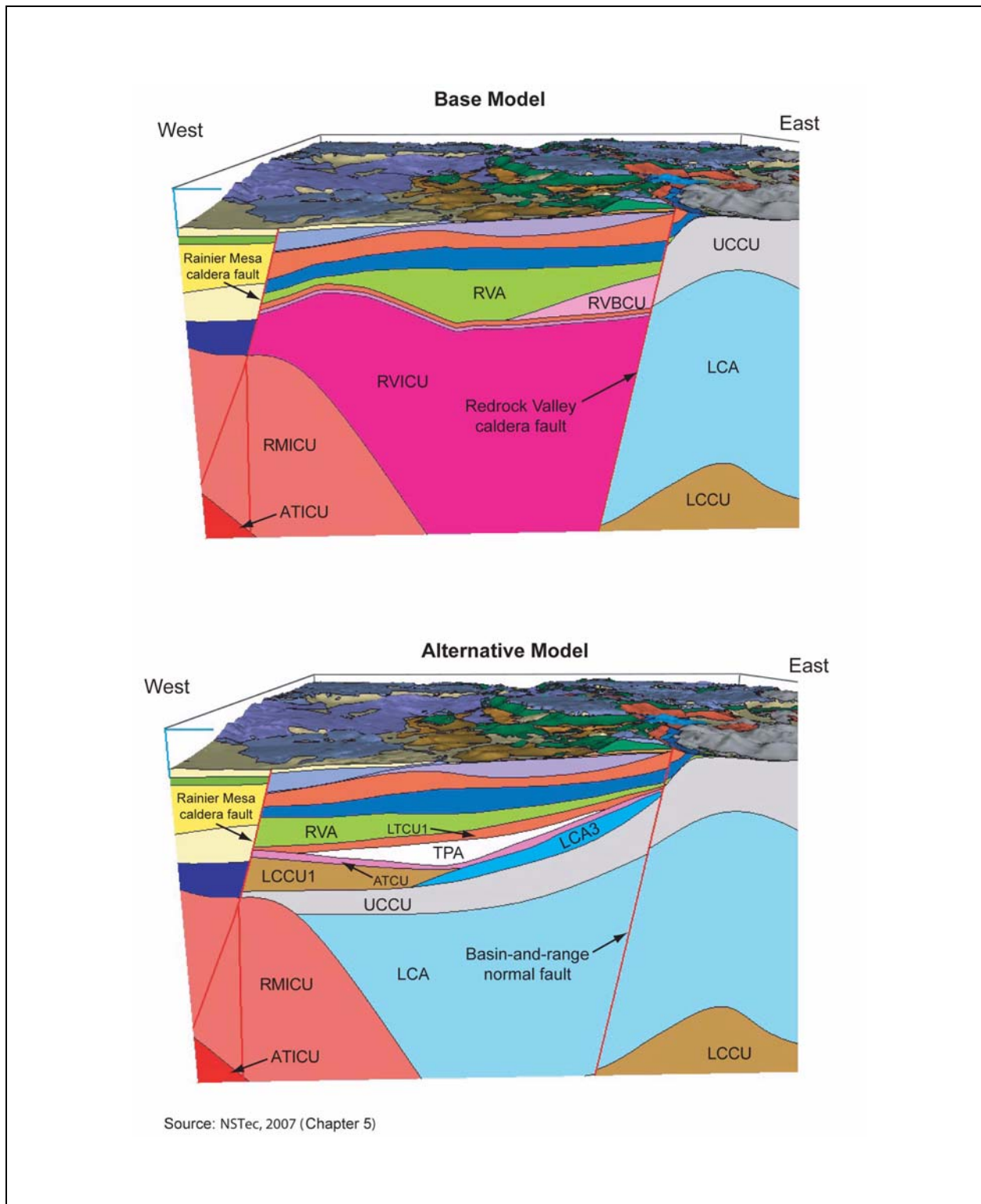


Figure 8-9
West-East Profiles through the Base Model and the
No Redrock Valley Caldera AFM

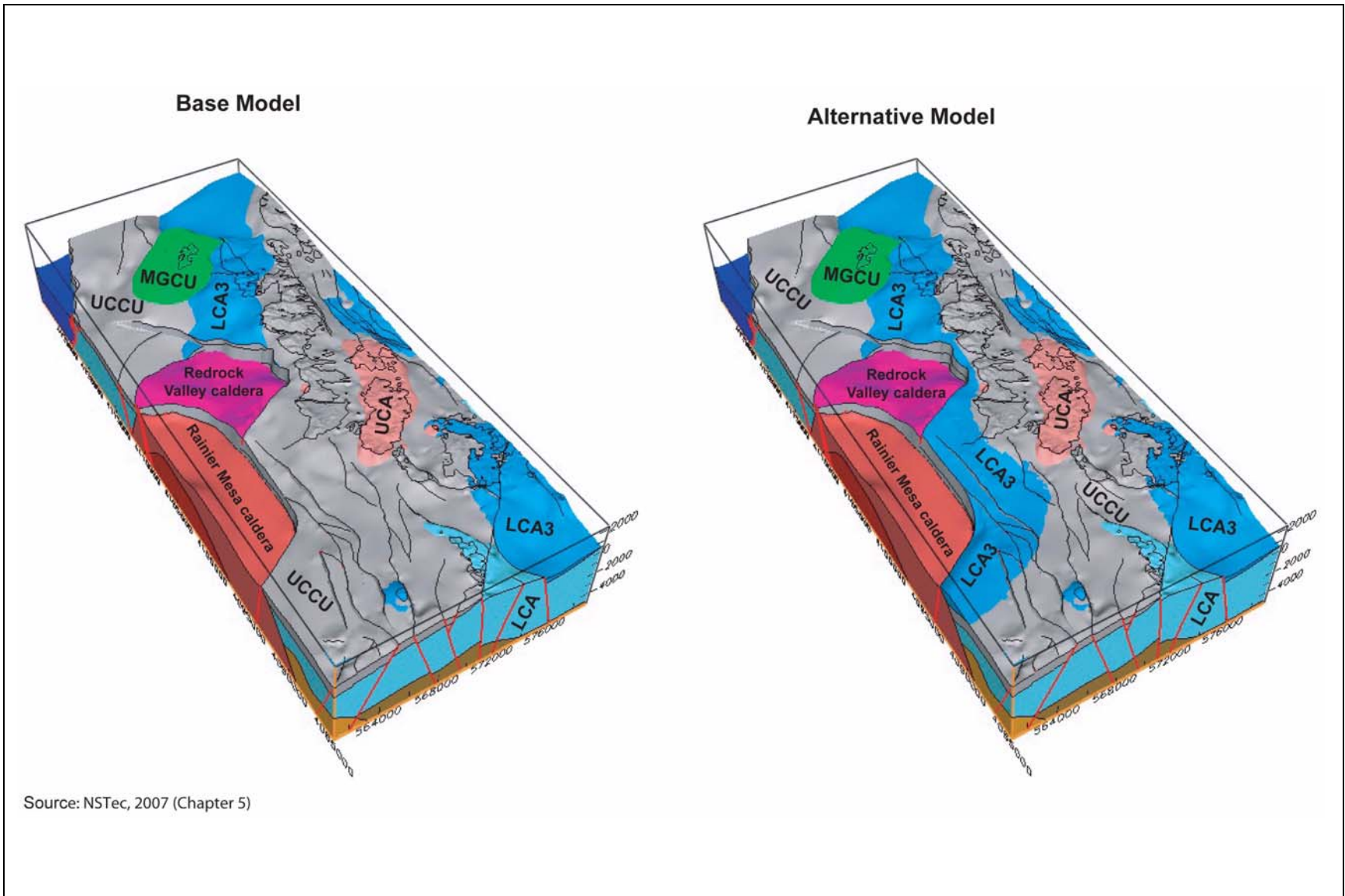


Figure 8-10
Comparison of the Base Model with the More Extensive LCA3 AFM
Perspective views with alluvium, volcanic rocks, and LCCU removed.

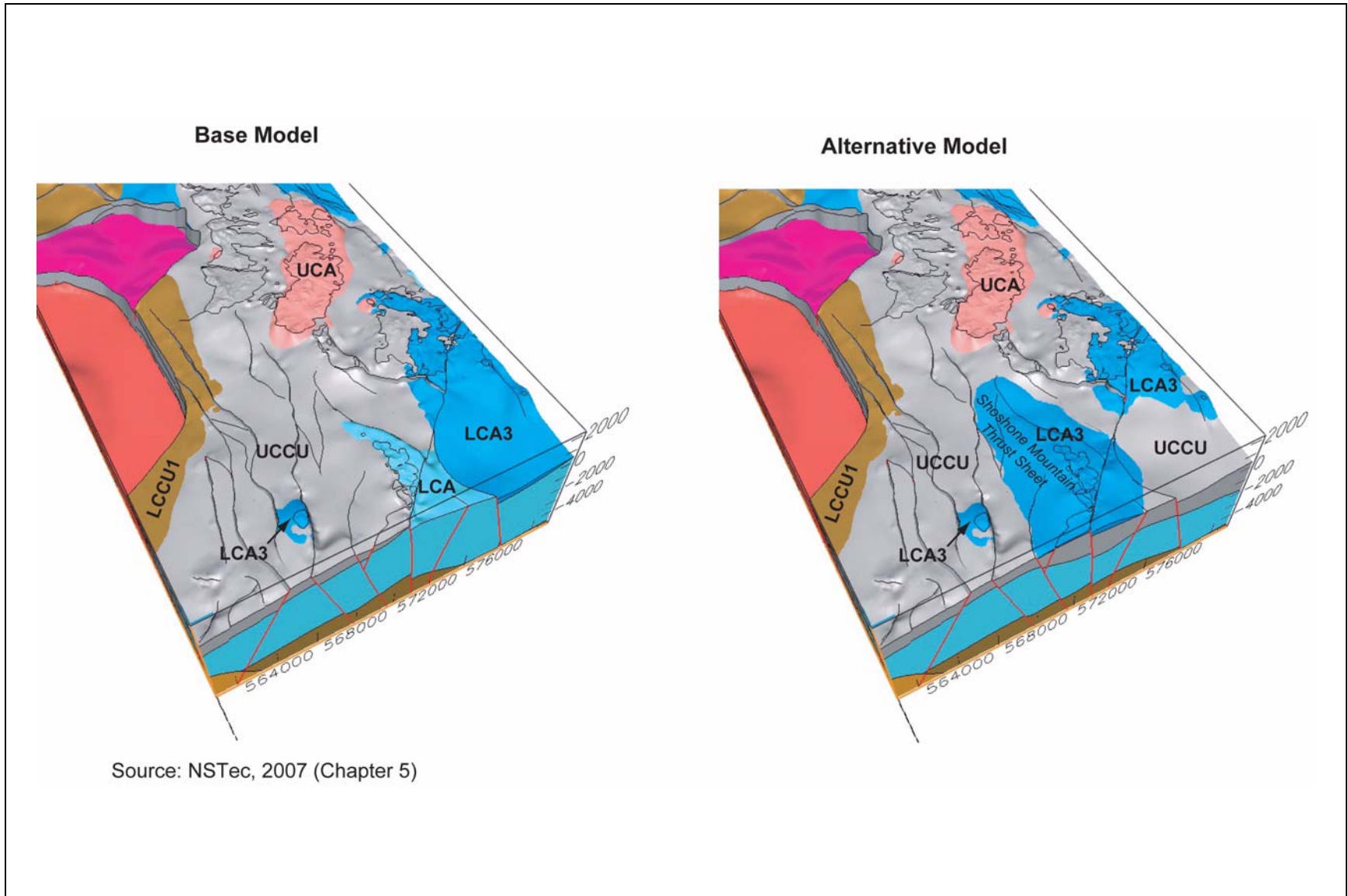


Figure 8-11
Comparison of the Base Model with the Shoshone Mountain Thrust Sheet AFM
Perspective views of the southern portion of the model area with alluvium and volcanic rocks removed.

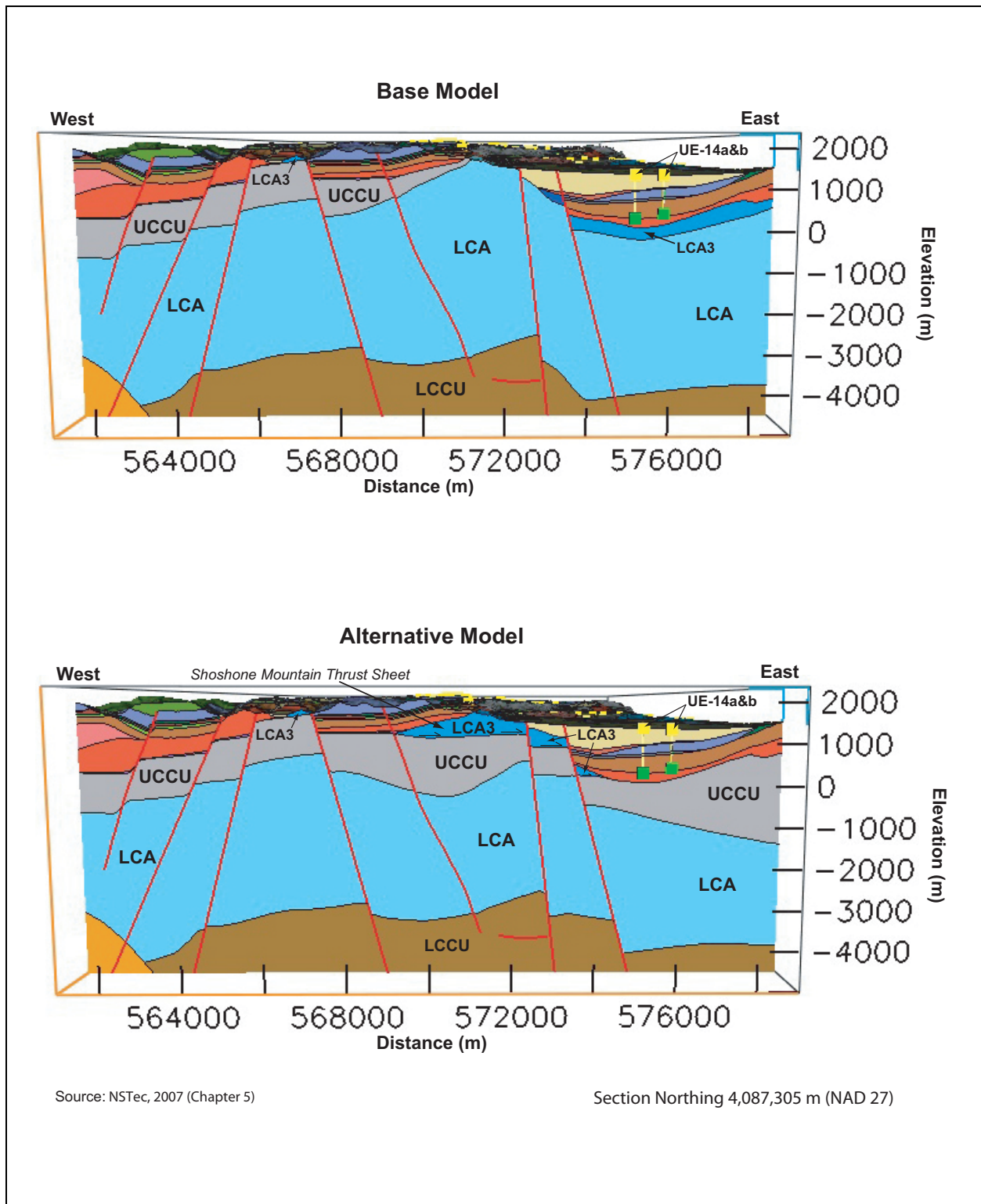


Figure 8-12
West-East Profiles through the Base Model and the
Shoshone Mountain Thrust Sheet AFM

These alternatives were modeled because they are possible configurations that the current data do not rule out and because they have the potential for developing flow fields different from those that result from the base conceptual model. These models are documented in [5]. The DVRFS model grid served as the base grid for the NTS CAU alternative models [2].

The sums of weighted residual errors calculated for the three AFMs were generally similar, ranging from a low of 19,533 for the DRI recharge scenario to a high of 22,401 for the No Redrock Caldera AFM. Table 8-4 presents a summary of the results.

Table 8-4 also presents a summary of the flows calculated passing through the top of the RMSM HFM area (recharge) as well as through the northern, southern, eastern, and western sides. The bottom of the model was simulated as a no-flow zone. Reference to the table shows a limited variation in the total flows calculated for each of the AFMs. The LCA3 Extension yielded the greatest overall flow through the RMSM HFM area at 19,883 m³/day and the No Redrock Valley Caldera AFM the lowest at 17,880 m³/day. For all three scenarios, there was net flow into the model area through the northern and eastern faces of the model area as well as at the surface (recharge). There was net flow out the southern and western boundaries with the greatest net flow out through the southern model face. In all cases, the net flow calculated through the model area was balanced with 0% difference, to two significant digits, between the flows in and out.

In terms of total flow through the entire DVRFS model area, the No Redrock Valley Caldera AFM at 516,167 m³/day exhibits the greatest flow volume here with the Shoshone Mountain Thrust Sheet AFM exhibiting the lowest flow volume at 491,849 m³/day. However, the LCA3 Extension AFM flow was only marginally higher at 497,318 m³/day, and all three flow volumes are similar. The results are summarized in Table 8-4.

Figures 8-13 through 8-15 show 2-D plots of the residual heads determined for each of the AFMs. The values shown are in meters and represent unweighted calculated minus observed heads for each of the data points used. Reference to the figures shows a broadly similar pattern overall in each. In the RMSM HFM area, the results are very similar. The majority of the residuals are in the range of no more than 50 m.

Figure 8-13 shows the residuals for the No Redrock Valley Caldera AFM. The initial runs done for this AFM showed a marked low in the residuals for Emigrant Valley and points northeast (Figure 8-16). Removing the Redrock Valley caldera and replacing it with an extension of the LCA (Figure 8-9) caused a significant change in the hydraulic heads calculated. The change in the conceptual model was significant enough to require decreasing the horizontal hydraulic conductivity for the LCA in this area (K221-LCA) from 60.09 to 3.09 m/day to prevent the underestimation of hydraulic head in the northeast quadrant of the model area for this alternative.

Table 8-4
Alternate Framework Model Run Results

| | AFMs | | |
|--|--------------------------|--------------------------|--------------------------|
| | No RV Cald | LCA3 Ext | SM Thrust |
| Sum of Squared Weighted Residuals | | | |
| Heads Only | 20,963.00 | 18,297.00 | 18,200.00 |
| Drain Flows Only | 1,343.20 | 1,299.30 | 1,287.70 |
| Constant Head Boundary Flows | 94.66 | 58.71 | 45.12 |
| Sum | 22,401.00 | 19,656.00 | 19,533.00 |
| RMSM HFM Area Boundary Flows | m³/day | m³/day | m³/day |
| North | 2,165.5 | 1,334.7 | 1,375.9 |
| South | -12,839.9 | -12,376.1 | -10,901.6 |
| East | 2,151.5 | 7,534.7 | 6,307.9 |
| West | -5,039.8 | -7,507.2 | -7,125.8 |
| Recharge | 13,562.7 | 11,013.9 | 10,343.6 |
| Total In | 17,879.7 | 19,883.4 | 18,027.4 |
| Total Out | -17,879.7 | -19,883.4 | -18,027.4 |
| Cumulative | 0.0 | 0.0 | 0.0 |
| Percent Difference ^a | 0.00% | 0.00% | 0.00% |
| DVRFS Model Area Flows | m³/day | m³/day | m³/day |
| IN | | | |
| CONSTANT HEAD | 182,889.25 | 196,157.48 | 197,991.67 |
| DRAINS | 0.00 | 0.00 | 0.00 |
| RECHARGE | 333,278.25 | 301,161.16 | 293,857.72 |
| TOTAL IN | 516,167.50 | 497,318.63 | 491,849.38 |
| OUT | | | |
| CONSTANT HEAD | 130,584.82 | 122,689.01 | 120,158.97 |
| DRAINS | 385,581.84 | 374,629.44 | 371,690.28 |
| RECHARGE | 0.00 | 0.00 | 0.00 |
| TOTAL OUT | 516,166.66 | 497,318.44 | 491,849.25 |
| IN - OUT | 0.84 | 0.19 | 0.13 |
| % DISCREPANCY | 0.00 | 0.00 | 0.00 |

^a Calculated as ((inflow + recharge) – (outflow)) / (outflow)

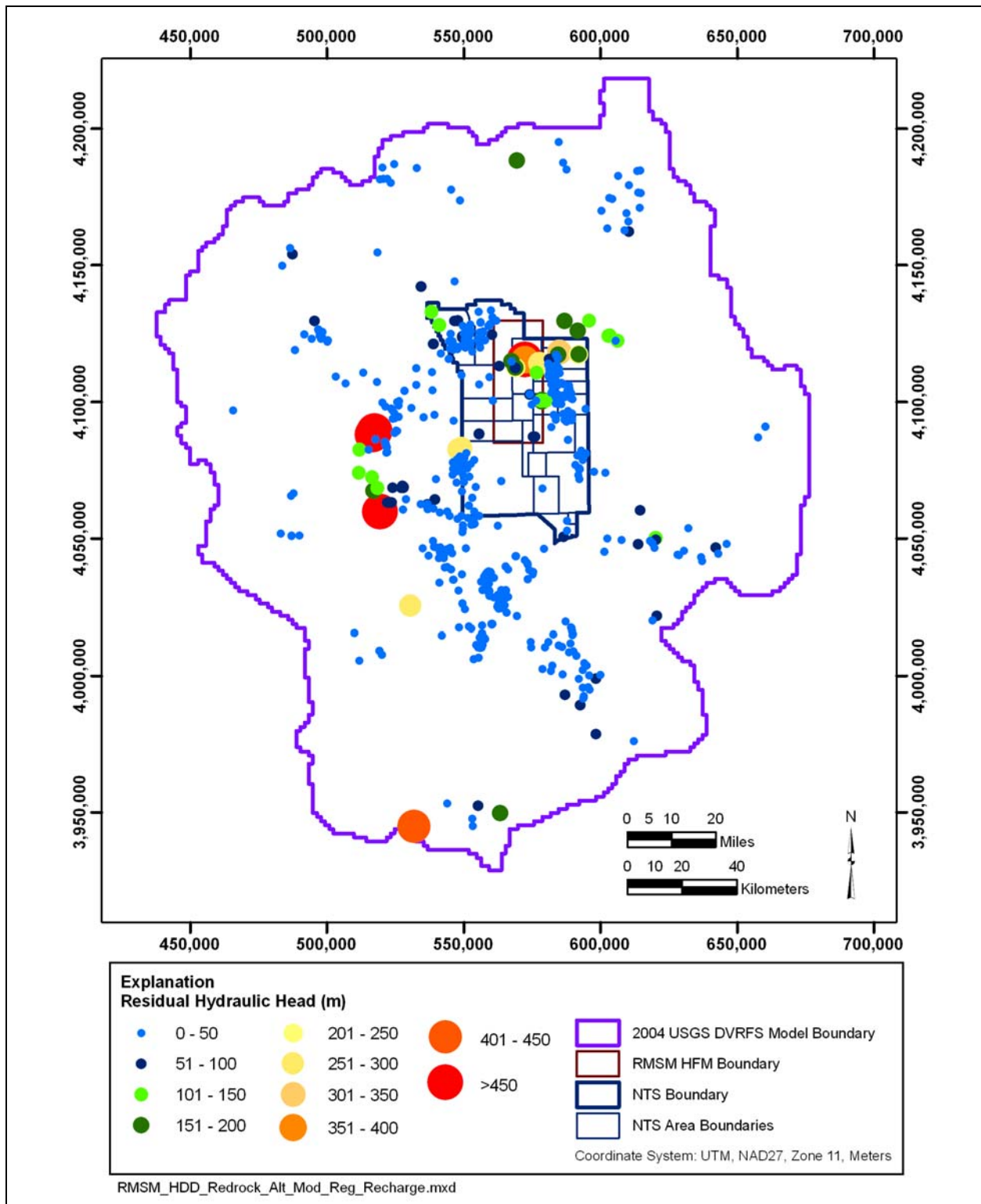


Figure 8-13
Unweighted Residual Hydraulic Heads for the No Redrock Valley Caldera
AFM Regional Recharge Scenario

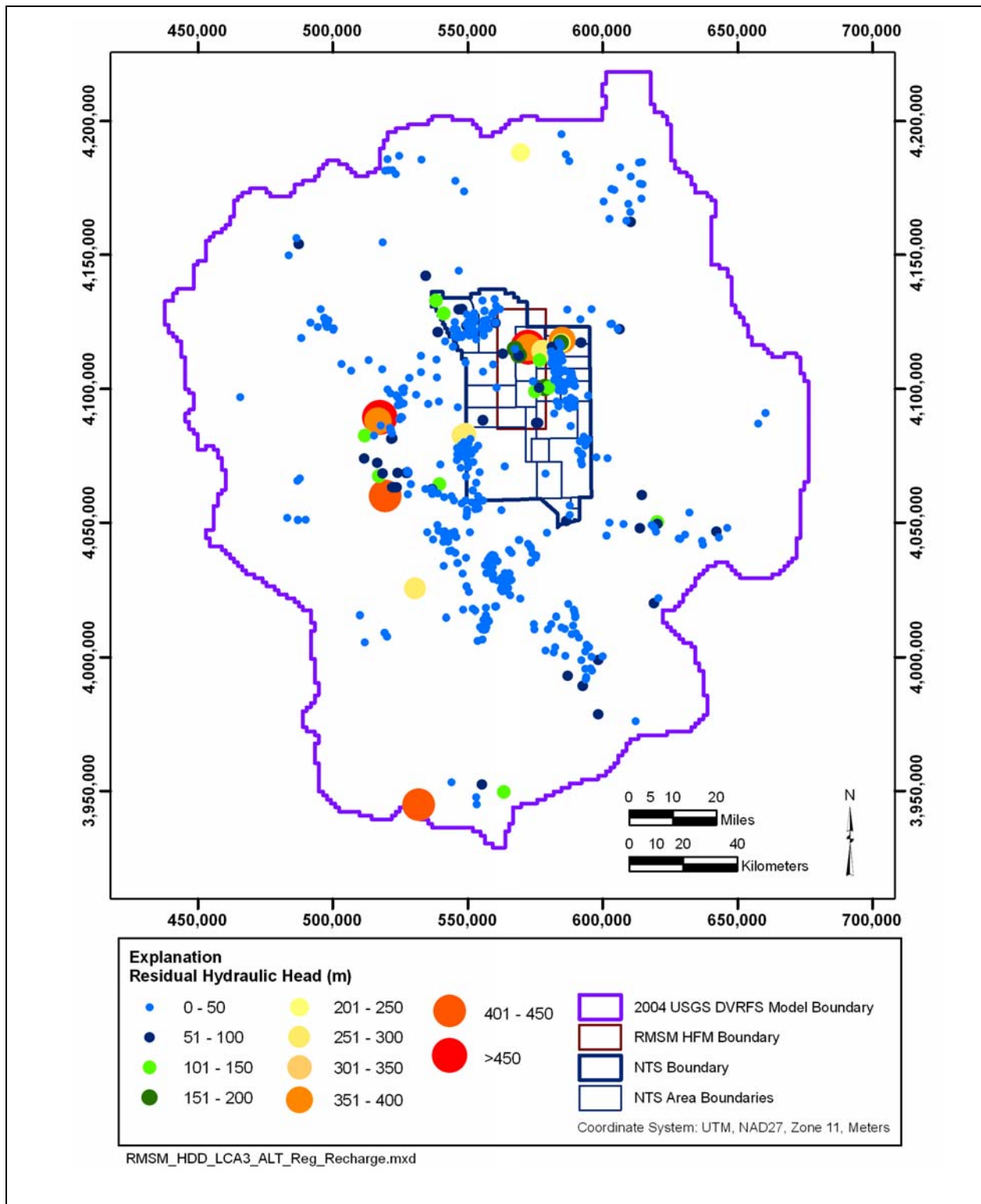


Figure 8-14
Unweighted Residual Hydraulic Heads for the More Extensive LCA3 AFM Regional Recharge Scenario

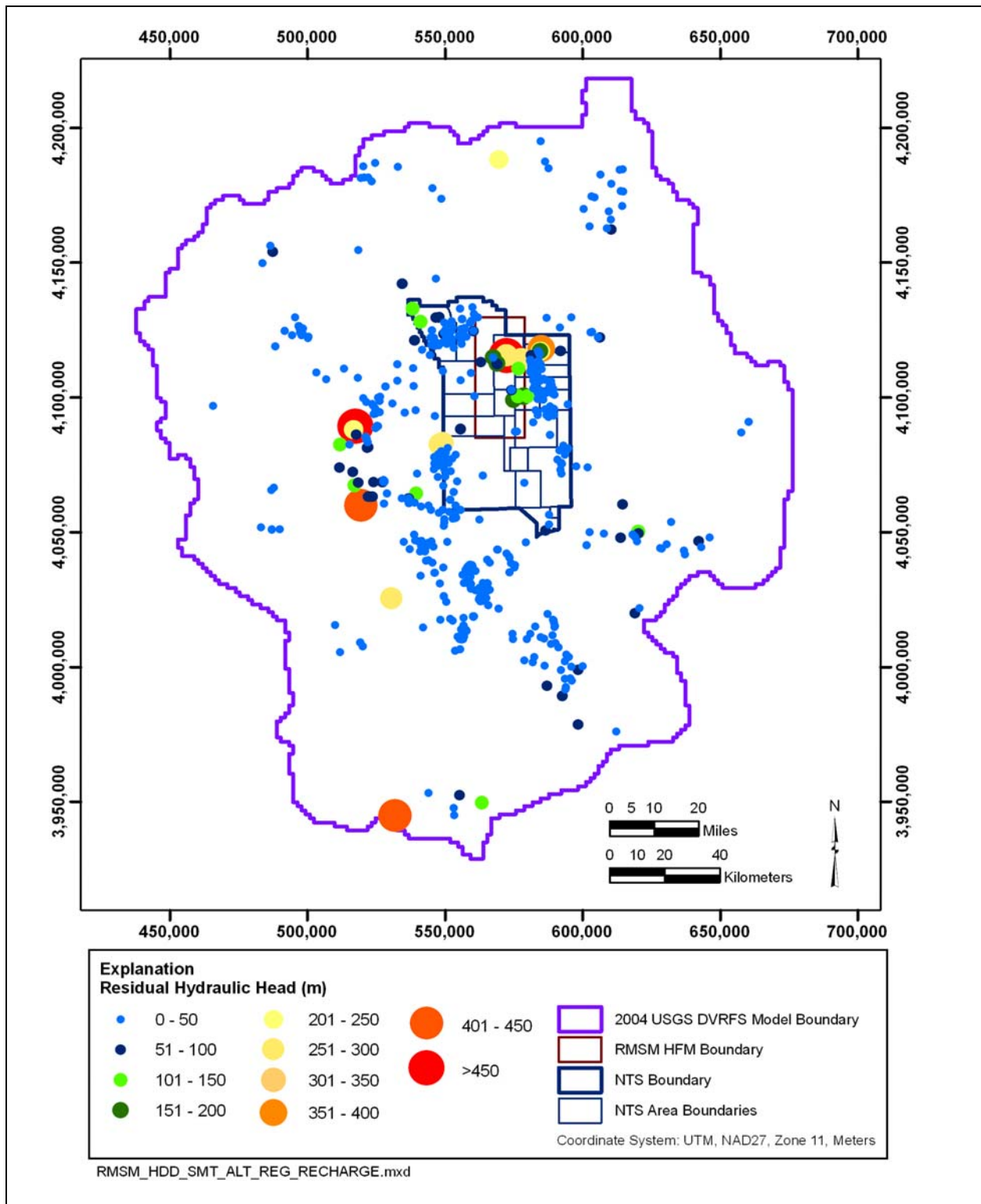


Figure 8-15
Unweighted Residual Hydraulic Heads for the Shoshone Mountain Thrust AFM Regional Recharge Scenario

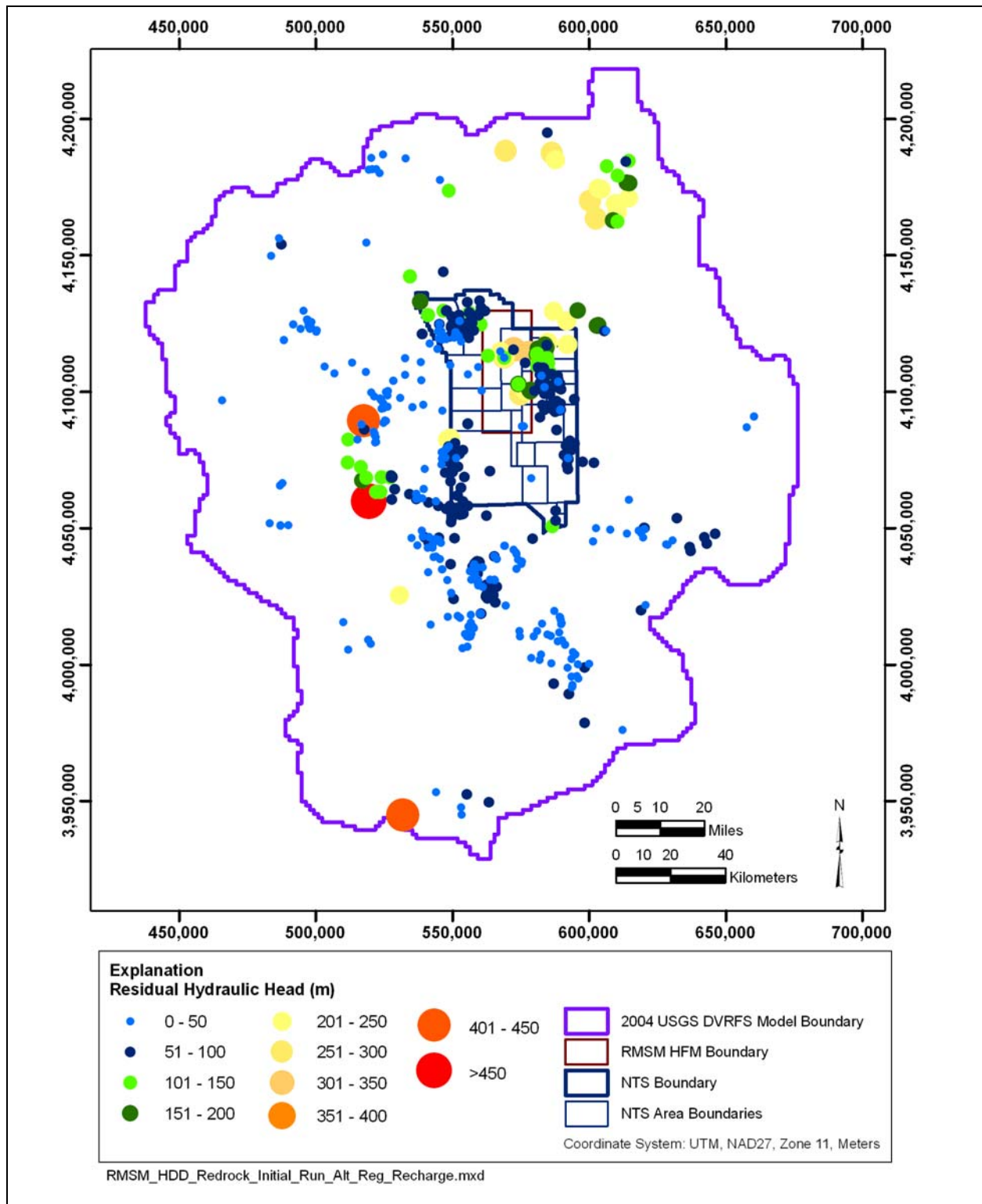


Figure 8-16
Unweighted Residual Hydraulic Heads for the Initial Run of the No Redrock Valley Caldera AFM Regional Recharge Scenario

8.6 Summary of Modeling Results

The preceding presents the results for the separate modeling runs with different recharge scenarios and model alternatives presented and compared. This section presents the modeling results by recharge scenario and model.

Table 8-5 presents a summary of the weighted residuals, RMSM HFM area boundary fluxes, and DVRFS model-wide flows. The model runs done under the regional recharge scenario, excluding the AFMs, are grouped in the first two columns. Reference to the table shows that the sum of squared weighted residuals for the two runs are generally similar at 12,611 and 19,253 for the DVRFS and NTS Flow Models, respectively. However, the changes to the model parameters made through the recalibration process for the NTS Flow Model run caused significant changes to the RMSM HFM boundary fluxes and to the full DVRFS model area constant head in and out flows calculated. Review of the RMSM HFM area boundary fluxes shows a lower total flow for the NTS Flow Model as compared to the DVRFS results. The DVRFS model shows flow into the RMSM HFM area across both the northern boundary and surface (recharge). In addition to these sources, the NTS Flow Model shows flow in along the eastern model boundary. Examining the results for the entire DVRFS model area, the flow into the model attributed to constant head is significantly smaller for the NTS Flow Model than for the original DVRFS model. Less flow in at the constant head boundaries translates to relatively reduced flows out.

Turning to the results for the revised UGTA recharge scenario, there is some difference to be noted in the sum of weighted residuals derived. The run with the NTS Flow Model yielded the highest values calculated for any of the runs. However, this result is still in the general range of the other results. Reference to the RMSM HFM area boundary flows for this scenario shows significantly less recharge for the NTS Flow Model which is directly reflected in the total flow through the RMSM HFM area. In addition, the NTS Flow Model predicts flow into the RMSM HFM area along the eastern boundary in contrast to the DVRFS model. Reviewing the results for the entire DVRFS model area, it can be noted that the difference in recharge between the two models is much less as compared to that for the RMSM HFM area alone. However, the NTS Flow Model has much less flow at the constant head boundaries, leading to a significantly lower flow volume through the model as a whole.

Turning to the results for the DRI recharge scenario, the sums of squared weighted residuals are similar as are the values of total flow through the RMSM HFM area. However, the distribution of flow is different. The NTS Flow Model shows a much smaller inflow through the northern boundary and flow into the model area along the eastern boundary rather than out. Review of the full DVRFS model area flow results show the NTS Flow Model to have significantly lower flow at the constant head boundaries and in terms of recharge.

The RMSM alternative HFMs were all run assuming the regional recharge scenario. Review of the results presented in Table 8-5 shows that the sums of the squared weighted residuals are similar to those determined for the other regional recharge runs. Total flow volumes through the RMSM HFM area are also comparable although, like the NTS Flow Model regional recharge run, flows through the northern boundary of the RMSM HFM area are lower than those calculated for the DVRFS model run. In addition, all three alternative model runs show flow into the RMSM HFM area along the

Table 8-5
Summary of Model Results

| | Regional Recharge | | Revised UGTA Recharge | | DRI Recharge | | Regional Recharge | | |
|--|--------------------------|--------------------------|--------------------------|--------------------------|--------------------------|--------------------------|---------------------------|--------------------------|--------------------------|
| | DVRFS | NTS Flow | DVRFS | NTS Flow | DVRFS | NTS Flow | No Redrock Valley Caldera | Southern LCA3 Ext. | SM Thrust |
| Sum of Squared Weighted Residuals | | | | | | | | | |
| Heads Only | 11531.0 | 18,049.0 | 19,130.0 | 30,049.0 | 16,800.0 | 19,372.0 | 20,963.0 | 18,297.0 | 18,200.0 |
| Drain Flows Only | 536.93 | 1,156.6 | 1,870.9 | 911.7 | 1,300.3 | 982.7 | 1,343.2 | 1,299.3 | 1,287.7 |
| Constant Head Boundary Flows | 543.34 | 48.2 | 1,114.4 | 222.8 | 284.0 | 127.7 | 94.7 | 58.7 | 45.1 |
| Sum | 12,611.27 | 19,253.0 | 22,115.0 | 31,183.0 | 18,385.0 | 20,482.0 | 22,401.0 | 19,656.0 | 19,533.0 |
| RMSM Model Area Boundary Flows | m³/day | m³/day | m³/day | m³/day | m³/day | m³/day | m³/day | m³/day | m³/day |
| North | 9,814.3 | 1,414.3 | 5,306.5 | 102.6 | 9,997.9 | 361.6 | 2,165.5 | 1,334.7 | 1,375.9 |
| South | -6,513.2 | -12,051.0 | -8,395.7 | -11,589.1 | -6,559.2 | -12,351.1 | -12,839.9 | -12,376.1 | -10,901.6 |
| East | -9,450.8 | 8,088.5 | -12,844.2 | 7,097.1 | -7,956.9 | 7,045.3 | 2,151.5 | 7,534.7 | 6,307.9 |
| West | -7,589.7 | -6,700.4 | -6,817.6 | -6,030.0 | -4,130.3 | -8,022.9 | -5,039.8 | -7,507.2 | -7,125.8 |
| Recharge | 13,739.3 | 9,248.7 | 22,751.0 | 10,419.3 | 8,648.4 | 12,967.1 | 13,562.7 | 11,013.9 | 10,343.6 |
| Total In | 23,553.7 | 18,751.4 | 28,057.5 | 17,619.0 | 18,646.3 | 20,373.9 | 17,879.7 | 19,883.4 | 18,027.4 |
| Total Out | -23,553.7 | -18,751.4 | -28,057.5 | -17,619.0 | -18,646.3 | -20,373.9 | -17,879.7 | -19,883.4 | -18,027.4 |
| Cumulative | 0.0 | 0.0 | 0.0 | 0.0 | 0.0 | 0.0 | 0.0 | 0.0 | 0.0 |
| Percent Difference ^a | 0.0 | 0.0 | 0.0 | 0.0 | 0.0 | 0.0 | 0.0 | 0.0 | 0.0 |
| DVRFS Model Area Flows | m³/day | m³/day | m³/day | m³/day | m³/day | m³/day | m³/day | m³/day | m³/day |
| IN | | | | | | | | | |
| CONSTANT HEAD | 349,591.3 | 201,144.3 | 388,437.3 | 238,172.1 | 346,831.2 | 204,860.6 | 182,889.3 | 196,157.5 | 197,991.7 |
| DRAINS | 0.0 | 0.0 | 0.0 | 0.0 | 0.0 | 0.0 | 0.0 | 0.0 | 0.0 |
| RECHARGE | 303,415.3 | 281,928.8 | 195,618.5 | 164,733.4 | 312,696.9 | 242,910.1 | 333,278.3 | 301,161.2 | 293,857.7 |
| TOTAL IN | 653,006.6 | 483,073.0 | 584,055.8 | 402,905.5 | 659,528.1 | 447,770.7 | 516,167.5 | 497,318.6 | 491,849.4 |
| OUT | | | | | | | | | |
| CONSTANT HEAD | 283,122.9 | 116,253.5 | 265,104.7 | 95,140.1 | 311,345.2 | 120,259.9 | 130,584.8 | 122,689.0 | 120,159.0 |
| DRAINS | 369,884.4 | 366,819.3 | 318,951.2 | 307,765.4 | 348,182.9 | 327,510.8 | 385,581.8 | 374,629.4 | 371,690.3 |
| RECHARGE | 0.0 | 0.0 | 0.0 | 0.0 | 0.0 | 0.0 | 0.0 | 0.0 | 0.0 |
| TOTAL OUT | 653,007.3 | 483,072.9 | 584,055.9 | 402,905.5 | 659,528.1 | 447,770.7 | 516,166.7 | 497,318.4 | 491,849.3 |
| IN - OUT | -0.6 | 0.2 | -0.1 | 0.1 | 0.0 | 0.0 | 0.8 | 0.2 | 0.1 |
| % DISCREPANCY | 0.0 | 0.0 | 0.0 | 0.0 | 0.0 | 0.0 | 0.0 | 0.0 | 0.0 |

^a Calculated as ((inflow + recharge) - (outflow)) / (outflow)

eastern boundary in contrast to the DVRFS model run. In comparison to the DVRFS model run data for the full DVRFS model area, flow at the constant head boundaries is lower, leading to lower overall flow volumes through the model.

8.7 Limitations

The primary limitation in estimating lateral boundary fluxes used for the CAU flow model stems from the indirect method of deriving the estimates. There are no practical means of directly measuring groundwater fluxes at the scale and spatial frequency needed, or measuring hydraulic gradients and hydraulic conductivities to derive the necessary groundwater fluxes. The limitations associated with deriving the fluxes from the regional-scale flow model are directly related to the degree to which the model accurately represents the physical system. The flow model representation of the physical system is a function of the: (1) appropriateness of the conceptual mode, (2) accuracy of the geologic model used to define parameter heterogeneity, (3) applicability of the recharge model, and (4) degree to which the model can be calibrated. The calibration of the model is dependent on not only how well the model mimics measured data but how the spatial distribution of target measurements compares to the spatial complexity of the system. Complexity of the physical system or the conceptual model in areas where there are no measurements is inherently uncertain. In addition, the model cannot be calibrated better than the uncertainty associated with the targets.

8.8 References

Belcher et al., 2004, see [2].

D'Agnese et al., 1997, see [9].

D'Agnese et al., 2002, see [10].

IT Corporation, 1996, see [11].

NSTec, 2007, see [5].

1. Blankennagel, R.K., and Weir, J.E., Jr. 1973. *Geohydrology of the Eastern Part of Pahute Mesa, Nevada Test Site, Nye County, Nevada*. U.S. Geological Survey Professional Paper 712-B, 35 p.
2. Belcher, W.R., J.B. Blainey, F.A. D'Agnese, C.C. Faunt, M.C. Hill, R.J. Laczniak, G.M. O'Brien, C.J. Potter, H.M. Putnam, C.A. San Juan, and D.S. Sweetkind. 2004. *Death Valley Regional Ground-Water Flow System, Nevada and California - Hydrogeologic Framework and Transient Ground-Water Flow Model*, Scientific Investigations Report 2004-5205. U.S. Geological Survey.
3. U.S. Geological Survey. 1988. *Techniques of Water-Resources Investigations of the United States Geological Survey, A Modular Three-Dimensional Finite-Difference Ground-Water Flow Model*. U.S. Government Printing Office, Washington DC.
4. Bechtel Nevada. 2002. *A Hydrostratigraphic Model and Alternatives for the Groundwater Flow and Contaminant Transport Model of Corrective Action Units 101 and 102: Central and Western Pahute Mesa, Nye County, Nevada*, DOE/NV/11718--706. Las Vegas, NV.

5. National Security Technologies, LLC. 2007. *A Hydrostratigraphic Model and Alternatives for the Groundwater Flow and Contaminant Transport Model of Corrective Action Unit 99: Rainier Mesa-Shoshone Mountain, Nye County, Nevada*, DOE/NV/29546--146. Las Vegas, NV.
6. Bechtel Nevada. 2006. *A Hydrostratigraphic Model and Alternatives for the Groundwater Flow and Contaminant Transport Model of Corrective Action Unit 97: Yucca Flat-Climax Mine, Lincoln and Nye Counties, Nevada*, DOE/NV/11718--1119. Las Vegas, NV.
7. Bechtel Nevada. 2005. *A Hydrostratigraphic Model and Alternatives for the Groundwater Flow and Contaminant Transport Model of Corrective Action Unit 98: Frenchman Flat, Clark, Lincoln, and Nye County, Nevada*, DOE/NV/11718--1064. Las Vegas, NV.
8. Environmental Modeling Systems, Inc. 2007. *Groundwater Modeling System (GMS)*, Version 6.0. South Jordan, UT.
9. D'Agnese, F.A., C.C. Faunt, A.K. Turner, and M.C. Hill. 1997. *Hydrogeologic Evaluation and Numerical Simulations of the Death Valley Regional Groundwater Flow System, Nevada and California*. USGS Professional Paper 1607. U.S. Geological Survey, Denver CO.
10. D'Agnese, F.A., G.M. O'Brien, C.C. Faunt, W.R. Belcher, W.R., and C. San Juan. 2002. *A Three-Dimensional Numerical Model of Predevelopment Conditions in the Death Valley Regional Ground-water Flow System, Nevada and California*. U.S. Geological Survey Water-Resources Investigations Report 02-4102, 114 p.
11. IT Corporation. 1996. *Regional Geologic Model Data Documentation Package (Phase I, Data Analysis Documentation, Volume I, Parts 1 and 2)*, ITLV/10972--181. Las Vegas, NV.

9.0 HYDRAULIC HEADS

Hydraulic head provides the state of hydraulic potential throughout a saturated media flow system. Hydraulic head is a spatial potential field that varies both laterally and vertically. The flux of water through the system is determined by the hydraulic conductivity of the saturated media and the hydraulic head gradient. Water always moves from areas of higher head to areas of lower head. The hydraulic head gradient is the amount of change in potential (head) over the distance of a change in spatial location. In the RMSM area, hydraulic heads are provided by measurements of water levels in wells. Hydraulic head is given as the height of the water level in a well above a fixed datum; this section uses meters above mean sea level (m amsl). Springs within the RMSM HFM area are perched and not discussed in this section.

9.1 Objectives

This section provides available hydraulic head data, an overview of the nature of the hydraulic head field in the RMSM area, and an overview of the types of data found in [Appendix E](#) of this report. The distribution of aquifers and confining units, saturation of the rocks in the HFM model, and hydraulic gradients within and between aquifers are also discussed.

9.2 Data Types

To evaluate hydraulic head by measurements in wells, numerous types of data must be compiled. The most important are the water levels themselves and the interval of saturated media that the well is open to, which is referred to in this report as the FAI. The location and hydrostratigraphy of the well must be established. Finally, information about factors that may affect the water levels measured at a well, such as production at the well or nearby wells, is necessary to ensure the quality of the measurements.

9.2.1 Data Uncertainties

There are a variety of factors that create uncertainty in the measurement of hydraulic heads at wells. The FAI or completion interval is the interval of a well in hydraulic communication with the saturated media. This interval is generally defined by a top and bottom depth or elevation of the open interval. The majority of wells are close to vertical, but deviation of the well can occur either intentionally and unintentionally. These deviations can create errors in both the position of the FAI and in the elevation of the hydraulic head measurement itself. Borehole directional surveys can accurately determine the position of a well in 3-D; however, these surveys are not available for all wells.

Because hydraulic head is a potential field and varies with location, the length over which the well is open creates some uncertainty in the location a head measurement is representative of, especially for

wells with large open intervals, or open intervals that cross multiple HSUs with varying hydraulic conductivities and large vertical gradients. Problems can also occur that make the FAI uncertain for a well. Wells with uncased FAIs are susceptible to borehole collapse, which may partially isolate the lower section of the well from measurements. Seals that isolate the FAI of a well can also leak, changing the representativeness of measurements in the FAI.

The drilling of a well can perturb the natural flow system at the well, and water levels taken immediately after drilling may not be representative of undisturbed conditions at the completion location. Among the problems that can occur are plugging of the formation by drilling fluid, and the introduction or removal of water to or from the formation. Production of water from a well or a nearby well can also significantly affect the water levels. These uncertainties can be reduced by monitoring hydraulic head responses over time.

Some natural variations in flux can create small fluctuations in the hydraulic head measured in a well completion over time. This analysis strives to determine representative steady-state estimates of hydraulic head, with the variation in head included as uncertainty. Measurement errors can also occur; however, the USGS water-level monitoring program through which most of the data in this document are acquired is highly accurate, and measurement uncertainty tends to be small and well characterized. There are a handful of useful measurements where the measurement error is significant in relation to other sources of uncertainty.

Finally, uncertainty in the hydraulic head measurements increases as distance from measurement points increases. Hydraulic head in the HFM model area is generally well characterized in the vicinity of the RMSM CAS locations, but there are some remote sections with few measurement locations, such as the southwest corner of the model area.

9.2.2 Data Sources

Water levels included in this report are compiled from databases produced specifically for the UGTA Project by the USGS [1-3] and from the USGS National Water Information System (NWIS) web interface [4]. The FAI information is compiled from drilling records produced by the various management and operating (M&O) contractors at the NTS; well completion and testing reports produced by various organizations that operate at the NTS; and other previously compiled sources, such as the UGTA Borehole Index and the USGS NWIS web interface. Well hydrostratigraphy is compiled from the well picks published in the HFM reports [5-8].

9.2.3 Data Compilation

Water-level data from the three NTS-specific USGS databases [1-3] and data from the USGS NWIS website [4] within 20 km of the RMSM HFM model boundary are merged into a single database for this analysis. The datasets in the three NTS-specific databases are updated with water levels from the NWIS website, measured after their dates of publication. It should be noted that the published databases contain some supporting data types not available on the USGS NWIS website.

Land-surface elevations compiled in the database are from the USGS databases. Coordinates for each location are from the UGTA Borehole Index database.

The FAI information is compiled in a table directly from a variety of sources. Often multiple sources containing complementary information are used for a single location. The HSU data used are from the well picks compiled to create the CAU HFM models. The latest CAU model is used for locations where one or more HFMs overlap. The HSU data for locations outside the boundaries of the existing CAU HFM models were provided via personal communication with the creators of the HFM models. Pumping data for the RMSM area are compiled in [Section 7.0](#) of this report. Other conditions that could disturb the water level in a well completion are compiled as notes in a database table that is linked to the well completion.

9.2.4 Data Analysis Methods

The purpose of this analysis is to produce a set of representative hydraulic heads with accurate uncertainties that can be used to characterize the state of hydraulic potential and gradient within the model area. To do this, the hydraulic head measurements at well completions were reviewed. Each set of hydraulic head measurements was evaluated to determine whether or not the levels are in equilibrium. Sets of hydraulic head measurements were flagged where there are few data points, there is a large variation in head, or for other reasons, as discussed in [Section 9.2.1](#), to believe measurements at the well are not representative. Comments are attached to flagged data in the database to explain why they are not used. Only the data that are not flagged are used in the development of the hydraulic head dataset. In some instances, suspect measurements of hydraulic head are intentionally included in averaging to better quantify uncertainty. The `RMSM_Hydraulic_Head_Data_Report.pdf` file included in the `Appendix\E` folder on the accompanying DVD contains complete hydrographs that show which measurements of head are used in the calculation of the mean values shown in [Figure 9-1](#). The HSUs that contribute water to the well completions are determined by comparing the well picks used to create the HFM at the location to the FAI and calculated mean water level. They are also shown in the report included in the `Appendix\E` folder. Finally, these representative hydraulic heads are examined within the larger context of the HFM shown in the block diagrams and cross sections (`RMSM_HFM_Figures.pdf`) included in the `Appendix\A` folder on the accompanying DVD.

9.3 RMSM Hydraulic Head Distribution

The LCA is the largest aquifer in the area. This aquifer is buried relatively deep in the RMSM HFM area. Only two wells in the model area are completed in the LCA: ER-16-1 and ER-12-1. The water level in ER-16-1 is roughly 763 m amsl with at least 4 m of uncertainty. Well ER-12-1 has only a single water-level measurement representative of the LCA. The level was taken with a pressure transducer used during a packer test before the well was fully cased. The water level is 931 m amsl with a measurement error of 7 m. The base geologic model assumes the completion is in LCA, but an alternative model assumes the rock that the well is completed in is an isolated LCA3 thrust sheet. Thus, the representativeness of the ER-12-1 measurement is highly uncertain. Water levels in wells in the LCA in Yucca Flat to the east of the model area vary from about 726 m amsl to about 740 m

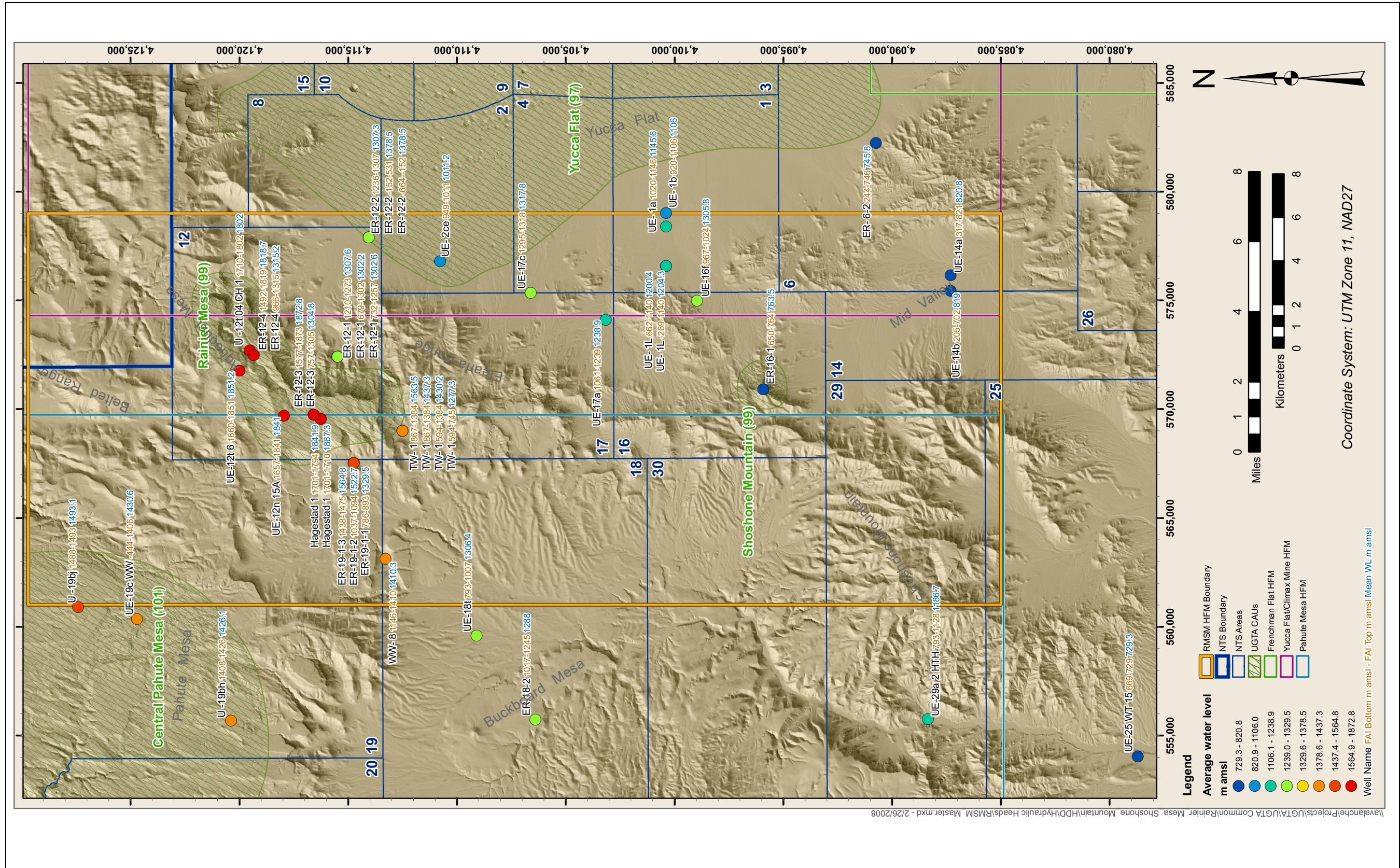


Figure 9-1
RMSM Hydraulic Head Calibration Targets

amsl. The similarity of water levels in Yucca Flat to the measurements in ER-16-1 show the characteristic low hydraulic gradient in the LCA in the area.

As discussed in [Section 4.0](#), the LCA is capped by a section of UCCU that isolates it from remainder of the HSUs in all but the southeast corner of the model. The LCA3 is the next major aquifer HSU above the UCCU. There are two distinct occurrences of LCA3 in the RMSM HFM as shown in the block diagram in the Appendix\A folder. The first occurrence is beneath Rainier and Aqueduct Mesas and runs from northeast to southwest. The second major occurrence is on the eastern edge of the HFM in western Yucca Flat and Mid Valley. The western Yucca Flat portion is separated from the Mid Valley portion in the RMSM HFM domain, but the two are connected to the east in the Yucca Flat HFM [9]. In the Rainier Mesa portion of the LCA3, water levels are at 1,315.2 m amsl at ER-12-4 main, 1,304.8 m amsl in ER-12-3 main, and 1,277.3 m amsl in TW-1. In the Yucca Flat portion of the LCA3, water levels are at 1,011 m amsl in UE-2ce and around 887 m amsl in UE-1c. At the northern tip of the LCA3 in Yucca Flat at ER-12-1, the bottom of the LCA3 is unsaturated at 1,460 m amsl.

Above the LCA3, the hydrostratigraphy becomes much more complicated. The hydrostratigraphic section just above the LCA3 includes four tuff confining units (argillic tuff confining unit [ATCU], Oak Spring Butte confining unit [OSBCU], lower tuff confining unit 1 [LTCU1], and lower tuff confining unit [LTCU]); however, there is an extensive but thin welded tuff aquifer (RVA) between the ATCU and the OSBCU in most of the western part of the model with some faulting that interrupts the continuity of the unit. The HFM shows some connection between the RVA and the LCA3 at Rainier Mesa. There are a number of aquifer units on top of the tuff confining units with varying extents and degrees of interconnection. There are also some smaller, less-extensive confining units mixed in as well. The block diagrams included in the Appendix\A folder illustrate the relationships.

In the immediate vicinity of Rainier Mesa, water levels in wells UE-12t 6, UE-12n 15A, U-12t.04 CH 1, ER-12-4 piezometer, and ER12-3 piezometer in tuff confining units are in the range of 1,800 to 1,875 m amsl. These high water levels are most likely caused by the low conductivity tuffs trapping the relatively high amount of recharge that occurs on the mesa. Data from ER-12-3 and ER-12-4 indicate that the vertical gradient is close to 1 and that water levels are between the top and bottom of the well FAI. Furthermore, there is a lack of a significant horizontal gradients. This shows that the largest portion of the hydraulic head measurements is elevation head with little pressure head from above and is consistent with a low permeability recharge zone.

Just west of Rainier Mesa, ER-19-1 contains three separate completions that provide a vertical profile of hydraulic head. The water level in ER-19-1-3 is about 1,565 m amsl in the OSBCU, and the level is about 70 m above the top of the FAI, indicating that the FAI is well within the saturated zone. Well ER-19-1-2 is completed in the RVA, and water levels are about 1,523 m amsl. The pressure component of the head at the FAI is roughly 450 m. The gradient between ER-19-1-3 and ER-19-1-2 is about 0.11. Well ER-19-1-1 is the deepest completion of the well in the LCCU1 with a water level at about 1,330 m amsl. The gradient between the deep and middle completion is about 0.86. The LCA3 is the next aquifer unit modeled below the well, and the gradient suggests that though the RVA is clearly saturated at the location, water levels in the unit are markedly disconnected from those in the LCA3. Water levels taken in WW-8 in the BRA in the western part of the model above the tuff

confining units are at about 1,410 m amsl, which is above the water levels in Rainier Mesa LCA3. The unit is separated from the RVA and LCA3 by tuff confining unit.

Areal recharge flux appears to play an important role in the hydraulic heads in many of the wells. Well UE-16f is located to the southeast of Syncline Ridge in the northeast quarter of Area 16. The well is completed in UCCU, but Syncline Ridge is an isolated block of UCA. There are no significant aquifer connections to the UCA as is shown by the outcropping of UCCU to the west of Syncline Ridge. The water level in UE-16f is 1,305 m amsl, and the well is surrounded by lower hydraulic heads as shown in [Figure 9-1](#). The most plausible explanation for the abnormally high water level in the well is that the head is controlled by recharge into the UCA on Syncline Ridge.

The HFM area to the north and west of Rainier and Aqueduct Mesas also receive significant recharge. There are few hydraulic head measurements here, but the presence of confining units mixed with aquifers combined with the recharge is likely to create steep vertical gradients as surface recharge works its way down.

9.4 References

1. Fenelon, J.M. 2005. *Analysis of Ground-Water Levels and Associated Trends in Yucca Flat, Nevada Test Site, Nye County, Nevada, 1951-2003*, Scientific Investigations Report 2005-5175. Carson City, NV: U.S. Geological Survey.
2. Fenelon, J.M. 2006. *Database of Ground-Water Levels in the Vicinity of Rainier Mesa, Nevada Test Site, Nye County, Nevada, 1957-2005*. Carson City, NV: U.S. Geological Survey.
3. Fenelon, J.M. 2006. Personal communication to SNJV. *Database of Ground-Water Levels in the Vicinity of Frenchman Flat and Eastern Pahute Mesa, Nevada Test Site, Nye County, Nevada, 1950-2006*. Henderson, NV: U.S. Geological Survey.
4. U.S. Geological Survey. 2007. "USGS Ground-Water Data for the Nation, National Water Information System: Web Interface." As accessed at <http://nwis.waterdata.usgs.gov/nwis/gwlevels> on 11 February 2008.
5. National Security Technologies, LLC. 2007. *A Hydrostratigraphic Model and Alternatives for the Groundwater Flow and Contaminant Transport Model of Corrective Action Unit 99: Rainier Mesa-Shoshone Mountain, Nye County, Nevada*, DOE/NV/29546--146. Las Vegas, NV.
6. Bechtel Nevada. 2006. *A Hydrostratigraphic Model and Alternatives for the Groundwater Flow and Contaminant Transport Model of Corrective Action Unit 97: Yucca Flat-Climax Mine, Lincoln and Nye Counties, Nevada*, DOE/NV/11718--1119. Las Vegas, NV.
7. Bechtel Nevada. 2002. *A Hydrostratigraphic Model and Alternatives for the Groundwater Flow and Contaminant Transport Model of Corrective Action Units 101 and 102: Central and Western Pahute Mesa, Nye Counties, Nevada*, DOE/NV/11718--706. Las Vegas, NV.

8. Bechtel Nevada. 2006. *A Hydrostratigraphic Model and Alternatives for the Groundwater Flow and Contaminant Transport Model of Corrective Action Unit 98: Frenchman Flat, Clark, Lincoln and Nye Counties, Nevada*, DOE/NV/11718--1064. Las Vegas, NV.
9. Stoller-Navarro Joint Venture. 2006. *Phase I Hydrologic Data for the Groundwater Flow and Contaminant Transport Model of Corrective Action Unit 97: Yucca Flat/Climax Mine, Nevada Test Site, Nevada*, S-N/99205-077. Las Vegas, NV.

10.0 SUBSURFACE TEMPERATURE DATA

Groundwater temperature is controlled by the conductive and advective heat flow in the geologic system. The proximity of the heat source at depth, thermal conductivity of the rocks between the heat source and the groundwater, advection of heat via groundwater flow, and the complexity of the faults and fracture zones all affect the heat flow and the temperature of groundwater.

This section refers the reader to the existing temperature data for potential use in the groundwater fate and transport model for the RMSM CAU. Temperature data can be used to correct the hydraulic head data or as a potential field in the case where non-isothermal groundwater flow modeling is deemed necessary. The groundwater temperature measurements referenced were collected by DRI, Lawrence Livermore National Laboratory (LLNL), and the USGS.

Groundwater temperature data collected during well testing and water-level measurements are necessary to convert the measured columns of water in wells to hydraulic head at the FAI. In addition, the spatial temperature variation and temperature gradients for the RMSM CAU may be used as the basis for specifying the appropriate temperature for use in conversion of hydraulic conductivity values to intrinsic permeabilities. This conversion requires the temperature data to calculate water density and viscosity (see [Section 3.1.6](#)). Subsurface temperatures can also be used to evaluate the movement of groundwater as was done for central and western Pahute Mesa [\[1\]](#). The selection of the appropriate thermal flow field (isothermal or non-isothermal) will be determined during the development of the groundwater fate and transport model.

10.1 Groundwater Temperature Data for the RMSM Model Area

Groundwater temperature measurements as well as the types of rock represented in a well and their thermal conductivities are needed to understand subsurface thermal conditions. [Table 10-1](#) identifies key reports that address temperature data for the NTS area. The Gillespie report [\[2\]](#) is one of the most recent and is the most comprehensive of those cited. The reader is directed to this document for temperature profiles in the RMSM CAU as well as NTS-wide. The USGS report [\[3\]](#) provides additional groundwater temperature profiles not found in Gillespie [\[2\]](#).

The data contained in the Gillespie report have been filtered [\[2\]](#). In an effort to include only data from wells in thermal equilibrium with the surrounding rock, groundwater temperature measurements taken less than one year after the installation of the wells are not used. In addition, the data were reviewed to eliminate those boreholes where vertical flow within the borehole might be present and for which the temperature profiles were collected from too short an interval relative to the borehole diameter to yield accurate heat flow values [\[4, 5\]](#).

[Tables 10-2](#) and [10-3](#) list the RMSM wells for which temperature profiles are found in references [\[2\]](#) and [\[3\]](#) respectively. [Figure 10-1](#) shows the locations of these wells.

Table 10-1
Key Reports Providing Temperature Data and Information for the NTS Area

| Report | Synopsis of Temperature Information Relevant to the RMSM Area |
|--|--|
| <i>Preliminary Interpretation of Thermal Data from the Nevada Test Site [6]</i> | Regional heat flow values within and adjacent to the NTS |
| <i>Temperature, Thermal Conductivity, and Heat Flow Near Yucca Mountain, Nevada: Some Tectonic and Hydrologic Implications [7]</i> | Laboratory measured thermal conductivity of major volcanic and dolomite rock types at the NTS |
| <i>Temperature Data Evaluation [8]</i> | Review of temperature logs available on the NTS, and the selection and evaluation of temperature log data from 13 boreholes deemed suitable for the determination of heat flow values |
| <i>Temperature Profiles and Hydrologic Implications from the Nevada Test Site Area [2]</i> | Compilation of temperature information related to the NTS, the presentation and analysis of temperature profiles from selected wells on the NTS, and identification of the thermal conductivity value for alluvium |
| <i>Ground-Water Temperature Data, Nevada Test Site and Vicinity, Nye, Clark, and Lincoln Counties, Nevada, 2000–2006 [3]</i> | Compilation of groundwater temperature information which includes some temperature profiles not found in Gillespie [1] |

The Gillespie report provides plots of each of the temperature profiles combined with depictions of the stratigraphy over which the data were collected [2]. In addition, it discusses thermal gradients, thermal conductivity, and heat flow. Tables are provided giving heat flow and thermal conductivity values for rock types found at the NTS. The USGS groundwater temperature data report provides additional temperature profiles for RMSM area wells ER-12-2, ER-19-1, and HTH-1 [3]. In addition, it provides a temperature profile for ER-12-1; no data for this well are given in Gillespie [2].

The most likely use for the temperature data referenced here is for the conversion of hydraulic conductivity values to intrinsic permeabilities. The data, as presented, will be the starting point of any such analysis. The YFCM HFM report provides an analysis of advective heat transport for the Yucca Flat CAU area [9]. Water levels and temperature data compiled for the NTS by the USGS are found at: http://nevada.usgs.gov/doe_nv/watertemp/temp_map.htm.

Table 10-2
Wells with Temperature Logs in the RMSM Model Area

| Well Name | Well Location Easting | Well Location Northing | Date of Temperature Log | Organization Providing Log | Depth to Logged Top (m) | Temperature at Top (°C) | Depth to Logged Bottom (m) | Temperature at Bottom (°C) | Temperature Gradient (°C/m) |
|-----------|-----------------------|------------------------|-------------------------|----------------------------|-------------------------|-------------------------|----------------------------|----------------------------|-----------------------------|
| ER-12-2 | 572,411.50 | 4,115,492.70 | 04/27/2004 | DRI | 45.35 | 17.42 | 1569.35 | 53.65 | 0.024 |
| ER-19-1 | 567,541.54 | 4,114,743.48 | 04/22/2003 | DRI | 517.73 | 23.57 | 1092.10 | 34.77 | 0.020 |
| HTH-1 | 569,000.27 | 4,112,499.01 | 08/19/1991 | DRI | 448.97 | 20.97 | 1127.49 | 28.40 | 0.011 |
| HTH-1 | 569,000.27 | 4,112,499.01 | 04/22/2003 | DRI | 425.84 | 15.43 | 1127.49 | 28.40 | 0.018 |
| UE-1L | 576,566.80 | 4,100,381.80 | 01/28/2002 | DRI | 160.02 | 20.21 | 237.29 | 22.31 | 0.027 |
| UE-2ce | 576,804.20 | 4,110,772.70 | 01/28/2002 | DRI | 441.66 | 31.10 | 459.94 | 32.78 | 0.092 |
| UE-14b | 575,427.20 | 4,087,304.10 | 08/21/1991 | DRI | 509.63 | 23.17 | 1097.89 | 32.13 | 0.015 |
| UE-14b | 575,427.20 | 4,087,304.10 | 04/16/2003 | DRI | 486.80 | 19.43 | 1100.36 | 30.72 | 0.018 |
| UE-16f | 574,999.70 | 4,098,960.00 | 05/02/1994 | LLNL | 115.13 | 21.02 | 424.31 | 25.07 | 0.013 |
| UE-16f | 574,999.70 | 4,098,960.00 | 04/16/2003 | DRI | 103.05 | 17.53 | 424.31 | 25.07 | 0.023 |
| UE-17a | 574,116.20 | 4,103,156.80 | 05/02/1994 | LLNL | 194.33 | 24.04 | 363.82 | 28.03 | 0.024 |
| UE-17a | 574,116.20 | 4,103,156.80 | 04/17/2003 | DRI | 180.01 | 14.94 | 366.25 | 24.27 | 0.050 |
| ER-12-1 | 572,411.50 | 4,115,493.00 | 06/24/2004 | USGS | 466.81 | 23.20 | 524.42 | 24.20 | 0.017 |

Source: [2]

Table 10-3
Wells with Temperature Logs in the RMSM Model Area

| Well Name | Well Location Easting | Well Location Northing | Date of Temperature Log | Organization Providing Log | Depth to Logged Top (m) | Temperature at Top (°C) | Depth to Logged Bottom (m) | Temperature at Bottom (°C) | Temperature Gradient (°C/m) |
|---------------------------|-----------------------|------------------------|-------------------------|----------------------------|-------------------------|-------------------------|----------------------------|----------------------------|-----------------------------|
| ER-12-2 main (lower zone) | 577,902.60 | 4,114,058.00 | 06/29/2004 | USGS | 63.64 | 18.90 | 370.86 | 29.10 | 0.033 |
| ER-12-2 main (upper zone) | 577,902.60 | 4,114,058.00 | 06/29/2004 | USGS | 57.60 | 18.90 | 1213.65 | 46.90 | 0.024 |
| ER-19-1-1 (deep) | 567,541.60 | 4,114,743.00 | 06/28/2004 | USGS | 542.88 | 27.10 | 1082.96 | 36.00 | 0.016 |
| ER-19-1-2 (middle) | 567,541.60 | 4,114,743.00 | 06/29/2004 | USGS | 350.38 | 22.50 | 435.42 | 24.20 | 0.020 |
| HTH-1 | 569,000.27 | 4,112,499.01 | 10/13/2004 | USGS | 447.09 | 21.00 | 1116.40 | 29.80 | 0.013 |

Source: [3]

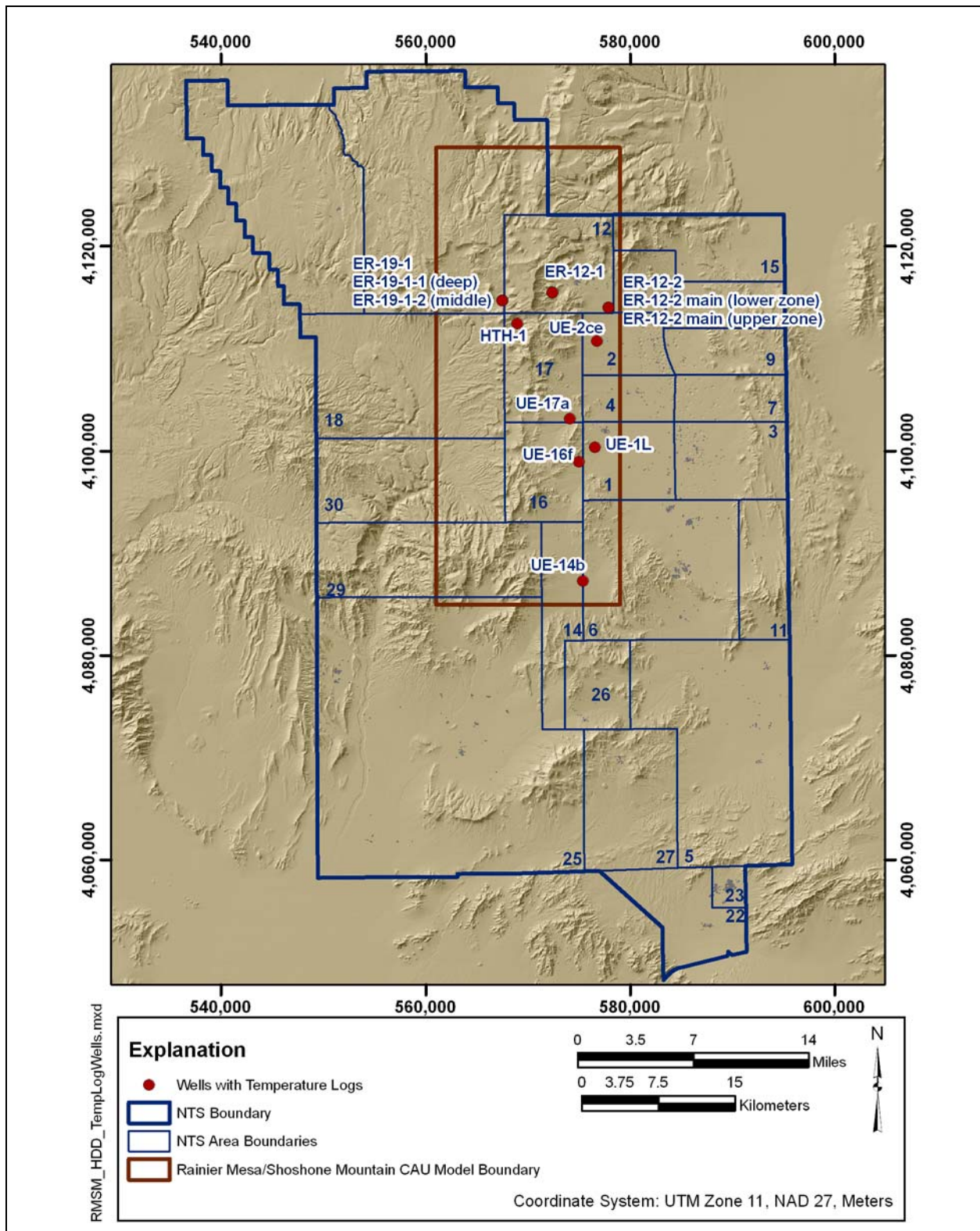



Figure 10-1
RMSM Locations of Existing Groundwater Temperature Profiles

10.2 References

1. Stoller-Navarro Joint Venture. 2006. *Groundwater Flow Model of Corrective Action Units 101 and 102: Central and Western Pahute Mesa, Nevada Test Site, Nye County, Nevada*, S-N/99205-076. Las Vegas, NV.
2. Gillespie, D. 2005. *Temperature Profiles and Hydrologic Implications from the Nevada Test Site Area*, DOE/NV/13609-40; Publication No. 45211. Las Vegas, NV: Desert Research Institute.
3. Reiner, S.R. 2007. *Ground-water Temperature Data, Nevada Test Site and Vicinity, Nye, Clark, and Lincoln Counties, Nevada, 2000–2006*. U.S. Geological Survey Data Series 269, 20 p.
4. Oberlander, P.L., and C.E. Russell. 2005. *Borehole Flow and Horizontal Hydraulic Conductivity with Depth at Well ER-12-3*, DOE/NV/13609-LTR2005-002.
5. Oberlander, P.L., and C.E. Russell. 2005. *Borehole Flow and Horizontal Hydraulic Conductivity with Depth at Well ER-12-4*, DOE/NV/13609-LTR2005-003.
6. Sass, J.H., and A.H. Lachenbruch. 1982. *Preliminary Interpretation of Thermal Data from the Nevada Test Site*. U.S. Geological Survey Open-File Report 82-973, 30 p.
7. Sass, J.H., A.H. Lachenbruch, W.W. Dudley, S.S. Priest, and R.J. Munro. 1987. *Temperature, Thermal Conductivity, and Heat Flow Near Yucca Mountain, Nevada: Some Tectonic and Hydrologic Implications*. U.S. Geological Survey Open-File Report, 87-649, 118 p.
8. Gillespie, D. 2003. *Temperature Data Evaluation*, DOE/NV/13609-22; Publication No. 45194. Las Vegas, NV: Desert Research Institute.
9. Stoller-Navarro Joint Venture. 2006. *Phase I Hydrologic Data for the Groundwater Flow and Contaminant Transport Model of Corrective Action Unit 97: Yucca Flat/Climax Mine, Nevada Test Site, Nye County, Nevada*, Rev. 0, S-N/99205--077. Las Vegas, NV.



Appendix A
RMSM HFM Data

A.1.0 INTRODUCTION

Supporting information for the RMSM HFM, as outlined in [Section 4.0](#), is provided in the Appendix\A folder on the accompanying DVD. The folder contains tables outlining the HSU and HGU system, geologic cross sections, and geologic block diagrams. The information contained in the accompanying files is also contained in the RMSM HFM RMSM HFM document [1] but is organized differently here.

A.2.0 DATASET SUMMARY

An Excel workbook file, RMSM_HFM.xls, contains four worksheets described in the Index worksheet in the file. The workbook outlines the HSUs and HGUs in the HFM, shows the relations between the two classification systems, and shows the relationships of the HSUs to previous models.

An Adobe portable document format (pdf) file, RMSM_HFM_Figures.pdf, contains block diagrams and cross sections of the HFM model. The file contains bookmarks for quick navigation. The up and down arrows on the keyboard can also be used to flip quickly back and forth between pages, which allows better visualization of the extent of HSUs in the block diagrams.

A.3.0 REFERENCES

1. National Security Technologies, LLC. 2007. *A Hydrostratigraphic Model and Alternatives for the Groundwater Flow and Contaminant Transport Model of Corrective Action Unit 99: Rainier Mesa-Shoshone Mountain, Nye County, Nevada*, DOE/NV/29546--146. Las Vegas, NV.



Appendix B

Hydraulic Properties Additional Analysis

B.1.0 INTRODUCTION

This appendix includes characterization group-specific figures for the K-dataset distributions and depth decay.

B.2.0 CHARACTERIZATION GROUP DATASETS

Figures B.2-1 through B.2-12 show the individual CG datasets developed for analysis and fitted lognormal distributions, bounded by the 95% confidence interval. The data points shown are not the values listed in the database for the analyses compiled from records and reports. Rather, they are the recalculated values following the analysis methodology described in [Section 5.9](#).

- AA Pumping-Scale CDF
- AA Pumping-Scale Depth Decay
- LFA Pumping-Scale CDF
- LFA Pumping-Scale Depth Decay
- WTA Pumping-Scale CDF
- WTA Pumping-Scale Depth Decay
- TCU Pumping-Scale CDF
- TCU Pumping-Scale Depth Decay
- LCA Pumping-Scale CDF
- LCA Pumping-Scale Depth Decay
- LCA3 Pumping-Scale CDF
- LCA3 Pumping-Scale Depth Decay

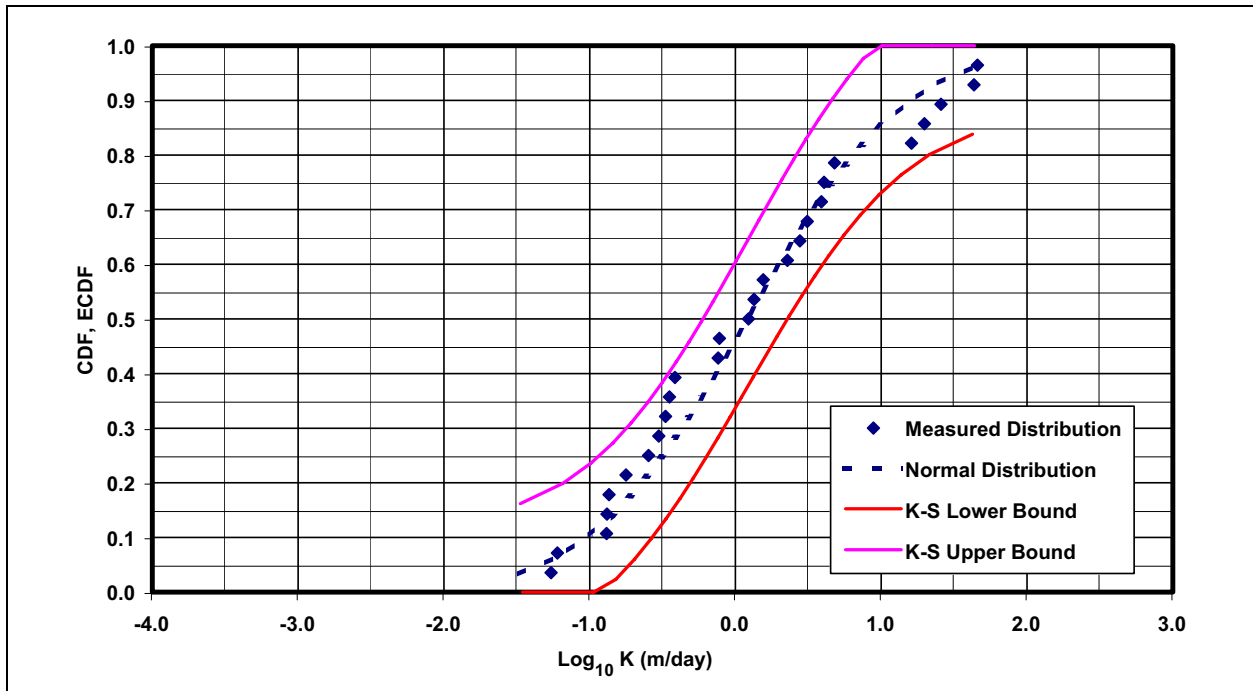


Figure B.2-1
AA Pumping-Scale CDF

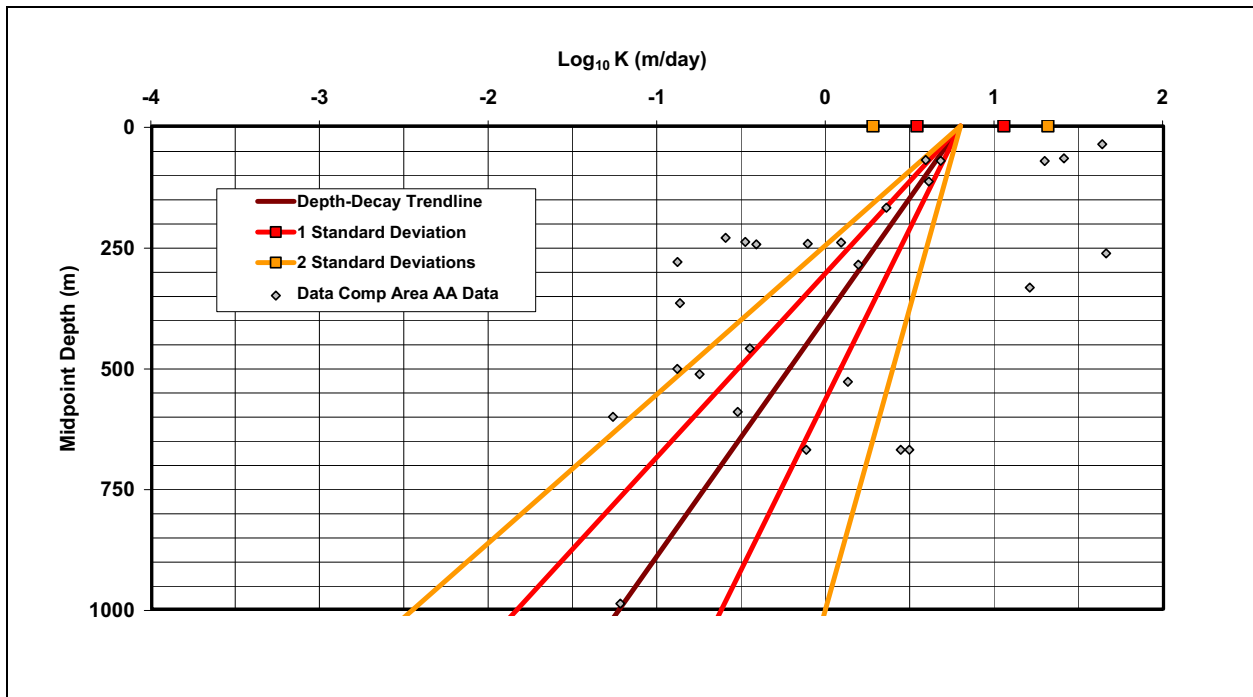


Figure B.2-2
AA Pumping-Scale Depth Decay

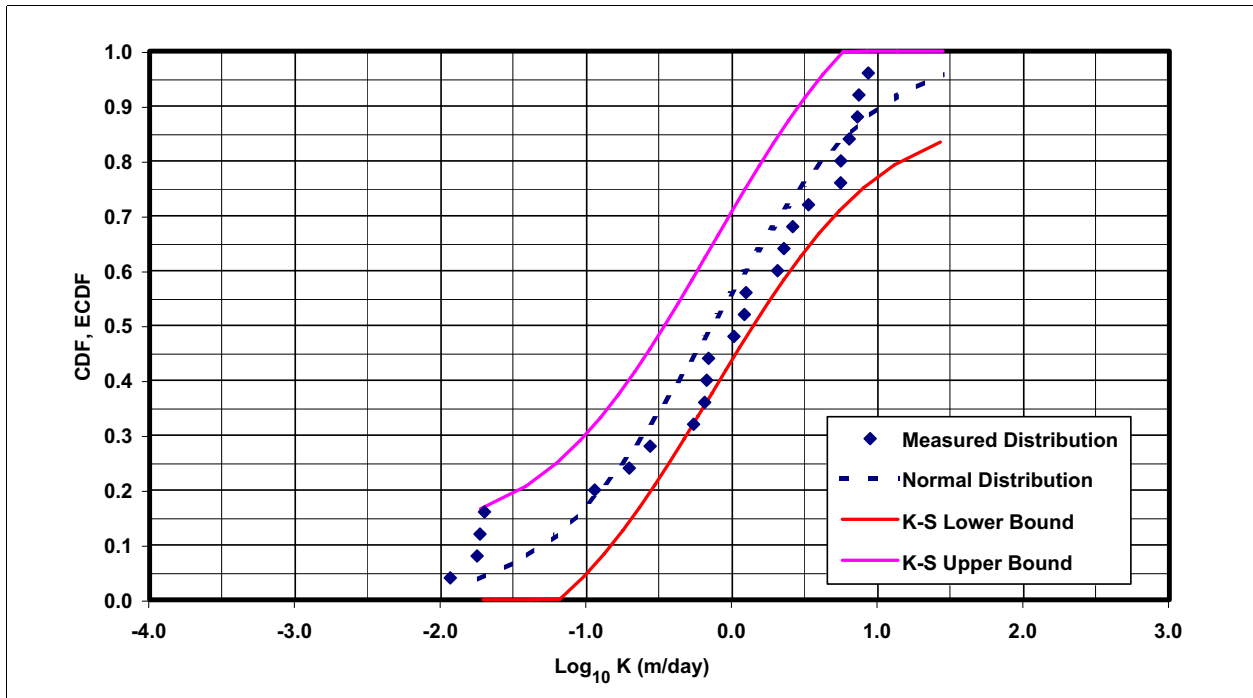


Figure B.2-3
LFA Pumping-Scale CDF

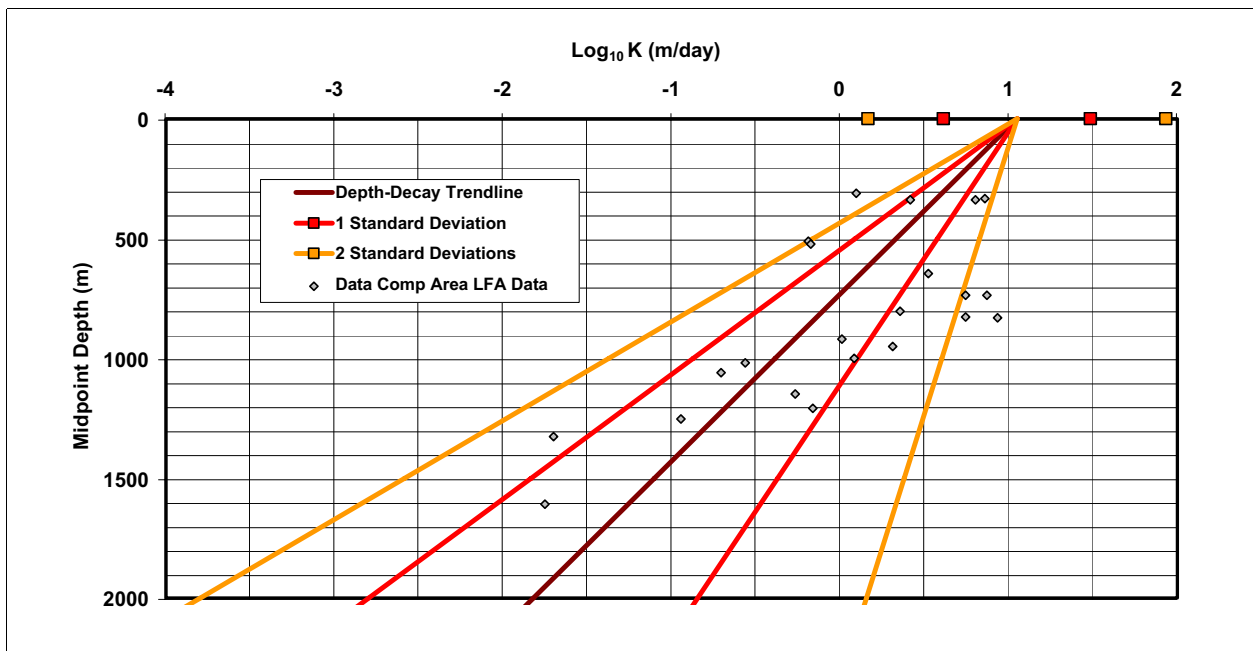


Figure B.2-4
LFA Pumping-Scale Depth Decay

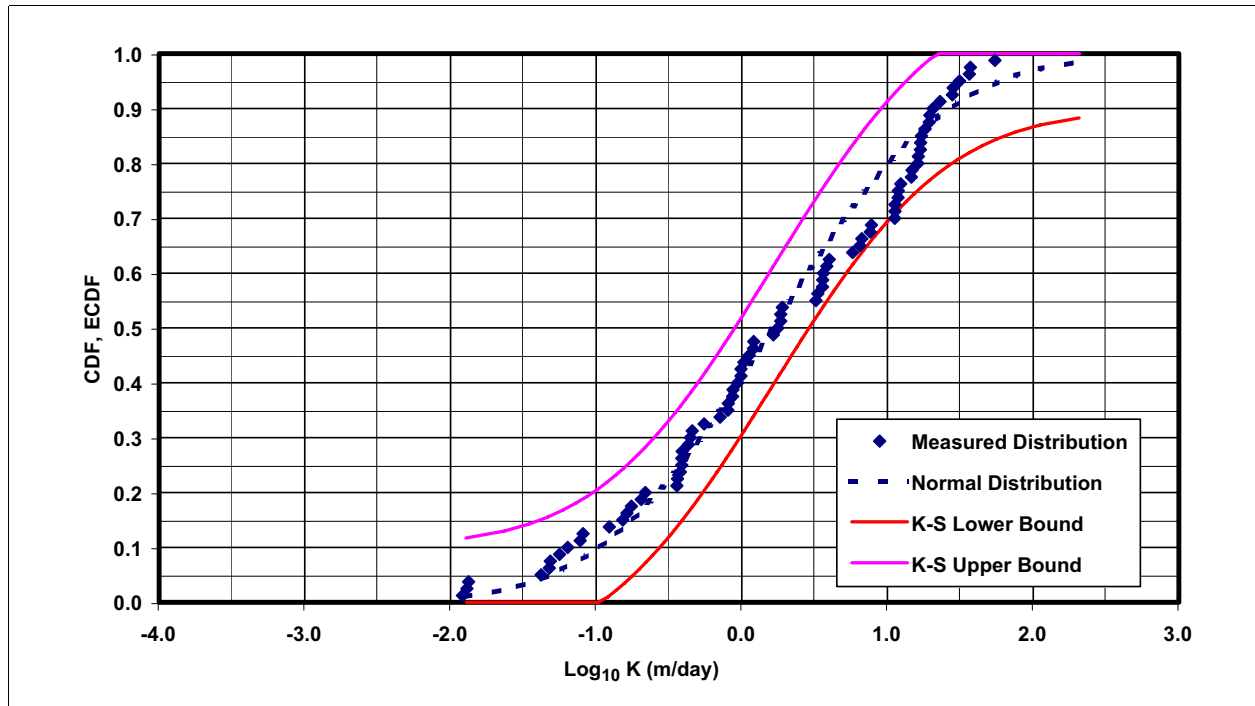


Figure B.2-5
WTA Pumping-Scale CDF

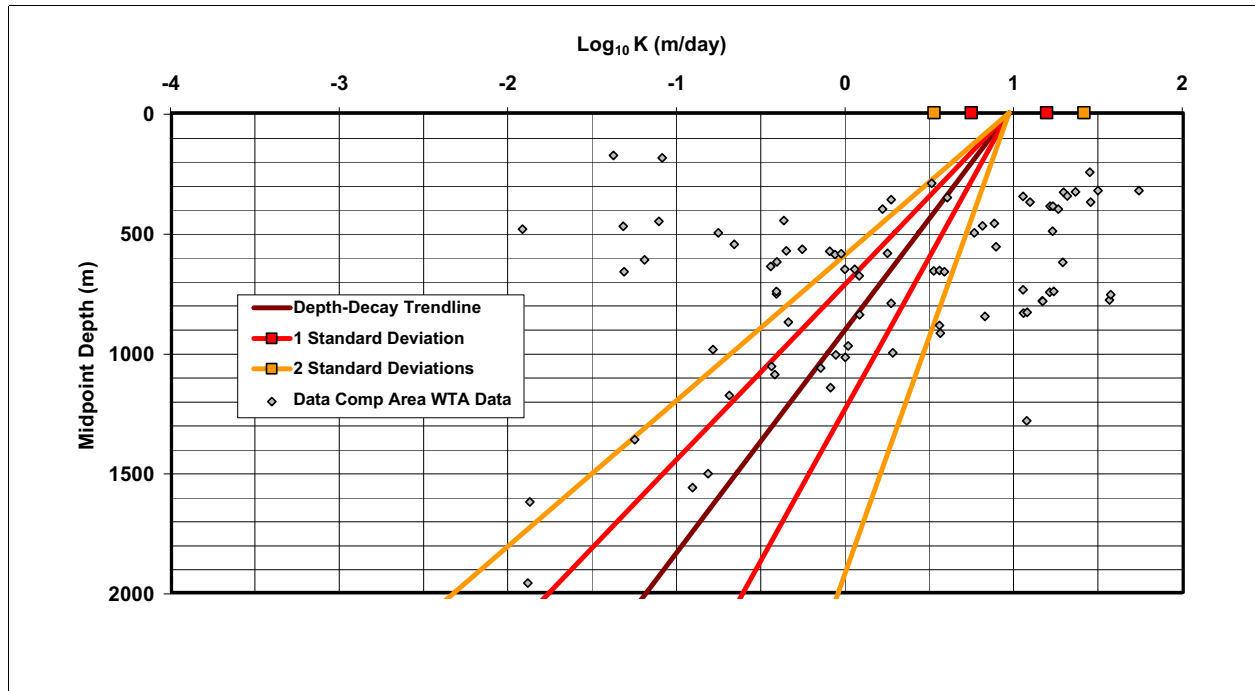


Figure B.2-6
WTA Pumping-Scale Depth Decay

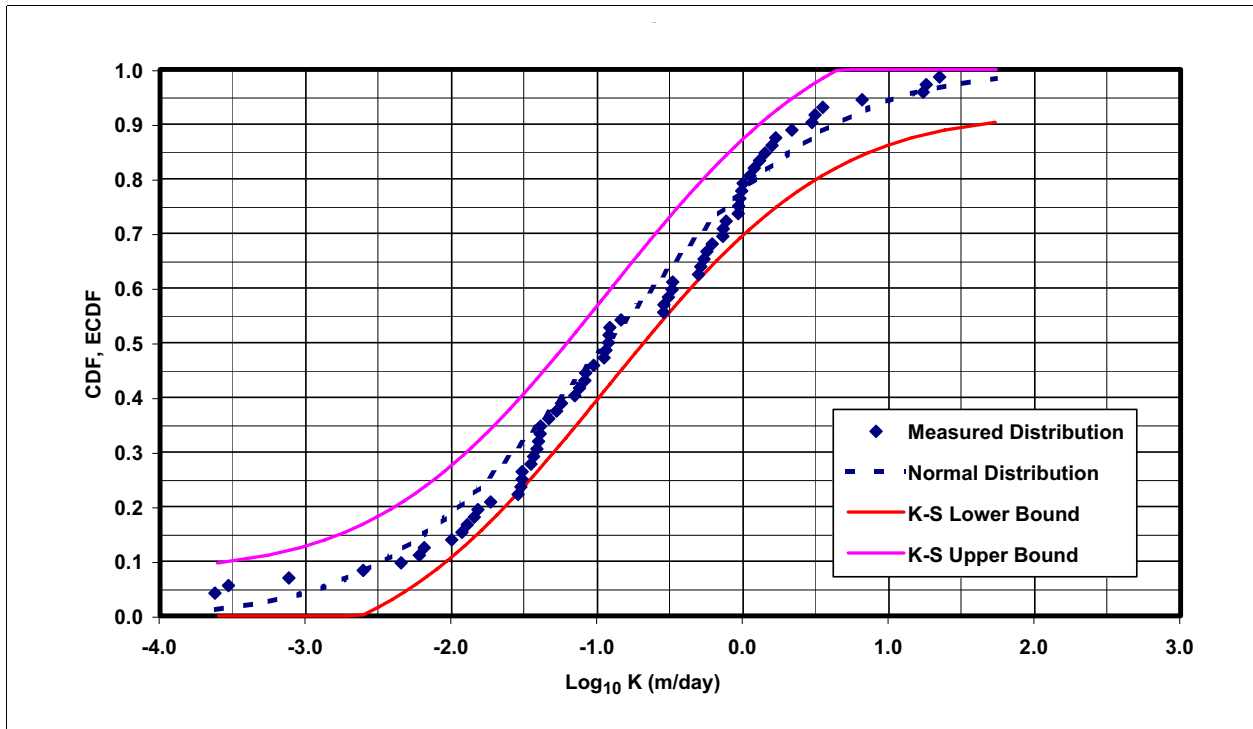


Figure B.2-7
TCU Pumping-Scale CDF

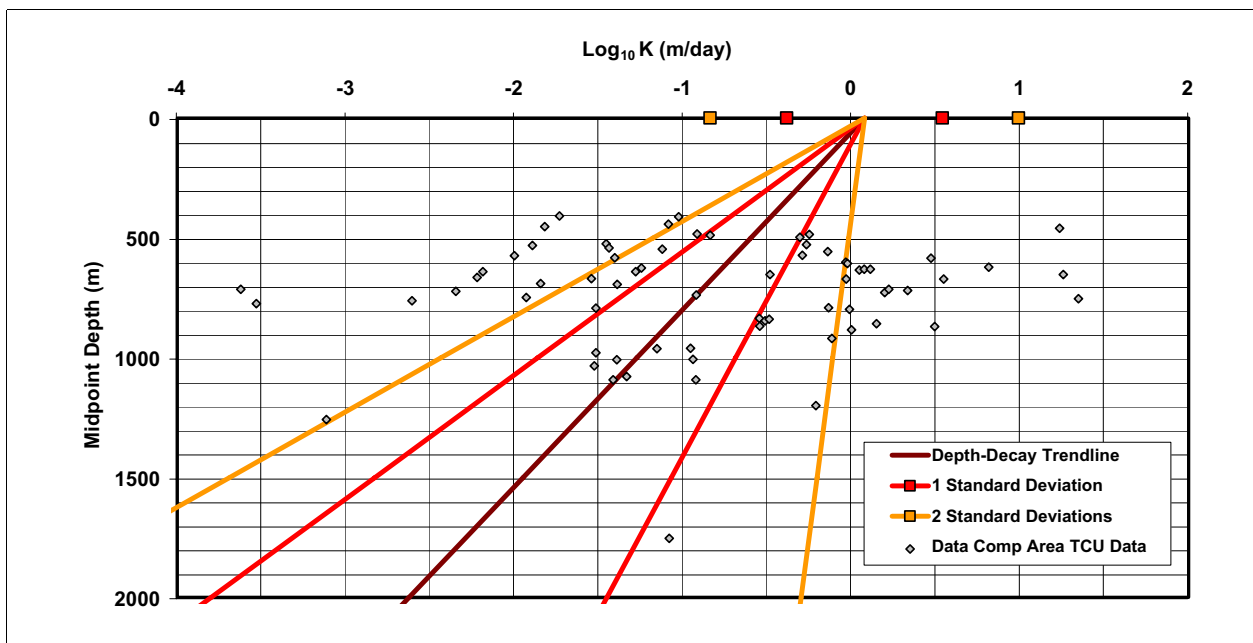


Figure B.2-8
TCU Pumping-Scale Depth Decay

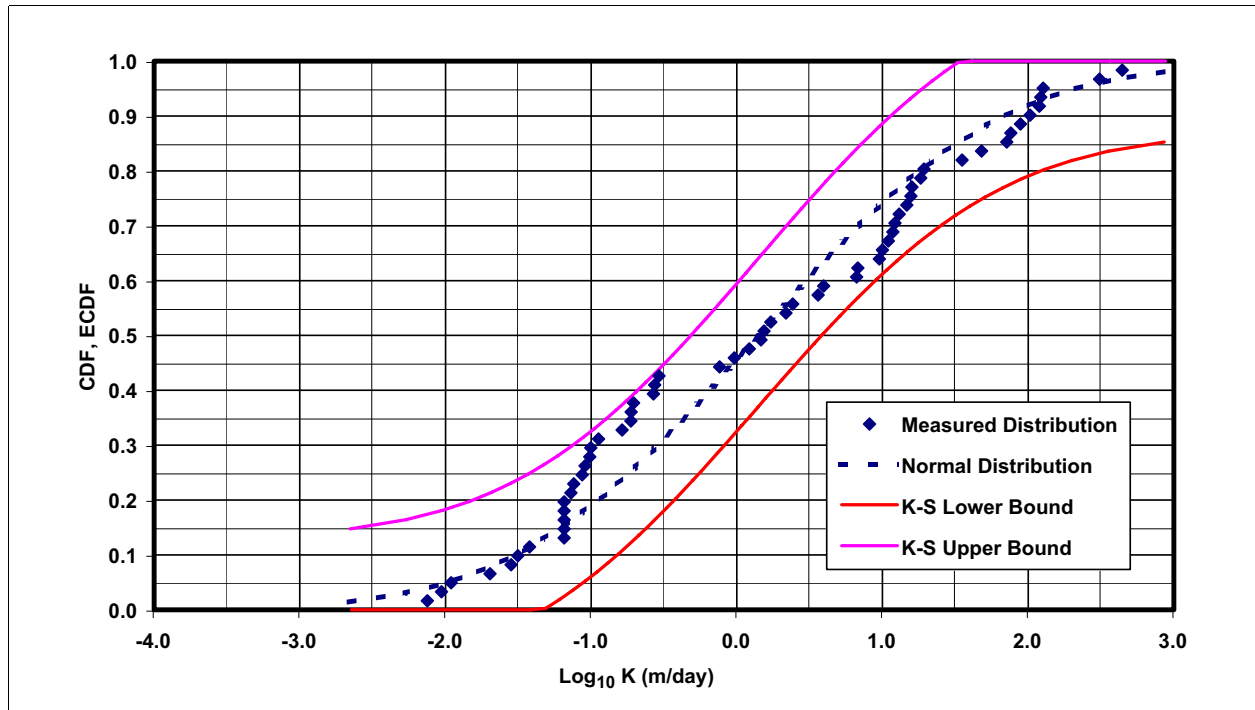


Figure B.2-9
LCA Pumping-Scale CDF

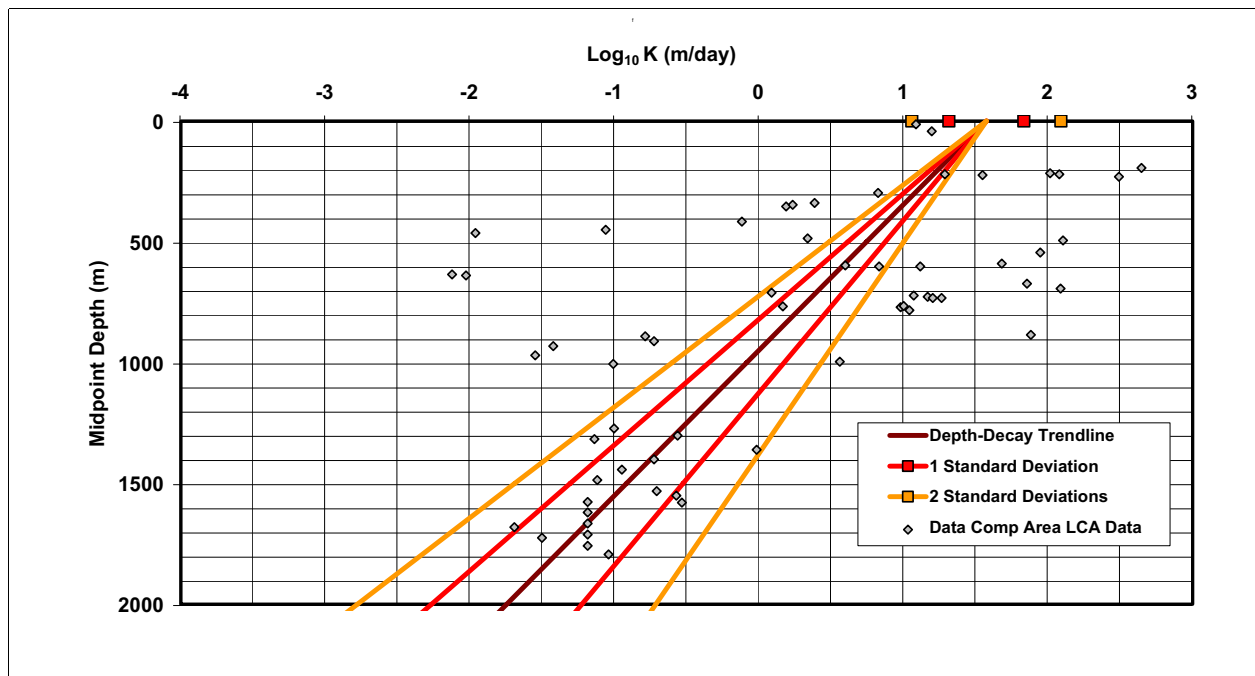


Figure B.2-10
LCA Pumping-Scale Depth Decay

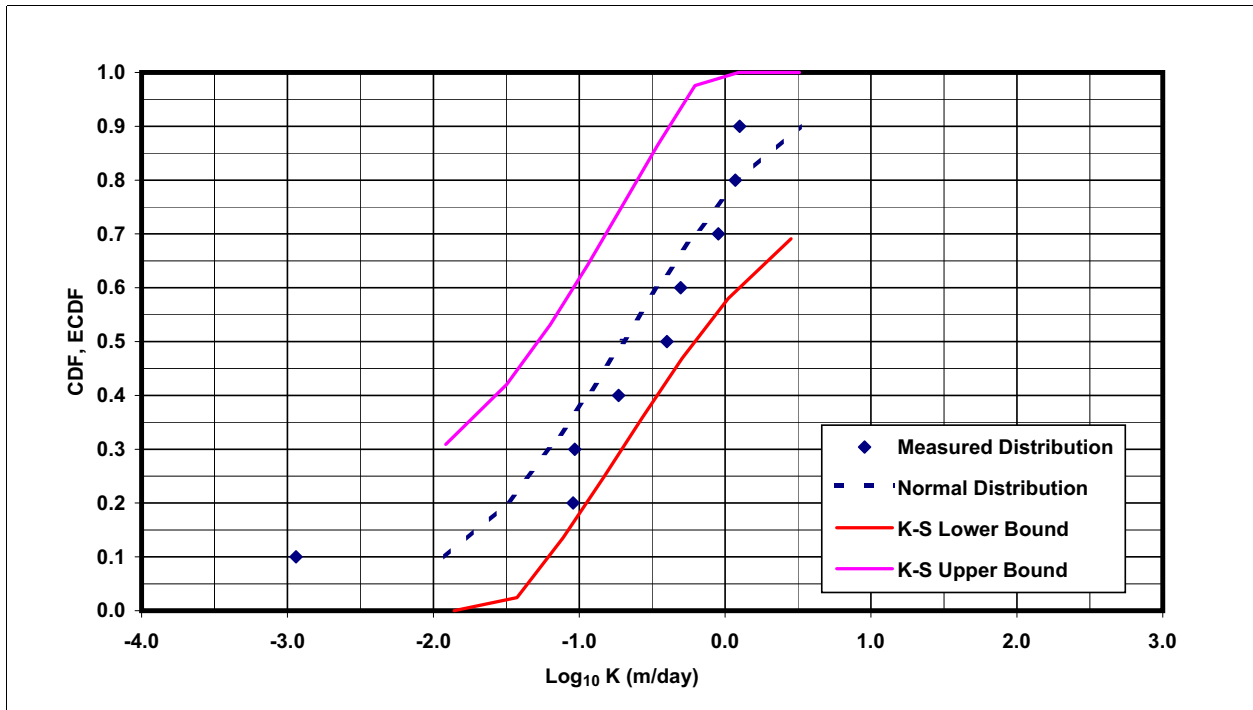


Figure B.2-11
LCA3 Pumping-Scale CDF

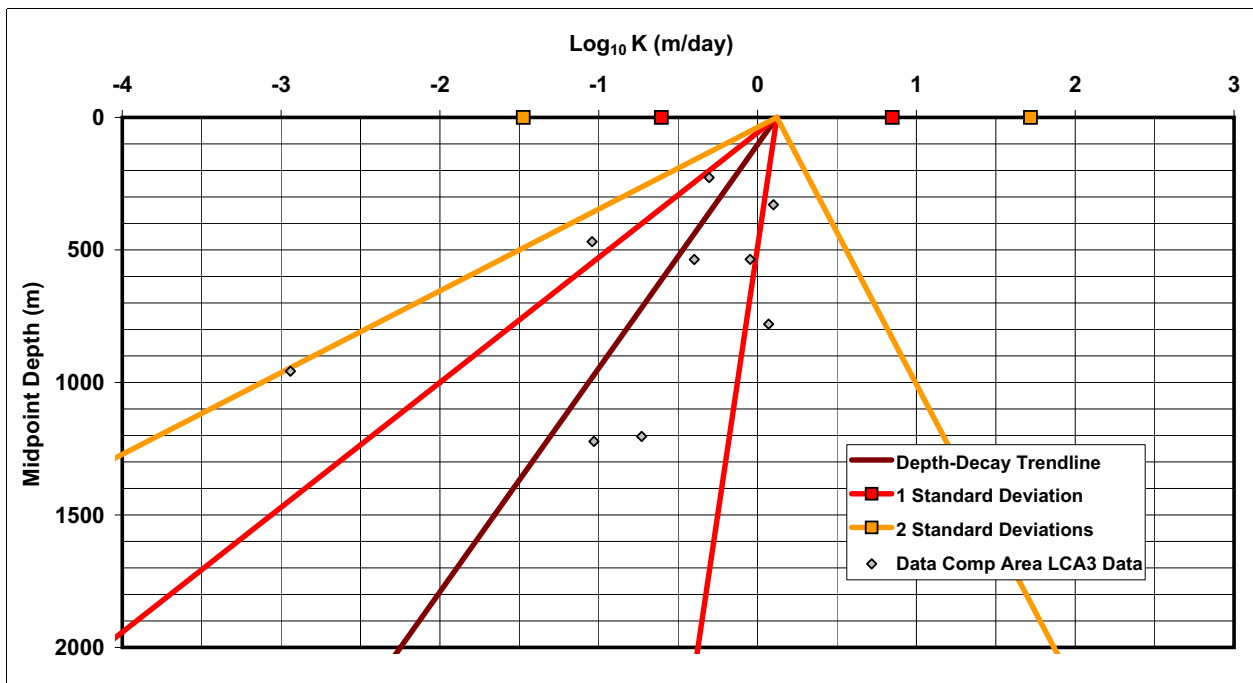


Figure B.2-12
LCA3 Pumping-Scale Depth Decay

B.3.0 ALTERNATE EVALUATION AND PRESENTATION OF DEPTH DECAY

An alternative evaluation of depth decay was developed to address concerns about the apparent poor correlation statistics of $\text{Log}_{10} K$ with depth and the scatter of the data. The characterization of the variation of hydraulic conductivity within formations is divided into two components: the natural variability within a formation and the effect of depth upon hydraulic conductivity. The regression of $\text{Log}_{10} K$ versus depth provides a measure of the overall variability of $\text{Log}_{10} K$ with depth that is a result of the variation in depth of the formation tested. In this alternate evaluation, the regression coefficient is used to calculate the K_0 , the value for $\text{Log}_{10} K$ at depth = 0, for each data point. A dataset of K_0 values can then be analyzed to determine the underlying intrinsic distribution of variability. This was performed for the CGs for which there were sufficient data to determine distributions. The results are tabulated in [Table B.3-1](#) and illustrated in [Figure B.3-1](#). [Table B.3-2](#) shows the regression statistics for the $\text{Log}_{10} K$ versus depth.

[Figure B.3-1](#) shows that the distributions for the LFA, WTA, and LCA/LCA3 are similar. They are all brittle, fractured rocks for which the hydraulic conductivity is dominated by fracturing and are grouped into one dataset. The other formations, AA/OAA/PCU and TCU, are better characterized as ductile, porous media. These divisions consider the difference in the effect of increasing overburden pressure on the formations, closing fracture apertures in the first case, and increasing consolidation in the second. The K_0 distributions for each of these combined datasets were determined based on regression of $\text{Log}_{10} K$ versus depth. [Figures B.3-2](#) and [B.3-3](#) show the raw data and distribution of $\text{Log}_{10} K$ for these datasets. The K_0 distributions are also shown with the regression trendline defining the variation of the mean and the 95% confidence bounds with depth. This presentation illustrates the characterization envelopes for the datasets, which contain approximately 95% of the data, respectively.

Table B.3-1
Statistics for K_0 Datasets

| CG | AA/OAA/PCU | LFA | WTA | TCU | LCA/LCA3 | Brittle Rock Data | Ductile Rock Data |
|-----------------------------|-----------------------------|-------|-------|-------|----------|-------------------|-------------------|
| Count | 31 | 24 | 79 | 71 | 69 | 176 | 102 |
| Parameter | Log ₁₀ K (m/day) | | | | | | |
| Mean | 0.62 | 0.95 | 1.14 | 0.43 | 1.14 | 1.04 | 0.49 |
| Standard Deviation | 0.72 | 0.76 | 0.87 | 1.17 | 1.05 | 1.03 | 1.06 |
| Minimum | -0.37 | -0.96 | -1.28 | -2.63 | -1.68 | -2.72 | -2.63 |
| Maximum | 2.14 | 2.03 | 2.76 | 2.72 | 3.04 | 3.04 | 2.72 |
| Max Abs Delta | 0.15 | 0.14 | 0.07 | 0.08 | 0.07 | 0.00 | 0.05 |
| K-S Statistic at 95% | 0.24 | 0.28 | 0.15 | 0.16 | 0.16 | 0.10 | 0.13 |
| Accept Lognormal Hypothesis | Yes | Yes | Yes | Yes | Yes | Yes | Yes |
| Lower Bound | -0.80 | -0.55 | -0.56 | -1.87 | -0.93 | -0.98 | -1.59 |
| Upper Bound | 2.04 | 2.45 | 2.84 | 2.73 | 3.20 | 3.07 | 2.56 |
| Range | 2.83 | 3.00 | 3.40 | 4.61 | 4.13 | 4.05 | 4.15 |

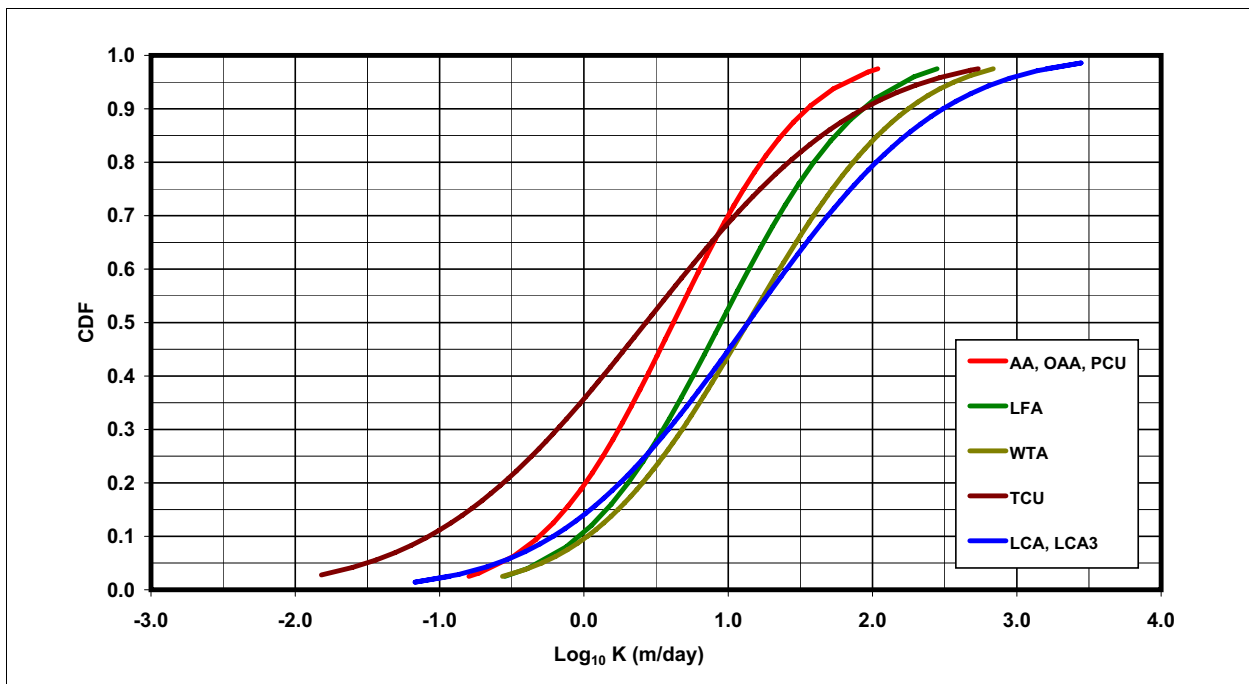


Figure B.3-1
Depth-Decay K HSU CDFs

Table B.3-2
Regression Statistics for Log₁₀ K Versus Depth

| CG | Par ^a | Value | SE ^b | t-Stat ^c | p-Value ^d | Confidence Bounds | | Data R ^e | Regression | | Par ^a R ^e |
|--------------|-----------------------------|-----------|-----------------|---------------------|----------------------|-------------------|-----------|---------------------|----------------|-----------------|---------------------------------|
| | | | | | | Lower 95% | Upper 95% | | R ² | SE ^b | |
| Brittle Rock | K ₀ ^f | 1.04E+00 | 1.65E-01 | 6.31E+00 | 2.19E-09 | 7.16E-01 | 1.37E+00 | -0.42 | 0.22 | 1.04 | -0.88 |
| | λ | -1.32E-03 | 1.88E-04 | -6.99E+00 | 5.52E-11 | -1.69E-03 | -9.44E-04 | | | | |
| Ductile Rock | K ₀ ^f | 4.88E-01 | 2.47E-01 | 1.98E+00 | 5.06E-02 | -1.28E-03 | 9.77E-01 | -0.42 | 0.21 | 1.06 | -0.90 |
| | λ | -1.82E-03 | 3.54E-04 | -5.14E+00 | 1.36E-06 | -2.52E-03 | -1.12E-03 | | | | |

^a Par = Parameter, referring to the two parameters in the depth-decay formula

^b Standard error

^c t-Statistic

^d Level of significance

^e Correlation coefficient

^f As log₁₀ (m/day)

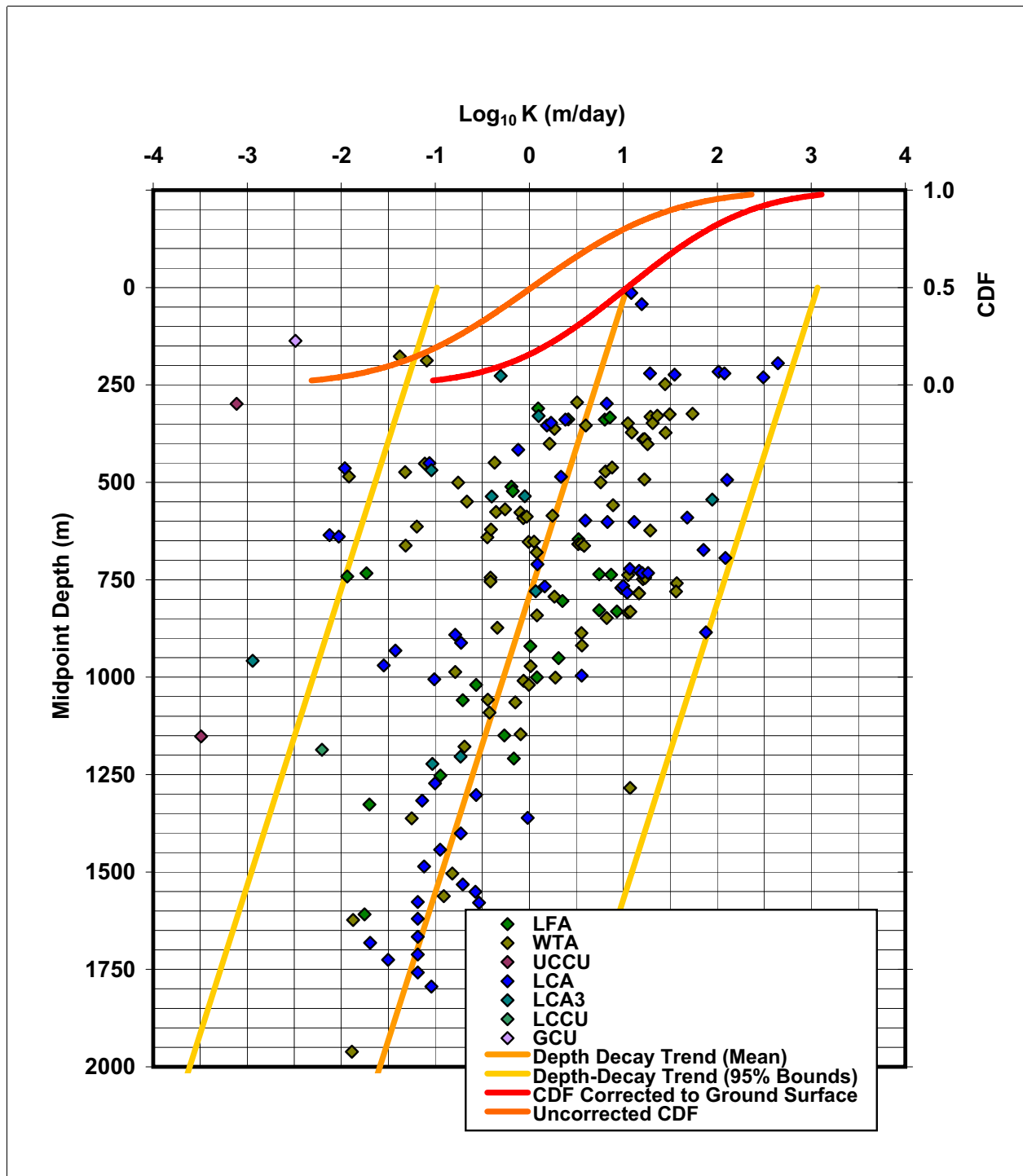


Figure B.3-2
Brittle Rock Depth Decay

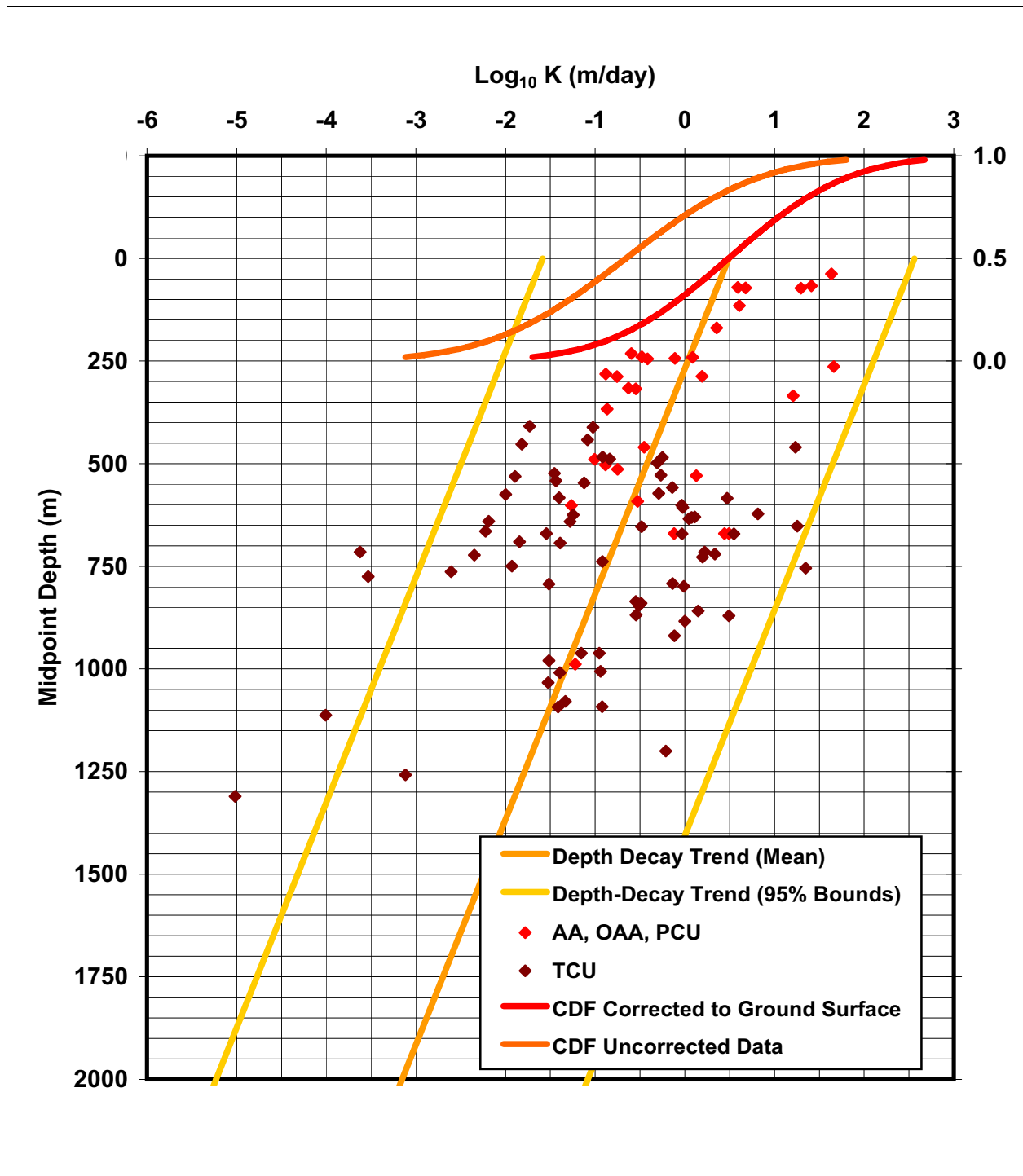


Figure B.3-3
Ductile Rock Depth Decay



Appendix C

Areal Recharge Supplementary Information

C.1.0 INTRODUCTION

Supporting information for the precipitation recharge is provided in the Appendix\C folder on the accompanying DVD. The supporting information includes a database of recharge model data for the models outlined in [Section 6.0](#).

C.2.0 DATASET SUMMARY

A database file, RMSM_Surface_Recharge_Geodatabase.mdb, contains recharge data for the four models presented in [Section 6.0](#). The database is a Microsoft Access file, and the data are accessible as tables through Access. The database has also been initialized as an ArcGIS geodatabase, and the tables can be accessed through ArcCatalog or ArcView. Data for each model are contained in separate tables/feature classes. Descriptions for the tables and fields in the tables are provided using the documentation features built into Access.



Appendix D

Groundwater Discharge Supplementary Information

D.1.0 INTRODUCTION

Supporting information for groundwater discharge is provided in the Appendix\D folder on the accompanying DVD. The supporting information includes several Microsoft Excel files with data for well, tunnel, and spring discharge for the RMSM area.

D.2.0 DATASET SUMMARY

An Excel workbook file, RMSM_Tunnel_Discharge.xls, contains data from a variety of sources on tunnel discharge in the RMSM area. Worksheets in the workbook are organized by tunnel and data source. The Index worksheet provides a description of the contents of each worksheet.

An Excel workbook file, RMSM_Spring_Discharge.xls, contains data from a variety of sources on discharge from springs in the RMSM area. Worksheets in the workbook are organized by spring and data source. The Index worksheet provides a description of the contents of each worksheet.

An Excel workbook file, RMSM_Well_Discharge.xls, contains data from a variety of sources on discharge from wells in the RMSM area. Worksheets in the workbook are organized by well. The Index worksheet provides a description of the contents of each worksheet.



Appendix E

Hydraulic Head Supplementary Information

E.1.0 INTRODUCTION

Well FAI and hydrograph data from a number of sources [1-8] is compiled, providing location information, a summary of water level data, FAI information, HSU information, and a hydrograph of available water levels. The report is provided in the Appendix\E folder on the accompanying DVD. A spreadsheet showing vertical gradient calculations (RMSM_Vertical_Gradient_Calculations.xls) is also included.

E.2.0 DATASET SUMMARY

An Adobe pdf file, RMSM_Hydraulic_Head_Data_Report.pdf, contains the “Formation Access Interval and Hydrograph Report.” The report has the following figures:

- Legend corresponding to each hydrograph
- Table describing each field within the hydrograph report
- Hydrograph report for each well

An Excel workbook file, RMSM_Vertical_Gradient_Calculations.xls, contains calculations of vertical gradients from several wells in the RMSM area with multiple completions. The workbook contains an index worksheet that explains the content of the file and four worksheets containing the vertical gradient calculations for each of the wells.

E.3.0 REFERENCES

1. Fenelon, J.M. 2005. *Analysis of Ground-Water Levels and Associated Trends in Yucca Flat, Nevada Test Site, Nye County, Nevada, 1951-2003*, Scientific Investigations Report 2005-5175. Carson City, NV: U.S. Geological Survey.
2. Fenelon, J.M. 2006. *Database of Ground-Water Levels in the Vicinity of Rainier Mesa, Nevada Test Site, Nye County, Nevada, 1957–2005*. Carson City, NV: U.S. Geological Survey.
3. Fenelon, J.M. 2006. Personal communication to SNJV. *Database of Ground-Water Levels in the Vicinity of Frenchman Flat and Eastern Pahute Mesa, Nevada Test Site, Nye County, Nevada, 1950-2006*. Henderson, NV: U.S. Geological Survey.
4. U.S. Geological Survey. 2007. “USGS Ground-Water Data for the Nation, National Water Information System: Web Interface.” As accessed at <http://nwis.waterdata.usgs.gov/nwis/gwlevels> on 11 February 2008.

5. National Security Technologies, LLC. 2007. *A Hydrostratigraphic Model and Alternatives for the Groundwater Flow and Contaminant Transport Model of Corrective Action Unit 99: Rainier Mesa-Shoshone Mountain, Nye County, Nevada*, DOE/NV/29546--146. Las Vegas, NV.
6. Bechtel Nevada. 2006. *A Hydrostratigraphic Model and Alternatives for the Groundwater Flow and Contaminant Transport Model of Corrective Action Unit 97: Yucca Flat-Climax Mine, Lincoln and Nye Counties, Nevada*, DOE/NV/11718--1119. Las Vegas, NV.
7. Bechtel Nevada. 2002. *A Hydrostratigraphic Model and Alternatives for the Groundwater Flow and Contaminant Transport Model of Corrective Action Units 101 and 102: Central and Western Pahute Mesa, Nye Counties, Nevada*, DOE/NV/11718--706. Las Vegas, NV.
8. Bechtel Nevada. 2006. *A Hydrostratigraphic Model and Alternatives for the Groundwater Flow and Contaminant Transport Model of Corrective Action Unit 98: Frenchman Flat, Clark, Lincoln and Nye Counties, Nevada*, DOE/NV/11718--1064. Las Vegas, NV.



Appendix F

Comments from Nevada Division of Environmental Protection

(5 Pages)

NEVADA ENVIRONMENTAL RESTORATION PROJECT DOCUMENT REVIEW SHEET

| 1. Document Title/Number: Phase I Hydrologic Data for the Groundwater Flow and Contaminant Transport Model of Corrective Action Unit 99; Rainier Mesa/Shoshone Mountain, Nevada Test Site, Nye County, Nevada (Final) | | | 2. Document Date: May 2008 | |
|---|-----------------------|--|--|-------------------|
| 3. Revision Number: Rev. 1 | | | 4. Originator/Organization: Nathan Bryant (702) 295-2374 | |
| 5. Responsible DOE NNSA/NSO Subproject Mgr.: Bill Wilborn | | | 6. Date Comments Due: April 7, 2008 | |
| 7. Review Criteria: Complete Document | | | | |
| 8. Reviewer/Organization Phone No.: State of Nevada; Mr. John J. Jones (702-486-2850) | | | 9. Reviewer's Signature: | |
| 10. Comment Responses transmitted via email from NDEP to Bill Wilborn on April 8, 2008 | | | 11. Comment Response Date: April 30, 2008 | |
| 12. Comment Number/Location | 13. Type ^a | 14. Comment | 15. Comment Response | 16. Accept/Reject |
| 1. Page 5-3, Section 5.2, seventh sentence | | The NDEP questions the use of unpublished data and interpretations from files because such data and interpretations are not peer reviewed. What procedures are in place to ensure such data and/or interpretations are credible? | The results from unpublished tests and analyses, sources identified in the hydraulic property database, are subject to the same QA/QC for use in this analysis as externally published analyses. The data in question, while not published, were evaluated using the same criteria as the published data. The text will be modified to state this. The available documentation was evaluated to determine the data documentation quality level, and the data quality was evaluated for suitability in general (see response to comment 2). Data quality levels were not assigned or weighted in the analysis for the reason stated in the response to comment 2. All of the data used in the saturated media hydraulic properties analyses has been reviewed before inclusion in the database to determine that the analysis is credible. Data described as unpublished indicates that the data has not been published in reports released for external distribution. Although unpublished, all of this data has undergone internal review prior to use, and has been incorporated into the analyses according to UGTA QA/QC requirements. Copies of all original data sources used for analysis is housed in the ER Contractor Central Files, Library, and/or electronic library. | Accept |

^aComment Types: M = Mandatory, S = Suggested.

^bCC has been replaced by CG (characterization group) in Rev. 1 final of the HDD and TDD

**NEVADA ENVIRONMENTAL RESTORATION PROJECT
DOCUMENT REVIEW SHEET**

| 12. Comment Number/Location | 13. Type ^a | 14. Comment | 15. Comment Response | 16. Accept/Reject |
|---|-----------------------|--|--|-------------------|
| 2. Page 5-4, Section 5.3, fifth paragraph | | ".....data quality evaluation flags (DQE-Fs) were not assigned to data entries." Not assigning data quality flags is not an acceptable way to indicate data quality. The UGTA QA/QC procedures must be followed. Data quality flags must be assigned or the data cannot be used. | <p>The general procedure to qualify data (UGTA QAPP, Sec.5.1.2 Data Quality Evaluation) includes assigning one or more flags, termed Data Quality Evaluation Flags, to each record or group of similar records compiled in the dataset. However, the opening statement of this section of the QAPP, "The criteria used to evaluate the quality of the different types of required data are dependent on the type and the intended use of the data.", provides leeway for alternate approaches. In this case, an evaluation of the objectives for characterizing hydraulic properties, in particular, variability and trends, has lead to use of an alternate approach. It has been judged that the most inclusive statistics would provide the best characterization, assuming the basic credibility of the data, which is addressed in the response to comment 1. Hydraulic property data (values) are not measured directly, but interpreted from tests. Consequently, there is inherent uncertainty in the correctness of the values depending upon the correctness of conceptual model, assumptions, and representativeness, which are open to interpretation. The approach used for hydraulic property characterization is to incorporate this uncertainty in the general analysis, and then reduce the uncertainty through evaluation and refinement of the characterization results.</p> <p>For the procedure used here, all of the data in the database were considered suitable for use and of equal weight. The argument for doing so relies on the fact that in cases where there were many data values for a CC* (Categorization Category, as defined in Sec. 5.4), the statistical analysis is expected to provide a good estimate of the mean and preclude the undue influence of any particular data value. In cases where there were few data for a CC, there is an insufficient basis to identify questionable data. Consequently, data quality evaluation flag levels (DQE_Fs) were not assigned to data entries and all data were used with equal weight.</p> | Reject |

^aComment Types: M = Mandatory, S = Suggested.

*CC has been replaced by CG (characterization group) in Rev. 1 final of the HDD and TDD

**NEVADA ENVIRONMENTAL RESTORATION PROJECT
DOCUMENT REVIEW SHEET**

| 12. Comment Number/Location | 13. Type ^a | 14. Comment | 15. Comment Response | 16. Accept/Reject |
|---|-----------------------|---|--|-------------------|
| 3. Page 5-6, Section 5.6, second paragraph | | It is stated that "The RMSM-specific parameter distributions and the NTS Data Compilation Area parameter distributions were compared to judge whether or not there are apparent discrepancies between the distribution determined. However, the RMSM-specific data sets are too sparse for a statistical comparison." How will the apparent discrepancies be determined? If the comparison was a subjective one to judge whether or not there are apparent discrepancies between the distributions, is the additional uncertainty considered throughout the CAU modeling? | <p>Reevaluation of the UCCU CC assignments since preparation of the Draft document led to the discovery of a discrepancy between the HSU assignments used, based on the HFM model, and detailed stratigraphic logs in drilling reports. The well completions in question were located in relatively thin intervals of LCA3 that were not mapped in the HFM. Since they are small, presumably disconnected blocks, within the UCCU, they were mapped as UCCU. All but two of the data points initially identified as UCCU were reassigned to LCA3. Since all the LCA3 data for the NTS is in the RMSM HFM area, the NTS and RMSM datasets for the LCA3 are the same and there is no need for a statistical comparison between them. The UCCU dataset is also entirely from the RMSM CAU. Consequently, there is no remaining issue regarding representativeness for these CCs.</p> <p>The RMSM WTA dataset has been statistically tested with respect to the NTS Data Compilation Area dataset for consistency of the variances and means, and was not found to be inconsistent. Text will be added to indicate this.</p> | Accept |
| 4. Page 5-9, Section 5.9.1, first paragraph, sixth sentence | | "... multiple K values were averaged (arithmetic average of K, assuming a normal distribution of errors is most likely) for multiple tests and analysis models used." In the literature, K has been shown to be lognormally distributed and the most appropriate average for K is the geometric average. Please quantify the discrepancy introduced by using the arithmetic mean instead of the geometric mean. | As stated in the text, multiple K values <i>determined for one test using alternate analysis models or assumptions</i> were averaged arithmetically. This is appropriate because it is assumed that analysis uncertainty is normally distributed, as stated. This is not related to the well-established lognormal distribution for K. There is no discrepancy introduced by the use of the arithmetic average for this analysis step. | Reject |
| 5. Page 5-10, Section 5.9.2, eighth and ninth sentences | | The statement, "The individual CC data sets were tested for conformity of the log K data to a normal distribution (lognormal distribution of K) ..." reflects the literature. If some of the K values used in this analysis were obtained using the averaging approach described in sentence eight, then there is a mismatch in the approach. A consistent approach should be used throughout the project. | Please see the response to Comment no. 4. | Reject |

^aComment Types: M = Mandatory, S = Suggested.

^bCC has been replaced by CG (characterization group) in Rev. 1 final of the HDD and TDD

**NEVADA ENVIRONMENTAL RESTORATION PROJECT
DOCUMENT REVIEW SHEET**

| 12. Comment Number/Location | 13. Type ^a | 14. Comment | 15. Comment Response | 16. Accept/Reject |
|--|-----------------------|---|--|----------------------|
| 6. Page 5-19, Section 5.13.1, first paragraph, third sentence | | As has been stated in the past, the NDEP does not agree with the statement given on Page 5-19, Section 5.13.1, first paragraph, third sentence in regards to the subject of decrease in hydraulic conductivity with depth (depth decay). It states, "In spite of the data scatter, which indicates that there is great variability of hydraulic conductivity at different depths for many formulations, the general conclusion in the literature is that hydraulic conductivity decreases with depth." A more appropriate statement the NDEP agrees with was given on Page 5-18, Section 5-13, first paragraph, second and third sentences. These statements are "The relationship of hydraulic conductivity to depth is controversial because the data contain great scatter and the regression of the log of hydraulic conductivity against depth exhibits poor correlation. However, there is considerable support in the literature for the relationship." The statements regarding depth decay should be consistent throughout the document. | These statements are not viewed as inconsistent by the authors. The general decrease of hydraulic conductivity with depth is controversial due to the great scatter in the data, which does not produce strong statistical correlation. However, the general conclusion in the literature <i>addressing the question of the relationship of hydraulic conductivity to depth</i> is that hydraulic conductivity decreases with depth. The reason(s) why the poor correlation (as indicated by a low correlation coefficient) is still considered are discussed in the text. The fact that some data has a correlation of 0.65 is taken as meaningful. The specific form of the relationship used to characterize the relationship in the RM HDD is the most common, simple and defensible relationship proposed, and serves the purpose for characterizing the relationship. The results of this analysis do not dictate the relationship that will be used for modeling. The above qualifier will be added to the statement in question to clarify the situation. Page 5-19, Section 5.13.1, first paragraph, third sentence will be reworded: "In spite of the data scatter, which indicates that there is great variability of hydraulic conductivity at different depths for many formulations, the general conclusion in the literature addressing the question of the relationship of hydraulic conductivity to depth is that hydraulic conductivity decreases with depth." | See Comment Response |
| 7. Page 5-19, Section 5.13.2, second paragraph, sixth sentence | | "The correlation coefficient values indicate that there is significant correlation (0.27-0.65) for many CCs of the NTS Data Compilation Area dataset. . ." Please justify how a correlation coefficient value of 0.27 can be considered significant because this leaves seventy-three percent of the variation due to error. | As stated in the text: 'By significant, it is meant that K appears correlated with depth to a degree that has proven significant for flow modeling. The relationship is understood to be superimposed upon natural variability....These values reflect the data scatter and are consistent with the understanding that other factors, such as heterogeneity and spatial variability, are also factors in the variability of hydraulic conductivity.' The remaining 73% of the variation is not due to error, but primarily to natural variability resulting from other factors. This does not argue that there may not be any error, but recognizes that other factors are present that affect the analysis. | Reject |
| 8. Page 5-23, Section 5.14, first paragraph, second sentence | | "... , which may be used for model verification." The term "verification" should be "validation." | Validation is a multistep process described in 5.1.4 of the RMSM CAIP. The referenced statement about the use of specific storage data for testing the flow model in transient mode follows the UGTA project use of the term verification to mean testing the model against an independent data set as described in Section 5.1.4.8 in the RMSM CAIP. | Reject |
| 9. Page 5-23, Table 5-27 | | A standard deviation for UCCU in the RMSM HFM area should not be included because there are only 2 data points which provides a range and is not enough data to calculate a standard deviation. | The UCCU is no longer included in this table due to the changes discussed in comment 3. | Accept |

^aComment Types: M = Mandatory, S = Suggested.

¹CC has been replaced by CG (characterization group) in Rev. 1 final of the HDD and TDD

**NEVADA ENVIRONMENTAL RESTORATION PROJECT
DOCUMENT REVIEW SHEET**

| 12. Comment Number/Location | 13. Type ^a | 14. Comment | 15. Comment Response | 16. Accept/Reject |
|---|-----------------------|---|---|-------------------|
| 10. Page 5-27, Section 5.15.2, Figure 5-8 | | Please explain the meaning of a non-integer flow dimension n, when the n values were defined as 1 (linear), 2 (radial) and 3 (spherical). | An explanation will be added: 'Non-integer flow dimension indicates an intermediate flow geometry such as bi-linear flow, n=1.5, which is simultaneous linear flow from the matrix to a fracture, and linear flow along the fracture.' | Accept |
| 11. Page 8-33, Section 8.7 | | What boundary fluxes and uncertainties or ranges are going to be used for the modeling? | Numerical modeling of the potential for migration of contaminants from the test locations through the vadose zone to the regional water table is planned for the Rainier Mesa and Shoshone Mountain test areas. If the modeling shows the potential for the migration of contaminants to the regional water table, saturated zone flow and transport modeling will be undertaken. This modeling, to include discussion of proposed model boundaries and boundary conditions, is the subject of the Modeling Approach/Strategy for Corrective Action Unit 99, Rainier Mesa and Shoshone Mountain report currently under review at NDEP. | Reject |
| 12. Section 5.13 and Appendix B | | Depth decay, though well researched and documented elsewhere, fails to be convincingly proven in the overall RMSM CAU. The graphs in Appendix B do show evidence for the application of depth decay in the LFA but the graphs for the other CCs show the same weak case for depth decay as the Frenchman Flat CAU did. For example, Figure B.2.2 for the AA has 13 data points within or close to the two standard deviation lines and 13 outside. The same general observation can be made for the WTA and LCA plots. No R~ values are given on the plots and they should be included. Conducting an analysis with 6 data points for the LCA3 shown on Page 8-7 for Figure B.2-12 is statistically questionable given the amount of scatter in the data. The overall graph, Figure 5-5, does not provide the confidence indicated by the text, nor does it provide a positive case for the overall use of depth decay in the RMSM CAU. | Depth-decay of hydraulic conductivity is a characteristic of hydraulic properties of formations which is well-supported in the literature, as referenced to Appendix E of the YF HDD. This document presents all of the data available and characterizes that data according to parameters that may be used in the flow model, which includes depth decay. The analysis of the data for depth decay is not purported to be strongly convincing, and this document does not presume to justify the specific use of depth decay in the RMSM flow model. However, the text does discuss the nature of the 'scatter' in the data and explains that the nature of much of the scatter is the superposition of natural variability within the formation at any particular depth upon the depth decay trend. The sparseness of many datasets contributes to the apparent randomness of the scatter. R values for all depth-decay analyses are listed on Table 5-6. | Reject |
| | | | | |

^aComment Types: M = Mandatory, S = Suggested.

^bCC has been replaced by CG (characterization group) in Rev. 1 final of the HDD and TDD



Plate

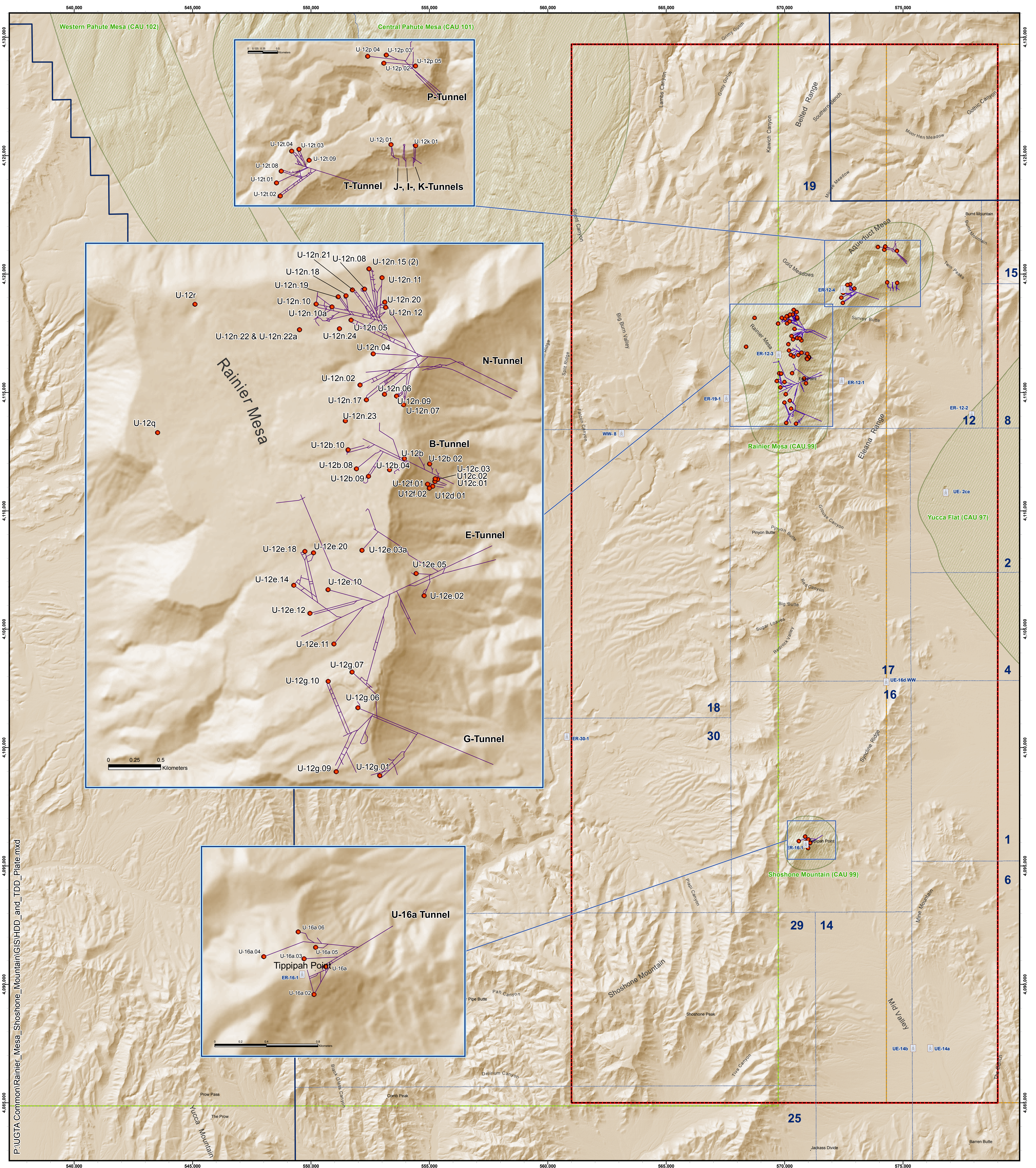


Plate 1
Rainier Mesa/Shoshone Mountain Hydrostratigraphic Area and Corrective Action Sites

| Explanation | |
|-------------|------------------------------|
| | RMSM Wells |
| | RMSM Corrective Action Sites |
| | NTS Boundary |
| | NTS Area Boundaries |
| | RMSM Tunnels |
| | RMSM HFM Boundary |
| | PMOV HFM Boundary |
| | YFCM HFM Boundary |
| | UGTA CAUs |

0 1.25 2.5 5

Miles

0 1.25 2.5 5 7.5

Kilometers

N

Coordinate System: UTM, NAD27, Zone 11, Meters



**DVD Containing This Document and
Supporting Datasets**

DISTRIBUTION

Copies

| | |
|---|----------------------|
| Tim Murphy State of Nevada Nevada Division of Environmental Protection 2030 E. Flamingo Road, Suite 230 Las Vegas, NV 89119-0818 | 2 Hard copies w/DVDs |
| W.R. Wilborn Environmental Restoration Division U.S. Department of Energy National Nuclear Security Administration Nevada Site Office P.O. Box 98518, M/S 505 Las Vegas, NV 89193-8518 | 2 Hard copies w/DVDs |
| K.C. Thompson Environmental Restoration Division U.S. Department of Energy National Nuclear Security Administration Nevada Site Office P.O. Box 98518, M/S 505 Las Vegas, NV 89193-8518 | 1 DVD |
| Alicia Tauber Environmental Management Records U.S. Department of Energy National Nuclear Security Administration Nevada Site Office P.O. Box 98518, M/S 505 Las Vegas, NV 89193-8518 | 1 Hard copy w/DVD |
| U.S. Department of Energy National Nuclear Security Administration Nevada Site Office Technical Library P.O. Box 62 Oak Ridge, TN 37831-0062 | 1 DVD |

| | <u>Copies</u> |
|---|-------------------|
| U.S. Department of Energy Office of Scientific and Technical Information P.O. Box 62 Oak Ridge, TN 37831-0062 | 1 DVD |
| Southern Nevada Public Reading Facility c/o Nuclear Testing Archive P.O. Box 98521, M/S NLV 400 Las Vegas, NV 89193-8521 | 2 DVDs |
| Manager, Northern Nevada FFACO ATTN: Kathryn Etcheverria Public Reading Facility c/o Nevada State Library & Archives 100 N Stewart Street Carson City, NV 89701-4285 | 2 DVDs |
| Celeste Sandoval Nye County Nuclear Waste Repository Project Office 1210 E. Basin Road, Suite #6 Pahrump, Nevada 89060 | 1 Hard copy w/DVD |
| Naomi Becker Los Alamos National Laboratory, M/S T003 Bikini Atoll Rd., SM30 Los Alamos, NM 87545 | 1 DVD |
| Gayle Pawloski Lawrence Livermore National Laboratory 7000 East Avenue, L-231 Livermore, CA 94550-9234 | 1 DVD |
| Mavrik Zavarin Lawrence Livermore National Laboratory 7000 East Avenue, L-231 Livermore, CA 94550-9234 | 1 DVD |
| Bonnie Thompson U.S. Geological Survey Water Resources Division 160 North Stephanie Street Henderson, NV 89074 | 1 DVD |

| | <u>Copies</u> |
|--|-------------------|
| Chuck E. Russell Desert Research Institute 755 E. Flamingo Las Vegas, NV 89119 | 1 DVD |
| Ken Ortego National Security Technologies, LLC P.O. Box 98521, M/S NLV 082 Las Vegas, NV 89193-8521 | 1 DVD |
| Sam Marutzky Stoller-Navarro Joint Venture 7710 W. Cheyenne, Bldg. 3 Las Vegas, NV 89129 | 1 Hard copy w/DVD |
| Greg Ruskauff Stoller-Navarro Joint Venture 7710 W. Cheyenne, Bldg. 3 Las Vegas, NV 89129 | 1 DVD |
| Bill Fryer Stoller-Navarro Joint Venture 105 Technology Drive, Suite 190 Broomfield, CO 80021 | 1 DVD |
| Nathan Bryant Stoller-Navarro Joint Venture 7710 W. Cheyenne, Bldg. 3 Las Vegas, NV 89129 | 1 DVD |
| Stoller-Navarro Joint Venture Central Files 7710 W. Cheyenne, Bldg. 3 Las Vegas, NV 89129 | 1 Hard copy w/DVD |